UNIVERSIDAD AUTÓNOMA DE MADRID
DEPARTAMENTO DE BIOQUÍMICA

CARACTERIZACIÓN MOLECULAR DE LOS FACTORES DE ENSAMBLAJE DE COMPLEJO I MITOCONDRIAL MidA y C20orf7 EN *Dictyostelium discoideum*

TESIS DOCTORAL

SERGIO CARILLA LATORRE
MADRID, 2011

DEPARTAMENTO DE BIOQUÍMICA
FACULTAD DE MEDICINA
UNIVERSIDAD AUTÓNOMA DE MADRID

CARACTERIZACIÓN MOLECULAR DE LOS FACTORES DE ENSAMBLAJE DE COMPLEJO I MITOCONDRIAL MidA y C20orf7 EN *Dictyostelium discoideum*

SERGIO CARILLA LATORRE
Licenciado en Bioquímica por la Universidad de Zaragoza
Director de Tesis: Dr. RICARDO ESCALANTE HERNÁNDEZ
Instituto de Investigaciones Biomédicas “Alberto Sols”, CSIC-UAM

MINISTERIO DE CIENCIA E INNOVACIÓN

CSIC
CONSEJO SUPERIOR DE INVESTIGACIONES CIENTÍFICAS

UAM
UNIVERSIDAD AUTONOMA DE MADRID

Ricardo Escalante Hernández, Científico Titular del Consejo Superior de Investigaciones Científicas adscrito al Instituto de Investigaciones Biomédicas "Alberto Sols" CSIC/UAM

CERTIFICA:

Qué Don Sergio Carilla Latorre, Licenciado en Bioquímica por la Universidad de Zaragoza, ha realizado bajo su dirección el trabajo titulado:

Caracterización molecular de los factores de ensamblaje de complejo I mitocondrial MidA y C20orf7 en *Dictyostelium discoideum*

y considera que el trabajo reúne las condiciones científicas necesarias para ser presentando como Tesis Doctoral.

Y para que así conste a los efectos oportunos, firma el presente documento en Madrid, a 5 de Julio de 2011.

Fdo: Dr. Ricardo Escalante Hernández

V^{O} B^{O} Dra. Amparo Cano García

C/Arturo Duperier, nº 4
28029 MADRID ESPAÑA
TEL.: 91 585 4400
FAX: 91 585 4401

http://www.iib.uam.es

A mis padres y **a** *mi hermana*

“Lo que sabemos es una gota de agua; lo que ignoramos es el océano”
Isaac Newton

“¡No corras, vete despacio, que a donde tienes que llegar es a ti mismo!”
Juan Ramón Jiménez

AGRADECIMIENTOS

Estos 4 años en el IIB han dado para mucho. Mucho trabajo sobre todo pero a la vez muchas risas, alegrías y fiestas. Además también he aprendido mucho, no sólo de ciencia, sino de aspectos de la vida que creo me han hecho ser mejor persona. Todo esto no hubiera sido capaz de hacerlo sólo, de no ser por la ayuda, apoyo y cariño de mucha gente que he querido recordar aquí.

En primer lugar quiero empezar agradeciendo al laboratorio, que es donde más rato me he pegado. A Ricardo creo que le tengo que agradecer mucho: por un lado me ha enseñado a ser un buen científico y por otro, yo he aprendido mucho con él gracias a que, además de ser un estupendo científico, es todavía mejor persona. Además creo que ha supuesto un auténtico ejemplo para mí. Y como amigo me ha dado un gran número de consejos y me ha apoyado siempre. A Rose, gracias por ser tan alegre y por los correos cachondos que envías de vez en cuando. Parte muy importante de este grupo es Javi. A Javi le quiero agradecer esas ganas de trabajar intensamente, que en definitiva y junto con un poco de cerebro, le llevan a uno a ser capaz de ser productivo en los tiempos tan difíciles que corren. Además nos lo hemos pasado muy bien subiendo a la montaña y olvidándonos de todas las penas que a veces surgen entre semana. También por las risas en Bilbao, Santander y Murcia. A Dani, que es un artista. Gracias por las risas, por los momentos en Barna, por la montaña, por los paseos, y por alegrarme un poco la vida cuando no estaba para tonterías. ….y por las finales y no finales del Barca. A Nata por su trabajazo. Y por alegrarme el cumple el año pasado, y por sus ideas estupendas sobre la vida. Y por la felicidad que trasmite, bueno, salvo cuando pone música dura.

Por el laboratorio vecino han pasado personas que también han sido la leche. Gracias Iván por tu forma fiestera de ver la vida y por acogerme en Sevilla. A Pilar que siempre tiene historias divertidas y a Iris, una tía grande que es supermaja. Y luego viene Pamper, creo que gracias por darme energía el día a día, sin necesidad, eso sí, de beber Redbull o cosas similares. A Ana que siempre me ha recibido con una sonrisa en la boca. A Mari Carmen que me da siempre besicos que se agradecen mucho. Y por ser tan maja y simpaticona conmigo.
Quiero agradecer a Carmen el hecho de su compresión y atención conmigo, y por Santander y por la fiefta. A Mª Jesús por los momentos de relax durante las comidas con todo el grupo y por tu aire vasco que tanto me mola. A Olivier y Antonio por su ayuda con el Pull-down y doble híbrido.

También hay mucha gente por la Facultad de Medicina que le quiero agradecer cositas tanto en el terreno profesional como en el personal. Primero a David. Gracias por estar como una regadera sana, por las muchas cervezas de la Yoli, por apoyarme cuando más lo necesitaba y por esas conversaciones sobre el espacio. Por ser un buen compañero de piso. A Lucía por unas conversaciones inteligentes y maduras. Del labo de Rafa, primero quiero agradecer a Susana. Gracias por resolver mis dudas y por las fiestas junto con David y los demás. Y por la ayuda con el BN-PAGE que se me hizo harto difícil al principio. A Miguel por las risas y el ping-pong en los Alpes. A Paula por su ayuda en el BN-PAGE y por las risas. Y por abrirme la puerta de la Facultad pero no rompérmela en la cabeza. A Ester por su paciencia y su gran trabajo en células. Y por las collejas creo que también. A Rafa, que con su habitual serenidad y conocimiento profundo de la mitocondria nos permitió dar ese pequeño saltito de unos cuantos millones de años.

A lo largo de estos años he disfrutado mucho con la gente Dicty. Quiero agradecer a Leandro lo primero su amabilidad. Su consejos, su ayuda tanto cuando estuvimos en su lab como más tarde. Siempre, y digo siempre, me ha ayudado sin reticencias. Y por su profundo conocimiento de Dicty. Por el abrebotellas y por arreglarme el cinturón. A María por sus expliaciones iniciales cuando no tenía ni idea de cómo trabajar con el cabezón. A Teresa por ayudarme a subir las escaleras del Guggenheim..¿o fue al revés? Y por presentarme a Pascale. A Anne que junto a María pasamos buenos ratos en Cardiff.

Antes de llegar al IIB pasé por el CNIO. Y quiero agradecer a todos mis amigos, que a pesar de irme de allí, nos hemos seguido viendo y pasando buenos momentos. A Lorenzo, un tío grande. Gracias por tus consejos, por tu apoyo en momentos difíciles, por las fiestas y por Londres. A Ros que junto con Loren son unos Frikis y "casi" consiguen que vuelva a jugar a rol. Por los buenos momentos. A Iñigo por las cervecillas y por los cumples. Y por el concierto de Bunbury. A Ricardo, por esos bailes brasileños y por Pilares con el resto de la pandilla. A Susana, por su paciencia en preguntas un tanto repetitivas..A Luisja o Javi por compartir junto con Iñigo la serie Lost y ver ese final tan maravilloso sin llorar..A Fernando por la afición que nos unía a los comics. A Alberto por sus grandes consejos y su ejemplo como persona, y bueno, por su gran conocimiento de grandes películas de la historia, como Contact..A Ana, Guille, Daniela y muchos más por esos momentos de cerves tras jornadas muy duras de trabajo. A Ellen por hacerme recordar y mejorar mi inglés, que luego me ha servido en no pocas ocasiones. Y por ayudarme con la charla de los Alpes, ¡qué miedo tenía!. A Osvaldo por ese trabajo tan profesional con MidA y por recordarme que, aparte de la ciencia de pipeta, me encanta la bioinformática.

Dada la importante ayuda que nos han prestado el grupo del Dr. Paul Fisher quiero agradecerle a él y a su grupo toda la entrega y trabajo que requirió el estudio de los genes *midA* y *C20orf7*. Por esos fantásticos artículos que hablan de las dos cosas que, por el momento, más me gustan en ciencia: Dicty y mitocondria.

Gracias a mis amigos de Zaragoza porque a pesar de que no he podido estar siempre a su lado, hemos mantenido el contacto. A Condor y Sueken por ser tan majos, por venir a visitarme y por conseguir que nos reuniésemos de nuevo con Yoda para recordar todas esas fantásticas frases y motes del pasado. Y chistes. A Diego, por esas conversaciones inteligentes y por tu visita.

Quiero agradecer a mi familia todo el cariño que me han prestado. A pesar de lo difícil que ha sido tener el corazón partido entre Madrid y Zaragoza siempre han estado conmigo. Siempre. A Susi y Rafa por esas escapadas a Cariñena. Y también por hacerme tito de la preciosa Lucía.

FINANCIACIÓN

Este trabajo ha podido llevarse a cabo gracias a la financiación de los proyectos BFU2006-00394 y BFU2009-09050 del Ministerio de Ciencia e Innovación y al contrato de Investigador de apoyo de la Comunidad de Madrid cofinanciado por el Fondo Social Europeo.

RESUMEN

En esta Tesis utilizamos *Dictyostelium* para la caracterización molecular de MidA, un nuevo factor de ensamblaje o estabilidad del complejo I (CI) mitocondrial, así como de C20orf7, otro factor previamente implicado en la función de dicho complejo.

La disrupción de los genes *midA* y *C20orf7* produce un defecto aislado de CI como hemos demostrado mediante la medición de cadena respiratoria. El uso de la técnica BN-PAGE en células humanas HEK293T, donde se reguló negativamente la expresión del homólogo humano de *midA* (*hMidA*), muestra también un defecto importante de complejo I ensamblado así como en la actividad. Mediante la técnica de doble híbrido en levadura y confirmación posterior mediante "pull-down" hemos descubierto que MidA y hMidA interaccionan con la subunidad de CI NDUFS2, tanto de *Dictyostelium* como de humano, sugiriendo la conservación de su función a lo largo de la evolución y su importante papel en el CI.

MidA es una proteína de función desconocida. Con el objetivo de conocer su posible función realizamos estudios *in silico* que nos han permitido generar un modelo 3D de nuestra proteína, así como predecir un posible dominio catalítico de unión de S-adenosilmetionina (SAM), donador de grupos metilo en reacciones catalizadas por metiltransferasas. Los estudios de mutagénesis dirigida indican que la mutación G170V en este dominio de unión de SAM produce una falta de función de la proteína MidA, sugiriendo una posible función metiltransferasa. Así mismo, la mutación G86V, en el posible dominio de unión de SAM descrito para C20orf7, produce de igual modo una aparente falta de función de la proteína indicando también un posible papel como metiltransferasa. Para avanzar en el conocimiento de la diferente citopatología producida por mutaciones en el gen *C20orf7* en pacientes humanos, hemos llevado a cabo la mutagénesis dirigida sobre los residuos homólogos en C20orf7 de *Dictyostelium* resultando en que ambas mutaciones producen una falta de función de la proteína.

midA^{-} presenta importantes defectos en fototaxis y termotaxis. Así mismo hemos descrito como la complementación de la cepa *midA*$^{-}$ con la proteína "wild type" es capaz de recuperar ambos fenotipos. Por otro lado, la transfección del mutante *midA*$^{-}$ con una construcción antisentido del gen *ampk* ("AMP-dependent protein kinase") consigue recuperar totalmente el fenotipo de fototaxis y parcialmente el de termotaxis sugiriendo que en *midA*$^{-}$ ambos fenotipos defectuosos podrían ser causados por la activación crónica de AMPK. Por otro lado la medición del flujo autofágico en los mutantes *midA*$^{-}$ y *C20orf7*$^{-}$ indica un aumento respecto al control WT y la presencia de agregados proteícos poliubiquitinados insolubles, similares a los encontrados en enfermedades neurodegenerativas donde la AMPK parece jugar un papel importante.

El mutante *C20orf7*$^{-}$ presenta, junto con los defectos de complejo I, defectos en crecimiento y desarrollo, similares a los hallados previamente para el mutante *midA*$^{-}$. La comparación de fenotipos entre ambos mutantes presenta similitudes, pero también diferencias importantes que son discutidas en este trabajo.

SUMMARY

In this thesis we have used *Dictyostelium* for the molecular characterization of MidA, a new mitochondrial complex I (CI) assembly/stability factor and C20orf7, another factor previously implicated in the function of this complex.

The *midA* and *C20orf7* gene disruption produces an isolated defect of CI in *Dictyostelium* as we have demonstrated by respiratory chain meassurements. The use of BN-PAGE technique in human HEK293T cells in wich the human homologue gene *hmidA* was downregulated, also showed an important defect in the CI assembly and activity. Yeast-two hybrid and pull-down techniques have shown that MidA and hMidA interact with the CI subunit NDUFS2 from both, *Dictyostelium* and human, suggesting the conservation of the function along the evolution and the important role of these proteins in CI.

MidA is a protein of unknown function. With the aim to discover its putative function we performed *in silico* studies wich allowed us to generate a 3D model of MidA and to predict the presence of a putative binding domain for S-adenosylmethionine (SAM), the main methyl donor in reactions catalyzed by methyltransferases. Site-directed mutagenesis experiments indicated that the G170V mutation in the putative SAM binding site produces aparently a loss of function of MidA, suggesting a putative methyltransferase function. Moreover the change G86V in the putative SAM binding site of C20orf7 also caused a loss of function of this protein indicating a similar role as a methyltransferase. To advance in the knowledge of the different cytopathology caused by diferent mutations found in the *C20orf7* gene in human patients, we have carried out site-directed mutagenesis in the homologous residues in *Dictyostelium* C20orf7 and both mutations resulted in an aparently loss of function of the protein.

midA$^-$ have important defects in phototaxis and thermotaxis. We have also described that the *midA*$^-$ complementation with the wild type protein is able to recover both phenotypes. The transfection of *midA*$^-$ mutant with an AMPK (AMP-dependent protein kinase) asRNA recovered the phototaxis phenotype and partially the thermotaxis phenotype suggesting that in *midA*$^-$, both phenotypes are caused by the chronic activation of AMPK. In adittion, the autophagic flux in the mutants *midA*$^-$ and *C20orf7*$^-$ was found to be increased and there were insoluble aggregates of polyubiquitinated proteins, similar to those observed previously in neurodegenerative diseases where AMPK seems to have an important role.

Apart form CI dysfunction, *C20orf7*$^-$ mutant showed defects in growth and development, similar to those reported in the *midA*$^-$ mutant. There are similarities but also differences in the phenotypes of both strains that are discussed in the present work.

ÍNDICE

ÍNDICE

ABREVIATURAS

2D-BN-PAGE	2-Dimensional Blue Native/SDS Gel Electrophoresis
7TM	Seven-transmembrane protein
ACA	Adenylyl cyclase
ACD	Autophagic Cell Death
AIF	Apoptosis Inducing Factor
AMPK	AMP-dependent Kinase
asAMPK	antisense AMPK
BN-PAGE	Blue Native Polyacrylamide Gel Electroforesis
BSr	Blasticidin resistance cassette
CAR	cAMP receptor
CI	Complex I; NADH dehydrogenase
CII	Complex II; Succinate dehydrogenase
CIII	Complex III; ubiquinol—cytochrome-c reductase
CIV	Complex IV; cytochrome c oxidase
CMF	Conditioned Medium Factor
CPN60	Chaperonine 60
CSA	Catalytic Site Atlas
CV	Complex V; ATP Synthase
DdNDUFS2	*Dictyostelium discoideum* NDUFS2
DIF-1	Differentiation Inducing Factor -1
GFP-Tkt-1	GFP-Transketolase
hMIDA	Human MidA
MidA	Mitochondrial disfunction gene A
MPTP	1-methyl-4-phenyl-1,2,3,6-tetrahydropyridine
mtDNA	mitochondrial DNA
mtRNA	mitochondrial RNA
OXPHOS	Oxidative Phosphorylation System
PDB	Protein Data Bank
PFAM	Protein Family Database
PIP2	Phosphatidylinositol 4,5-bisphosphate
PIP3	Phosphatidylinositol (3,4,5)-trisphosphate
PSF	Pre Starvation Factor
PTEN	Phosphatase and tensin homolog
SAM	S-adenosylmethionine
SCOP	Structural Clasification of Proteins Database

TAP	Tandem Affinity Purification tag
TIM	Translocase of the Inner Mitochondrial membrane
TOM	Translocase of the Outer Mitochondrial membrane

INTRODUCCIÓN

1. *Dictyostelium discoideum*

1.1. Descubrimiento y filogenia.

Dictyostelium discoideum es una ameba social de vida libre que se encuentra de manera natural en los suelos donde se alimenta de bacterias y otros microorganismos por fagocitosis. Su tamaño medio como organismo unicelular es de 10µm. Sin embargo cuando los nutrientes escasean es capaz de desarrollar una estructura multicelular de aproximadamente 100.000 células denominada cuerpo fructífero. Así mismo este cuerpo fructífero mantiene en la parte superior un soro que contiene un elevado número de formas resistentes denominadas esporas que aseguran la supervivencia de la especie.

La especie *Dictyostelium discoideum* fue descubierta por primera vez en 1935 por Raper en los bosques de Ashville en Carolina del Norte [1,2,3]. Los estudios filogenéticos y la secuenciación completa del genoma de *Dictyostelium* han permitido, por un lado, fijar la aparición del grupo *Dictyostelida* hace unos 500 millones de años [1,2,1] y, por otro, clasificarlo dentro del grupo monofilético Eumycetazoa [4,6] **(Fig. 1)** . Este grupo, que se separó después de la división de las plantas y antes de la división de metazoos y hongos, mantiene características de los tres grupos.

Reconocido como organismo modelo por el NIH (National Institutes of Health) presenta un gran número de ventajas. Al compartir dos ciclos de vida, unicelular y multicelular, nos permite estudiar un elevado rango de fenotipos como motilidad, quimiotaxis, agregación, diferenciación o morfogénesis no presentes en organismos modelo más simples como *S.cerevisiae*. Por otro lado, el hecho de que sea un organismo haploide y con su genoma totalmente secuenciado, permite trabajar a nivel génico o transcriptómico de un modo sencillo.

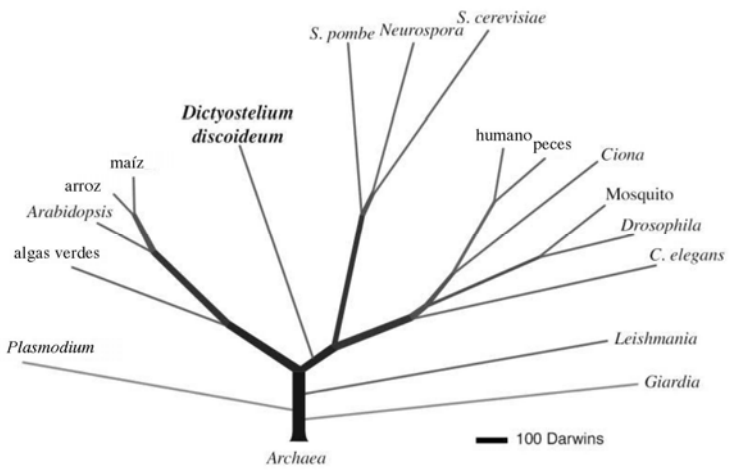

Fig. 1. Árbol filogenético basado en proteómica. Este árbol fue generado utilizando 5279 proteínas ortólogas de 17 especies eucariotas diferentes [4,6]. La longitud de las ramas se da en Darwin. (1 Darwin= 1/2000 la divergencia entre *S.cereviase* y humano). A pesar de la temprana división de *D.discoideum* (antes de la división de hongos y metazoos pero después de plantas) muchas de sus proteínas son más parecidas a sus ortólogos humanos que a *S.cerevisiae.*

1.2. Genoma

El genoma nuclear de *Dictyostelium discoideum* fue secuenciado en 2005 [46] mientras que el mitocondrial ya había sido publicado anteriormente [109]. En este apartado nos centramos en el primero dado que del segundo se hablará más en detalle en otro capítulo.

El genoma nuclear consta de 6 cromosomas y comprende 34 Mb que permiten codificar 12600 proteínas. Esto lo hace un genoma altamente compacto. El contenido de adeninas y timinas (A+T) es muy elevado sobre todo en regiones no codificantes. En general este valor es de 78% siendo de 65% para regiones codificantes. El espaciamiento intergénico es de 2.5 Kb mientras que en humano es de 128 Kb. El codigo genético utilizado es universal. Como en el genoma humano, el genoma de *Dictyostelium discoideum* presenta intrones aunque su número es reducido y el tamaño medio es de 146pb frente a los 3365pb en humano. Las secuencias señal de procesamiento en las uniones intron-exón son las mismas que en mamíferos lo que hace pensar en un mecanismo de procesamiento similar que se habría mantenido a lo largo de la evolución. Por otro lado los ARN ribosómicos (rRNA) 5S, 17S y 26S son codificados a partir de un DNA lineal extracromosómico palindrómico de 88Kb donde se ha estimado en 100 el número de copias por núcleo [46]. Así mismo existen otros elementos extracromosómicos como plásmidos, retrotransposones y LINEs, ocupando estos dos últimos un importante porcentaje del genoma como ocurre en humanos [46].

La información genómica y transcriptómica así como información funcional se encuentra depositada en la base de datos Dicty-base (www.dictybase.org). Destaca especialmente por su relevancia el apartado Dictyexpress donde se puede consultar información de expresión génica de los diferentes genes obtenida tanto por microarrays de expresión como por secuenciación masiva.

Uno de las aplicaciones inmediatas de la secuenciación del genoma de *D.discoideum* fue corroborar la presencia o ausencia de ortólogos a proteínas humanas. Esto se hace especialmente relevante si estas proteínas se encuentran implicadas en enfermedad, sobre todo en el caso de proteínas cuya información es limitada y con ella también la etiología de la enfermedad. Proteínas implicadas en cáncer de colon (MSH2, MLH1, MSH3, PMS2) , oncogenes como AKT2 o Ras o implicadas en enfermedades neurológicas como adrenoleucodistrofia (ABCD1), angelman (UBE3A), TaySachs (HEXA), esclerosis lateral amiotrófica (SOD1) o Parkinson (UCHL1) son sólo unos pocos ejemplos. Sin embargo existen un gran número de genes ortólogos no implicados en enfermedad igualmente interesantes. Mediante una clasificación de las proteínas con bases de datos como SCOP (Structural Clasification of Proteins Database) o PFAM (Protein Family Database) se descubrió que existía un elevado número de proteínas homólogas no sólo con humanos sino también con hongos y plantas. Especialmente interesante resulta el grupo de proteínas conservadas entre humano y *Dictyostelium* pero ausente en levaduras o plantas. Esto es debido en gran parte al interés que tiene el uso de *Dictyostelium* como modelo experimental frente a otros organismos modelo más sencillos como *Sacharomyces cerevisae*, dado que permite el estudio de diferentes fenotipos no presentes en levadura relacionados por ejemplo con la

pluricelularidad como son la quimiotaxis, agregación, morfogénesis o diferenciación. Dominios encontrados en familias de proteínas como son los receptores de GABA, implicados en señalización como PBK o β-catenina o en citoesqueleto como espectrina y el complejo motor de microtúbulos son sólo unos pocos ejemplos de homologías entre *Dictyostelium discoideum* y humano no presentes en S.cerevisiae [46]. Otro ejemplo importante lo constituyen las proteínas STAT ("Signal Transducers and Activators of Transcription"), que son factores de transcripción que desempeñan papeles esenciales en rutas de transducción de señales reguladas por citoquinas y factores de crecimiento. El genoma de *S.cerevisiae* ha sido secuenciado en su totalidad y no se han encontrado proteínas homólogas a STAT, sin embargo en *Dictyostelium* estas proteínas desempeñan papeles fundamentales en su etapa de desarrollo multicelular [69]

1.3. Ciclo de vida unicelular

Dictyotelium es una ameba de vida libre que se divide por fisión binaria simple cada 8-10 horas. Como organismo unicelular presenta una serie de fenotipos que lo hacen muy útil como modelo, entre los que se cuentan fagocitosis, macropinocitosis o quimiotaxis.

Dictyostelium se alimenta por fagocitosis de las bacterias que encuentra en el suelo como las de los géneros Shigella o Klebsiella (siendo *Klebsiella aerogenes* la bateria utilizada para crecimento en laboratorio) aunque también se alimenta de levaduras. De hecho se comporta como un fagocito profesional que puede consumir hasta 300 bacterias por hora y constituye por tanto un factor esencial en la ecología microbiana del suelo así como un modelo válido en el estudio de la relación patógeno-huésped. El mecanismo de fagocitosis consiste en el reconocimiento de la bacteria por receptores de membrana [27] y el englobamiento con una doble membrana que conlleva una reorganización del citoesqueleto de actina, con la consecuente formación del fagosoma. Finalmente el fagosoma se fusiona con el lisosoma donde el material es digerido [27].

Por otro lado, y debido a su facilidad de crecimiento y tratamiento en laboratorio se aislaron determinadas cepas que eran capaces de crecer, no solo alimentándose de bacterias por fagocitosis, sino también en medio líquido por pinocitosis (cepas axénicas). Se pueden formar dos tipos de estructuras: los pinosomas, pequeños (0.1-0.2 μm), que se envuelven de una cubierta de clatrina, o macropinosomas, más grandes (1.6 μm), siendo esta última estructura la que principalmente ultiliza para alimentarse. [27, 58]

La quimiotaxis, el proceso por el cual la ameba realiza movimientos direccionales en respuesta a un agente químico, se produce gracias a la rápida reorganización del citoesqueleto. Hasta ahora se conocen dos agentes quimiotácticos en *Dictyostelium discoideum*: el folato secretado por las bacterias y que le sirve para "medir" la cantidad de alimento y capturar las bacterias [112] y el adenosin monofosfato cíclico (AMPc) que se produce al inicio del proceso de agregación de manera cíclica para permitir su agregación y la entrada en la fase de desarrollo [148], como se explicará más adelante.

1.4. Ciclo de vida pluricelular

Como se ha mencionado anteriormente *Dictyostelium* es capaz de formar un organismo pluricelular en condiciones de ayuno. Esta estructura final denominada cuerpo fructífero le permite sobrevivir esparciendo formas altamente resistentes, las esporas. El proceso total, que se produce de manera secuencial a través de diversas estructuras, es relativamente complejo e incluye agregación, morfogénesis, fototaxis o termotaxis en caso de formación del "slug" y finalmente la culminación y maduración de esporas.

1.4.1. Agregación

Antes de que se produzca la falta de alimento las células de *Dictyostelium* se preparan para esa situación. Continuamente se secreta al medio extracelular una proteína de 68 KDa llamada PSF ("Prestarvation Factor"). La expresión de esta proteína se encuentra inhibida en caso de haber suficiente alimento (bacterias), de modo que *Dictyostelium* utiliza el PSF como sonda para testar la relación entre el número de células y el de bacterias [32]. Uno de los efectos del PSF es la inducción de discoidinas, lectinas implicadas en procesos de adhesión celular necesarios para el correcto proceso de polarización y movimiento celular.

Más tarde se libera al medio otra proteína, CMF ("Conditionated Medium Factor") que se ha visto fundamental para la posterior liberación de AMPc. CMF funciona controlando la densidad celular durante el crecimiento, antes de la agregación. Esto es muy importante dado que la futura forma de resistencia debe tener un número determinado, ni muy alto ni muy bajo, de células. Ambos factores, ayuno y densidad celular, son factores imprescindibles para la agregación [31].

Es ahora cuando entra en juego el AMPc. Los receptores de AMPc (cAR) del tipo 7TM ("Seven-transmembrane protein") y ACA ("Adenylyl cyclase") que se encarga de transformar AMP (Adenosin Monofosfato) en AMPc, son altamente expresados en la membrana. Dentro de los 4 receptores conocidos cAR solo dos de ellos (1 y 3) son altamente afines por AMPc y solo cAR1 se ha visto esencial para la agregación. La molécula de AMPc al ser reconocida por el receptor desencadena una cascada de transducción de la señal que se inicia con la disociación de la proteína G heterotrimérica en $G_{\alpha 2}$ y $\beta\gamma$. La subunidad $\beta\gamma$ activa de manera indirecta el enzima ACA que se encuentra anclado en la membrana plasmática. Esto produce un aumento de AMPc que, por un lado sale al exterior actuando como agente quimiotáctico y otra parte se queda en citosol donde, a través de la activación de PKA (Protein quinasa A dependiente de AMPc) , producirá cambios en la expresión génica de genes necesarios. Por otro lado la subunidad $G_{\alpha 2}$ activa la proteína AKT/PKB dando lugar a cambios en el citoesqueleto necesarios para la agregación [47].

Los cambios en citoesqueleto vienen determinados principalmente por las proteínas PI3K ("Phosphatidylinositol-3-Kinase") y PTEN ("Phosphatase and tensin homolog") [101]. Cuando la molécula de AMPc se une y activa el receptor cAR1 se produce el reclutamiento de la proteína PI3K a la membrana en la parte anterior de la célula. Debido a la fosforilación de PIP2

(“Phosphatidylinositol 4,5-bisphosphate”) por PI3K, se produce la acumulación de PIP3 (“Phosphatidylinositol (3,4,5)-triphosphate”). Sin embargo en la parte posterior de la célula predomina la presencia en membrana de la proteína PTEN, que cataliza la desfosforilación de PIP3 para dar lugar a PIP2, antagonizando la función de PI3K. De este modo se produce un gradiente antero-posterior con la presencia de las proteínas PI3K y PTEN junto con los fosfolípidos PIP3 y PIP2 respectivamente. La presencia de PIP3 en la parte anterior promueve el reclutamiento de proteínas con dominios PH (Homología con Pleckstrina) como CRAC o AKT/PKB. Esto producirá a su vez la polimerización de actina en la parte delantera e inhibición de polimerización de miosina II. Por otro lado en la parte posterior ocurre el hecho contrario. En su conjunto estos cambios en citoesqueleto permiten a la célula el movimiento quimiotáctico direccional.

Es muy importante que la producción de AMPc se produzca de manera controlada y pulsátil para que las células puedan decidir en cortos períodos de tiempo qué orientación tomar. Para ello el AMPc extracelular será degradado por el enzima PDE (Fosfodiesterasa extracelular) que a su vez se encuentra regulado por el inhibidor PDI (Inhibidor de Fosfodiesterasa). De este modo la cantidad disponible para el receptor cAR1 disminuye, lo que produce una disminución en la producción de AMPc por ACA. Estos ciclos pulsátiles se producen cada 6 min durante horas. De este modo las células quedan polarizadas unas detrás de otras, moviéndose hacia un centro de agregación formando hileras denominadas “streams” (**Fig. 2**).

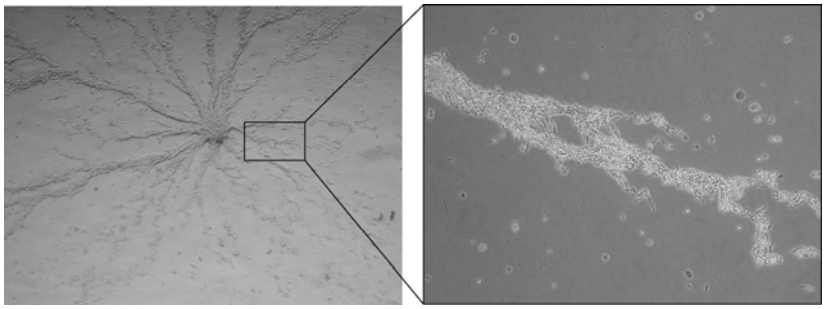

Fig.2. Polarización de células de *D. discoideum* y formación de “streams”. Como puede en el panel izquierdo un gran número de células se polarizan, se mueven por quimiotaxis y forman torrenteras de células o “streams” gracias a la señalización por AMPc y se mueven hacia el centro de agregación, donde, si las condiciones son buenas, se producirá la formación, tras 24 horas, del cuerpo fructífero. El panel de la derecha muestra en detalle la polarización que produce un alargamiento característico en la célula.

1.4.2. Morfogénesis

Tras la formación de los "streams" el centro de agregación se enriquece en células dando lugar al cabo de 10h a una estructura denominada "loose mound" que 2 horas después da lugar a otra llamada "tight mound" (**Fig. 3**). Estas estructuras se mantienen gracias a la interacción de moléculas de adhesión célula-célula y a una matriz extracelular compuesta de polisacáridos y celulosa (una de las características que lo asemejan al reino de las plantas). Es en esta fase temprana de desarrollo cuando se va a producir el inicio de la diferenciación de ciertas células que, posteriormente, darán lugar a las células tallo y esporas, conocidas respectivamente como células pretallo y células preespora. El factor GBF (G-box binding factor) se ha visto muy importante como regulador transcripcional de un gran número de genes necesarios para la diferenciación inicial de estos dos grupos celulares así como de genes necesarios para la adhesión celular [129]. En este momento y gracias a movimientos diferenciales las células pretallo se sitúan en la parte anterior mientras que las células preespora se sitúan en la parte posterior. La parte anterior produce un apéndice abultado denominado "tip" que se va a convertir en un verdadero centro de control del desarrollo. En este momento la estructura, denominada "finger" puede seguir dos caminos totalmente diferentes: Si el pH del medio se encuentra tamponado (pH = 6-7) o bien existe una fuente de luz zenital, esta estructura continúa hasta dar lugar al cuerpo fructífero tras un tiempo total de desarrollo de 24 horas. Sin embargo, si el pH del medio no se encuentra tamponado o bien la luz incide de manera lateral, la estructura cae sobre el substrato, formando una babosa denominada "slug" o gusano, que es capaz de moverse sobre el substrato mediante el movimiento coordinado de todas sus células hasta que las condiciones imperantes sean mejores.

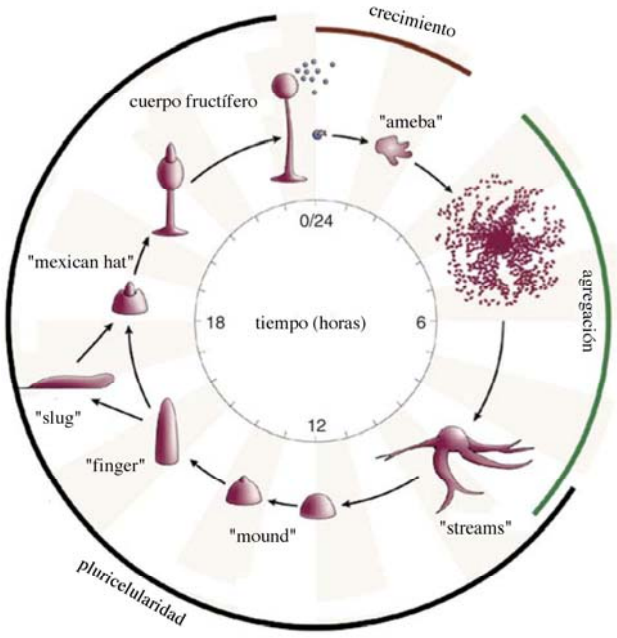

Fig. 3. Ciclo de vida de *Dictyostelium discoideum*. Combina tanto una fase unicelular (ameba) como una pluricelular. En condiciones de ayuno las células se polarizan y generan "streams" donde las células se dirigen a un centro de agregación. Al cabo de 10 horas se forma el "loose mound", a las 12 el "tight mound" (indicadas como fase "mound") y a las 15 h el "finger". Posteriormente si las condiciones no son las adecuadas se forma la estructura "slug" que migra hacia otra región donde las condiciones sean mejores. Si son las adecuadas continúa hacia la fase "mexican hat" (19 horas) y finalmente se produce el cuerpo fructífero o estructura culminante (24 horas) que esparce esporas que más tarde podrán germinar para continuar el ciclo [36].

1.4.3. “Slug”

La forma “ slug” del desarrollo, como se ha comentado anteriormente, se forma bajo ciertas condiciones. Esta estructura es capaz de moverse mediante fototaxis o termotaxis. En el primer caso se ha descrito que responde a longitudes de onda en el espectro visible de 425nm a 550nm acercándose a la fuente, mientras que en el caso de ser luz del espectro UV, se aleja [53, 117]. En el caso de termotaxis, el “slug” responde a temperaturas ligeramente superiores al crecimiento en laboratorio (22ºC) entre 25ºC y 30ºC con gradientes tan pequeños como 0.009ºC/m [19, 118].

Tanto en esta forma “slug” como en la forma finger se distinguen diferentes tipos celulares en función de las proteínas que expresan (**Fig. 4**). La parte anterior ocupa un 20 % del “slug” y se compone de células “prestalk” o pretallo. Dentro de este grupo y en función de si expresan o no las proteínas de matriz extracelular EcmA y/o EcmB se distinguen las células pstA, pstAB o pst0. Por otro lado las células “anterior like-cells” o “células como las anteriores”, es una pequeña proporción de células que se distribuyen a lo largo del resto del “slug” entre las células preespora.

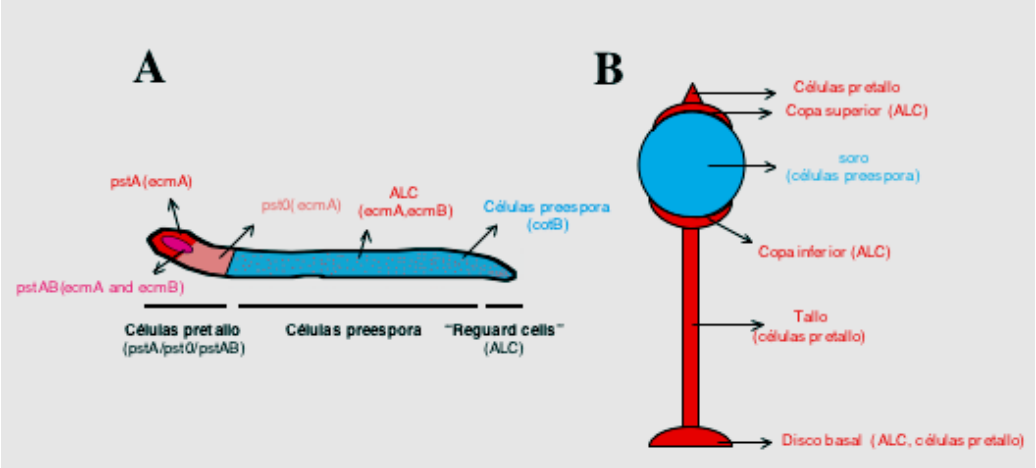

Fig. 4. Tipos celulares en el “slug” y su destino final en el cuerpo fructífero. La figura **A** muestra las diferentes células que forman parte del “slug” y la figura **B** muestra una estructura culminante o cuerpo fructífero, donde los colores corresponden al tipo celular implicado en la formación de los diferentes componentes y se corresponden a su vez con los tipos celulares del slug. Las células pretallo (pst) darán lugar al tallo; las células ALC o “anterior like cells” junto con las células pretallo darán lugar al disco basal que une la estructura con el sustrato y a las “copas” por encima y por debajo del soro; las células preespora dan lugar a las esporas contenidas en el soro [47].

1.4.4. Culminación

La culminación es el proceso por el que, mediante la migración de células y su diferenciación terminal, se construye la estructura final denominada cuerpo fructífero (**Fig 4**). Durante este proceso las células “prestalk” bajan desde la parte superior o “tip” dirigiéndose al sustrato. Finalmente y tras la diferenciación final darán lugar a las células que forman el tubo del tallo. Estas células se encuentran altamente vacuolizadas y terminan muriendo por muerte celular autofágica (ver más adelante). A su vez, este movimiento descendente de las células tallo empuja a las células preespora que se encuentran en la parte inferior elevándose sobre el sustrato. Por su parte las células “anterior-like cell” darán lugar a la cubierta superior sobre el soro o “upper cup”, a

la cubierta inferior o " lower cup" y finalmente al disco basal que fija la estructura al sustrato. La diferenciación final de las células tallo o espora se produce por factores secretados por un tipo celular y reconocidos por receptores en el otro. Así por ejemplo las células pretallo necesitan del factor DIF ("Differentiation Inducing Factor"), una alquil fenona, producida por las células preespora [71, 72]. Por otro lado, los péptidos SDF-1 y SDF-2 ("Spore Differentiation Factors") son requeridos para el encapsulamiento de las esporas. Un dato interesante es que la proporción entre células tallo y espora es de 20% y 80% respectivamente y se mantiene siempre constante. La diferenciación final de esporas requiere, por su parte, de la secreción de una matriz extracelular formada por una capa de celulosa recubierta por dos de proteína. Para que estas estructuras sean realmente resistentes a calor, PH extremos u otras situaciones de estrés, es necesario un período de maduración de al menos una semana [154].

2. *Dictyostelium* como modelo de enfermedades humanas

D. discoideum ha sido utilizado como modelo de un gran numero de enfermedades humanas y su interés sigue creciendo. Esto es debido a que posee una serie de características que lo hacen especialmente interesante. Entre estas características destaca que su genoma se encuentra totalmente secuenciado y de este modo se conocen un gran número de proteínas ortólogas en humano [46]. Por supuesto es de gran ayuda el hecho de que es un organismo haploide y por tanto la generación de mutaciones se traduce rápidamente en fenotipos observables.

La presión selectiva ejercida por Dictyostelium y otras amebas sobre las bacterias de su entorno se cree que ha modelado durante la evolución los complejos mecanismos de virulencia que permite a las bacterias patógenas evadir el sistema inmune como es el caso por ejemplo de los patógenos intracelulares. Por otro lado el huésped ha evolucionado diseñando mecanismos de resistencia a los patógenos que implican moléculas que se han mantenido en la evolución. En esta línea y también debido a su facilidad de crecimiento y a la posibilidad de evaluar diversos fenotipos, *Dictyostelium discoideum* ha sido utilizado ampliamente como modelo para infectividad por *Pseudomonas aeruginosa* [28, 88] , *Legionella pneumophila*, *Mycobacterium avium*, *Mycobacterium tuberculosis*, *Salmonella typhimurium*, *Klebsiella pneumoniae*, *Yersinia pseudotuberculosis*, *Vibrio cholerae* y *Neisseria meningitidis* [136]. Dictyostelium no sólo es capaz de fagocitar bacterias en su forma ameba sino que incluso en su estado pluricelular de "slug" existen todavía una serie de células centinela que son capaces de fagocitar bacterias y eliminar toxinas[34].
Otra característica típica, la motilidad celular, que le permite agregarse y también dar forma al organismo pluricelular, ha sido aprovechada para el estudio de enfermedades de motilidad celular que afectan al sistema inmune y neurológico como la Lisencefalia, donde se han descrito dos proteínas importantes LIS1 y DCX [104]. También ha sido utilizado como modelo en farmacogenómica. Por ejemplo se ha descrito el papel que determinados lípidos como esfingosina y ceramida juegan en la resistencia al tratamiento en cáncer por cisplatino [6]. Otro ejemplo es el

avance llevado a cabo para entender las bases moleculares implicadas en el uso de ácido valproico o de litio para el tratamiento de transtorno bipolar[94]. Las bases moleculares de enfermedades como el síndrome de Chediak-Higashi o Nieman Pick, relacionadas con la exocitosis y endocitosis de células, han sido establecidas también en este organismo modelo [96]. Por último *Dictyostelium*, como se explica en el siguiente apartado, se utiliza como modelo de enfermedad mitocondrial.

3. Biología mitocondrial en *Dictyostelium*

3.1. Introducción

La mitocondria es el orgánulo celular donde se llevan a cabo múltiples procesos metabólicos como la β-oxidación, el ciclo de Krebs, la fosforilación oxidativa y otros muchos más. Como en humanos y otras especies, las mitocondrias de *Dictyostelium* poseen una doble membrana externa e interna, separadas por un espacio intermembrana. La membrana interna se invagina dentro de la matriz dando lugar a las crestas mitocondriales donde se produce mayoritariamente la respiración o fosforilación oxidativa.

Existen un gran número de enfermedades asociadas a mutaciones que afectan a proteínas mitocondriales. Han sido descritos numerosos síndromes, todos ellos causados por mutaciones tanto en genes mitocondriales como en genes nucleares, que codifican proteínas mitocondriales. Estas enfermedades son complejas y están a menudo asociadas a una variedad de síntomas patológicos que pueden incluir ceguera, sordera, epilepsia, ataxia, disfunción cardiaca y muscular entre otros. En muchos casos la etiología de le enfermedad es completamente desconocida por lo que se hace necesario ir a los mecanismos moleculares que causan dichas enfermedades. Para ello resulta de gran utilidad la utilización de organismos modelo que permitan, como en *Dictyostelium discoideum*, la posibilidad de generar mutantes y de estudiar con relativa facilidad un gran número de fenotipos (macropinocitosis, fagocitosis, señalización extracelular, motilidad, fototaxis, termotaxis, diferenciación, morfogénesis entre otros). Además, el genoma mitocondrial de *Dictyostelium* se encuentra totalmente secuenciado y el mecanismo de transcripción y procesamiento del RNA está estudiado al detalle [14]. El análisis de la disfunción mitocondrial en *Dictyostelium* puede aportar un mejor conocimiento de las complejas relaciones entre fenotipo y genotipo a nivel celular, sin la gran complejidad asociada con los sistemas de mamíferos.

3.2. Genoma mitocondrial.

Dictyostelium discoideum contiene 200 copias por célula de un mtDNA (“mitochondrial DNA”) covalentemente cerrado. Su tamaño es de 55564 pb frente a las 16569 pb en humano [85] y, como este último, se encuentra totalmente secuenciado [109]. El genoma se encuentra altamente empaquetado existiendo incluso solapamiento entre genes pero por otro lado existen regiones intergénicas de hasta más de 2 Kb. El código genético utilizado es el universal. Se ha descrito que codifica 33 proteínas, 6 ORFs, 2 rRNA y 18tRNA que en su conjunto son utilizados para diferentes

procesos como son respiración, traducción o maduración de RNA. Los ORFs no se encuentran en otros organismos lo que hace pensar que no desempeñan un papel universal. [135, 153].

La transcripción del mtDNA se produce en un sentido desde un único sitio de inicio de la trasncripción situado en una región no codificante "upstream" respecto al gen *rnl* (que codifica para rRNA de la subunidad grande ribosomal) [84] **(Fig. 5)**. Este RNA primario es rápidamente procesado para dar lugar a 8 mensajeros secundarios que serán posteriormente procesados para dar lugar a mensajeros terciarios mono, di o tricistrónicos [13]. Las señales de procesamiento son generalmente las secuencias de tRNA presentes entre estos genes.

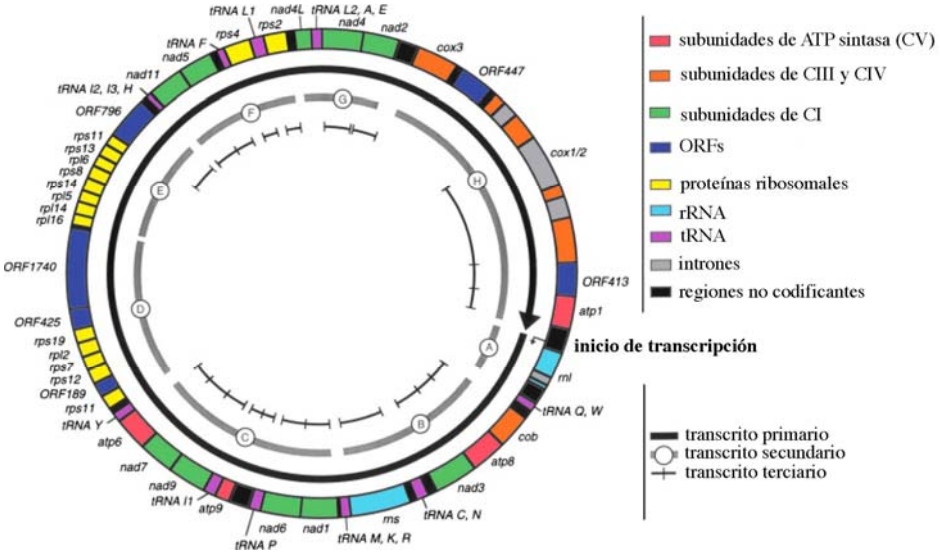

Fig. 5. Genoma mitocondrial en *Dictyostelium*. Organización de los genes, transcripción y procesamiento. Se indica el sitio de inicio de la transcripción junto al gen *rnl*. Como puede verse, el transcrito primario se procesa para dar 8 transcritos secundarios que a su vez darán lugar a transcritos terciarios mono, di o tri-cistrónicos [84].

3.3. Importación de proteínas

Como se ha dicho anteriormente, la mayor parte de las proteínas mitocondriales son codificadas en el núcleo aunque existen algunos genes como *nad7, nad9, nad11 y atp1* que son mitocondriales en *Dictyostelium* pero sin embargo son codificados en el núcleo en mamíferos . Estas proteínas mitocondriales codificadas en el núcleo no sólo incluyen la maquinaria metabólica sino también el resto de las 70 subunidades de los complejos de la cadena respiratoria, como también las proteínas necesarias para replicación o transcripción. Un simple error en esta maquinaria de importe puede conducir a un defecto del OXPHOS ("Oxidative Phosphorylation System") acompañado de un defecto en el contenido de ATP celular como ocurre en el Síndrome de distonia y sordera humano [77]. Por otro lado un defecto indirecto en OXPHOS también afecta a la maquinaria de transporte debido a que un correcto potencial transmembrana mitocondrial ($\Delta\Psi m$) en la membrana interna es un requisito necesario, junto con otros factores como la chaperona Hsp70 o el factor MSF (Factor de estimulación del importe mitocondrial) [11, 63]. Por supuesto esta

maquinaria está altamente controlada, diferenciando qué proteínas están destinadas a la matriz, membrana mitocondrial interna, externa o espacio intermembrana [18].

El conocimiento de las proteínas implicadas proviene sobre todo de los organismos modelo *S.cerevisiae* y *N.crassa*. Sin embargo se ha observado que la maquinaria básica se mantiene conservada en la evolución entre diferentes especies. El transporte a través de la membrana externa se regula por el complejo TOM ("Translocase of the Outer Mitochondrial membrane") que reconoce la proteína y la transloca. Tres subunidades "core" de TOM (TOM40, TOM7, TOM22) se encuentran altamente conservados en la evolución y también en *Dictyostelium* [95]. La translocación a través de membrana interna mediado por TIM ("Translocase of the Inner Mitochondrial membrane") se produce por TIM23 en el caso de proteínas destinadas a matriz o por TIM22 en el caso de proteínas de membrana [56].

Sorprendentemente, y al igual que se ha visto en levadura, la translocación de proteínas mitocondriales en *Dictyostelium* se puede producir en ciertos casos de manera cotraduccional [4]. Para ello, secuencias en regiones UTR del mRNA son reconocidas por la mitocondria mientras éste se está leyendo por la maquinaria ribosomal en el citoplasma [5].

3.4. Morfología

A pesar de la visión clásica estática, lo cierto es que las mitocondrias se encuentran bajo continuos procesos de fusión-fisión . Estos ciclos de fusión-fisión controlan no sólo el tamaño sino también el número de mitocondrias [155, 156]. Además las mitocondrias no están "suspendidas" en el citosol sino más bien ancladas a proteínas motoras que las mueven a lo largo de "carreteras" que son los microtúbulos o microfilamentos de actina que constituyen el citoesqueleto. Mientras que en ciertas especies como *S.pombe* o humano se mueven a lo largo de microtúbulos en *S.cerevisae* o plantas lo hacen usando los microfilamentos de actina [60, 139, 147].

En *Dictyostelium* las mitocondrias se encuentran distribuidas por toda la célula donde aparecen con tres formas diferentes: esfera, varillas y túbulos. Las dos primeras son las predominantes y aunque es posible encontrarlas a la par en una misma célula, es mucho más corriente que todas las mitocondrias dentro de una única célula tengan la misma forma [55]. No se conoce si existe alguna diferencia funcional atribuible a estas diferencias morfológicas.

Por otro lado se han identificado en *Dictyostelium* diferentes proteínas homólogas a otras descritas previamente en organismos como *S.cerevisae* que están implicadas en la división y movimiento mitocondrial. Entre ellas se encuentran : CluA (andamio entre las mitocondrias y sus proteínas motoras asociadas) que se ha visto implicada además en la dinámica de membranas [50, 165], dinamina A (proteína GTPasa implicada en la organización del citoesqueleto) [157] o también FtsZ (proteína homóloga a la implicada en la fisión bacteriana) [55].

3.5. Mitocondria, autofagia y muerte celular

En muchos organismos, sobre todo pluricelulares, se ha visto que la mitocondria juega un papel muy importante en la muerte celular programada o apoptosis. Esto es debido al papel que juegan proteínas como las de la familia Bcl-2, citocromo c o AIF, todas ellas mitocondriales. En estos organismos la liberación de citocromo c tras una alteración en el ΔΨm produce una cascada de señales mediadas por caspasas o bien mediante mecanismos independientes de caspasas como es el caso de AIF ("Apoptosis Inducing Factor") que, en último término, producen la fragmentación nuclear, la formación de cuerpos apoptóticos y muerte celular [120].

En *Dictyostelium discoideum* no existen homólogos de caspasas y se ha comprobado que no existe apoptosis mediada por caspasas [81, 124]. Así mismo sí existe un homologo para AIF que guarda alta similitud con el factor AIF humano [10]. Como este último presenta dos secuencias de localización, una mitocondrial y la otra nuclear. Cuando se encuentra en mitocondria AIF juega un papel importante como factor de ensamblaje del complejo I [145]. Cuando se altera el ΔΨm el factor AIF escapa de mitocondria y se dirige al núcleo donde produce la degradación del genoma nuclear y muerte celular apoptótica. En *Dictyostelium* este tipo de muerte solo se consigue en laboratorio bajo ciertas condiciones donde se impide la agregación y desarrollo en condiciones de ayuno. Sin embargo, y de manera muy interesante, las células pretallo en ayuno y bajo condiciones normales de desarrollo padecen una muerte conocida como muerte celular autofágica o ACD ("Autophagic Dell Death") [22]. Para entender mejor la relación entre autofagia y muerte se hace necesario explicar bien las características de estos dos procesos y las diferencias que existen entre ellos.

La autofagia es , en esencia, un mecanismo de supervivencia celular utilizado en todos los organismos eucariotas [30, 102, 103]. En condiciones de crecimiento normal las células necesitan regenerar ciertos orgánulos que por diferentes razones pueden presentar defectos y ya no son útiles. Diferentes orgánulos como mitocondrias, retículo endoplásmico, peroxisomas o aparato de Golgi son continuamente degradados por autofagia para generar orgánulos nuevos más funcionales. Por otro lado, en condiciones de ayuno, las células necesitan responder de manera inmediata a la falta de alimento. Para ello activan rutas catabólicas (como la autofagia) e inhiben rutas anabólicas con un objetivo final: la obtención de energía en forma de ATP. La AMPK ("AMP-dependent Kinase"), un sensor energético esencial en la célula, como se verá mas adelante, ha sido implicado directamente en la activación de autofagia [44, 45, 116, 149]. Así mismo la autofagia se activa también en procesos como la eliminación de agregados proteicos o para luchar contra bacterias intracelulares lo que la relaciona con procesos patológicos, así como con envejecimiento [86]. El mecanismo autofágico implica la formación de pequeñas estructuras de doble membrana llamadas autofagosomas que envuelven el cargo (que pueden ser orgánulos o partes del citosol). Posteriormente estos autofagosomas se fusionan a los lisosomas dando lugar a autofagolisosomas. Durante el proceso el pH del interior de este orgánulo va disminuyendo. Finalmente se activan las enzimas lisosomales que degradarán las proteínas y lípidos que serán transportados de nuevo al

citoplasma y utilizados para su reciclaje y obtención de energía. El proceso y toda la maquinaria necesaria se encuentra altamente conservada en todos los organismos, incluido *Dictyostelium*, donde ha sido revisado extensamente por nuestro laboratorio [22] (Anexo).

La muerte celular autofágica (ACD) tiene lugar en las células tallo. Como se explicó anteriormente *Dictyostelium discoideum* desarrolla una estructura denominada cuerpo fructífero donde un soro que contiene las esporas es sostenido sobre un tallo que lo eleva sobre el sustrato. Las células del tallo en realidad terminan muriendo por ACD que se caracteriza por la condensación de la cromatina, vacuolización y secreción de una pared celular rígida de celulosa. Sin embargo, estas células muertas retienen la integridad y no son digeridas por las células vecinas como ocurre en apoptosis [33, 70, 87]. Se llama muerte autofágica porque requiere de la autofagia para activarse aunque no es el único estímulo necesario. Con la inducción de autofagia por ayuno y secreción de AMPc se completa un primer paso en esta vía de muerte [16, 161], que solo es completada tras la secreción del factor DIF-1 [22].

Por tanto, y a pesar de que no existe apoptosis mediada por caspasas, sí que existe apoptosis mediada por AIF (condiciones *in vitro*) y muerte celular autofágica (condiciones *in vivo* e *in vitro*). En ambos casos el papel de la mitocondria es esencial dado el papel que juegan AIF y la AMPK, la última activada por una disminución del ATP producido en mitocondria.

3.6. Patología mitocondrial

3.6.1. Enfermedades mitocondriales humanas y complejo I

Las enfermedades mitocondriales humanas son causadas en su mayoría por mutaciones en genes mitocondriales o nucleares que codifican proteínas de la maquinaria de traducción o el sistema OXPHOS. Presentan una serie de características generales. Por un lado el tipo de herencia es materna, en el caso de las mutaciones en genes mitocondriales, dado que en la formación del zigoto solo las mitocondrias del óvulo participan mientras que las del espermatozoide (que tiene muchas menos) se pierden [134]. Debido a que todas las células del organismo (salvo excepciones) tienen mitocondrias todas deberían quedar afectadas por la mutación. Sin embargo la variación en el número, la diferente proporción de mitocondrias dañadas (heteroplasmia), las diferentes necesidades energéticas de las células o las diferentes isoformas de proteínas nucleares que van a mitocondria hace que esto no sea así, siendo en parte la causa de la gran complejidad de estas enfermedades. Esto hace que diferentes mutaciones puedan causar el mismo síndrome, mientras que la misma mutación puede dar lugar a diferentes síndromes. Además, los síntomas clínicos sólo se manifiestan a veces cuando se alcanza una determinada proporción de mitocondrias mutantes o carga mutante (efecto umbral o “threshold effect”) y esto además es dependiente del tejido [125] .

Aproximadamente un 40% de las enfermedades mitocondriales del OXPHOS son directa o indirectamente causadas por defectos del complejo I. Este complejo que cataliza la transferencia de electrones desde el NADH a la ubiquinona produce también la transferencia de protones desde la

matriz al espacio intermembrana [78]. La estructura del complejo homólogo en bacteria ha sido determinada lo que ha supuesto un importante avance en el conocimiento del mecanismo que consigue acoplar la transferencia electrónica al transporte transmembrana de protones [43]. Debido al elevado número de subunidades que lo forman (45 en humano), requiere de un elevado número de factores de ensamblaje. Hasta ahora han sido descritos 9 factores de ensamblaje (NDUFAF1, NDUFAF2, NDUFAF3, NDUFAF4, C8orf38, C20orf7 ,ACAD9, IndI y FOXRED1) [54, 62, 110, 111, 127, 137, 150, 57, 108, 130, 48, 25] que, junto con las 14 subunidades estructurales esenciales o "core" presentan mutaciones en pacientes. Existen además otros 2 factores de ensamblaje sin mutaciones patológicas descritas (Ecsit, AIF) [145, 151, 100] aunque se piensa que deben existir muchos más por el gran tamaño del complejo. Aunque existen un gran número de síndromes asociados a mutaciones, todos ellos cursan siempre con neurodegeneración o degeneración neuromuscular. Por otro lado, defectos en el complejo I han sido asociados también a enfermedades neurodegenerativas como Parkinson o Alzheimer [67, 83, 131].

3.6.2. Métodos para generar la disfunción mitocondrial en *Dictyostelium discoideum*

A parte de los métodos químicos como en el caso del BrEt (Bromuro de etidio) utilizado en la generación de células ρ^0 sin mtDNA, se han utilizado otros de tipo genético. Por un lado la disrupción heteroplásmica, que se utiliza para suprimir la expresión de genes mitocondriales, se ha aplicado para los genes *rnl*, *rps4* y otros [66, 158]. En cuanto a la alteración de genes nucleares depende de si el gen es esencial, en cuyo caso se utilizan métodos de interferencia del RNA o si el gen es no esencial en cuyo caso se puede proceder a la deleción o disrupción del gen. El primer caso ha sido aplicado para el gen nuclear que codifica Cpn60 ("Chaperonin 60") de matriz mitocondrial [79, 17]. Esta proteína está implicada en el correcto plegamiento de proteínas dirigidas precisamente a la matriz y cuya alteración en humano produce neurodegeneración, retraso del desarrollo y depleción de enzimas mitocondriales [3, 20, 64]. La interferencia de RNA también ha sido usada en *Dictyostelium* para la regulación negativa de la expresión de genes del CII y para la chaperona Hsp90. Mediante diferentes técnicas se puede saber el número de copias de la construcción de RNAi introducido y se puede correlacionar con la intensidad del efecto generado (dosis génica). Por último es posible realizar el KO ("Knock out") de genes nucleares no esenciales como se ha hecho con *cluA*[165], *torA*[146], *fszA y fszB* [55], *aoxA*[75] o *midA*[142]. Estas construcciones llevan un casete de resistencia (generalmente blasticidina) que les hace resistentes a este antibiótico y que , gracias a la interrupción del gen mediante recombinación homóloga, produce un cambio en el patrón de lectura que da lugar a la interrupción del RNA mensajero.

3.6.3. Fenotipos defectuosos en mutantes del OXPHOS

Como se ha comentado anteriormente la presencia en *Dictyostelium* de un gran número de características fenotípicas lo hace único para el estudio de enfermedades. En particular en el caso de las mutaciones mitocondriales, que no parecen afectar por igual a todos los fenotipos, lo que equivale a lo que ocurre en mamíferos. De este modo fenotipos como fototaxis, termotaxis o morfogénesis son más sensibles que otros a las disfunciones mitocondriales.

Tradicionalmente se ha pensado que células mutantes en OXPHOS deberían presentar un defecto importante en la producción de ATP y que es precisamente este defecto en ATP el responsable de la patología asociada. Sin embargo recientes estudios llevados a cabo en *Dictyostelium discoideum* indican que la patología mitocondrial es producida por defectos en rutas de señalización que son reguladas de manera errónea como se comentará más adelante en el apartado dedicado a AMPK.

En primer lugar tanto la fototaxis como la termotaxis en *Dictyostelium* se encuentran afectadas en todos los defectos del OXPHOS, ya sean farmacológicos o genéticos. Las rutas que regulan estos dos procesos, aunque no conocidas por completo, convergen temprano con lo que un gran número de proteínas son compartidas, entre ellas proteínas G heterotriméricas, segundos mensajeros como cAMP, cGMP, IP3 o Ca^{2+}, proteínas señalizadoras como RasD o GefE, GelL, proteínas quinasas como PKB o ErKB y otras muchas. Se ha observado que estas proteínas señalizadoras se asocian a través de una proteína andamio, la filamina, formando el complejo de señalización fotosensorial [9, 12].

El segundo fenotipo afectado que es común a todos los defectos del OXPHOS en *Dictyostelium* es el crecimiento tanto en líquido (crecimiento axénico) como en asociación con bacterias [17, 79, 158]. De manera muy interesante se observó que este defecto no se encontraba asociado a defectos en la macropinocitosis o fagocitosis [17], a excepción del mutante *midA*$^-$ que sí presentaba estos dos defectos asociados [142]. A excepción de este último se observó que la causa era más bien un defecto en la regulación del ciclo celular o de crecimiento. Diferentes proteínas han sido implicadas entre las que se cuentan 6 ciclinas, 6 proteínas quinasas dependientes de ciclina y el homólogo en *Dictyostelium* (*rblA*) del gen supresor de tumores en retinoblastoma.

El tercer fenotipo común a este tipo de defectos mitocondriales es la diferenciación a células tallo y esporas. Se ha observado un aumento de células que se diferencian a tallo cuya consecuencia es la formación de tallos aberrantes. Esto ocurre tanto en el tratamiento con BrEt [35] como por métodos genéticos [17, 79]. Como se comentó anteriormente las células tallo terminan muriendo por muerte celular autofágica. Parece ser que la disfunción mitocondrial podría conducir a un aumento del flujo autofágico y finalmente conducir a muerte, pero esta hipótesis no ha sido todavía confirmada.

3.6.4. El culpable de todo: ¿AMPK?

La quinasa dependiente de AMP o AMPK es un sensor energético celular además de ser regulador de la homeostasis energética [59]. Esta serin-treonin quinasa heterotrimérica está compuesta por una subunidad catalítica α, una subunidad reguladora γ y una subunidad β que sirve de andamio para las dos anteriores. En mamíferos tres genes codifican diferentes isoformas α, mientras que dos genes codifican para distintas subunidades β y γ. En *Dictyostelium* sólo existe un gen para cada subunidad. La AMPK responde a la relación AMP/ATP. Cuando esta relación es alta como consecuencia, por ejemplo, de un defecto mitocondrial, la AMPK se activa. El AMP se une a la subunidad γ, produciendo un cambio conformacional que libera de su inhibición a la subunidad α que queda ahora susceptible de ser fosforilada en un residuo treonina por quinasas upstream como CaMMKα y β [65] , TAK1 [106] o LKB1 [159], siendo esta última la más importante. A su vez este cambio conformacional hace que la subunidad α no sea accesible a proteínas fosfatasas. El ATP compite con el AMP por su sitio de unión, de modo que cuando el ATP aumenta como consecuencia de los cambios metabólicos llevados a cabo, entonces la AMPK queda inhibida.

La AMPK regula diferentes aspectos del metabolismo celular para restaurar los niveles de ATP: por un lado inhibe rutas anabólicas que agotan el ATP y por otro induce rutas catabólicas que tienen como fin la obtención de energía en forma de ATP. Como ejemplos de esto tenemos la inhibición de enzimas como acil-coA carboxilasa o 3-HMG-CoA implicados en síntesis de lípidos y colesterol, respectivamente, la inducción de la translocación de proteínas a membrana como por ejemplo del transportador GLUT4 [80] o también produciendo un aumento del factor transcripcional NRF-1 que en último término lleva al aumento de masa mitocondrial [15, 166]. Todos estos cambios consiguen restablecer la relación AMP/ATP.

Fue por primera vez Bokko et al. quien demostró molecularmente que los fenotipos asociados a la enfermedad mitocondrial se producían por la sobreexpresión crónica de la AMPK [17] en el modelo *Dictyostelium*. Dos experimentos fueron determinantes: por un lado la expresión de una forma constitutivamente activa de AMPK (AMPKαT) en células WT (“wild-type”) producía una fenocopia de todos los defectos mitocondriales (fototaxis, termotaxis, crecimiento y desarrollo) mientras que por otro lado la inhibición de AMPK en mutantes mitocondriales como el de Cpn60 (ver antes) usando una construcción antisentido de AMPK, conseguía paliar dichos defectos. Esto llevó a la propuesta de un modelo en el que a pesar de que la activación de AMPK consigue parcialmente restaurar los defectos mitocondriales a través de diferentes rutas, esta sobreactivación de manera crónica conduce a un estado patológico.

4. MidA

MidA (DDB_G0282615, Mitochondrial disfunction gene A) es una proteína de función desconocida y sin ningún dominio conocido que muestra una alta homología de secuencia con la proteína humana C2orf56 (NP_653337). A lo largo de la tesis el homólogo humano se denominará hMidA. Esta proteína se encuentra altamente conservada a lo largo de la evolución, no sólo entre metazoa y plantas, sino también en α-proteobacteria , los parientes más próximos de las mitocondrias. Con el objetivo de conocer algo sobre su función se generó previamente en el laboratorio una cepa deficiente en MidA mediante la disrupción del gen por recombinación homóloga [141]. Este mutante presentaba diferentes defectos fenotípicos, como la reducción en la velocidad de crecimiento en líquido o en asociación con bacterias y también una reducción en el tamaño celular, así como defectos en fagocitosis y macropinocitosis. También se encontró que las células *midA*$^-$ presentaban retraso en la agregación y desarrollo, con estructuras "slug" que permanecían durante un elevado periodo de tiempo sin culminar. Además, la viabilidad de las esporas estaba reducida. En estos estudios se determinó que la proteína estaba localizada en mitocondria y que junto con los defectos anteriores presentaban una importante caída del 30% en el contenido de ATP [142].

Esta caída en la cantidad de ATP, la localización mitocondrial, la ausencia de homólogos en especies que carecen de Complejo I funcional como *S.cerevisiae* o *S.pombe* y otros factores que se comentarán en detalle llevaron a nuestro grupo a un estudio más profundo de la función molecular y el papel biológico de esta proteína, lo que constituye la primera parte de la tesis.

5. C20orf7

C20orf7 ha sido descrito en humanos como un factor de ensamblaje del complejo I mitocondrial, pero nada se conoce acerca de la función o papel biológico que juega. La proteína fue localizada en mitocondria asociada, aunque no de manera integral, a la membrana mitocondrial interna [137]. Han sido descritas tres mutaciones que cursan con enfermedad mitocondrial en humanos. La primera , L229P , conduce a una enfermedad neonatal letal [137]. La segunda, L159F y tercera, G250V, producen síndrome de Leigh [54, 126]. Tanto en células provinientes de estos pacientes como en líneas celulares donde se interrumpió la expresión del gen *C20orf7* con shRNA, se observó que la actividad del complejo I bajaba respecto a los controles. Además, el ensamblaje del complejo I se encontraba gravemente afectado. Otros estudios consiguieron demostrar la ausencia tanto de la subunidad ND1 como la ausencia del intermedio asociado a membrana que contiene ND1 (aprox 400 KDa) y que interviene en la ruta de ensamblaje del complejo I. De este modo los autores llegaron a la conclusión de que el papel de C20orf7 podría ser como activador traduccional de ND1, estar implicado en la inserción de ND1 en la membrana o bien ayudar en el ensamblaje de ND1 previamente en el intermedio de membrana [100, 137]. Sin embargo todavía no se conocen los mecanismos moleculares por los que actúa. Su estudio en el organismo modelo

Dictyostelium discoideum se hace realmente importante dada la existencia de pacientes con mutaciones y más cuando la etiología de la enfermedad es desconocida. Este estudio constituye la segunda parte de la tesis.

OBJETIVOS

1. Caracterización de MidA

    1.1. Determinar si la disrupción del gen *midA* produce un defecto específico de complejo I mitocondrial en *Dictyostelium* y células humanas en cultivo.

    1.2. Aproximación a su posible función bioquímica.

    1.3. Búsqueda de interacciones proteína – proteína.

    1.4. Papel de AMPK y relación con autofagia.

2. Caracterización de C20orf7

    2.1. Determinar si la ausencia en *Dictyostelium* del gen *C20orf7* produce un defecto específico de complejo I mitocondrial como ocurre en humano.

    2.2. Caracterización de fenotipos defectuosos.

    2.3. Recreación de las mutaciones patogénicas L159F y L229P.

    2.4. Aproximación a su posible función bioquímica.

    2.5. Papel de AMPK y relación con autofagia.

3. Comparación de fenotipos en los mutantes nulos *midA*$^{-}$ y *C20orf7*$^{-}$

MATERIALES Y MÉTODOS

1. Crecimiento de las cepas, transformación y desarrollo

Células de *Dictyostelium* , tanto WT como de diferentes mutantes, se cultivaron en medio HL5 (Formedium) o en asociación con *Klebsiella aerogenes* en placas agar-SM [138]. Las transformaciones fueron llevadas a cabo por electroporación, como se describió previamente [113]. Para el desarrollo sincrónico, células en crecimiento axénico exponencial fueron lavadas por centrifugación para eliminar restos de medio HL5, resuspendidas en medio PDF (20mM KCl, 9mM K_2HPO4, 13mM KH_2PO_4, 1mM $CaCl_2$, 1mM $MgSO_4$; pH 6.4) y depositadas sobre filtros de nitrocelulosa [132].

2. Generación de las cepas antisentido de AMPK (AMPKas)

Para la "downregulación" del gen de la quinasa dependiente de AMP (AMPK) de *Dictyostelium*, una construcción antisensentido (pPROF362) fue transfectada sobre la cepa *midA*$^-$ como se describió previamente [17]. Posteriormente se seleccionaron clones que presentaban diferente número de copias de la construcción. Este trabajo se hizo en estrecha colaboración con el grupo del Profesor Paul Fisher (Melbourne, Australia).

3. Cultivo de células humanas y RNA de interferencia

Células HEK293T y HeLa se obtuvieron del depósito "American Type Culture Collection" (ATCC), (Manassas, VA), que posteriormente fueron cultivadas siguiendo las especificaciones. Dos construcciones shRNA ("short hairpin RNA") clonadas en el vector pGIPZ (V2HLS_31857 y V2HLS_31862; Open Biosystems) fueron usadas para hacer el "knockdown" estable del gen humano que codifica MidA (*C2orf56*). Para la transfección de tales construcciones se utilizó Lipofectamine 2000 (Invitrogen) según el protocolo del fabricante. Para la selección de líneas estables se utilizó el marcador de resistencia a puromicina. Por otro lado se utilizó la técnica de RT-PCR para evaluar la "downregulación" en la expresión de las cepas transformadas usando el termociclador 7900HT Fast Real Time PCR system (Applied Biosystems) . Con este objetivo se utilizaron dos sondas diferentes: una para detectar los niveles de mRNA que codifica hMidA (Hs00218600; Applied Biosystems) y otra como control endógeno dirigida contra el RNA ribosomal 18S (4308329; Applied Biosystems).

4. Localización mitocondrial

La localización mitocondrial en *Dictyostelium* de las proteínas MidA y C20orf7 (WT y mutantes) se llevó a cabo mediante el clonaje de estas dos proteínas en el vector PDV-cGFP- cTAP (GenBank: EF028672) donde se produce la fusión de la proteína GFP y del marcador TAP ("Tandem Affinity Purification") en C-terminal. El control de la expresión queda regulado por el promotor de actina-15. Estas construcciones con las proteínas WT o bien las proteínas mutantes (ver la sección mutagénesis dirigida) fueron transfectadas en las correspondientes cepas *midA*$^-$ y

C20orf7⁻ obteniendo, en el caso de las proteínas salvajes, las cepas complementadas o recuperadas. Para la colocalización por microscopía confocal con un marcador mitocondrial, $1x10^6$ células transfectadas creciendo exponencialmente en HL5 (Formedium) fueron incubadas durante 1 h a 22ºC con MitoTracker Red CMXRos (Molecular probes) a una concentración final 500nM. Después de lavar durante 1 hora con nuevo medio HL5, las células fueron depositadas sobre un cubre y fijadas con 3.7 % formaldehído en HL5 durante 15 min. Tras lavar con PBS 1X se llevo a cabo el montaje con Prolong (Molecular probes).

Para la localización mitocondrial de la proteína MidA humana el cDNA fue clonado en el vector pEGFP-N1 (GenBank: U55762) y transfectado transitoriamente en células HEK293T y HeLa. Para la visualización del núcleo se utilizo el marcador Hoechst 33342.

Las imágenes fueron tomadas con el microscopio confocal LeicaTCS SP5 usando un objetivo PL APO 63X/1.4- 0.6 y el software LAS-AF (Leica Application Suite).

5. Análisis espectrofotométrico de los complejos del OXPHOS

$5x10^7$ células creciendo en cultivo exponencial fueron centrifugadas y lavadas una vez con PBS 1X. El "pellet" se resuspendió en 2 ml de solución SETH (250mM sacarosa, 2mM EDTA, 10mM Tris-Hcl, 100 U/l heparin; pH 7.4) y se sonicó 3 veces durante 10s en baño de hielo con intervalos de descanso de 30s. Para eliminar las células resistentes a la sonicación se centrifugó el lisado, recuperando el sobrenadante que se utilizó como muestra para el análisis espectrofotométrico como se describió anteriormente [140].

6. BN-PAGE

El análisis de electroforesis nativa en gel o BN-PAGE ("Blue Native"- PAGE) se llevó a cabo de modo muy similar a como se describió previamente [21], pero con pequeñas diferencias. Brevemente $1 x10^7$ células se resuspendieron en "gel buffer" 3X (750mM ácido aminocaproico, 150mM Bis-Tris; pH 7) y se cuantificó la proteína por el método de Bradford. El detergente N-dodecyl-β-D-maltósido (Sigma) fue añadido en una relación de 20μg por cada μg de proteína y llevado a un volumen final de 40 μl con gel buffer 3X. Para la detección de complejo I se añadieron 40 μg por pocillo pero sólo 10 μg para la detección de MidA. Para el análisis por "western-blot" el gel se transfirió O/N a potencial constante (30V) y a temperatura de laboratorio a una membrana PVDF de 0.45μm (PALL life sciences). Posteriormente esta mebrana fue lavada (2% SDS, 62.5 mM Tris-HCl; pH 6.8) durante 90 min para eliminar los restos del colorante azul de Coomassie que pudiesen interferir con el reconocimiento del anticuerpo. Para estudiar el complejo I ensamblado se utilizó un cocktail de anticuerpos para detectar todos los complejos del OXPHOS (total OXPHOS Human WB Antibody cocktail; Mitosciences). Para estimar los tamaños de los complejos se utilizó un marcador de proteínas nativas (Native protein Standard; Invitrogen). El anticuerpo secundario anti-

mouse IgG-HRP se obtuvo de Santa Cruz Biotechnology. Para los experimentos de dimerización de MidA se corrió una segunda dimensión como ha sido descrito anteriormente [21]. En este caso se utilizaron los anticuerpos anti-GFP (Sigma) y anti-rabbit IgG-HRP (Santa Cruz).

7. Mutagénesis dirigida

Las mutaciones G170V y G172V en MidA se llevaron a cabo por PCR usando como molde el gen *midA* clonado en P-GEMTeasy (Promega), mientras que las mutaciones en la proteína C20orf7 G86V, L165F y L235P se obtuvieron por PCR sobre dicho gen clonado también en el mismo vector. Los oligonucleótidos utilizados se encuentran descritos en el apartado oligonucleótidos. La reacción de PCR fue digerida con enzima DpnI y transformada en la cepa DH5α de *E.coli* para la amplificación del plásmido. El DNA fue extraído por miniprep y, tras la confirmación de la mutación por secuenciación, fue clonado en el vector PdV-cGFP-cTAP. Las construcciones fueron entonces transfectadas en células *midA*$^-$ y *C20orf7*$^-$ respectivamente. El crecimiento en líquido (axénico) y en asociación con bacterias en placas de agar-SM fue testado. La localización mitocondrial de las proteínas mutadas fue analizada por microscopía confocal como se ha descrito en el apartado localización mitocondrial.

8. Pull-down

La fracción N-terminal de las proteínas NDUFS2 tanto de humano como de *Dictyostelium discoideum* fue amplificada por PCR y clonada en el plásmido PGEX (Pharmacia-Biotech) donde se fusionan a la proteína glutation S- transferasa (GST) para la sobreexpresión en *E.coli* y posterior purificación según las instrucciones del fabricante. La construcción NDUFS2 de *Dictyostelium* abarca los aminoácidos 8-176 mientras que el de humano abarca la región 38-234. La proteína GST sóla fue usada como control. Las proteínas fueron mantenidas en asociación con “beads” de glutation sepharosa 4B (Amersham Biosciences) hasta que fueron usadas para el pull-down. $5x10^6$ células de *Dictyostelium* o HEK293T expresando MidA fusionado a GFP se resuspendieron en 500 µl de buffer STE+T (10mM Tris-HCl pH 8, 1mM EDTA pH 8, 150mM NaCl, 5mM DTT, 1% Tritón X-100, 1X cocktail de inhibidor de proteasas). Esta suspensión se agitó durante 30 min a 4ºC. Después de una centrifugación para eliminar las células no lisadas, el sobrenadante se incubó 1 hora a 4ºC con 30µl de la suspensión de proteína unida a sepharosa que había sido obtenida previamente. Las “beads” se lavaron 3 veces con solución STE+T y finalmente se resuspendieron en 30 µl solución de carga de proteína. La muestra se dividió en dos geles de SDS- PAGE : uno fue teñido con Coomassie como control de la presencia de las proteínas expresadas en bacteria y el otro fue transferido a una membrana de PVDF para detección con el anticuerpo anti-GFP (Sigma) de las proteínas expresadas.

9. Cuantificación de mtDNA y mtRNA

Para la cuantificación de mtDNA, células de *Dictyostelium* se crecieron exponencialmente en HL5 . El DNA genómico de $6x10^6$ células se extrajo con 300 µl de Quick Extract DNA Extraction solution 1.0 (Epicentre). Una dilución 1:50 fue usada como molde en la reacción de PCR llevada a cabo en el termociclador 7900 HT Fast Real- Time PCR system usando Power Sybergreen PCR Master Mix 2 con los oligos a una concentración final de 300 nM en un volumen final de 10µl. Los resultados fueron adquiridos con el software SDS 2.3 (Applied Biosystems) y tratados con Excel (Microsoft). Estos oligos, que estaban dirigidos tanto a la detección de mtDNA (DDB_G0294054) como a un gen control nuclear (DDB_G0277273) son descritos en el apartado Oligonucleótidos.

Para la cuantificación de mtRNA previamente se extrajo el RNA total de $1X10^7$ células creciendo en HL5 con Tri-reagent (Sigma). Este RNA se ajustó a una concentración final de 2 µg/µl. La posible contaminación de DNA fue eliminada mediante la incubación con 10U DNasa (New England Biolabs) a 10 µg de RNA en un volumen final de 10 µl. Esta mezcla se incubó por 30 min a 37 ºC y posteriormente a 70 ºC 5 min para destruir la actividad DNasa. Este RNA fue entonces ajustado a 100 ng/µl con agua DEPC. 250 ng de esta solución (2.5 µl) se usaron como molde para la reacción de RT-PCR con "high capacity cDNA reverse transcription kit" (Applied Biosystems) en un volumen final de 20 µl. El cDNA fue usado como molde para la reacción de PCR posterior. La expresión de 8 genes representativos de los 8 transcritos policistrónicos secundarios descritos en *Dictyostelium discoideum* [84] se estudió en cada muestra y posteriormente fue normalizada frente a un gen nuclear (DDB_G0277273) y frente a los niveles en WT.

10. Fototaxis y termotaxis

Los ensayos cualitativos de fototaxis de los "slug" fueron llevados a cabo para las cepas WT y *midA*$^-$ como se describió previamente [40], transfiriendo una colonia de *Dictyostelium discoideum* crecida en asociación con *K.aerogenes* al centro de placas de agar-carbón (5% carbón activado, 1% agar). Los datos se obtuvieron tras una incubación de 48h a 21ºC con una fuente de luz lateral. Para los ensayos cuantitativos de fototaxis se aisló *Dictyostelium* creciendo en placas agar-SM, se lavó para eliminar las bacterias arrastradas y se suspendieron en salino a las diluciones apropiadas. Finalmente se inocularon 20 µl sobre un área de $1cm^2$ en el centro de cada placa de agar-carbono. Las densidades resultantes estaban entre $1.5x10^6$ a $3.7x10^7$ células/cm^2. La fototaxis fue de nuevo medida tras 48h a 21ºC con luz lateral.

Para la termotaxis de los "slug" se utilizaron las mismas células lavadas de antes y se plaquearon a $3x10^6$ células/cm^2. Una alíquota de 20 µl se plaqueó en $1cm^2$ en el centro de placas de agar (1%) y se incubó durante 72h en oscuridad en una barra de calor produciendo un gradiente en la superficie del agar de 0.2ºC/cm.

Los “trails” del “slug” fueron transferidos a discos de PVC, teñidos con azul de Coomassie y digitalizados. La orientación de la migración del “slug” fue analizada usando estadística direccional [52].

11. Fagocitosis y macropinocitosis

Las cepas WT, mutante *midA*$^-$ y la cepa complementada con MidA-GFP fueron crecidas en medio HL5 sin antibióticos hasta la fase exponencial antes de su uso en los experimentos de fagocitosis y macropinocitosis. La captación de bacterias por *Dictyostelium* fue determinada usando una cepa de *E.coli* expresando la proteína fluorescente DsRed [99] como se describió anteriormente [17]. Los ensayos de macropinocitosis se llevaron a cabo midiendo la captación de medio conteniendo un indicador fluorescente, fenilisotiocianato (FITC)- dextrano (Sigma, masa molecular media 70 KDa) como se describió previamente [17].

12. Construcción de una cepa deficiente en *C20orf7*

Los fragmentos N-terminal y C-terminal del gen *C20orf7* de *Dictyostelium* fueron generados por PCR usando DNA genómico extraído previamente de la cepa WT AX4 y posteriormente clonados a ambos lados del casete de resistencia a blasticidina (BSr) derivado del vector pUCBsrBam [1]. La inserción del BSr interrumpió el gen en el nucleòtido 206 (aminoácido 69) localizado 10 nucleótidos “upstream” del pequeño intrón que contiene el gen. Dado que el fragmento C-terminal empieza en el aminoácido 85 se produce, además de la inserción del BSr, una deleción de 16 aa.

Después de la transfección y selección posterior con blasticidina las células fueron cultivadas en placas SM para el aislamiento clonal y se analizó por PCR si tenían insertada la construcción en el gen diana.

Para verificar la ausencia del mRNA en el mutante, RNA total de células tanto WT como de *C20orf7*$^-$ fue extraído a 14 horas de desarrollo usando Tri-reagent (Sigma) y usado como molde en la reacción de RT-PCR con los oligos indicados en el apartado oligonucleótidos.

13. Medidas de contenido en ATP

5 x10^6 células WT o *C20orf7*$^-$ creciendo exponencialmente en medio HL5 fueron lavadas y resuspendidas en 1 ml de agua. 900 µl fueron entonces mezclados con 100 µl de ácido tricloroacético (TCA) diluido al 10% y agitados en vortex durante 10 min. Después de una centrifugación (10.000g, 5 min) para eliminar el material insoluble, se midió el ATP en el sobrenadante usando el ATP Determination Kit-time stable assay (Proteinkinase.de) con las instrucciones del fabricante. La luminiscencia se midió en el luminómetro GloMax96 (Promega).

14. Análisis por "western-blot" de flujo autofágico en medio con nutrientes

Células WT, *midA*$^-$ y *C20orf7*$^-$ fueron transfectadas con la proteína de fusión GFP- transketolasa (GFP-Tkt-1) introducida en el vector pTX-GFP (GenBank AF269237). Las células transfectadas creciendo en HL5 se lavaron y se resuspendieron en medio HL5 fresco a concentración final de $1x10^6$ células/ml. Estas suspensiones se plaquearon sobre placas multiwell de 6 pocillos. Diferentes cantidades de NH_4Cl (0 mM, 100mM, 250mM y 400mM) fueron añadidas. Tras 2 horas se volvió a añadir la misma cantidad dejando en total 4 horas de exposición a la droga. Se recogieron las células y se centrifugaron 9000 rpm durante 4 min, retirando completamente el sobrenadante y resuspendiendo el pellet en 50 μl de medio RIPA 1X (NP-40 1%, SDS 0.1%, deoxicolato sódico 0.5% w/v, 150mM NaCl, 2mM EDTA, 50mM Tris-HCl pH 8, 1X cocktail de inhibidores de proteasas). Tras 30 min en hielo se cuantificaron las muestras por el método de Bradford. Se cargaron por pocillo 3,5 μg de proteína en un gel SDS-PAGE del 12%, que fueron llevados a 25 μl con agua y buffer de proteínas 5X. Tras la transferencia a membrana de PVDF la proteína GFP-Tkt-1 fue detectada con el anticuerpo anti-GFP (Sigma).

15. Análisis por microscopía confocal del flujo autofágico en medio con nutrientes y estudio de los agregados poliubiquitinados

La construcción RFP-GFP-Atg8 fue generada usando el fragmento GFP-Atg8 amplificado por PCR sobre el vector pA15/GFP-Apg8 (depositado amablemente en el Dicty Stock Center por Grant Otto). Este fragmento fue clonado en fase sobre un sitio XhoI en el extremo C-terminal de la proteína RFP del vector pTX-RFPmars (depositado en el mismo almacén amablemente por Clement Nizak). La construcción fue entonces transfectada en células WT, *midA*$^-$, *C20orf7*$^-$ y *atg1*$^-$, usado este último como control negativo de autofagia.

Para la visualización *in vivo,* células en crecimiento exponencial en HL5 fueron lavadas y resuspendidas con medio HL5 fresco a una concentración final de $1x10^6$ células/ml y finalmente depositadas sobre placas P35 con IBITREAT (IBIDI). De modo similar a como se ha descrito en el apartado anterior, diferentes cantidades de NH_4Cl (0 mM, 100mM, 250mM) fueron añadidas a las diferentes placas. Tras 2 horas se añadió de nuevo la misma cantidad y finalmente tras 4 horas se visualizaron en el microscopio confocal LeicaTCS SP5 usando un objetivo PL APO 63X/1.4- 0.6 y el software LAS-AF (Leica Application Suite).

El análisis de los agregados poliubiquitinados se llevó a cabo según describimos previamente en el laboratorio [24] **(Anexo)**. Mientras que para la inmunocitoquímica se utilizaron las cepas WT, *midA*$^-$, *C20orf7*$^-$ todas ellas expresando la proteína RFP-GFP-Atg8, para la detección por "western-blot" con anticuerpo α-ubiquitina se utilizaron las cepas WT, *midA*$^-$ y *C20orf7*$^-$ sin transfectar.

16. Microscopía de transmisión electrónica

Células WT y *C20orf7*⁻ creciendo en HL5 fueron incubadas en placas Petri durante una noche para permitir su adhesión a la superficie y una vez eliminado el sobrenadante las células se fijaron rápidamente en glutaraldehído 1.25% según describimos previamente en el laboratorio [23] **(Anexo)**. Se utilizó un microscopio electrónico de transmisión JEOL 1010 operando a 80 kV.

17. Oligonucleótidos

Oligos usados en la verificación del KO de *C20orf7*:

1. AAC TTG AGA ATC CAA TAG TTG C
2. CAA ATA ATA ATT AAC CAA CCC AAG
3. TAG GAT CCA TGT TAA GAA CAA CAT TTA GAA AAG G
4. CCC AAT GTA ATG AGA AAT TAC TTA TAA TTA AAT C

ATG10_F. CGG GAT CCG CAT GTA ACA TCC AAA GAT TTT AG

ATG10_R. CGGGATCCCTATATTATTATTTTTTAATAAATCAAATGG

Oligos usados en la cuantificación de mtRNA y mtDNA en el mutante *midA*⁻:

DDB_G0294054_F. AAC AAT CAT GTG GCT TTA GTA CGT AAA

DDB_G0294054_R. TCG GCC CTG CAT TTC GT

DDB_G0277273_F. CCG TTG CCC TAA CTT ACT TCC A

DDB_G0277273_R. GCC GCC ATT GAT GAA ACT ATT C

DDB_G0294022_F. GAT GTT TAA AGT GGC GTA TGA GGA T

DDB_G0294022_R. TCT TGC ATT ACC AAA AGG ATC AAA

DDB_G0294048_F. CAG TAA AAA TTC CAA TAG CAC CAT TAC A

DDB_G0294048_R. ACT GAT CCT GCT GTT GGT GCT T

DDB_G0294026_F. GAT ATG TCG CGG CAT TTG G

DDB_G0294026_R. CTT CAT GAA CTC CTG CAA TTG TTT

DDB_G0294030_F. GTA GAT ATT GGA ATA GTA AGC GCA GAA G

DDB_G0294030_R. TCA TAT ACG ATC CCT GCT CCT CTT

DDB_G0269220_F. CGT GGT TAT GCC GGC AAT

DDB_G0269220_R. AGC TAC ATC TGG TGA TCC TAC CAT T

DDB_G0294070_F. GCA GGA GTA CAA GGA TTT AGT CAA GA

DDB_G0294070_R. TGC AAG CTC GAG CAA GAC TAT AA

DDB_G0294054_F. AAC AAT CAT GTG GCT TTA GTA CGT AAA

DDB_G0294054_R. TCG GCC CTG CAT TTC GT

DDB_G0294034_F. GCA CCT CGA TGT CGG CTT AA

DDB_G0294034_R. CAC CCC AAC CCT TGG AAA CT

Oligos usados para mutagénesis dirigida de la proteína MidA

G170V_F. CAA ATA GTT GAA ATG GTT CCA GGT AGA GGC ACA CTA ATG

G170V_R. CAT TAG TGT GCC TCT ACC TGG AAC CAT TTC AAC TAT TTG

G172V_F. CAA ATA GTT GAA ATG GTT CCA GTT AGA GGC ACA CTA ATG

G172V_R. CAT TAG TGT GCC TCT AAC TGG AAC CAT TTC AAC TAT TTG

Oligos usados para mutagénesis dirigida de la proteína C20orf7

G86V_F. GGT AAT GTT TTA GAT TTT GTT AGT AGA AAT GGA GC

G86V_R. GCT CCA TTT CTA CTA ACA AAA TCT AAA ACA TTA CC

L165F_F. GAT TTA ATT ATA AGT AAT TTC TCA TTA CAT TGG G

L165F_R. CCC AAT GTA ATG AGA AAT TAC TTA TAA TTA AAT C

L235P_F. GAT ATT GGT AAC ATT CCA TCA AAG AAT AGA TAC

L235P_R. GTA TCT ATT CTT TGA TGG AAT GTT ACC AAT ATC

RESULTADOS

MIDA

1.1. La proteína MidA tanto de *Dictyostelium* como de humano es necesaria para la actividad del complejo I

Las proteínas MidA de humano (hMidA) y *Dictyostelium* (MidA) son altamente homólogas. Nuestros estudios previos en *Dictyostelium* mostraron que MidA es una proteína mitocondrial implicada en bioenergética y la alta homología de secuencia entre diferentes especies sugería la posibilidad de una posible conservación con humanos, donde la función de esta proteína no había sido todavía abordada [142]. Quisimos testar esta hipótesis y aumentar nuestro conocimiento sobre la función de estas proteínas. Por tanto nuestro primer objetivo fue determinar la localización subcelular de hMidA en células humanas. Una construcción expresando la proteína humana fusionada a GFP fue transitoriamente transfectada en células humanas HELA y HEK293T que fueron entonces teñidas con el marcador mitocondrial Mitotracker Red **(Fig. 6)**. Como puede observarse hMidA se localizó también en mitocondria.

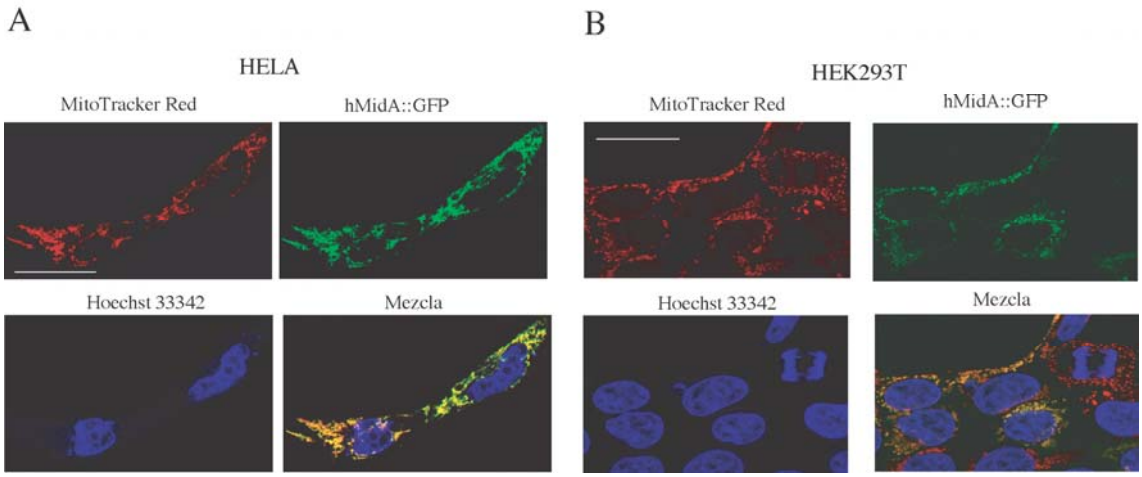

Fig. 6. hMidA es una proteína mitocondrial.
La secuencia completa del cDNA de hMidA fue clonado en el vector pEGFP-N1 y fusionado en N-terminal de la proteína eGFP. Posteriormente esta construcción se transfectó transitoriamente en células HeLa y HEK293T. La fluorescencia de GFP colocalizó con el marcador mitocondrial MitoTracker Red. Hoechst 33342 se utilizó para visualizar el núcleo. La colocalización se muestra en los paneles mezcla en color amarillo-naranja. Barra de escala = 25μm

Posteriormente aprovechamos las herramientas de genómica comparativa para diseñar hipótesis de trabajo sobre la función de MidA. Así, existen homólogos de *Dictyostelium* en muchos organismos, pero parece encontrarse ausente en otros y este perfil filogenético podría darnos pistas funcionales. Se espera que proteínas trabajando juntas en una función dada tengan el mismo perfil filogenético. Utilizando el servidor String (http://string.embl.de/) obtuvimos perfiles muy similares entre MidA y subunidades del complejo I mitocondrial (CI) así como con factores de ensamblaje del mismo complejo. Un análisis manual en detalle es mostrado en la **Tabla S1** (pág. 97). Existe una correlación clara entre la presencia de MidA y una subunidad representativa del complejo I (NDUFS7). Es bien conocido que el complejo I no se encuentra presente en todos los eucariotas (como en las levaduras *S.cerevisiae* y *S.pombe*), pero se encuentra presente en otros eucariotas y

Dictyostelium, donde juega un papel clave en la generación de ATP. Como cabría esperar, MidA no tiene homólogos en *S.cerevisiae y S.pombe*. De modo muy interesante MidA se encuentra presente en α-proteobacterias, los parientes vivos más próximos de los posibles precursores bacterianos de las mitocondrias.

Para testar la hipótesis de una posible conexión funcional entre MidA y el CI medimos la actividad de los complejos del OXPHOS (I, II, III y IV) en el mutante nulo *midA*$^-$ comparándolos con los niveles de la cepa "wild type". Un descenso del 50% en la actividad del CI fue observado **(Fig. 7A)**. Debe resaltarse que el resto de los complejos, o bien no se vieron afectados (CII), o incluso su actividad era significantemente más alta (CIII y CIV) en el mutante. Esto podría significar un posible mecanismo compensatorio de la célula en respuesta a la caída de actividad del complejo I mitocondrial. Consistente con este posible mecanismo compensatorio también se observaron incrementos, tanto de DNA mitocondrial (mtDNA) como de la mayoría de transcritos secundarios de RNA mitocondrial (mtRNA) **(Fig. 7 B,C)** . También parece haber un pequeño, pero significativo, incremento en la actividad del enzima citrato sintasa **(Fig 7 C)**, usada como una medida de la masa mitocondrial.

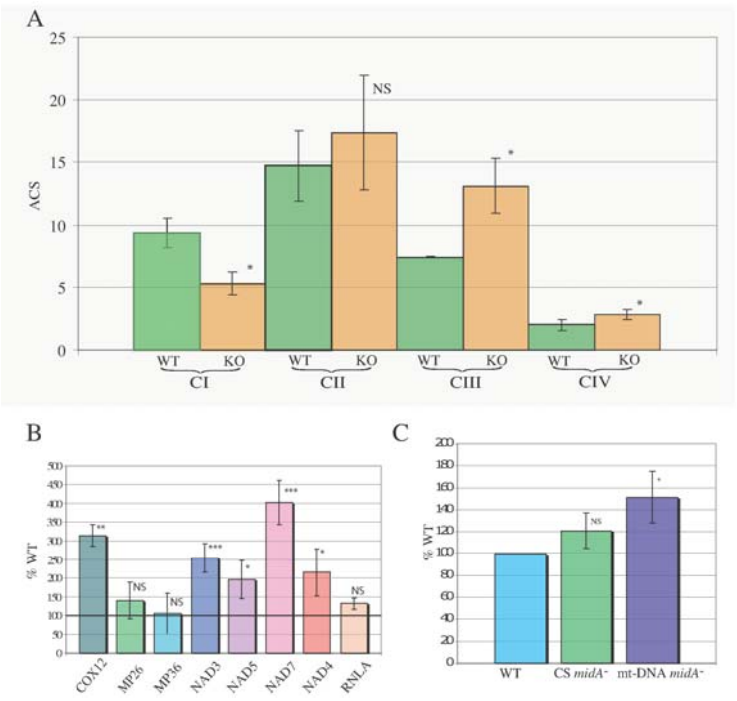

Fig. 7. La actividad del complejo I disminuye en células deficientes en MidA.
(A) Análisis espectrofotométrico de la actividad de los complejos I, II, III y IV en células WT y *midA*$^-$. Al menos se realizaron tres experimentos independientes para cada complejo y las barras representan la media ± d.s. La significanción de las diferencias fue determinada con el test t de Student; * P<0.05; ** P<0.01; *** P<0.001; NS, no significativo. ACS, actividad corregida por citrato sintasa. **(B)** Los niveles de expresión de 8 genes representativos de los 8 transcritos secundarios mitocondriales se midieron y se compararon con los niveles en células WT. Cinco de ellos mostraron incrementos significativos. Tres experimentos independientes se llevaron a cabo y las barras representan la media ± d.s. La significancia y la representación estadística se realizaron igual que en el apartado anterior. **(C)** El nivel de actividad de la enzima mitocondrial citrato sintasa (CS) y la cantidad de DNA mitocondrial (mt-DNA) se midieron y se corrigió por los niveles de WT (ajustado al 100%). De nuevo tres experimentos independientes se llevaron a cabo y el cálculo estadístico se llevo a cabo como antes.

1.2. Los niveles de complejo I ensamblado se encuentran reducidos en células HEK293T donde se ha disminuido la expresión del gen *midA*

Con el fin de conocer si el defecto en actividad del complejo I se encontraba asociado a un defecto en el ensamblaje o estabilidad del complejo I estudiamos el nivel de complejo I ensamblado por geles nativos "blue native (BN)-PAGE". Fue imposible utilizar células de *Dictyostelium* debido a la falta de los anticuerpos necesarios para la detección de los diferentes complejos del OXPHOS y a la falta de suficiente señal en BN-PAGE mediante la tinción por azul Coomassie. Por tanto se utilizaron células transfectadas estables HEK293T en los cuales la expresión del gen humano que codifica hMidA había sido disminuida con la correspondiente construcción shRNA. Se obtuvieron dos clones diferentes (S1 y S19), con un nivel de represión génica del mRNA de h*midA* del 93% y 87% respectivamente. Un clon control transfectado con el vector "scrambled" no mostró reducción en el mRNA de h*midA*. La **figura 8A** muestra 2 geles representativos con los dos clones y la **figura 8B** la cuantificación por densitometría de tres experimentos independientes donde los niveles de CI fueron normalizados usando la señal del complejo III. Resultados similares se obtuvieron utilizando la señal de los complejos II, IV o V para normalizar. Encontramos un defecto modesto aunque reproducible en los niveles de complejo I ensamblado que van desde el 60% a 80% respecto al control.

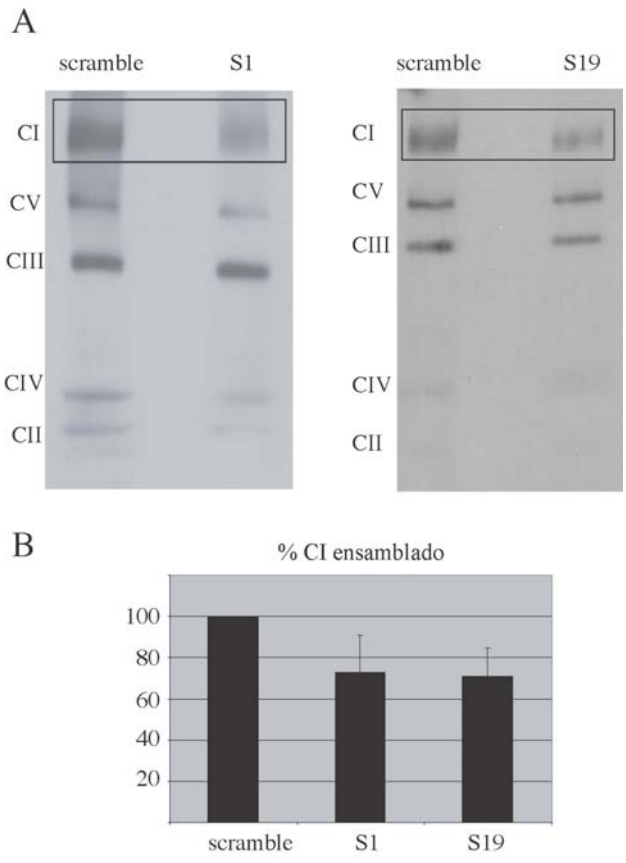

Fig. 8. Reducción del CI ensamblado en células humanas con regulación negativa de h*midA*. (A) Los complejos mitocondriales de los clones S1 y S19 de células HEK293T así como del control fueron extraídos con el detergente N-dodecil β-D-maltósido para el análisis por BN-PAGE. El gel fue transferido a una membrana de PVDF que fue incubada con un cocktail de anticuerpos para la detección de los complejos. Las diferentes bandas fueron asignadas gracias al patrón esperado y al tamaño aproximado calculado con un marcador de de proteínas nativo. Se observó reducción en los niveles de CI (indicado con un rectángulo). **(B)** La cuantificación densitométrica de tres experimentos independientes mostró una reducción de CI a aprox 60-80% respecto al clon que portaba un vector scrambled (control). El programa ImageJ 1.33u (NIH, USA) se utilizó para la densitometría y los valores de CI se normalizaron frente a CIII. Las barras representan la media ± d.s. P = 0.06 para S1 y P = 0.033 para S19 (test t-Student).

Así mismo se midió la actividad del complejo I por métodos espectrofotométricos. Sólo se observó reducción de actividad en el clon S1, el cual tenía una mayor porcentaje de inhibición del mRNA. Este clon mostró una actividad que era del 75% respecto al control. En definitiva, todos estos resultados sugieren que las proteínas MidA de humano y *Dictyostelium* están implicadas en el ensamblaje o estabilidad del complejo I.

1.3. MidA interacciona con la subunidad NDUFS2 del complejo I

En un estudio en paralelo para elucidar la función de MidA llevamos a cabo un análisis de doble híbrido en levadura buscando posibles interacciones proteína-proteína. Como "cebo" se utilizó la proteína entera MidA de *Dictyostelium* salvo los 21 primeros aminoácidos correspondientes a la secuencia señal mitocondrial. El vector usado fue pB29 que contiene una fusión "N-bait-LexA-C" y 57.4 millones de interacciones fueron analizadas por la empresa Hybrigenics. Curiosamente se obtuvieron 10 clones independientes que codificaban la proteína NADH- ubiquinona oxidoreductasa- cadena 49 (DDB_G0294030; DdNDUFS2) el homólogo de la subunidad de 49 KDa del complejo I humano NDUFS2 (hNDUFS2). La **Figura 9A** muestra la región común a todos los clones que nos permitió restringir la zona de interacción a 40 aminoácidos. Esta interacción fue clasificada como de alta confianza por el programa de la compañía Hybrigenics "Global PBS Predicted Biological Score" que representa la probabilidad de una interacción dada de ser específica [122].

No obstante, se llevó a cabo una validación posterior usando ensayos de pull-down. El fragmento N-terminal de la proteína DdNDUFS2 que contiene la región mínima de interacción se fusionó a la proteína glutation-S transferasa (GST), se purificó de bacterias y se incubó con extractos celulares de *Dictyostelium* conteniendo la proteína MidA fusionada a GFP (cepa complementada). Como se muestra en la **Figura 9B**, MidA-GFP fue arrastrado por la proteína GST-DdNDUFS2 pero no por GST sólo, que se utilizó como control. También quisimos validar la interacción usando hMidA, expresado en células HEK293T donde se encuentra fusionado a GFP (la misma cepa utilizada para la localización de hMidA; ver apartado 1.1). El resultado fue de nuevo positivo indicando por tanto, y de nuevo, una conservación funcional entre las proteínas MidA de humano y *Dictyostelium*.

Lo siguiente que nos preguntamos es si esta interacción con NDUFS2 requiere del dominio metiltransferasa nativo y funcional de MidA (ver apartados 1.4 y 1.5). De este modo llevamos a cabo el "pull-down" usando tanto la cepa que expresa la proteína nativa MidA-GFP como la proteína mutada con el cambio G170V en el cual el dominio metiltransferasa se presume que se encuentra inactivado (ver más adelante). Como se muestra en la **Figura 9C** ambas proteínas, mutada y "wild-type", fueron arrastradas por GST-DdNDUFS2 sugiriendo que el dominio metiltransferasa activo no es necesario para la interacción.

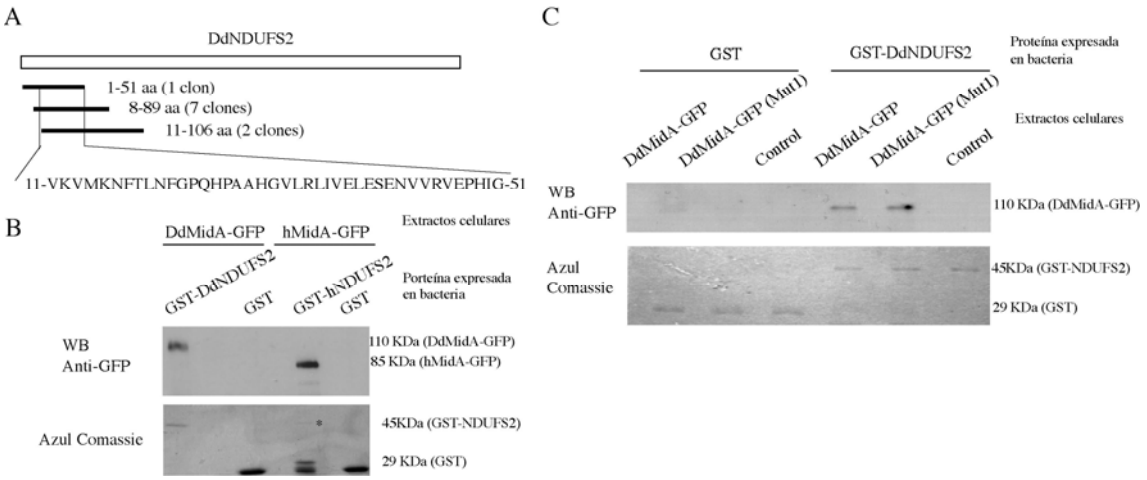

Fig. 9. MidA interacciona con NDUFS2. **(A)** El estudio de doble híbrido en levadura usando la proteína DdMidA de *Dictyostelium* como cebo nos proporcionó una posible interacción con el extremo N-terminal de la subunidad de Complejo I DdNDUFS2. El rectángulo abierto representa la secuencia de aminoácidos completa de DdNDUFS2 y las líneas de abajo marcan la posición y el número de los diferentes clones que dieron positivo en la búsqueda. Se muestra también la secuencia aminoacídica común a todos los clones. **(B)** La interacción fue validada por pull-down usando NDUFS2, tanto humano como de *Dictyostelium*, expresado en bacteria y fusionado a GST, y extractos celulares expresando MidA, tanto de humano como de *Dictyostelium*, fusionados a GFP. Después de la incubación con los extractos celulares y posterior lavado las muestras fueron divididas en dos geles. Uno que fue teñido con azul de Comassie para la detección de las proteínas expresadas en bacteria (panel inferior) y otro que se transfirió a membrana PVDF para incubación con anticuerpo anti-GFP (panel superior). La proteína humana NDUFS2 es muy sensible a degradación y sólo una pequeña cantidad fue purificada (marcada con asterisco). Tanto la proteína de *Dictyostelium* como la humana fueron arrastradas en el "pull-down" y mostraban el peso molecular esperado. **(C)** Estudios similares se llevaron a cabo usando la proteína DdMidA nativa (control positivo) así como la proteína mutada en la glicina 170, G170V (Mut1). Un extracto de células WT sin transfectar fue utilizado como control negativo. El panel superior indica la detección con anti-GFP no sólo de la proteína WT sino también de la mutada. El panel inferior indica la tinción con azul de Comassie de las proteínas expresadas en bacteria.

Por otro lado, si la proteína MidA interacciona con NDUFS2 podría ser que forme parte del complejo I mitocondrial o, por el contrario, que interaccione en algún subcomplejo previo a la formación del CI completamente ensamblado. Para distinguir entre estas posibilidades se utilizó la cepa complementada (que expresa MidA-GFP) para llevar a cabo un 2D-BN-PAGE ("2-Dimensional Blue Native/SDS Gel Electrophoresis"). Para ello, después de correr un gel nativo en su primera dimensión, se cortó la calle del gel y resolvió en perpendicular en un segundo gel desnaturalizante SDS-PAGE, identificando la proteína MidA-GFP por "western-blot" **(Fig. 10B)**. MidA tiene un peso molecular aparente en la primera dimensión que es compatible con la estructura de homodímero (aproximadamente 200 KDa teniendo en cuenta la masa conjunta de MidA y del GFP junto con el marcador TAP). Aunque la mayor parte de MidA se encuentra como dímero, señales discretas fueron detectadas a mayores pesos moleculares entre 450 y 750 KDa **(Fig. 10B)**. El complejo I de *Dictyostelium discoideum* tiene un peso molecular aproximado de 880 KDa como se determinó por análisis " MALDI-TOF" de la correspondiente banda extraída de geles BN-PAGE **(Fig. 10A)**. Así pues, no parece que MidA se encuentre ensamblado en el complejo I, pero quizá esté presente en subcomplejos pertenecientes a la cadena de ensamblaje del CI. Este

resultado está de acuerdo con estudios proteómicos previos que no han detectado MidA como componente del CI [49]. Un estudio similar fue llevado a cabo usando células HEK293T expresando la fusión hMidA-GFP (ver apartado 3.1) pero en este caso no se encontró una asociación estable de la proteína humana con subcomplejos, aunque su tamaño sugiere que es también un homodímero (datos no mostrados). Quizás la interacción en *Dictyostelium* con los subcomplejos es más estable que en humano, permitiendo su detección por medio de esta técnica, o pueden existir diferencias funcionales entre las dos especies que no alcanzamos a comprender todavía.

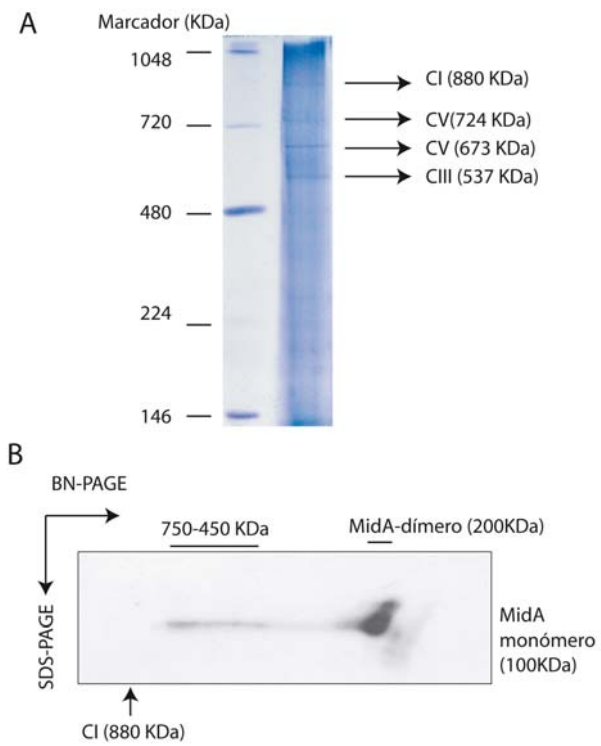

Fig. 10. Análisis por BN-PAGE de células de *Dictyostelium* expresando DdMidA-GFP. (A) Una tinción de azul de Comassie de la primera dimensión reveló una serie de bandas que fueron analizadas por espectroscopia de masas MALDI-TOF . Esto nos permitió identificar diferentes complejos, entre ellos el complejo I. **(B)** Se diseñó una segunda dimensión desnaturalizante con SDS-PAGE y el gel se transfirió a membrana de PVDF para detección con anticuerpo anti-GFP. La señal de DdMidA se detectó en la 1D a 200KDa mientras que en la 2D mostraba un tamaño de 100KDa consistente con su conformación de homodímero. Se detectaron así mismo señales adicionales más pequeñas que el tamaño del complejo I de *Dictyostelium.*

1.4. MidA tiene un dominio metiltransferasa conservado

La falta de motivos funcionales identificables en la secuencia aminoacídica de MidA usando los programas habituales de comparación de secuencias nos impidió previamente especular sobre la posible función molecular [142]. En este trabajo hemos buscado posibles similitudes estructurales con otras proteínas cuya función es conocida y hemos llevado a cabo una modelización bioinformática que nos ha permitido avanzar en su función molecular.

Para obtener un modelo estructural de MidA, llevamos a cabo una búsqueda por Blast en la base de datos PDB (Protein Data Bank, http://www.pdb.org/pdb/home/home.do), una base de datos de estructuras de proteínas, buscando una proteína homóloga de estructura conocida [7, 76].

Encontramos así un candidato con un 32 % de identidad de secuencia con MidA y con "E-value" en Blast de 2e-52 perteneciente a la bacteria *Rhodopseudomonas palustris*. El análisis de la estructura de esta proteína fue realizado por el consorcio de genómica estructural (Uniprot: Q6N1P6; PDB: 1zkd). Su función es hasta ahora desconocida como se demuestra por su clasificación en la base de datos de dominios conservados PFAM, como DUF185, una familia de proteínas de función desconocida [51]. Sin embargo, en la base de datos estructural de proteínas SCOP, 1zkd fue clasificada como un posible miembro de la superfamilia de metiltransferasas dependientes de S- adenosilmetionina (SAM) que incluye 52 familias de proteínas [8].

La alta homología existente entre MidA de *Dictyostelium* y 1zkd de *Rhodopseudomonas* sugería que ambas proteínas podrían ser ortólogas y por tanto se diseñó un modelo 3D de MidA con el servidor "Phyre server" [73] usando como base la estructura de 1zkd que aparecía en dicho programa, de nuevo, como la proteína más parecida a MidA de estructura conocida. El alineamiento de tipo secuencia-estructura entre MidA y 1zkd englobaba a casi toda la proteína MidA **(Fig. 11A)**. Por supuesto la secuencia señal mitocondrial en N-terminal es excluida del modelo.

El siguiente paso fue definir los residuos funcionales que podría haber en el sitio catalítico usando FireStar, un servidor web que predice residuos funcionales importantes usando FireDB [93]. FireDB es una base de datos de estructuras depositadas en la base de datos PDB junto con sus ligandos asociados y contiene una serie de anotaciones funcionales. Estas anotaciones se extraen de los contactos atómicos entre proteína y ligando y también se derivan del CSA ("Catalytic Site Atlas") [119]. De un modo impactante para nosotros, la información contenida en FireStar indicaba una correlación entre MidA, 1zkd y una proteína metiltransferasa humana (PDB: 1zq9). Siguiendo por otro lado las anotaciones en FireStar derivadas del CSA, el sitio catalítico de 1zq9 contiene tres residuos relevantes: G64, E85 y N128. Los dos primeros se encuentra conservados en MidA (G170 y E200) mientras que el tercero está reemplazado por glutamina (Q257). La estructura cristalina de 1zq9 ya había sido previamente obtenida con su ligando SAM (el donador de grupos metilo de esta familia de metiltransferasas), que se encuentra en contacto con los tres residuos comentados. Nosotros superpusimos nuestro modelo 3D de MidA con la región catalítica de 1zq9 usando alineamiento local-global (LGA) [163] y encontramos que ambas estructuras se superponen perfectamente **(Fig. 11B)**.

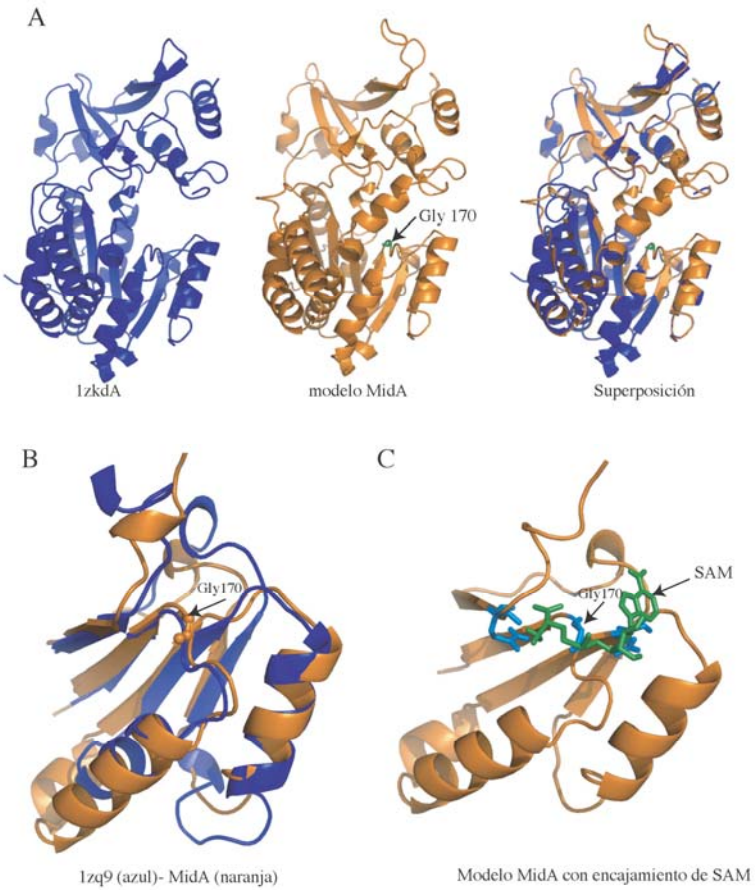

Fig. 11. MidA contiene un dominio metiltransferasa. **(A)** Presentación del modelo 3D de MidA construido usando como molde la proteína 1zkd de *Rhodopseudomonas Palustris*, que pertenece a la familia DUF185 y cuya estructura se encuentra depositada en el PDB. El diagrama azul representa 1zkd_A (la proteína es un homodímero y la cadena B no se muestra). En naranja se muestra el modelo de MidA. El alineamiento estructural entre MidA y 1zkd se muestra en la derecha y abarca la mayor parte de la secuencia de MidA. **(B)** Detalle del alineamiento entre MidA y 1zq9. La región catalítica del modelo MidA (naranja) se superpone perfectamente con aquella de 1zq9 (azul), una adenosín metiltransferasa humana, y muestra un plegamiento característico con varios aminoácidos conservados, entre ellos G170 que fue seleccionado para posteriores análisis funcionales. **(C)** El donador de grupos metilo SAM encaja en el modelo MidA. El encaje o "docking" fue llevado a cabo con el programa Haddock. SAM mantiene las distancias adecuadas a los residuos catalíticos equivalentes de la metiltransferasa 1zq9. Los residuos G170, E200 y Q257 se muestran en azul y SAM en verde.

Para determinar si el ligando SAM puede ser acomodado en nuestro modelo MidA de un modo correcto (energéticamente favorable) se llevó a cabo el "docking" o encaje usando el software "Haddock biomolecular docking" buscando entre 1.000 modelos posibles [41, 42]. La única restricción espacial ordenada al programa fue que la molécula de SAM se encontrase en estrecho contacto a los tres residuos catalíticos equivalentes en nuestro modelo 3D. Se obtuvieron múltiples modelos y finalmente se seleccionaron los 10 mejores modelos (mejor valor Haddock). El mejor modelo es mostrado en la **Figura. 11C**. La red de contactos entre los tres residuos catalíticos de MidA y la molécula SAM **(Fig. 12)**, obtenida con Ligplot [152], permanecía inalterada, siendo por tanto compatible.

El último paso, antes de pasar a ensayos funcionales, fue simular la mutación del residuo catalítico crítico G170. Primero reemplazamos G170 por Valina (G170V) con el programa Pymol (The PyMol Molecular Graphics System. DeLano Scientific, Palo Alto, CA) sobre el modelo de "docking", seleccionando el rotámero más frecuente en proteínas. Obviamente el efecto de esta mutación produce nuevos choques entre la molécula de SAM y los aminoácidos, de modo que el nuevo modelo requiere un nuevo modelo de "docking" de la molécula de SAM en el modelo mutado. De nuevo, y como se había hecho anteriormente, seleccionamos los 10 primeros modelos que presentaban mejor valor Haddock y observamos la conservación de la distancia entre SAM y los 3 residuos catalíticos. El nuevo modelo nos permitió ver que la red de contactos existentes se perdía y que la molécula de SAM se acomodaba ahora hacia el exterior de la proteína, causando presumiblemente una pérdida de función de la enzima. Esta modelización ponía de relieve la importancia del residuo G170 que como veremos en el siguiente apartado fue confirmada por estudios de mutagénesis dirigida.

Otro aspecto interesante a resaltar de estos estudios es el hecho de que la estructura cristalina de 1zq9 indica que es un homodímero, como ha sido descrito para otras muchas metiltransferasas. Esto es compatible con nuestros resultados mostrados anteriormente usando 2D-BN-PAGE, donde se mostró que MidA es también un homodímero **(Fig. 10)**.

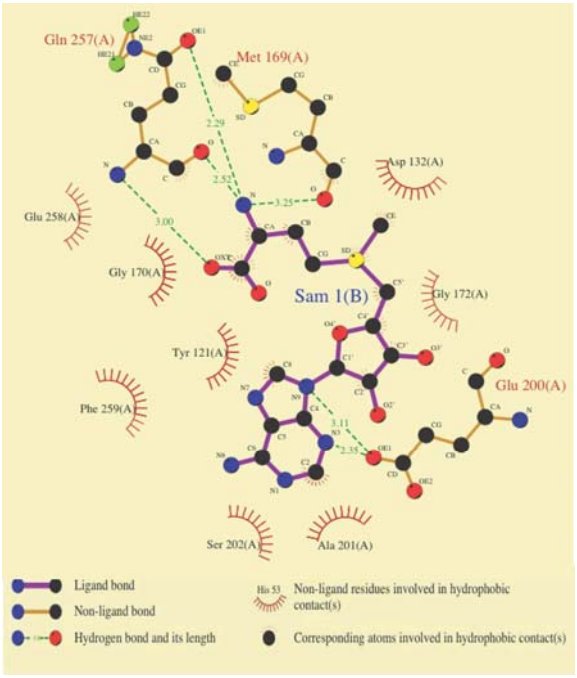

Fig. 12. Red de contactos entre MidA y SAM. Los enlaces entre el ligando SAM y MidA se representaron con el programa Ligplot (versión inglesa).

1.5. El dominio metiltransferasa es necesario para la función de MidA

El modelo estructural mostrado arriba sugiere fuertemente la presencia de un motivo de unión a SAM en MidA, el cual es característico de proteínas metiltransferasas. Para confirmar esta hipótesis llevamos a cabo la mutagénesis dirigida para cambiar el residuo G170 que se encuentra en el dominio conservado y, cuyo cambio a Valina, según la modelización, provocaba un efecto claramente perjudicial en la unión de SAM. También se llevó a cabo una doble mutación G170V y G172V. Se ha sugerido previamente que ambos residuos son importantes para la unión de SAM y están claramente conservados en la superfamilia de metiltransferasas [107]. Las formas WT y mutadas de MidA se fusionaron a GFP, para determinar su localización subcelular, y fueron transfectadas en células de *Dictyostelium midA*$^-$ **(Fig. 13A)**. Como se describió previamente, las células *midA*$^-$ muestran defectos en crecimiento, tanto en líquido como en asociación a bacterias, debidos a la disfunción mitocondrial [142]. Mientras que la proteína "wild-type" MidA era capaz de complementar el fenotipo como ya habíamos descrito antes, el mutante G170V no era capaz de hacerlo **(Fig. 13C)**. Un resultado similar se obtuvo con el doble mutante G170V y G172V (datos no mostrados). Para excluir la posibilidad de que la falta de complementación fuese debida a un fallo en la expresión o en la localización de la proteína en mitocondria, estudiamos la localización subcelular por microscopía confocal de las proteínas mutantes y pudimos ver que, al igual que la proteína WT, colocalizaban en mitocondria con el marcador MitoTracker Red (la **Fig. 13B** muestra el resultado para el mutante G170V como ejemplo). La falta de reversión del fenotipo sugiere fuertemente que una simple mutación G170V en el dominio metiltransferasa es suficiente para mantener la proteína inactiva. Estos resultados también sugieren que el posible dominio metiltransferasa es requerido para la función de MidA en *Dictyostelium*.

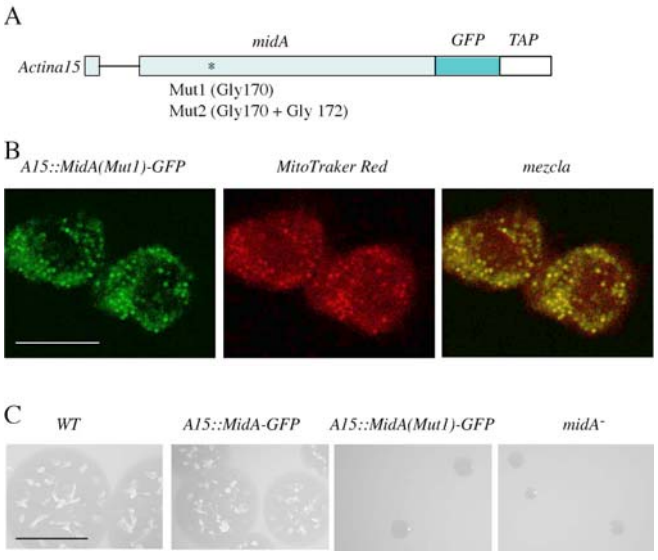

Fig. 13. La mutagénesis dirigida confirma la presencia del dominio metiltransferasa. **(A)** Esquema de la construcción utilizada para la complementación. La región codificante de midA, fusionada a GFP y TAP es dirigida por el promotor del gen actina15 (A15) y es dibujado como cajones. La línea delgada representa el pequeño intron en N-terminal. El asterisco indica la zona donde se llevó a cabo la mutagénesis dirigida. **(B)** Las construcciones WT y las mutantes se transfectaron en el mutante *midA*$^-$ y clones transfectados establemente fueron estudiados para ver la expresión y localización subcelular. Todas las construcciones mostraron localización mitocondrial de la proteína como muestra su colocalización con MitoTracker Red. Barra de escala = 10µm. **(C)** Análisis del crecimiento en asociación con bacterias de transformantes WT y mutantes. La construcción WT complementó el fenotipo de crecimiento WT así como otros fenotipos (no mostrado). Sin embargo los mutantes no fueron capaces de complementar el fenotipo y su aspecto era de colonias pequeñas como ocurre en el mutante *midA*$^-$. Un estudio representativo se muestra para el mutante Mut1 (G170V). Barra de escala = 1cm.

1.6. Caracterización de la deficiencia de complejo I y su relación con la señalización de AMPK.

Con el objetivo de avanzar más en el conocimiento en la relación genotipo-fenotipo en disfunción mitocondrial hicimos uso del mutante *midA*$^-$ en *Dictyostelium* como modelo celular de enfermedad asociada a CI. Quisimos caracterizar en detalle el mutante nulo *midA*$^-$ y estudiar la relación con la señalización de la quinasa dependiente de AMP (AMPK). Las células de *Dictyostelium* agregan tras un período de ayuno para formar un organismo pluricelular. En la fase de "slug" estas estructuras muestran una remarcable capacidad para moverse a través de gradientes de luz y térmicos (ver apartado 1.4.3). Se vió anteriormente que estos procesos eran más sensibles a la deficiencia mitocondrial que otras funciones celulares [79, 158]. El mutante *midA*$^-$ mostró un fuerte defecto en fototaxis como se puede observar en el ensayo del rastro del "slug" **(Fig. 14A)** y en la cuantificación de la precisión de la fototaxis (κ) **(Fig. 14 B)**. κ mide como de concentrados son los rastros del gusano alrededor de la dirección de la fuente de luz. Varía entre 0 cuando no hay orientación en ninguna dirección preferencial a infinito en caso de una orientación perfecta. Este defecto en fototaxis fue recuperado cuando se analizó la cepa *midA*$^-$ transfectada con la proteína MidA fusionada a GFP (cepa complementada). Por otro lado se observó también un defecto en termotaxis **(Fig. 14 C)**. En este estudio se midió el valor κ en las cepas wild-type, *midA*$^-$ y complementada. Como se puede ver en la **Figura 14C** este defecto también se recuperó en la cepa complementada.

Por otro lado los mutantes *midA*$^-$ mostraron un defecto en crecimiento que se acompaña de defectos en macropinocitosis y fagocitosis [142] **(Fig. 15)**. Estos defectos de macropinocitosis y fagocitosis no han sido observados previamente en otros mutantes mitocondriales de *Dictyostelium*, sugiriendo un escenario complejo que será comentado en la discusión [14].

Posteriormente quisimos estudiar la contribución de la señalización de AMPK en el complejo fenotipo de las células *midA*$^-$. La sobreexpresión de una construcción antisentido de AMPK, AMPKas (pPROF362), se ha visto previamente que inhibe la expresión de AMPK y que restaura el fenotipo de fototaxis en diferentes mutantes mitocondriales en *Dictyostelium*. Como se esperaba, encontramos que la fototaxis y parcialmente la termotaxis eran restaurados en el mutante *midA*$^-$ cuando la expresión de la proteína AMPK era disminuida sugiriendo que estos fenotipos defectuosos se deben, en realidad, a la activación crónica de esta quinasa **(Fig. 14A)**. Esta es la primera vez que se describe que un defecto fenotípico causado por una deficiencia específica del complejo I mitocondrial puede ser rescatado por disminución de la proteína AMPK. Resulta interesante que los defectos en crecimiento, macropinocitosis y fagocitosis no pudieron ser rescatados de esta manera, sugiriendo que estos fenotipos son independientes de la señalización por AMPK en el mutante *midA*$^-$ **(Fig. 15)**.

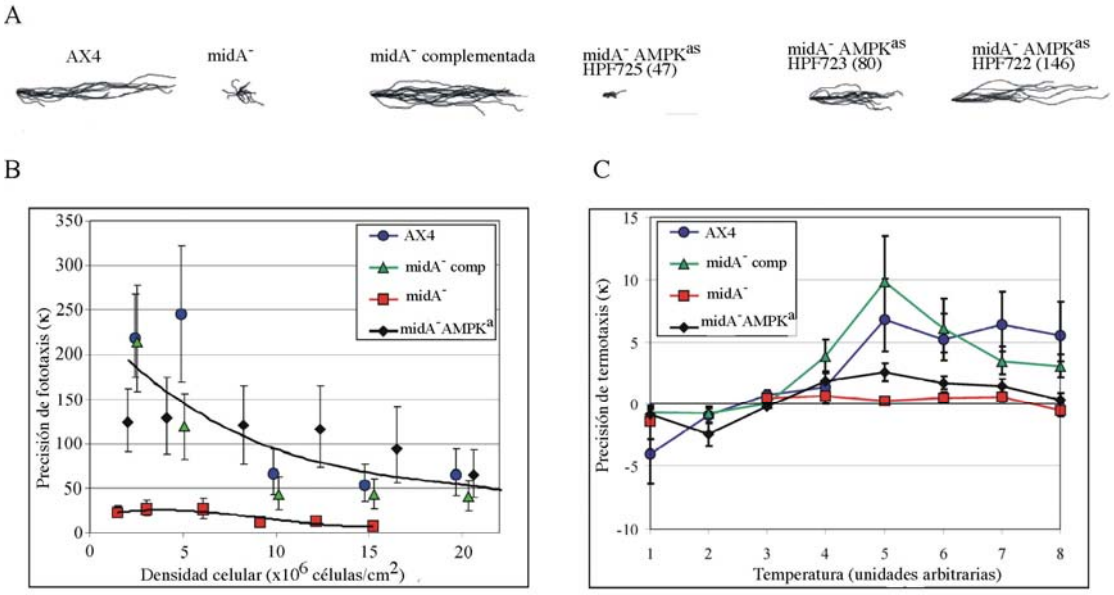

Fig.14. Los defectos de fototaxis en el mutante *midA*⁻ de *Dictyostelium* pueden ser revertidos por inhibición de AMPK. **(A)** Se permitió que diferentes cepas de *Dictyostelium* formasen "slugs" y se expusieron a luz lateral para determinar su capacidad de fototaxis. Las cepas utilizadas son : células wild-type de *Dictyostelium* (AX4), mutante nulo *midA*⁻, cepa complementada del gen *midA* y diferentes cepas transfectadas de la cepa *midA*⁻ expresando diferente nº de copias de la construcción antisentido de AMPK pPROF362 (el nombre de cepas comienzan por HPF). El nº de copias de la construcción es indicado entre paréntesis. Los defectos de fototaxis y migración (rastros cortos y sin orientación) del mutante *midA*⁻ fueron suprimidos de un modo dependiente del nº de copias de asAMPK. **(B)** La precisión de la fototaxis (κ) se midió en las cepas indicadas a diferentes densidades celulares. La cepa *midA*⁻ asAMPK utilizada fue HPF722. **(C)** La precisión de la termotaxis en un gradiente de 0.2º C/cm se midió para los "slugs" formados a una densidad de $3x10^6$ células/cm^2 y migrando a temperaturas desde 1 a 8 (unidades arbitrarias que se corresponden a experimentos de calibración de 14 ºC a 28 ºC). La cepa *midA*⁻ asAMPK utilizada era HPF723 y exhibía una supresión parcial del defecto, pero no completa (como ocurre en la cepa complementada).

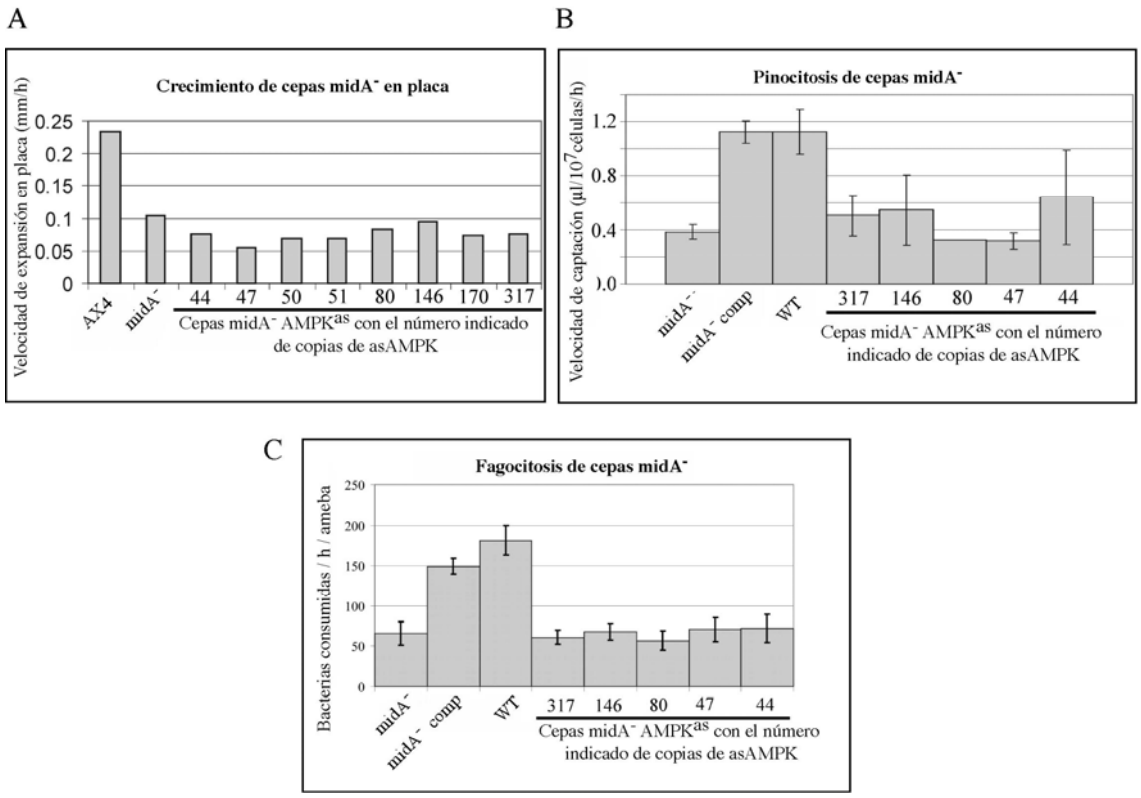

Fig. 15. Defectos en velocidades de crecimiento, fagocitosis y macropinocitosis en el mutante *midA*⁻ y cepas AMPKas. Las cepas AMPKas utilizadas se derivan del mutante nulo *midA*⁻ por transfección con la construcción antisentido de AMPK pPROF362. Las cepas y el correspondiente nº de copias de pPROF362 fueron: HPF727 (44), HPF725 (47), HPF724 (50), HPF721 (51), HPF723 (80), HPF722 (146), HPF726 (170) y HPF720 (317). **(A)** Las velocidades de crecimiento fueron medidas por la velocidad de expansión de la zona de lisis bacteriana en las cepas indicadas. El mutante *midA*⁻ mostró una marcada disminución de crecimiento que no fue rescatada por la inhibición de AMPK independientemente del nº de copias de la construcción. **(B)** La macropinocitosis se analizó midiendo la captación de FITC-dextrano en las cepas indicadas. Una vez más este fenotipo no fue rescatado por inhibición de AMPK. **(C)** La fagocitosis en diferentes cepas se analizó midiendo la captación de bacterias expresando DsRed. Este fenotipo no se recupera por inhibición de AMPK.

C20ORF7

2.1. "Knock-out" del gen homólogo a *C20orf7* humano en *Dictyostelium*

La proteína C20orf7 de humano (Uniprot: Q5TEU4) ha sido descrita previamente como un factor de ensamblaje de complejo I mitocondrial que presenta mutaciones en pacientes con síndrome de Leigh y con un tipo de enfermedad neonatal letal [54, 137]. Sin embargo poco o nada se conoce de su función bioquímica o de su papel citopatológico en enfermedad mitocondrial. El gen codifica dos posibles isoformas (NP_077025.2 y NP_001034464.1) con la menor de ellas presentando un "splicing" alternativo en la región codificante.

C20orf7 está presente a lo largo de la evolución en plantas, metazoos y de manera muy similar a como ocurre en MidA se encuentra presente en α-proteobacterias **(Tabla. S2, pág. 98),** los "parientes" más próximos de las mitocondrias según la teoría endosimbiótica. Sin embargo la proteína se encuentra ausente en las levaduras *S.cerevisiae* y *S.pombe*, que precisamente carecen de complejo I. El homólogo en *Dictyostelium* (C20orf7) **(Fig. 16A)** presenta un "Blast e-value" muy alto de 6e-62 a pesar de la gran distancia evolutiva y una identidad de secuencia del 41%. Dada la poca información que se posee de esta proteína, el interés que suscita debido a la presencia de mutaciones en pacientes y su similitud con MidA por ser otro factor de ensamblaje de complejo I con una posible función metiltransferasa, decidimos comenzar su estudio en *Dictyostelium*. Se llevó a cabo la generación de una cepa KO del gen *C20orf7* y para ello se utilizó una construcción donde el gen *C20orf7* es interrumpido por el gen de resistencia a blasticidina **(Fig. 16B)**. La construcción fue transfectada en células "wild-type" AX4 y se llevo a cabo la búsqueda de mutantes con fenotipo defectuoso en placa. La confirmación de la interupción a nivel genómico se llevó a cabo por PCR usando oligos tanto del gen de resistencia al antibiótico como de la región "upstream" del gen **(Fig. 16C)**. Por otro lado la confirmación de la ausencia de mensajero se llevo a cabo por RT-PCR utilizando en este caso oligos de la zona N-terminal y C-terminal del gen **(Fig. 16D)**.

2.2. La eliminación de *C20orf7* conduce a una serie de fenotipos defectuosos en *Dictyostelium*

Primero se analizó el fenotipo de crecimiento y desarrollo en la cepa *C20orf7*¯. El mutante presentaba un importante defecto de crecimiento tanto en líquido como en asociación con bacterias **(Fig. 17A)**. En el caso de crecimiento axénico en líquido, el tiempo de generación fue de 14 horas respecto a las 10 horas del "wild-type". Para el estudio del desarrollo sincrónico, células de *Dictyostelium* tanto "wild-type" como *C20orf7*¯ se depositaron en filtros de nitrocelulosa. Como puede observarse en la **Figura 17B**, mientras que las células WT son capaces de alcanzar la estructura culminante al cabo de 24 horas, las células mutantes *C20orf7*¯ sufren un retraso en el desarrollo, mostrando al cabo de 24 horas un gran número de "slugs". Esta cepa solo es capaz de culminar al cabo de 48 horas, aunque los cuerpos fructíferos son aberrantes, siendo más pequeños que en el wild-type. Más aún, las esporas tomadas tras 10 días, tiempo necesario para la completa

maduración, presentan una morfología inadecuada y son menos refringentes que las esporas "wild-type", lo que puede ser debido a un defecto de maduración o de diferenciación **(Fig. 17B)**.

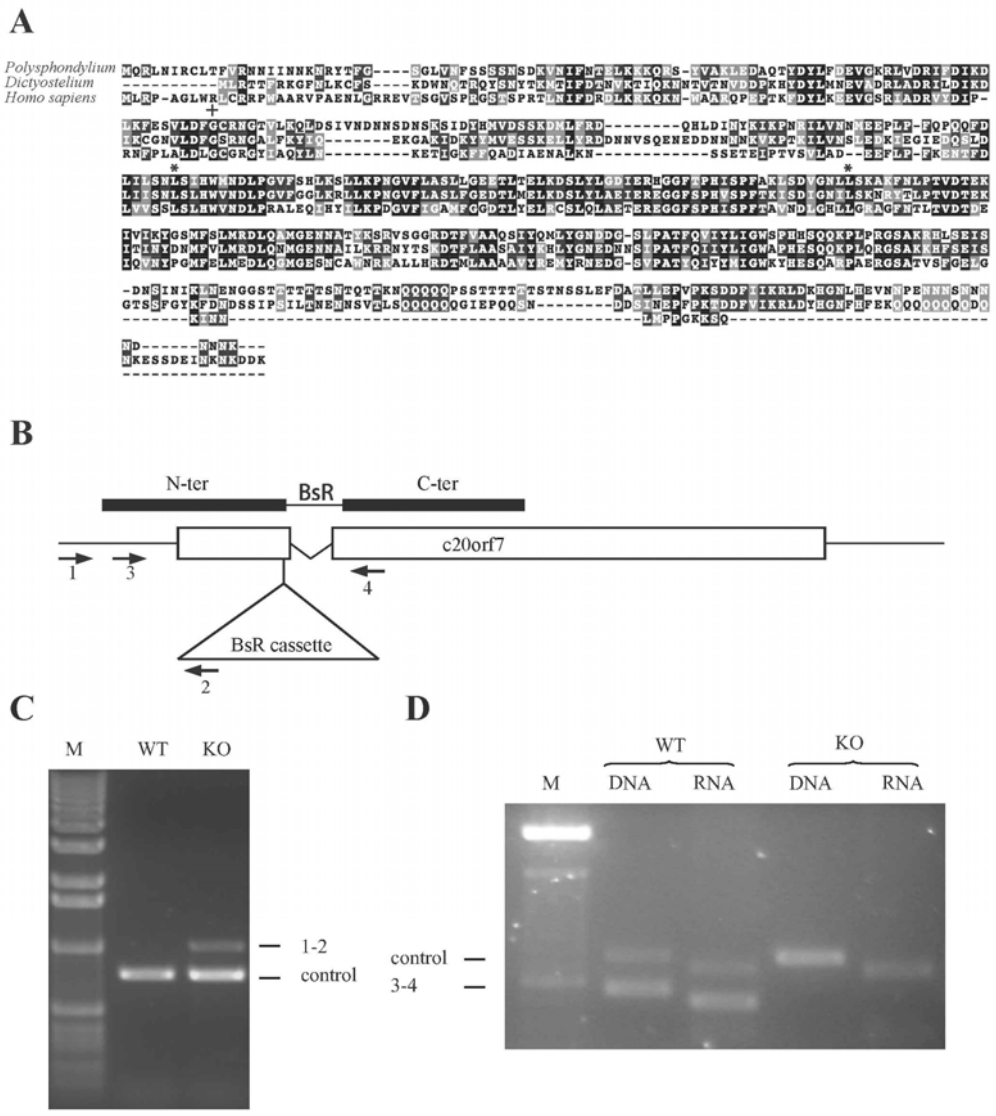

Fig. 16. Knock out de *C20orf7* y pérdida de expresión. (A) La secuencia de C20orf7 se alineó con la proteína humana (NP_0077025.2) y con la proteína homóloga de *Polysphondylium pallidum* (EFA86651.1) usando el programa ClustalW. El fondo negro indica aminoácidos idénticos en las 3 proteínas, el gris oscuro indica residuos idénticos en dos de las proteínas y el gris claro indica residuos similares (en polaridad y carga). La localización de las dos mutaciones homólogas a las descritas en pacientes humanos (L159F y L229P) se marcan con asteriscos. La Gly conservada del posible sitio de unión de SAM se marca con +. **(B)** Esquema del locus *C20orf7* y del vector KO. El casete de resistencia a blasticidina (BsR) interrumpió el gen en el nucleótido 206 de la secuencia codificante antes del intrón y delecionó el intron marcado con línea en V. Las cajas abiertas representan la secuencia codificante de *C20orf7*. Las cajas negras representan el vector de KO con la posición de las regiones N-terminal y C-terminal usadas para permitir la recombinación homóloga. Las flechas indican los diferentes oligonucleótidos usados para la verificación de las cepas KO (listado en Materiales y métodos). **(C)** Verificación genómica. El DNA extraído de cepas AX4 y *C20orf7*⁻ se utilizó como molde en la PCR usando oligos 1-2. La presencia de una banda indica que la recombinación ha tenido lugar en el locus *C20orf7*. El gen DDB_G0268840 fue utilizado como control. **(D)** Verificación de la falta de expresión a nivel de mRNA usando los oligos 3-4. Las diferencias en el tamaño usando como molde DNA o RNA son debidas a la presencia del pequeño intrón tanto en *C20orf7* como en el control (DDB_G0268840). La ausencia de la banda de menor tamaño indica que el gen ha sido interrumpido y que no se produce mRNA de *C20orf7*.

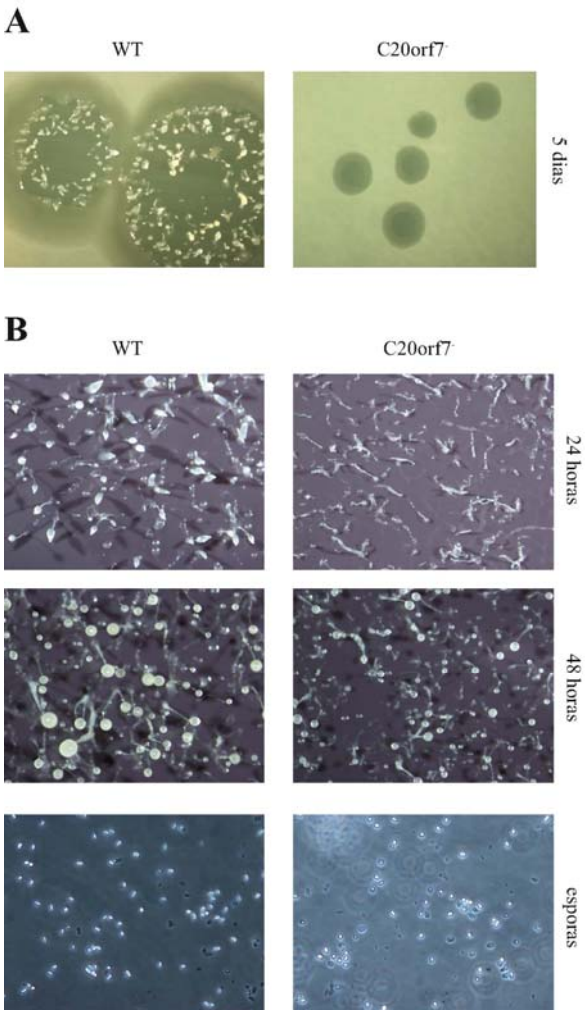

Fig. 17. Fenotipos de crecimiento y desarrollo aberrantes. (A) Células "wild-type" y *C20orf7-* fueron sembradas en placas SM en asociación a la bacteria *Klebsiella aerogenes* y dejadas crecer 5 días. Las células *C20orf7-* mostraron un importante defecto, como muestra el diámetro de la zona de crecimiento. Las fotografías fueron tomadas al mismo aumento. **(B)** Células "wild-type" y *C20orf7-* creciendo en medio HL5, fueron aisladas, lavadas con medio PDF y depositadas en filtros de nitrocelulosa. Las fotografías fueron tomadas con lupa a los tiempos indicados y al mismo aumento. El mutante nulo *C20orf7-* mostró un importante retraso en la fase "slug" que sólo le permitió culminar tras 48 horas. Además estas estructuras son más pequeñas como puede observarse en el panel intermedio. En el panel inferior se muestran las fotos de microscopía de campo claro obtenidas de esporas de ambas cepas al cabo de 10 días de desarrollo. Las esporas del mutante son más redondas y menos refringentes. Las imágenes mostradas son representativas de al menos tres experimentos independientes.

2.3. C20orf7 es necesaria para la actividad del complejo I en *Dictyostelium*

Previamente ha sido descrito que la regulación negativa del gen *C20orf7-* en células humanas en cultivo o incluso la mutación de esta proteína en pacientes producía un defecto, no sólo de ensamblaje de complejo I, sino también de su actividad [54, 137]. En *Dictyostelium* no es posible el estudio de estabilidad de complejos por la técnica de BN- PAGE, dado que no disponemos de los anticuerpos necesarios para la detección de todos ellos. De este modo nos centramos en el estudio de la actividad de los complejos de cadena respiratoria **(Fig. 18A)**. Se observó una caída significativa del 60% de actividad de complejo I en el mutante nulo *C20orf7-* . Esto parece confirmar que la función de C20orf7 como factor de ensamblaje/ actividad del complejo I se mantiene en la evolución desde *Dictyostelium* a humano. Así mismo, no se observaron cambios en la actividad del resto de complejos. Por otro lado, la actividad del enzima citrato sintasa (enzima del ciclo de Krebs anclado a la membrana mitocondrial interna), que se utiliza como marcador de masa mitocondrial, mostraba un aumento significativo del 70% respecto al WT **(Fig. 18B)**.

Como medida del status energético de la célula quisimos testar los niveles de ATP celular en células "wild-type" y en el mutante *C20orf7-* **(Fig. 18C)**. Sorprendentemente los niveles de ATP

eran significativamente superiores en la cepa *C20orf7*⁻ (70% más que en "wild-type"). Conjuntamente con el aumento de masa mitocondrial esto podría significar la existencia de un mecanismo compensatorio llevado a cabo por las células mutantes *C20orf7*⁻ para intentar restaurar la deficiencia produciendo más mitocondrias y de algún modo generando más ATP.

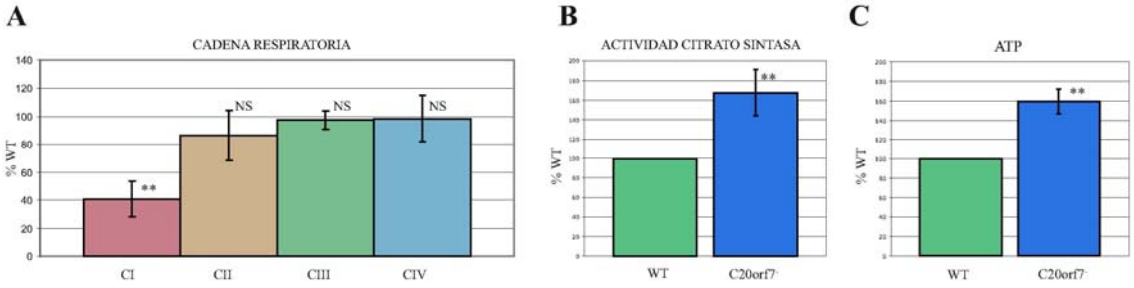

Fig. 18. La deficiencia de complejo I de *C20orf7*⁻ se acompaña con altos niveles de masa mitocondrial y de ATP celular. (A) Las actividades de los complejos I, II, III y IV de células WT y mutantes *C20orf7*⁻ se midieron por el método espectrométrico y finalmente se corrigieron por proteína total, por la actividad de citrato sintasa y se normalizaron frente a los valores WT. La actividad del complejo I se ve reducida en el mutante *C20orf7*⁻ pero no el resto de complejos. Los valores medios ± s.d se obtuvieron de al menos tres experimentos independientes para cada complejo. La significancia se calculó usando el test t-Student. NS = no significativo. ** p< 0.001. **(B)** La actividad citrato sintasa se midió por espectroscopia en las células WT y *C20orf7*⁻, se corrigió por proteína total y se normalizó frente a WT. Se realizaron al menos tres experimentos independientes. Se observó un fuerte incremento que indica un aumento de masa mitocondrial. Los cálculos estadísticos se realizaron como en A. **(C)** Los niveles de ATP celular fueron medidos en células WT y *C20orf7*⁻ usando el ensayo de bioluminiscencia y se normalizaron frente a WT. Los niveles de ATP son superiores en el mutante *C20orf7*⁻. Al menos se realizaron tres experimentos independientes. La significancia se obtuvo del mismo modo que anteriormente.

Por otro lado pensamos que la disfunción mitocondrial de complejo I tal vez pudiese llevar, en el caso de *C20orf7*⁻, a defectos morfológicos en la mitocondria como ha sido observado para mutantes del factor de ensamblaje IndI [133]. Sin embargo, el análisis detallado y comparativo de fotos de microscopía electrónica de transmisión no mostraba diferencias o defectos morfológicos mitocondriales **(Fig. 19)**.

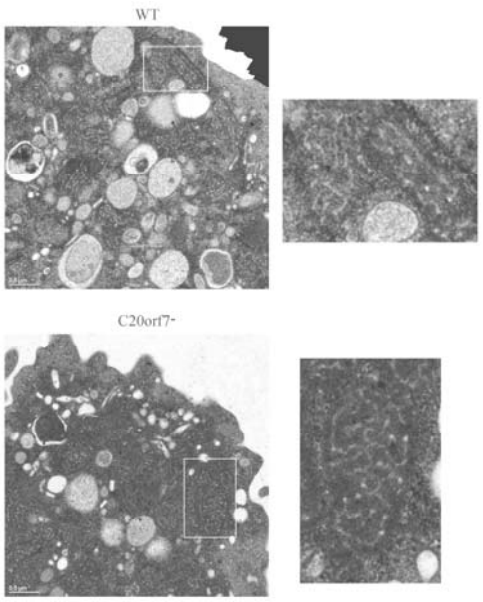

Fig. 19. Microscopía electrónica de células WT y *C20orf7*⁻. Células WT y *C20orf7*⁻ creciendo exponencialmente se sometieron al tratamiento descrito en Materiales y métodos. Se muestran en detalle (marco blanco y a la derecha de la imagen) las mitocondrias de ambas cepas, mostrando que no existen diferencias morfológicas apreciables.

2.4. El dominio metiltransferasa es necesario para la función de C20orf7

Utilizando la secuencia de aminoácidos de C20orf7 en la base de datos "Conserved Domains" de NCBI se pudo observar que la proteína contiene un dominio metiltransferasa dependiente de SAM (cd02440). Esta predicción se da en las dos isoformas existentes de C20orf7 en humano. De modo similar a como se había hecho para la proteína MidA, se intentó construir un modelo 3D que nos permitiese estudiar *in-silico* la posible interacción con la molécula de SAM o incluso modelizar las diferentes mutaciones patogénicas. Sin embargo no se encontraron proteínas homólogas de otras especies cuya estructura se encontrase depositada en la base de datos PDB. En cualquier caso, la predicción del dominio metiltransferasa de tipo I en "Conserved Domains" de la proteína C20orf7 humana es muy significativa y nos permitió identificar la secuencia aminoacídica conservada GxGxG dentro del motivo característico de unión de la molécula de SAM. Como ocurriese en el caso de MidA se seleccionó el primer residuo Glicina para mutagénesis dirigida (G86V) y la proteína mutante se denominó M1. Las formas wild-type y mutante de la proteína C20orf7 se fusionaron a GFP (para el estudio de su localización subcelular) y se transfectaron en el mutante *C20orf7*$^{-}$ **(Fig. 20A)**. La proteína "wild-type" fue capaz de complementar el fenotipo de crecimiento tanto en líquido (no mostrado) como en asociación a bacterias **(Fig. 21)**. Este estudio de complementación confirma que los fenotipos defectuosos del mutante *C20orf7*$^{-}$ son debidos única y exclusivamente a la disrupción de este gen. Además la proteína colocalizó en mitocondria con el marcador MitoTracker Red de igual modo a como se había descrito previamente en células humanas [111, 137] **(Fig. 20B)**. Por otro lado la proteína mutante no fue capaz de complementar el fenotipo de crecimiento, ni en líquido ni en asociación a bacterias, siendo defectuoso en igual medida al observado en el mutante *C20orf7*$^{-}$ **(Fig. 21)**. Para eliminar la posibilidad de que la falta de complementación fuese debida a una incorrecta expresión o localización subcelular de la proteína mutante, estudiamos esta posibilidad y vimos que colocalizaba en mitocondria, de nuevo, con el marcador MitoTracker Red **(Fig. 20B)**. La falta de recuperación del fenotipo sugiere por tanto que la mutación en Gly 86 es suficiente para inactivar la proteína y producir por tanto una falta de función. Así mismo esto indica que el posible dominio metiltransferasa es necesario para la función de C20orf7 en *Dictyostelium*.

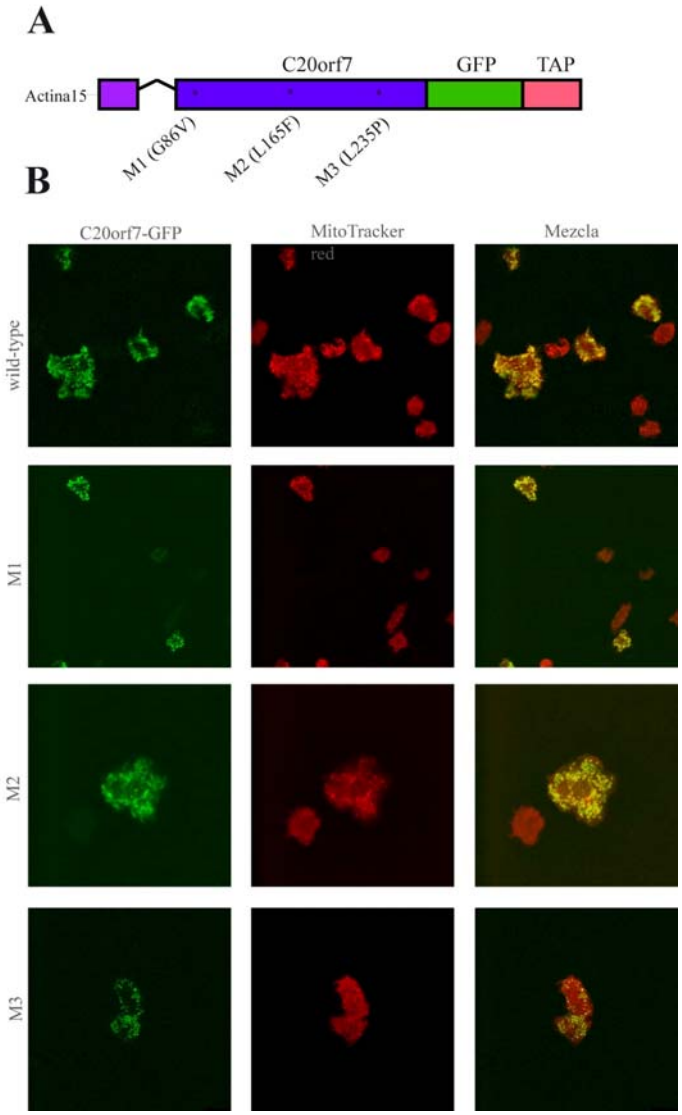

Fig. 20. Localización mitocondrial, complementación y mutagénesis dirigida. (A) Esquema de la construcción usada para la complementación o para los ensayos de mutagénesis dirigida. El gen *C20orf7* se fusionó a GFP y TAP donde la expresión del gen es dirigida bajo la acción del promotor de actina 15. La línea con forma de v representa el intrón en N-terminal. La proteína wild-type o diferentes proteínas mutantes (representadas por asteriscos y el cambio de aminoácido debajo) fueron transfectadas en células *C20orf7*. M1 es la mutación en el supuesto dominio de unión de SAM. M2 y M3 son las mutaciones en *Dictyostelium* homólogas a los cambios L159F y L229P de humano respectivamente. **(B)** Las proteínas wt y mutadas se transfectaron para determinar la localización subcelular. Todas ellas colocalizaron en mitocondria con el marcador MitoTracker Red.

2.5. Las mutaciones patogénicas de C20orf7 en pacientes de enfermedad mitocondrial recrean un estado citotopatológico en *Dictyostelium*.

Se han descrito previamente tres mutaciones diferentes en el gen *C20orf7* en pacientes. La primera (L159F) producía síndrome de Leigh en una familia de Marruecos. La segunda (L229P), descrita en una familia de Egipto, era más severa y producía un tipo de enfermedad neonatal letal. Por último el cambio G250V se ha visto en una familia Ashkenazi con síndrome de Leigh. En ninguno de los casos ha quedado claro si la presencia de estas mutaciones afecta o no a la estructura de la proteína o al posible dominio metiltransferasa. Los dos primeros residuos se encuentran altamente conservados a lo largo de la evolución y también en *Dictyostelium*. Con el objetivo de analizar el diferente efecto citopatológico que pudiesen tener ambas mutaciones llevamos acabo la mutagénesis dirigida sobre los residuos equivalentes a L159 y L229 (M2 (L165F) y M3 (L235P)) y los cambiamos por el mismo aminoácido que se encuentra presente en los pacientes **(Fig. 16A)**. De modo similar a como se hizo con el mutante M1 se fusionaron las

proteínas a GFP y se transfectaron en la cepa *C20orf7*$^{-}$. Ninguno de los dos mutantes fue capaz de complementar el fenotipo ni en asociación a bacterias ni en líquido, siendo igual al observado para el mutante nulo *C20orf7*$^{-}$ **(Fig. 21)**. Ambas proteínas mutantes colocalizaron en mitocondria con el marcador MitoTracker Red indicando que la falta de recuperación no era debida a una incorrecta localización de las proteínas **(Fig. 20B)**. Este resultado indica que la presencia de las mutaciones recrea un estado citopatológico en *Dictyostelium* de modo similar a como ocurriría en humano. Es más, ambas mutaciones parecen producir una falta de función de la proteína ya que no son capaces de revertir el fenotipo de crecimiento ni siquiera parcialmente. No se han analizado con detalle el resto de los fenotipos por lo que no podemos excluir la existencia de una recuperación parcial en algún otro fenotipo.

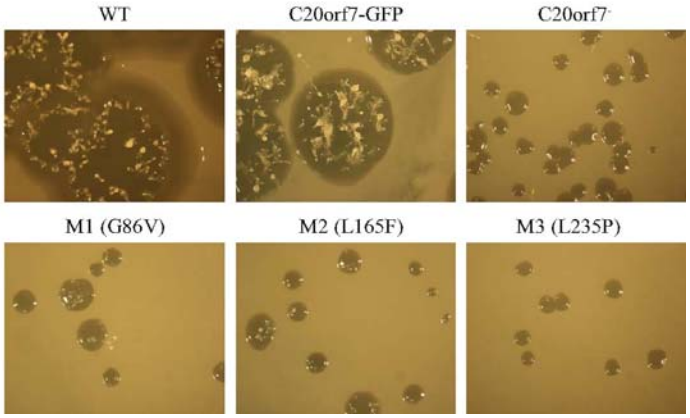

Fig. 21. Fenotipos de crecimiento defectuosos en los mutantes M1, M2 y M3. Células *C20orf7*$^{-}$ fueron transfectadas con la construcción mostrada en Fig. 20. Diferentes cepas fueron sembradas sobre placas SM en asociación a bacterias para testar el tamaño de la zona de crecimiento al cabo de 5 días. Se puede observar que la cepa transfectada con la construcción WT (cepa complementada) complementó el fenotipo con un tamaño de colonia similar al observado para WT. Sin embargo ninguna de las cepas mutantes fue capaz de recuperar el fenotipo, siendo similar al encontrado para el mutante *C20orf7*$^{-}$.

2.6. Los mutantes *C20orf7*$^{-}$ y *midA*$^{-}$ presentan agregados poliubiquitinados a pesar de tener un aumento de flujo autofágico

Como se describió en el apartado previo, parte de los fenotipos defectuosos encontrados en el mutante nulo *midA*$^{-}$ son debidos a la activación crónica de AMPK. En estudios llevados a cabo en células humanas se ha relacionado la activación de AMPK con una activación de autofagia [44, 45, 91]. Con el objetivo de comprobar si el mutante *C20orf7*$^{-}$ presentaba aumento de flujo autofágico y compararlo con el mutante *midA*$^{-}$ hemos aplicado una técnica puesta a punto previamente en nuestro laboratorio para su aplicación en *Dictyostelium*. Para ello se transfectaron células wild-type, *C20orf7*$^{-}$, *midA*$^{-}$ y *atg1*$^{-}$ (éste último utilizado como control negativo) con dos tipos de construcciones: por un lado con el marcador autofágico Atg8 fusionado a GFP y RFP (RFP-GFP-Atg8) y por otro lado con la proteína de fusión GFP-Tkt-1. La primera técnica utiliza el fenómeno de apantallamiento de la fluorescencia debido a la acidez que se produce a lo largo del flujo

autofágico por la fusión de los autofagosomas a los lisosomas. La proteína GFP es mas sensible que la RFP al ambiente acídico y proteolítico tras dicha fusión y por tanto la presencia de estructuras punteadas rojas (y no verdes) indica que el cargo ha llegado a los lisosomas y es por tanto un modo de medir el flujo autofágico. La segunda técnica nos permite visualizar por "western-blot" la degradación progresiva que se produce del marcador GFP-Tkt-1, un marcador citoplásmico que codifica la proteína transquetolasa y cuya degradación por autofagia es revelada por la aparición de un fragmento de proteolisis detectable con un anticuerpo anti-GFP. Ambas técnicas han sido ampliamente utilizadas previamente en otras especies [105]. Como puede observarse en la **Figura 22A** (panel superior) las células WT presentan un cierto flujo autofágico en condiciones de crecimiento normal, como muestra la aparición de ciertos puntos sólo rojos en algunas células. Este resultado concuerda con el obtenido utilizando la construcción GFP-Tkt-1, donde puede verse una cierta degradación de la proteína con la aparición del fragmento GFP libre **(Fig. 22B)**. Sin embargo ambos mutantes de complejo I, *C20orf7*$^-$ y *midA*$^-$, presentan un aumento de flujo autofágico, como muestra la acumulación de estructuras autofágicas coloreadas sólo en rojo **(Fig. 22A)** así como el aumento significativo de degradación de la proteína GFP-Tkt-1 (relación GFP libre/ GFP-Tkt-1) **(Fig. 22 B)**.

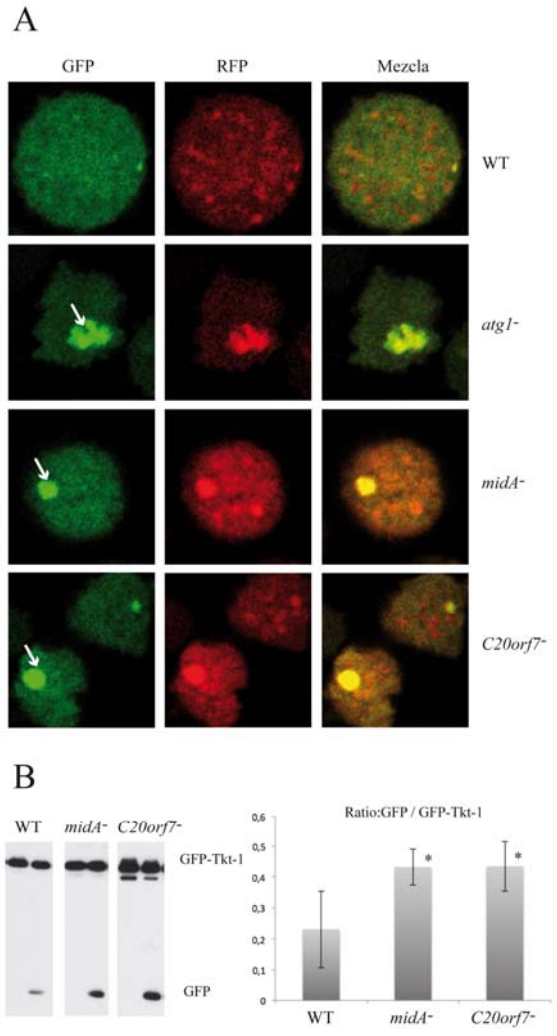

Fig. 22. *C20orf7*$^-$ y *midA*$^-$ tienen un aumento de autofagia. (A) Las cepas mostradas fueron transfectadas con la construcción RFP-GFP-Atg8, crecidas en fase exponencial en medio HL5, tratadas con 100mM de NH_4Cl (tratamiento que aumenta el ph lisosomal y permite la acumulación de productos intermedios de degradación) y visualizadas por microscopía confocal. La cepa WT presenta puntos rojos no verdes que indican un cierto flujo autofágico en medio HL5. El mutante *atg1*$^-$ presenta agregados (marcado con una flecha) que ya habían sido descritos previamente y no tiene flujo autofágico (no hay puntos rojos ni verdes en el resto del citoplasma). Por otro lado las células *C20orf7*$^-$ y *midA*$^-$ contienen agregados (marcados con flechas) pero además presentan un mayor número de estructuras sólo en rojo que podrían corresponder a fagolisosomas, indicando un posible aumento de flujo autofágico. **(B)** Células WT, *midA*$^-$ y *C20orf7*$^-$ creciendo en HL5 se transfectaron con la construcción GFP-Tkt-1 y fueron tratadas con 100mM de NH_4Cl. El panel de la izquierda muestra un experimento de "western-blot" representativo, donde se puede ver la mayor degradación de GFP-Tkt-1 en los mutantes, tratando en todos los casos con NH_4Cl (carril derecho). El panel de la derecha muestra la cuantificación con los valores medios ± d.s. Las cepas *midA*$^-$ y *C20orf7*$^-$ tienen un mayor ratio que indica aumento de flujo autofágico. Al menos tres experimentos independientes fueron llevados a cabo. Para el análisis de significancia se utilizó el test t-Student. * $p<0.05$.

Curiosamente los mutantes presentaban un enorme agregado del marcador RFP-GFP-Atg8 al igual que se ve en el mutante Atg1. Estos agregados presentan fluorescencia roja y verde por lo que no se corresponden con verdaderas estructuras autofágicas fusionadas a lisosomas (autolisosomas). En el caso del mutante *atg1*$^-$, como cabía esperar de un mutante autofágico, no se observa punteado rojo adicional en el resto del citoplasma como sí ocurre en *midA*$^-$ y *C20orf7*$^-$.

La presencia de agregados proteicos ha sido descrita previamente en enfermedades neurodegenerativas como Parkison, Alzheimer o Hungtinton donde la activación de AMPK parece jugar un papel fundamental [37, 39, 92]. En muchos casos estos agregados están formados por un gran número de proteínas poliubiquitinadas y pueden reclutar proteínas con tendencia a agregarse, como el marcador autofágico Atg8 fusionado a proteínas fluorescentes como hemos descrito previamente en mutantes autofágicos [24]. Quisimos por tanto caracterizar estos agregados en los mutantes *C20orf7*$^-$ y *midA*$^-$. Como se muestra en la **Figura 23A**, la inmunocitoquímica de células *C20orf7*$^-$ y *midA*$^-$ que habían sido transfectadas con la construcción RFP-GFP-Atg8 mostró colocalización de esta proteína en los agregados con el anticuerpo α-ubiquitina.

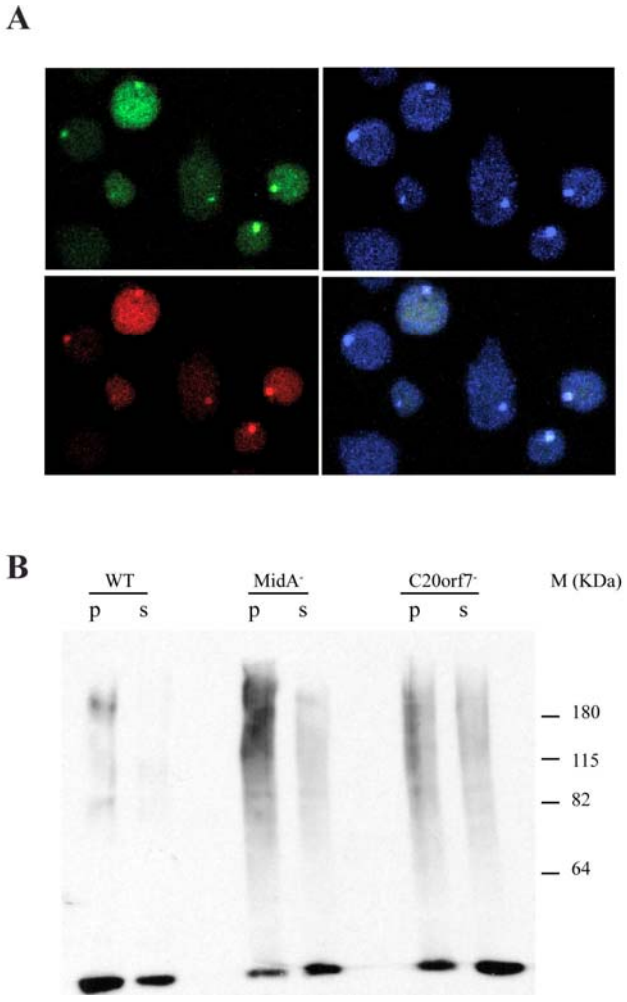

Fig. 23. Agregados de proteínas poliubiquitinadas en los mutantes *C20orf7*$^-$ y *midA*$^-$. (A) Microscopía confocal. Las células *C20orf7*$^-$ que habían sido transfectadas con la construcción RFP-GFP-Atg8 fueron fijadas e incubadas con el anticuerpo α-ubiquitina. La fotografía de *C20orf7*$^-$ muestra que los agregados positivos para el marcador RFP-GFP-Atg8 (verde-rojo, izquierda) colocalizan con el anticuerpo α-ubiquitina (azul, derecha). El mismo resultado se obtuvo para *midA*$^-$ (no mostrado). Sin embargo las células WT no presentaron dichos agregados (datos no mostrados). **(B)** Ensayo de confirmación por "western-blot". Células WT, *C20orf7*$^-$ y *midA*$^-$ fueron lisadas en buffer con 1% tritónX-100 y 0.1 % NP40. Después de centrifugar, los sobrenadantes y pellets fueron separados y cargados en un gel de poliacrilamida (8%) y transferidos por "western-blot" para detectar las proteínas poliubiquitinadas usando el anticuerpo α-ubiquitina. Un experimento representativo es mostrado. Se puede observar una clara acumulación de proteínas ubiquitinadas de alto peso molecular en *C20orf7*$^-$ y *midA*$^-$ pero no en WT.

De manera independiente, y utilizando en este caso células “wild-type”, *C20orf7*$^{-}$ y *midA*$^{-}$ que no expresan el marcador autofágico se pudo observar por “western-blot” que sólo los mutantes presentaban una acumulación insoluble de proteínas poliubiquitinadas de alto peso molecular **(Fig. 23 B)** . En conjunto estos resultados indican por primera vez que un defecto específico de complejo I mitocondrial conlleva la formación de agregados poliubiquitinados. La autofagia es un mecanismo implicado en la eliminación de agregados proteicos ubiquitinados [74] y resulta por tanto interesante que en este modelo las células mutantes no son capaces de eliminar dichos agregados a pesar del aumento observado de flujo autofágico.

Tabla S1. Distribución filogenética de MidA y Complejo I

	NDUFS7	MidA
VERTEBRADOS		
Homo sapiens	+	+
Rattus norvegicus	+	+
Danio rerio	+	+
INSECTOS		
Drosophila melanogaster	+	+
Anopheles gambiae	+	+
NEMÁTODOS		
Brugia malayi	-	-
Caenorhabditis elegans	+	+
EQUINODERMOS		
Strongylocentrotus purpuratus	+	+
HONGOS		
Aspergillus fumigatus	+	+
Aspergillus terreus	+	+
Candida albicans	+	+
Candida glabrata	-	-
Ashbya gossypii	-	-
Debaryomyces hansenii	+	+
Kluyveromyces lactis	-	-
Pichia stipitis	+	+
Saccharomyces cerevisiae	-	-
Yarrowia lipolytica	+	+
Schizosaccharomyces pombe	-	-
Cryptococcus noeformans	+	+
PROTOZOOS		
Plasmodium falciparum	-	-
Babesia bovis	-	-
Cryptosporidium parvum	-	-
Theileria parva	-	-
Leishmania major	+	+
Trypanosoma brucei	+	+
Bigelowiella natans	-	-
Cyanophora paradoxa	-	-
Monosiga brevicollis	-	-
Tetrahymena thermophila	+	-
Dictyostelium discoideum	+	+
PLANTAS		
Oriza sativa	+	+
Arabidopsis thaliana	+	+
ALGAS VERDES		
Chlamydomonas reinhardtii	+	+
ALGAS ROJAS		
Guillardia theta	-	-
Hemiselmis andersenii	+	-
ALFAPROTEOBACTERIA		
Breadyrhizobium sp	+	+
Magnetospirillum sp	+	+
Rhodopseudomonas palustris	+	+
Rickettsia felis	+	+

Tabla S2. Distribución filogenética de los homólogos de C20orf7

Organismo	E-value	Eucariotas	Bacterias	Código GenBank
Polysphondylium	7e-102	Metazoo		EFA86651.1
Drosophila	3e-67	Metazoo		NP_610922.1
Laccaria	6e-66	Hongo		XP_001877001.1
Danio rerio	3e-65	Metazoo		NP_001076363.1
Xenopus	2e-64	Metazoo		NP_001016398.1
Homo sapiens	6e-62	Metazoo		NP_077025.2
Mus musculus	2e-60	Metazoo		NP_081369.2
Anopheles	4e-60	Metazoo		XP_309862.3
Aspergillus	8e-60	Hongo		XP_662522.1
Neurospora	4e-57	Hongo		XP_956725.2
Pichia	9e-54	Hongo		XP_002492537.1
Yarrowia	5e-51	Hongo		XP_501354.1
Oriza sativa	2e-50	Planta		EEC69002.1
Vitis vinifera	4e-50	Planta		XP_002279511.1
Arabidopsis	1e-46	Planta		XP_002890535.1
Rhodospirillum	5e-46		alfaproteobacteria	YP_425827.1
Magnetospirilum	1e-45		alfaproteobacteria	YP_420968.1
Rhodomicrobium	1e-45		alfaproteobacteria	YP_004013051.1
Ochrobactrum	4e-45		alfaproteobacteria	YP_001369577.1
Brucella	6e-44		alfaproteobacteria	YP_001628309.1
Agrobacterium	3e-41		alfaproteobacteria	NP_357097.2
Caenorhabditis	7e-41	Metazoo		NP_496949.1
Rhodoseudomonas	1e-40		alfaproteobacteria	YP_530416.1
Rickettsi	4e-19		alfaproteobacteria	YP_001492229.1

DISCUSIÓN

MidA es un posible factor de ensamblaje del CI

En este trabajo hemos utilizado técnicas *in-silico* y experimentales, tanto en *Dictyostelium discoideum* como en células humanas en cultivo, que sugieren que la proteína MidA es una metiltransferasa que tiene un papel claro en la regulación del complejo I mitocondrial. Además, y gracias al uso de las dos especies, *Dictyostelium* y humano, hemos podido demostrar que las dos proteínas ortólogas mantienen su función a lo largo de la evolución.

Aproximadamente el 40 % de las enfermedades relacionadas con defectos en cadena de transporte de electrones (OXPHOS) se presentan o bien de manera aislada, o asociadas a otros genes, con mutaciones en componentes del complejo I, el más grande de todos los complejos del OXPHOS. Sin embargo existe un gran número de pacientes con defectos de complejo I donde la etiología de la enfermedad es desconocida. Dado que estos pacientes no muestran mutaciones en ninguna de las subunidades estructurales del complejo I (cuya composición ha quedado perfectamente definida desde hace tiempo), solo queda la posibilidad de que estos defectos, en caso de ser genéticos, se asocien a proteínas que regulen la actividad o que afecten al ensamblaje o estabilidad del complejo I. Dado que este complejo es enorme se piensa que todavía quedan por identificar un gran número de factores de ensamblaje y con ellos posibles mutaciones en pacientes. El mutante nulo *midA*$^-$ en *Dictyostelium* produce un importante defecto de actividad de CI y la regulación negativa de este gen en células humanas en cultivo produce un defecto de CI ensamblado, sugiriendo que MidA tiene un papel importante como factor de ensamblaje o estabilidad de CI. En células deficientes en MidA, la actividad del CI se reduce un 30% respecto a los controles, una disminución tal vez no muy fuerte, pero dentro del umbral necesario para producir un impacto en la bioenergética celular [114] o incluso producir enfermedad en humanos [89]. El complejo I está compuesto por un gran número de subunidades (hasta 45 en humano) que necesitan ensamblarse de manera correcta y secuencial en la membrana mitocondrial interna [100]. Hasta la fecha han sido descritos 9 factores de ensamblaje de CI que presentan mutaciones en pacientes, como son NDUFAF1 - F4 , C20orf7, C8orf38, ACAD9, IndI o FOXRED1 (ver Introducción). Por otro lado existen otros factores de ensamblaje como son Ecsit o AIF donde no se han descrito mutaciones hasta la fecha. De este modo proponemos *midA* como un nuevo gen candidato que debería ser tenido en cuenta en el "screening" de pacientes con defectos, posiblemente aislados, de complejo I.

El CI contiene lo que denominamos subunidades "core" o básicas, 14 subunidades codificadas tanto en el genoma nuclear como en el mitocondrial, que se encuentran presentes en el "ancestro" del complejo I en bacterias y que se consideran esenciales para la función del complejo I [43]. En todas ellas se han descrito mutaciones causando enfermedad en humanos incluyendo NDUFS2 [89, 143, 144], que en este trabajo hemos demostrado que interacciona con MidA. Curiosamente MidA presenta ortólogos en α-proteobacterias, los parientes más próximos de los ancestros de la mitocondria, lo que parece indicar una estrecha relación entre MidA y estas

subunidades básicas. NDUFS2 es codificada en el núcleo en mamíferos. Sin embargo es codificada en la mitocondria en *Dictyostelium*, apoyando el hecho aceptado de que la bacteria endosimbionte, que más tarde se convertiría en mitocondria, fue perdiendo a lo largo de la evolución gran parte de sus genes, que pasarían al control del núcleo, mucho más estricto [82, 97].

MidA contiene un dominio metiltransferasa

Las enzimas metiltransferasa dependientes de SAM no muestran una gran homología de secuencia entre ellas, pero sí que contienen un plegamiento estructural característico que sí está conservado. Sorprendentemente hay muy pocos residuos dentro de este plegamiento que sean claramente identificables en todos los casos y esto ha dificultado la asignación de MidA como una posible metiltransferasa [90, 130]. Nuestros estudios *in-silico* y experimentales sugieren fuertemente que DUF185 (a cuya familia pertenece MidA) tiene un dominio metiltransferasa. A nivel de secuencia, DUF185 presenta una pequeña región de homología con metiltransferasas, el denominado motivo I, que se corresponde precisamente a la región catalítica implicada en la unión de SAM [107]. Este motivo, que contiene tanto hélices-α como hebras-β, es el más frecuente en la superfamilia de las metiltransferasas (existen en total 5 motivos descritos) [98, 130]. La secuencia consenso es hh(D/E)hGxGxG donde h es cualquier aminoácido hidrofóbico y x puede ser cualquier residuo [107]. Es la simple presencia de esta secuencia de 9 aminoácidos lo que llevó en el pasado a la presunción de que DUF185 podría ser una familia de metiltransferasas [128]. En este trabajo hemos alterado por mutagénesis dirigida la primera y la segunda glicina de esta secuencia en MidA, observando que la primera y tal vez las dos son necesarias para la función de la proteína y por tanto sugerimos que MidA contiene este dominio metiltransferasa. Se hace necesario en el futuro testar bioquimicamente la posible función metiltransferasa e identificar los sustrados de dicha metilación.

Las metiltransferasas son una amplia familia de proteínas que pueden metilar diferentes substratos como DNA, RNA o proteínas en átomos de carbono, oxígeno, nitrógeno o azufre. Sin embargo no existen dominios o plegamientos característicos dependiendo del substrato metilado, por lo que es imposible predecir el substrato de una metiltransferasa desconocida. De hecho este es el caso del motivo I, que está presente en metiltransferasas de DNA, RNA o proteínas [68]. Por otro lado se han descrito metiltransferasas mitocondriales que utilizan como substrato DNA, tRNA o rRNA [61, 115] así como una proteína transportadora de SAM en membrana mitocondrial [2]. En el complejo I han sido descritos dos substratos de metilación : uno en diferentes histidinas en N-terminal de la proteína NDUFB3 en bovino [29] y la otra en la Arg323 en NDUFS2 de humano [160]. Dado que MidA interacciona con NDUFS2 es posible que NDUFS2 sea metilado por MidA, hipótesis muy atractiva que quedaría por confirmar en nuestro laboratorio. De este modo se abren al menos dos posibilidades: una es que MidA ejerciese su papel de factor de ensamblaje de complejo I a través de una metilación en NDUFS2 que pudiera dar estabilidad al complejo I. Dado que hemos observado MidA en intermedios de ensamblaje de complejo I en *Dictyostelium*, esta

parece la hipótesis más probable. Otra posibilidad que no podemos descartar es que tal vez MidA tenga una doble función: como factor de ensamblaje y por otro lado como metiltransferasa. La hipótesis de una doble función ha sido planteada ya anteriormente con otros factores de ensamblaje del complejo I. Por ejemplo AIF ha sido implicado como factor de ensamblaje del complejo I en mitocondria, pero durante el proceso que dispara la apoptosis independiente de caspasas, se dirige al núcleo donde curiosamente ejerce una función endonucleasa cortando el genoma nuclear .Así mismo, en estudios dirigidos generalmente a la búsqueda de mutaciones en otros factores de ensamblaje de CI, siempre se ha querido separar, con poco rigor científico, su función como posibles chaperonas de su posible función inferida por programas bioinformáticos. Esta separación de funciones sin fundamento puede estar conduciendo a la comunidad científica a un error de interpretación importante.

La compleja citopatología del mutante *midA*$^-$ y su relación con la AMPK

Los fenotipos del mutante de complejo I *midA*$^-$ presentan muchas características en común con otros defectos mitocondriales en *Dictyostelium*, pero también diferencias. Defectos en fototaxis y termotaxis se han observado previamente también en otras deficiencias mitocondriales que afectan la respiración como son la depleción de mtDNA por tratamiento con BrEt y la regulación negativa de la chaperonina Cpn60 [17, 35, 79, 158]. Del mismo modo que había sido descrito previamente para otros mutantes mitocondriales de *Dictyostelium*, la regulación negativa de AMPK en la cepa *midA*$^-$ consiguió recuperar el fenotipo de fototaxis y parcialmente el de termotaxis, demostrando que es la expresión crónica de esta quinasa la responsable al menos de estos fenotipos. No obstante las células *midA*$^-$ presentaban defectos de macropinocitosis y fagocitosis que de hecho no habían sido observados previamente en otros mutantes mitocondriales. La regulación negativa del gen que codifica AMPK no fue capaz de restaurar ninguno de los dos fenotipos, lo que deja dos posibilidades en el aire: la primera es que estos dos fenotipos sean específicos de un defecto concreto del complejo I . Cabe, en este sentido, recordar que este es el primer mutante mitocondrial de complejo I en *Dictyostelium* descrito. La segunda posibilidad es que este fenotipo sea específico del mutante *midA*$^-$. De este modo, la medida de los fenotipos de fagocitosis y macropinocitosis en el mutante *C20orf7*$^-$ se hace muy importante aunque el resultado de dichos experimentos no se pudo incluir en este trabajo.

Hemos observado un aumento en los niveles y actividad del resto de complejos de la cadena respiratoria, así como en los niveles de mtDNA, lo que sugiere un mecanismo compensatorio de la célula que intenta aumentar el número de mitocondrias y los niveles de ATP, pero que es incapaz de recuperar la función del complejo I en el mutante *midA*$^-$. La AMPK parece estar implicada en esto ya que su activación crónica produce un aumento de mitocondrias y de ATP en *Dictyostelium* así como en otros organismos [17]. De este modo, parte de los complejos fenotipos observados responden a una activación crónica de AMPK y a una defectuosa respuesta que es

incapaz de corregir la deficiencia de complejo I. Se revela de nuevo una compleja citopatología, especialmente en enfermedades asociadas a complejo I. La AMPK, que juega un papel importante en un defecto específico de complejo I en *Dictyostelium*, produciendo ciertos fenotipos aberrantes, podría ser el responsable, al menos, en parte, de ciertos fenotipos en enfermedad mitocondrial humana. De ser así, el estudio de tratamientos destinados a su regulación debería ser profundamente evaluado.

Modelización de una disfunción del gen *C20orf7* en *Dictyostelium*

En este estudio hemos podido comprobar como la función de la proteína C20orf7 parece conservarse en la evolución, desde humano a *Dictyostelium*. Prueba de esto es que la eliminación completa de C20orf7 produce un defecto específico de complejo I mitocondrial en *Dictyostelium*, de modo similar a como se ha descrito en pacientes con mutaciones en este gen y en células donde se había regulado negativamente la expresión de *C20orf7* [54, 137]. Previamente se ha descrito el posible papel de C20orf7 como factor de ensamblaje en etapas tempranas de la cadena de ensamblaje de CI dado que las diferentes mutaciones en el gen humano conducen a la desaparición de un intermedio temprano (400KDa) que contiene la subunidad ND1 [137]. A pesar de que la proteína ha sido localizada asociada a membrana mitocondrial interna no se ha hallado su localización en subcomplejos de CI.

De modo similar a como ocurría para MidA, la función de C20orf7 es desconocida y las únicas pistas provienen de predicciones usando complejos programas bioinformáticos, pero ningún estudio funcional había sido llevado a cabo hasta la fecha. Ha sido predicho un motivo tipo I metiltransferasa, que como se comentó anteriormente es el más común entre las metiltransferasas dependientes de SAM. Como en el caso de MidA este motivo contiene la secuencia consenso hh(D/E)hGxGxG donde h es cualquier aminoácido hidrofóbico y x puede ser cualquier residuo [107]. Esta secuencia se encuentra altamente conservada en la evolución y entre humano y *Dictyostelium* aunque la segunda glicina se encuentra cambiada por una arginina **(ver Fig. 16A)**. Curiosamente las regiones que contienen las mutaciones patogénicas L159F y L229P se encuentran también altamente conservadas, sobre todo en el primer caso, con un alto grado de identidades. Esto indica que los plegamientos correspondientes a estos residuos pueden ser funcionalmente importantes. A pesar de todo, los programas de predicción de estructuras generan resultados muy ambiguos. De modo que dada la imposibilidad de generar un modelo 3D de la proteína (no hay proteínas homólogas depositadas en el PDB) no podemos predecir el cambio estructural que suponen dichas mutaciones. Así y todo, llevamos a cabo la mutagénesis dirigida de los diferentes residuos, tanto del posible dominio de unión a SAM , M1 (G86V), como de las mutaciones homólogas a las encontradas en pacientes: M2 (L165F) y M3 (L235P). Curiosamente todas ellas producían una falta de función de la proteína, con fenotipos defectuosos iguales a los encontrados en el mutante KO *C20orf7*.

La importancia de la metilación en el complejo I

El mutante M1 y su falta de función nos indican que el dominio metiltransferasa es necesario para la función de C20orf7 y por tanto parece indicar que esta proteína es una posible metiltransferasa. Sin embargo, y como se ha dicho anteriormente, no somos capaces de predecir el substrato de metilación en base a la secuencia del dominio metiltransferasa. No obstante, dos subunidades de complejo I son portadoras de metilaciones. La primera, NDUFS2, es metilada en Arg323 [160]. Dado que MidA interacciona con NDUFS2 pensamos que esta metilación podría ser llevada a cabo por MidA. La otra subunidad (NDUFB3) tiene metilaciones en al menos dos residuos de histidina en N-terminal [29]. Sin embargo, utilizando la secuencia de aminoácidos y el programa Blast, no existe una proteína homóloga a NDUFB3 en *Dictyostelium*. Si ambas proteínas se encuentran relacionadas funcionalmente, esperaríamos la presencia, o ausencia, a la vez, de ambas proteínas entre diferentes especies a lo largo de la evolución. De este modo parece improbable que NDUFB3 sea metilada por C20orf7 como ha sido sugerido previamente [100, 137]. Dado que las modificaciones postraduccionales no se han estudiado en detalle en las subunidades de complejo I (sólo fragmentos N-terminal [29]) es posible que existan más metilaciones en otras subunidades de CI, que además puedan ser importantes para la estabilidad o actividad de CI. Por último C20orf7, a diferencia de MidA, no ha sido observado asociado a subcomplejos de CI. Cabe la posibilidad que el efecto producido en CI por la alteración del gen *C20orf7* sea debido a un mecanismo indirecto, lo que abre la puerta de posibles metilaciones fuera del contexto del complejo I.

Recreación de mutaciones patogénicas de C20orf7 en *Dictyostelium*

Los mutantes M2 y M3 correspondientes a las mutaciones descritas en pacientes, recrean un estado citopatológico en *Dictyostelium* con fenotipos similares a los hallados en *C20orf7*⁻ , lo que sugiere una falta de función de la proteína. Estas mutaciones afectan a una región de la proteína que parece alejada del dominio de unión de SAM, y podrían estar afectando a la estructura de la proteína más que al dominio catalítico. De modo muy interesante se han descrito diferencias importantes entre las dos mutaciones patogénicas en humano [54]. El cambio L159F (Síndrome de Leigh), equivalente a M2, conduce a un estado menos severo que permite a los pacientes llegar a edad adulta mientras que el cambio L229P (Enfermedad neonatal letal), equivalente a M3, lleva a un cuadro muy severo con muerte prematura neonatal, aunque también se ha descrito muerte prenatal. Esta severidad se correlaciona con un mayor defecto de complejo I, tanto de ensamblaje como de actividad, siendo prácticamente nula la existencia de CI en el caso de la mutación L229P. Como se comentó, el gen humano *C20orf7* codifica dos isoformas (NP_077025.2 y NP_001034464.1) que se diferencian por un splicing alternativo que lleva a una de ellas a ser más pequeña (NP_001034464.1). Mientras que la mutación L159F se encuentra solo en la primera isoforma (NP_077025.2), la mutación L229P afecta a ambas. Dado que ambas isoformas se

encuentran igualmente expresadas en todos los tejidos humanos, se ha postulado que la diferencia de severidad del cuadro clínico podría venir debida, o bien al diferente efecto estructural que puedan producir ambas mutaciones, o bien a la presencia de la segunda isoforma intacta en el caso de la mutación L159F que produciría un rescate parcial fenotípico. Esto último implicaría posiblemente que ambas isoformas tienen la misma función. La base de datos "Conserved Domains" predice un dominio metiltransferasa en ambas isoformas lo que podría apoyar esta hipótesis. Sin embargo la evolución podría haber dado lugar a la divergencia de ambas proteínas, que a pesar de tener la misma función, pudiesen metilar substratos diferentes. Aprovechando que en *Dictyostelium* sólo existe una isoforma C20orf7, hemos podido comprobar que la recreación de ambas mutaciones produce el mismo efecto de falta de función. Si las mutaciones tuviesen un efecto estructural y con ello funcional diferente, se esperaría que ambas mutaciones produjesen difrentes cuadros fenotípicos. Sin embargo, en *Dictyostelium*, ambas mutaciones parecen producir un efecto de falta de función. Esto podría apoyar la hipótesis de que la segunda isoforma juega un papel importante en el rescate parcial que conduce a un estado menos severo en pacientes con la mutación L159F.

***Dictyostelium* como un modelo de agregación proteíca en disfunción mitocondrial**

A pesar de no existir evidencias de formación de agregados proteicos en defectos genéticos específicos de OXPHOS, si que existen numerosos estudios donde el tratamiento farmacológico con inhibidores específicos de CI , como MPTP (1-methyl-4-phenyl-1,2,3,6-tetrahydropyridine) y rotenona produce, no sólo estos agregados, sino el mejor modelo existente en la actualidad para estudiar la enfermedad de Parkinson en modelos experimentales [26]. En el modelo que hace uso de MPTP se ha observado que se produce una sobreactivación de AMPK y que ésta protege en cierta medida de la muerte celular de neuronas dopaminérgicas [37]. En otro estudio independiente se observó que el tratamiento con MPTP conducía a un aumento de autofagia [164]. Dado que ha sido claramente demostrado en diferentes especies que la activación de AMPK conduce a una activación de autofagia (indirectamente a través de la activación de mTOR y directamente a través de la fosforilación de Atg1), [44, 45, 91] no sería de extrañar que la activación de autofagia en modelos de Parkinson y en nuestro modelo sea debida a la activación de AMPK. Esta es una hipótesis que quedaría pendiente de confirmar también en nuestras cepas *midA*$^{-}$ y *C20orf7*$^{-}$.

La activación de AMPK y la formación de agregados proteicos (cuerpos de Levy) no sólo es específica de Parkinson sino que también se ha visto en modelos experimentales de las enfermedades de Alzheimer y Hungtinton aunque no a través de una relación directa con el complejo I [39, 92]. Este hecho parece estar en contraposición con la activación del flujo autofágico, que se ha demostrado previamente efectivo en la eliminación de este tipo de agregados en enfermedades neurodegenerativas [86]. La poliubiquitinación es una señal que marca las proteínas que han de ser degradadas bien por el proteasoma o bien por macroautofagia. Previamente se ha

descrito que la activación de AMPK conduce a una inhibición del proteasoma en células en cultivo [149]. Y de nuevo, en otros estudios independientes se ha visto como el inhibidor de CI rotenona afecta a la función del proteasoma [38]. Parece posible pues el siguiente escenario: en nuestros mutantes mitocondriales la activación de AMPK conduciría a un aumento de autofagia para obtener energía que no es capaz de obtener por oxidación del alimento. Sin embargo el sistema del proteasoma, debido a que gasta una elevada cantidad de energía en forma de ATP, sería inhibido por la acción de AMPK. Esto produciría un exceso de proteínas ubiquitinadas favoreciendo la formación de agregados. Por tanto es posible que a pesar de que la autofagia se encuentrase activada, no fuese capaz de eliminar todas las proteínas poliubiquitinadas que deberían ser eliminadas por el sistema del proteasoma. Esta es otra hipótesis que deberá ser confirmada en el futuro mediante el estudio del proteasoma en este modelo de disfunción mitocondrial en *Dictyostelium discoideum*.

MidA, C20orf7 y balance energético

Las células *midA*$^-$ y *C20orf7*$^-$ presentan un defecto específico de complejo I, que en ambos casos se asocia con un aumento de masa mitocondrial. Sin embargo este aumento de masa mitocondrial es mayor para *C20orf7*$^-$ (68% de aumento frente a 20% en *midA*$^-$) **(ver Tabla 1)**. Así mismo el mutante *C20orf7*$^-$ presenta una subida de ATP total del 70% respecto a una bajada del 30% que se produce en el mutante *midA*$^-$. A pesar de que en pacientes de enfermedad mitocondrial se han observado niveles de ATP normales, una subida del 70% resulta muy sorprendente. No obstante existe un precedente en *C.elegans* donde la presencia de una mutación en NDUFB4, una subunidad del complejo I mitocondrial producía, del mismo modo que hemos visto para *C20orf7*$^-$, un aumento de ATP total [162]. Es más, este aumento era de hasta tres veces los niveles encontrados en controles a pesar de que la actividad del complejo I era prácticamente indetectable. Este aumento de ATP en el mutante *C20orf7*$^-$ podría ser debido, o bien a un bloqueo excesivo de las rutas anabólicas en relación a la poca producción de ATP, dado el defecto de entrada de electrones por complejo I, o bien a un defecto en rutas de retroregulación del "sensing" del ratio AMP/ATP. De nuevo parece ser que la AMPK podría jugar un papel fundamental en ambas hipótesis. En definitiva las diferencias observadas en contenido en ATP entre *midA*$^-$ y *C20orf7*$^-$ podrían ser debidas a una todavía mayor activación de AMPK en el mutante *C20orf7*$^-$, como parece indicar el aumento de masa mitocondrial que, a su vez, podría también colaborar a una mayor producción de ATP mediante la entrada de electrones en cadena respiratoria a través sobre todo de complejo II y la lanzadera del glicerol fosfato.

Tabla 1. Comparación de fenotipos

Fenotipo	*C20orf7*$^-$	*midA*$^-$
Actividad de complejo I	- 60%	- 50%
Actividad citrato sintasa	**+68%**	**+20%**
ATP	**+60%**	**- 30%**
Crecimiento en placa SM	colonias pequeñas	colonias pequeñas
Crecimiento en líquido	crecimiento lento (t_g = 14h)	crecimiento lento(t_g = 14h)
Fagocitosis	¿?	- 60%
Macropinocitosis	¿?	- 64%
Desarollo	retraso, cuerpos pequeños	retraso, cuerpos pequeños
Esporas	defectuosas	defectuosas
Fototaxis	¿?	defecto
Agregados poliubiquitinados	positivo	positivo
Flujo autofágico	aumento	aumento

Estudios previos llevados a cabo en el organismo *Dictyostelium* determinaron que la disfunción mitocondrial no afectaba de igual manera a todos los fenotipos, siendo más sensibles los fenotipos de fototaxis , termotaxis, crecimiento o desarrollo [17]. Ambos mutantes presentaron defectos en crecimiento y desarrollo, y además el mutante *midA*$^-$ presentó defectos importantes en fototaxis y termotaxis. A pesar de que el defecto de crecimiento en el mutante *midA*$^-$ se asocia a defectos en macropinocitosis y fagocitosis, en el caso de *C20orf7*$^-$ podría no ser así. Se están llevando a cabo los experimentos necesarios en *C20orf7*$^-$ para discernir sobre estos aspectos. Por otro lado, el fenotipo de desarrollo se ve afectado de igual modo en ambos mutantes con un retraso importante y un bloqueo en la fase “slug”. Además las estructuras culminantes son más pequeñas que en los controles. También las esporas de *C20orf7*$^-$ y *midA*$^-$ presentan una morfología diferente y la viabilidad , estudiada en el mutante *midA*$^-$, se ve reducida. En otros modelos de deficiencia mitocondrial de *Dictyostelium*, como la regulación negativa de Cpn60 o por tratamiento farmacológico con BrEt, se ha observado que las estructuras culminantes presentan cuellos más cortos y anchos [17, 35, 79]. Dado que la sobreactivación de AMPK es responsable de este fenotipo, se ha hipotetizado que la sobreactivación de AMPK podría conducir a un aumento de autofagia y con ello dar el primer paso necesario para la muerte celular autofágica que se ha demostrado necesaria en la diferenciación terminal de las células tallo en *Dictyostelium* y que también se ha observado en neurodegeneración en humanos [22]. Sin embargo, los fenotipos de *midA*$^-$ y *C20orf7*$^-$ en relación a la morfología del tallo son diferentes y no presentan este aspecto corto y ancho, aunque las estructuras son más pequeñas que el WT. Como hemos visto a lo largo del trabajo, las deficiencias de MidA y C20orf7 en *Dictyostelium* afectan ambas, a la actividad del CI y aunque existen aspectos comunes, también existen diferencias relevantes entre ellos en cuanto a ciertos aspectos del balance energético como la cantidad de ATP y efectos compensatorios sobre los otros complejos. No tenemos todavía una explicación plausible sobre estas diferencias, así como las que existen entre

estos mutantes y otros más generales como los inducidos por la falta de función de la Cpn60. Es posible que estas proteínas afecten de un modo diferente la actividad residual del CI o su regulación, aunque tampoco podemos rechazar la posibilidad de que ejerzan funciones adicionales en otros procesos mitocondriales. Estos estudios ponen de relieve la enorme complejidad de las deficiencias mitocondriales incluso en organismos tan sencillos como *Dictyostelium discoideum* y abre el camino para usar este modelo en el estudio de los procesos citopatológicos en las enfermedades mitocondriales.

CONCLUSIONES

CONCLUSIONES

1. La proteína MidA, tanto en *Dictyostelium discoideum* como en humano, es necesaria para la correcta función del complejo I mitocondrial. Además el mutante nulo *midA*$^{-}$ muestra un aumento generalizado de mtRNA, masa mitocondrial y aumento de actividad de otros complejos de cadena lo que puede indicar un fenómeno compensatorio para restaurar la deficiencia mitocondrial.

2. MidA interacciona con la subunidad de complejo I NDUFS2 tanto en *Dictyostelium* como en humano. Así mismo, MidA no forma parte del complejo I, aunque sí ha sido observado en asociación a subcomplejos de la cadena de ensamblaje del complejo I en *Dictyostelium discoideum.*

3. MidA es posiblemente un homodímero, de manera similar a como ha sido observado en otras metiltransferasas previamente.

4. Los estudios *in-silico* indican que MidA tiene un dominio metiltransferasa y los experimentos de mutagénesis dirigida apuntan a una posible función metiltransferasa dependiente de SAM. Este dominio metiltransferasa no es necesario en su forma nativa para la interacción con NDUFS2.

5. Los fenotipos defectuosos de fototaxis y termotaxis en *midA*$^{-}$ son debidos a la sobreactivación crónica de AMPK. Así mismo, otros fenotipos defectuosos como el crecimiento, fagocitosis o macropinocitosis son independientes de la señalización mediada por AMPK.

6. La eliminación del gen *C20orf7* en *Dictyostelium discoideum* conduce a una serie de fenotipos defectuosos en crecimiento, desarrollo y diferenciación de esporas.

7. C20orf7 es necesario para la correcta función del complejo I en *Dictyostelium discoideum*. La cepa *C20orf7*$^{-}$ no sólo produce un defecto específico de complejo I sino también un aumento de masa mitocondrial y ATP, lo que puede indicar un mecanismo compensatorio para restaurar la deficiencia mitocondrial.

8. C20orf7 es una posible metiltransferasa como demuestran los ensayos de mutagénesis dirigida en la región de unión de SAM que producen una falta de función de la proteína. Además la recreación de las mutaciones humanas L159F y L229P en los residuos homólogos L165F y L235P en *Dictyostelium discoideum* produce una falta de función de ambas proteínas.

9. Las cepas *C20orf7*$^{-}$ y *midA*$^{-}$ presentan un aumento de flujo autofágico cuando se comparan con controles, que se acompaña de la presencia de agregados poliubiquitinados similares a los encontrados en enfermedades neurodegenerativas.

10. En conjunto nuestros resultados sugieren que la función de las proteínas C20orf7 y MidA se ha conservado en la evolución desde *Dictyostelium* a humanos. Esto nos ha permitido comenzar el estudio y la modelización de su función fisiológica y patológica en *Dictyostelium discoideum*.

BIBLIOGRAFÍA

1. **Adachi, H., T. Hasebe, K. Yoshinaga, T. Ohta, and K. Sutoh**. 1994. Isolation of Dictyostelium discoideum cytokinesis mutants by restriction enzyme-mediated integration of the blasticidin S resistance marker. Biochem. Biophys. Res. Commun. **205**:1808-1814.
2. **Agrimi, G., M. A. Di Noia, C. M. Marobbio, G. Fiermonte, F. M. Lasorsa, and F. Palmieri**. 2004. Identification of the human mitochondrial S-adenosylmethionine transporter: bacterial expression, reconstitution, functional characterization and tissue distribution. The Biochemical journal **379**:183-190.
3. **Agsteribbe, E., A. Huckriede, M. Veenhuis, M. H. Ruiters, K. E. Niezen-Koning, O. H. Skjeldal, K. Skullerud, R. S. Gupta, R. Hallberg, O. P. van Diggelen, et al.** 1993. A fatal, systemic mitochondrial disease with decreased mitochondrial enzyme activities, abnormal ultrastructure of the mitochondria and deficiency of heat shock protein 60. Biochem Biophys Res Commun **193**:146-154.
4. **Ahmed, A. U., P. L. Beech, S. T. Lay, P. R. Gilson, and P. R. Fisher**. 2006. Import-associated translational inhibition: novel in vivo evidence for cotranslational protein import into Dictyostelium discoideum mitochondria. Eukaryot Cell **5**:1314-1327.
5. **Ahmed, A. U., and P. R. Fisher**. 2009. Import of nuclear-encoded mitochondrial proteins: a cotranslational perspective. Int Rev Cell Mol Biol **273**:49-68.
6. **Alexander, S., and H. Alexander**. 2011. Lead genetic studies in Dictyostelium discoideum and translational studies in human cells demonstrate that sphingolipids are key regulators of sensitivity to cisplatin and other anticancer drugs. Semin Cell Dev Biol **22**:97-104.
7. **Altschul, S. F., T. L. Madden, A. A. Schaffer, J. Zhang, Z. Zhang, W. Miller, and D. J. Lipman**. 1997. Gapped BLAST and PSI-BLAST: a new generation of protein database search programs. Nucleic Acids Res **25**:3389-3402.
8. **Andreeva, A., D. Howorth, J. M. Chandonia, S. E. Brenner, T. J. Hubbard, C. Chothia, and A. G. Murzin**. 2008. Data growth and its impact on the SCOP database: new developments. Nucleic Acids Res **36**:D419-425.
9. **Annesley, S. J., E. Bandala-Sanchez, A. U. Ahmed, and P. R. Fisher**. 2007. Filamin repeat segments required for photosensory signalling in Dictyostelium discoideum. BMC Cell Biol **8**:48.
10. **Arnoult, D., I. Tatischeff, J. Estaquier, M. Girard, F. Sureau, J. P. Tissier, A. Grodet, M. Dellinger, F. Traincard, A. Kahn, et al.** 2001. On the evolutionary conservation of the cell death pathway: mitochondrial release of an apoptosis-inducing factor during Dictyostelium discoideum cell death. Mol Biol Cell **12**:3016-3030.
11. **Baker, M. J., A. E. Frazier, J. M. Gulbis, and M. T. Ryan**. 2007. Mitochondrial protein-import machinery: correlating structure with function. Trends in cell biology **17**:456-464.
12. **Bandala-Sanchez, E., S. J. Annesley, and P. R. Fisher**. 2006. A phototaxis signalling complex in Dictyostelium discoideum. Eur J Cell Biol **85**:1099-1106.
13. **Barth, C., U. Greferath, M. Kotsifas, Y. Tanaka, S. Alexander, H. Alexander, and P. R. Fisher**. 2001. Transcript mapping and processing of mitochondrial RNA in Dictyostelium discoideum. Curr. Genet. **39**:355-364.
14. **Barth, C., P. Le, and P. R. Fisher**. 2007. Mitochondrial biology and disease in Dictyostelium. Int Rev Cytol **263**:207-252.
15. **Bergeron, R., J. M. Ren, K. S. Cadman, I. K. Moore, P. Perret, M. Pypaert, L. H. Young, C. F. Semenkovich, and G. I. Shulman**. 2001. Chronic activation of AMP kinase results in NRF-1 activation and mitochondrial biogenesis. Am J Physiol Endocrinol Metab **281**:E1340-1346.
16. **Berks, M., and R. R. Kay**. 1988. Cyclic AMP is an inhibitor of stalk cell differentiation in Dictyostelium discoideum. Dev. Biol. **126**:108-114.
17. **Bokko, P. B., L. Francione, E. Bandala-Sanchez, A. U. Ahmed, S. J. Annesley, X. Huang, T. Khurana, A. R. Kimmel, and P. R. Fisher**. 2007. Diverse cytopathologies in mitochondrial disease are caused by AMP-activated protein kinase signaling. Mol Biol Cell **18**:1874-1886.
18. **Bolender, N., A. Sickmann, R. Wagner, C. Meisinger, and N. Pfanner**. 2008. Multiple pathways for sorting mitochondrial precursor proteins. EMBO reports **9**:42-49.

19. **Bonner, J. T., W. W. Clarke jr, C. h. L. Neely jr, and M. K. Slifkin**. 1950. The orientation to light and the extremely sensitive orientation to temperature gradients in the slime mold Dictyostelium discoideum. J. Cell. Compar. Physiol. **36**:149-158.
20. **Briones, P., M. A. Vilaseca, A. Ribes, A. Vernet, M. Lluch, V. Cusi, A. Huckriede, and E. Agsteribbe**. 1997. A new case of multiple mitochondrial enzyme deficiencies with decreased amount of heat shock protein 60. J Inherit Metab Dis **20**:569-577.
21. **Calvaruso, M. A., J. Smeitink, and L. Nijtmans**. 2008. Electrophoresis techniques to investigate defects in oxidative phosphorylation. Methods **46**:281-287.
22. **Calvo-Garrido, J., S. Carilla-Latorre, Y. Kubohara, N. Santos-Rodrigo, A. Mesquita, T. Soldati, P. Golstein, and R. Escalante**. 2010. Autophagy in Dictyostelium: genes and pathways, cell death and infection. Autophagy **6**:686-701.
23. **Calvo-Garrido, J., S. Carilla-Latorre, F. Lazaro-Dieguez, G. Egea, and R. Escalante**. 2008. Vacuole membrane protein 1 is an endoplasmic reticulum protein required for organelle biogenesis, protein secretion, and development. Mol Biol Cell **19**:3442-3453.
24. **Calvo-Garrido, J., and R. Escalante**. 2010. Autophagy dysfunction and ubiquitin-positive protein aggregates in Dictyostelium cells lacking Vmp1. Autophagy **6**:100-109.
25. **Calvo, S. E., E. J. Tucker, A. G. Compton, D. M. Kirby, G. Crawford, N. P. Burtt, M. Rivas, C. Guiducci, D. L. Bruno, O. A. Goldberger, et al.** 2010. High-throughput, pooled sequencing identifies mutations in NUBPL and FOXRED1 in human complex I deficiency. Nature genetics **42**:851-858.
26. **Cannon, J. R., and J. T. Greenamyre**. 2010. Neurotoxic in vivo models of Parkinson's disease recent advances. Prog Brain Res **184**:17-33.
27. **Cardelli, J.** 2001. Phagocytosis and macropinocytosis in Dictyostelium: phosphoinositide-based processes, biochemically distinct. Traffic **2**:311-320.
28. **Carilla-Latorre, S., J. Calvo-Garrido, G. Bloomfield, J. Skelton, R. R. Kay, A. Ivens, J. L. Martinez, and R. Escalante**. 2008. Dictyostelium transcriptional responses to Pseudomonas aeruginosa: common and specific effects from PAO1 and PA14 strains. BMC Microbiol **8**:109.
29. **Carroll, J., I. M. Fearnley, J. M. Skehel, M. J. Runswick, R. J. Shannon, J. Hirst, and J. E. Walker**. 2005. The post-translational modifications of the nuclear encoded subunits of complex I from bovine heart mitochondria. Mol Cell Proteomics **4**:693-699.
30. **Cecconi, F., and B. Levine**. 2008. The role of autophagy in mammalian development: cell makeover rather than cell death. Developmental cell **15**:344-357.
31. **Clarke, M., and R. H. Gomer**. 1995. PSF and CMF, autocrine factors that regulate gene expression during growth and early development of Dictyostelium. Experientia **51**:1124-1134.
32. **Clarke, M., J. Yang, and S. Kayman**. 1988. Analysis of the prestarvation response in growing cells of Dictyostelium discoideum. Dev. Genet. **9**:315-326.
33. **Cornillon, S., C. Foa, J. Davoust, N. Buonavista, J. D. Gross, and P. Golstein**. 1994. Programmed cell death in Dictyostelium. J. Cell Sci. **107**:2691-2704.
34. **Chen, G., O. Zhuchenko, and A. Kuspa**. 2007. Immune-like phagocyte activity in the social amoeba. Science **317**:678-681.
35. **Chida, J., H. Yamaguchi, A. Amagai, and Y. Maeda**. 2004. The necessity of mitochondrial genome DNA for normal development of Dictyostelium cells. J. Cell Sci. **117**:3141-3152.
36. **Chisholm, R. L., and R. A. Firtel**. 2004. Insights into morphogenesis from a simple developmental system. Nature Rev. Mol. Cell Biol. **5**:531-541.
37. **Choi, J. S., C. Park, and J. W. Jeong**. 2010. AMP-activated protein kinase is activated in Parkinson's disease models mediated by 1-methyl-4-phenyl-1,2,3,6-tetrahydropyridine. Biochem Biophys Res Commun **391**:147-151.
38. **Chou, A. P., S. Li, A. G. Fitzmaurice, and J. M. Bronstein**. 2010. Mechanisms of rotenone-induced proteasome inhibition. Neurotoxicology **31**:367-372.
39. **Chou, S. Y., Y. C. Lee, H. M. Chen, M. C. Chiang, H. L. Lai, H. H. Chang, Y. C. Wu, C. N. Sun, C. L. Chien, Y. S. Lin, et al.** 2005. CGS21680 attenuates symptoms of Huntington's disease in a transgenic mouse model. J Neurochem **93**:310-320.
40. **Darcy, P. K., Z. Wilczynska, and P. R. Fisher**. 1994. Genetic analysis of Dictyostelium slug phototaxis mutants. Genetics **137**:977-985.

41. **de Vries, S. J., A. D. van Dijk, M. Krzeminski, M. van Dijk, A. Thureau, V. Hsu, T. Wassenaar, and A. M. Bonvin**. 2007. HADDOCK versus HADDOCK: new features and performance of HADDOCK2.0 on the CAPRI targets. Proteins **69**:726-733.
42. **Dominguez, C., R. Boelens, and A. M. Bonvin**. 2003. HADDOCK: a protein-protein docking approach based on biochemical or biophysical information. J Am Chem Soc **125**:1731-1737.
43. **Efremov, R. G., R. Baradaran, and L. A. Sazanov**. 2010. The architecture of respiratory complex I. Nature **465**:441-445.
44. **Egan, D., J. Kim, R. J. Shaw, and K. L. Guan**. 2011. The autophagy initiating kinase ULK1 is regulated via opposing phosphorylation by AMPK and mTOR. Autophagy **7**:643-644.
45. **Egan, D. F., D. B. Shackelford, M. M. Mihaylova, S. Gelino, R. A. Kohnz, W. Mair, D. S. Vasquez, A. Joshi, D. M. Gwinn, R. Taylor, et al.** 2011. Phosphorylation of ULK1 (hATG1) by AMP-activated protein kinase connects energy sensing to mitophagy. Science **331**:456-461.
46. **Eichinger, L., J. A. Pachebat, G. Glockner, M. A. Rajandream, R. Sucgang, M. Berriman, J. Song, R. Olsen, K. Szafranski, Q. Xu, et al.** 2005. The genome of the social amoeba Dictyostelium discoideum. Nature **435**:43-57.
47. **Escalante, R., and J. J. Vicente**. 2000. Dictyostelium discoideum: a model system for differentiation and patterning. Int. J. Dev. Biol. **44**:819- 835.
48. **Fassone, E., A. J. Duncan, J. W. Taanman, A. T. Pagnamenta, M. I. Sadowski, T. Holand, W. Qasim, P. Rutland, S. E. Calvo, V. K. Mootha, et al.** 2010. FOXRED1, encoding an FAD-dependent oxidoreductase complex-I-specific molecular chaperone, is mutated in infantile-onset mitochondrial encephalopathy. Hum Mol Genet **19**:4837-4847.
49. **Fearnley, I. M., J. Carroll, and J. E. Walker**. 2007. Proteomic analysis of the subunit composition of complex I (NADH:ubiquinone oxidoreductase) from bovine heart mitochondria. Methods in molecular biology (Clifton, N.J **357**:103-125.
50. **Fields, S. D., Q. Arana, J. Heuser, and M. Clarke**. 2002. Mitochondrial membrane dynamics are altered in cluA- mutants of Dictyostelium. Journal of muscle research and cell motility **23**:829-838.
51. **Finn, R. D., J. Tate, J. Mistry, P. C. Coggill, S. J. Sammut, H. R. Hotz, G. Ceric, K. Forslund, S. R. Eddy, E. L. Sonnhammer, et al.** 2008. The Pfam protein families database. Nucleic Acids Res **36**:D281-288.
52. **Fisher, F. R., E. Smith, and K. L. Williams**. 1981. An extracellular chemical signal controlling phototactic behavior by D. discoideum slugs. Cell **23**:799-807.
53. **Francis, D. W.** 1964. Some studies on phototaxis of Dictyostelium. J. Cell. Compar. Physiol. **64**:131-138.
54. **Gerards, M., W. Sluiter, B. J. van den Bosch, E. de Wit, C. M. Calis, M. Frentzen, H. Akbari, K. Schoonderwoerd, H. R. Scholte, R. J. Jongbloed, et al.** 2009. Defective complex I assembly due to C20orf7 mutations as a new cause of Leigh syndrome. J Med Genet **47**:507-512.
55. **Gilson, P. R., X. C. Yu, D. Hereld, C. Barth, A. Savage, B. R. Kiefel, S. Lay, P. R. Fisher, W. Margolin, and P. L. Beech**. 2003. Two Dictyostelium orthologs of the prokaryotic cell division protein FtsZ localize to mitochondria and are required for the maintenance of normal mitochondrial morphology. Eukaryot Cell **2**:1315-1326.
56. **Gordon, D. M., A. Dancis, and D. Pain**. 2000. Mechanisms of mitochondrial protein import. Essays Biochem **36**:61-73.
57. **Haack, T. B., K. Danhauser, B. Haberberger, J. Hoser, V. Strecker, D. Boehm, G. Uziel, E. Lamantea, F. Invernizzi, J. Poulton, et al.** 2010. Exome sequencing identifies ACAD9 mutations as a cause of complex I deficiency. Nature genetics **42**:1131-1134.
58. **Hacker, U., R. Albrecht, and M. Maniak**. 1997. Fluid-phase uptake by macropinocytosis in Dictyostelium. J. Cell Sci. **110**:105-112.
59. **Hardie, D. G.** 2007. AMP-activated/SNF1 protein kinases: conserved guardians of cellular energy. Nature reviews **8**:774-785.
60. **Heggeness, M. H., M. Simon, and S. J. Singer**. 1978. Association of mitochondria with microtubules in cultured cells. Proc Natl Acad Sci U S A **75**:3863-3866.

61. **Helm, M., H. Brule, F. Degoul, C. Cepanec, J. P. Leroux, R. Giege, and C. Florentz**. 1998. The presence of modified nucleotides is required for cloverleaf folding of a human mitochondrial tRNA. Nucleic Acids Res **26**:1636-1643.
62. **Hoefs, S. J., C. E. Dieteren, R. J. Rodenburg, K. Naess, H. Bruhn, R. Wibom, E. Wagena, P. H. Willems, J. A. Smeitink, L. G. Nijtmans, et al.** 2009. Baculovirus complementation restores a novel NDUFAF2 mutation causing complex I deficiency. Hum Mutat **30**:E728-736.
63. **Hood, D. A., and A. M. Joseph**. 2004. Mitochondrial assembly: protein import. Proc Nutr Soc **63**:293-300.
64. **Huckriede, A., and E. Agsteribbe**. 1994. Decreased synthesis and inefficient mitochondrial import of hsp60 in a patient with a mitochondrial encephalomyopathy. Biochim Biophys Acta **1227**:200-206.
65. **Hurley, R. L., K. A. Anderson, J. M. Franzone, B. E. Kemp, A. R. Means, and L. A. Witters**. 2005. The Ca2+/calmodulin-dependent protein kinase kinases are AMP-activated protein kinase kinases. J Biol Chem **280**:29060-29066.
66. **Inazu, Y., S. C. Chae, and Y. Maeda**. 1999. Transient expression of a mitochondrial gene cluster including rps4 is essential for the phase-shift of Dictyostelium cells from growth to differentiation. Developmental genetics **25**:339-352.
67. **Janssen, R. J., L. G. Nijtmans, L. P. van den Heuvel, and J. A. Smeitink**. 2006. Mitochondrial complex I: structure, function and pathology. J Inherit Metab Dis **29**:499-515.
68. **Kagan, R. M., and S. Clarke**. 1994. Widespread occurrence of three sequence motifs in diverse S-adenosylmethionine-dependent methyltransferases suggests a common structure for these enzymes. Archives of biochemistry and biophysics **310**:417-427.
69. **Kawata, T., A. Shevchenko, M. Fukuzawa, K. A. Jermyn, N. F. Totty, N. V. Zhukovskaya, A. E. Sterling, M. Mann, and J. G. Williams**. 1997. SH2 signaling in a lower eukaryote: A STAT protein that regulates stalk cell differentiation in Dictyostelium. Cell **89**:909-916.
70. **Kay, R. R.** 1987. Cell differentiation in monolayers and the investigation of slime mold morphogens. Methods in cell biology **28**:433-448.
71. **Kay, R. R., and K. A. Jermyn**. 1983. A possible morphogen controlling differentiation in Dictyostelium. Nature **303**:242-244.
72. **Kay, R. R., and C. R. L. Thompson**. 2001. Cross-induction of cell types in Dictyostelium: evidence that DIF-1 is made by prespore cells. Development **128**:4959-4966.
73. **Kelley, L. A., and M. J. Sternberg**. 2009. Protein structure prediction on the Web: a case study using the Phyre server. Nature protocols **4**:363-371.
74. **Kim, D. H., R. C. Davis, R. Furukawa, and M. Fechheimer**. 2009. Autophagy contributes to degradation of Hirano bodies. Autophagy **5**:44-51.
75. **Kimura, K., H. Kuwayama, A. Amagai, and Y. Maeda**. 2010. Developmental significance of cyanide-resistant respiration under stressed conditions: experiments in Dictyostelium cells. Development, growth & differentiation **52**:645-656.
76. **Kirchmair, J., P. Markt, S. Distinto, D. Schuster, G. M. Spitzer, K. R. Liedl, T. Langer, and G. Wolber**. 2008. The Protein Data Bank (PDB), its related services and software tools as key components for in silico guided drug discovery. Journal of medicinal chemistry **51**:7021-7040.
77. **Koehler, C. M., D. Leuenberger, S. Merchant, A. Renold, T. Junne, and G. Schatz**. 1999. Human deafness dystonia syndrome is a mitochondrial disease. Proc Natl Acad Sci U S A **96**:2141-2146.
78. **Koopman, W. J., L. G. Nijtmans, C. E. Dieteren, P. Roestenberg, F. Valsecchi, J. A. Smeitink, and P. H. Willems**. 2010. Mammalian mitochondrial complex I: biogenesis, regulation, and reactive oxygen species generation. Antioxid Redox Signal **12**:1431-1470.
79. **Kotsifas, M., C. Barth, A. De Lozanne, S. T. Lay, and P. R. Fisher**. 2002. Chaperonin 60 and mitochondrial disease in Dictyostelium. J. Muscle Res. Cell Motil. **23**:839-852.
80. **Kurth-Kraczek, E. J., M. F. Hirshman, L. J. Goodyear, and W. W. Winder**. 1999. 5' AMP-activated protein kinase activation causes GLUT4 translocation in skeletal muscle. Diabetes **48**:1667-1671.

81. **Lam, D., J. P. Levraud, M. F. Luciani, and P. Golstein**. 2007. Autophagic or necrotic cell death in the absence of caspase and bcl-2 family members. Biochem Biophys Res Commun **363**:536-541.
82. **Lang, B. F., M. W. Gray, and G. Burger**. 1999. Mitochondrial genome evolution and the origin of eukaryotes. Annual review of genetics **33**:351-397.
83. **Lazarou, M., D. R. Thorburn, M. T. Ryan, and M. McKenzie**. 2009. Assembly of mitochondrial complex I and defects in disease. Biochim Biophys Acta **1793**:78-88.
84. **Le, P., P. R. Fisher, and C. Barth**. 2009. Transcription of the Dictyostelium discoideum mitochondrial genome occurs from a single initiation site. RNA (New York, N.Y **15**:2321-2330.
85. **Leonard, J. V., and A. H. Schapira**. 2000. Mitochondrial respiratory chain disorders I: mitochondrial DNA defects. Lancet **355**:299-304.
86. **Levine, B., and G. Kroemer**. 2008. Autophagy in the pathogenesis of disease. Cell **132**:27-42.
87. **Levraud, J. P., M. Adam, M. F. Luciani, C. de Chastellier, R. L. Blanton, and P. Golstein**. 2003. Dictyostelium cell death: early emergence and demise of highly polarized paddle cells. J. Cell Biol. **160**:1105-1114.
88. **Lima, W. C., E. Lelong, and P. Cosson**. 2011. What can Dictyostelium bring to the study of Pseudomonas infections? Semin Cell Dev Biol **22**:77-81.
89. **Loeffen, J., O. Elpeleg, J. Smeitink, R. Smeets, S. Stockler-Ipsiroglu, H. Mandel, R. Sengers, F. Trijbels, and L. van den Heuvel**. 2001. Mutations in the complex I NDUFS2 gene of patients with cardiomyopathy and encephalomyopathy. Ann Neurol **49**:195-201.
90. **Loenen, W. A.** 2006. S-adenosylmethionine: jack of all trades and master of everything? Biochemical Society transactions **34**:330-333.
91. **Loffler, A. S., S. Alers, A. M. Dieterle, H. Keppeler, M. Franz-Wachtel, M. Kundu, D. G. Campbell, S. Wesselborg, D. R. Alessi, and B. Stork**. 2011. Ulk1-mediated phosphorylation of AMPK constitutes a negative regulatory feedback loop. Autophagy **7**:696-706.
92. **Lopez-Lopez, C., M. O. Dietrich, F. Metzger, H. Loetscher, and I. Torres-Aleman**. 2007. Disturbed cross talk between insulin-like growth factor I and AMP-activated protein kinase as a possible cause of vascular dysfunction in the amyloid precursor protein/presenilin 2 mouse model of Alzheimer's disease. J Neurosci **27**:824-831.
93. **Lopez, G., A. Valencia, and M. L. Tress**. 2007. firestar--prediction of functionally important residues using structural templates and alignment reliability. Nucleic Acids Res **35**:W573-577.
94. **Ludtmann, M. H., K. Boeckeler, and R. S. Williams**. 2011. Molecular pharmacology in a simple model system: Implicating MAP kinase and phosphoinositide signalling in bipolar disorder. Semin Cell Dev Biol **22**:105-113.
95. **Macasev, D., J. Whelan, E. Newbigin, M. C. Silva-Filho, T. D. Mulhern, and T. Lithgow**. 2004. Tom22', an 8-kDa trans-site receptor in plants and protozoans, is a conserved feature of the TOM complex that appeared early in the evolution of eukaryotes. Molecular biology and evolution **21**:1557-1564.
96. **Maniak, M.** 2011. Dictyostelium as a model for human lysosomal and trafficking diseases. Semin Cell Dev Biol **22**:114-119.
97. **Margulis, L.** 1975. Symbiotic theory of the origin of eukaryotic organelles; criteria for proof. Symposia of the Society for Experimental Biology:21-38.
98. **Martin, J. L., and F. M. McMillan**. 2002. SAM (dependent) I AM: the S-adenosylmethionine-dependent methyltransferase fold. Curr Opin Struct Biol **12**:783-793.
99. **Maselli, A., G. Laevsky, and D. A. Knecht**. 2002. Kinetics of binding, uptake and degradation of live fluorescent (DsRed) bacteria by Dictyostelium discoideum. Microbiology **148**:413-420.
100. **McKenzie, M., and M. T. Ryan**. 2010. Assembly factors of human mitochondrial complex I and their defects in disease. IUBMB life **62**:497-502.
101. **McMains, V. C., X. H. Liao, and A. R. Kimmel**. 2008. Oscillatory signaling and network responses during the development of Dictyostelium discoideum. Ageing Res Rev **7**:234-248.
102. **McPhee, C. K., and E. H. Baehrecke**. 2009. Autophagy in Drosophila melanogaster. Biochim Biophys Acta **1793**:1452-1456.

103. **Melendez, A., and B. Levine**. 2009. Autophagy in C. elegans. WormBook:1-26.
104. **Meyer, I., O. Kuhnert, and R. Graf**. 2011. Functional analyses of lissencephaly-related proteins in Dictyostelium. Semin Cell Dev Biol **22**:89-96.
105. **Mizushima, N., T. Yoshimori, and B. Levine**. 2010. Methods in mammalian autophagy research. Cell **140**:313-326.
106. **Momcilovic, M., S. P. Hong, and M. Carlson**. 2006. Mammalian TAK1 activates Snf1 protein kinase in yeast and phosphorylates AMP-activated protein kinase in vitro. J Biol Chem **281**:25336-25343.
107. **Niewmierzycka, A., and S. Clarke**. 1999. S-Adenosylmethionine-dependent methylation in Saccharomyces cerevisiae. Identification of a novel protein arginine methyltransferase. J Biol Chem **274**:814-824.
108. **Nouws, J., L. Nijtmans, S. M. Houten, M. van den Brand, M. Huynen, H. Venselaar, S. Hoefs, J. Gloerich, J. Kronick, T. Hutchin, et al.** 2010. Acyl-CoA dehydrogenase 9 is required for the biogenesis of oxidative phosphorylation complex I. Cell Metab **12**:283-294.
109. **Ogawa, S., R. Yoshino, K. Angata, M. Iwamoto, M. Pi, K. Kuroe, K. Matsuo, T. Morio, H. Urushihara, K. Yanagisawa, et al.** 2000. The mitochondrial DNA of Dictyostelium discoideum: complete sequence, gene content and genome organization. Mol Gen Genet **263**:514-519.
110. **Ogilvie, I., N. G. Kennaway, and E. A. Shoubridge**. 2005. A molecular chaperone for mitochondrial complex I assembly is mutated in a progressive encephalopathy. J Clin Invest **115**:2784-2792.
111. **Pagliarini, D. J., S. E. Calvo, B. Chang, S. A. Sheth, S. B. Vafai, S. E. Ong, G. A. Walford, C. Sugiana, A. Boneh, W. K. Chen, et al.** 2008. A mitochondrial protein compendium elucidates complex I disease biology. Cell **134**:112-123.
112. **Pan, P., E. M. Hall, and J. T. Bonner**. 1972. Folic acid as second chemotactic substance in the cellular slime moulds. Nature New Biol. **237**:181-182.
113. **Pang, K. M., M. A. Lynes, and D. A. Knecht**. 1999. Variables controlling the expression level of exogenous genes in Dictyostelium. Plasmid **41**:187-197.
114. **Pathak, R. U., and G. P. Davey**. 2008. Complex I and energy thresholds in the brain. Biochim Biophys Acta **1777**:777-782.
115. **Pintard, L., J. M. Bujnicki, B. Lapeyre, and C. Bonnerot**. 2002. MRM2 encodes a novel yeast mitochondrial 21S rRNA methyltransferase. EMBO J **21**:1139-1147.
116. **Poels, J., M. R. Spasic, P. Callaerts, and K. K. Norga**. 2009. Expanding roles for AMP-activated protein kinase in neuronal survival and autophagy. BioEssays **31**:944-952.
117. **Poff, K. L., and D. P. Hader**. 1984. An action spectrum for phototaxis by pseudoplasmodia of Dictyostelium discoideum. Photochem. Photobiol. **39**:433-436.
118. **Poff, K. L., and M. Skokut**. 1977. Thermotaxis by pseudoplasmodia of Dictyostelium discoideum. Proc. Natl. Acad. Sci. USA **74**:2007-2010.
119. **Porter, C. T., G. J. Bartlett, and J. M. Thornton**. 2004. The Catalytic Site Atlas: a resource of catalytic sites and residues identified in enzymes using structural data. Nucleic Acids Res **32**:D129-133.
120. **Pradelli, L. A., M. Beneteau, and J. E. Ricci**. 2010. Mitochondrial control of caspase-dependent and -independent cell death. Cell Mol Life Sci **67**:1589-1597.
121. **Raff, R. A.** 1996. The Shape of Life: Genes, Development, and the Evolution of Animal Form.
122. **Rain, J. C., L. Selig, H. De Reuse, V. Battaglia, C. Reverdy, S. Simon, G. Lenzen, F. Petel, J. Wojcik, V. Schachter, et al.** 2001. The protein-protein interaction map of Helicobacter pylori. Nature **409**:211-215.
123. **Raper, K. B.** 1935. Dictyostelium discoideum, a new species of slime mold from decaying forest leaves. J. Agr. Res. **50**:135-147.
124. **Roisin-Bouffay, C., M. F. Luciani, G. Klein, J. P. Levraud, M. Adam, and P. Golstein**. 2004. Developmental cell death in Dictyostelium does not require paracaspase. J Biol Chem **279**:11489-11494.
125. **Rossignol, R., B. Faustin, C. Rocher, M. Malgat, J. P. Mazat, and T. Letellier**. 2003. Mitochondrial threshold effects. The Biochemical journal **370**:751-762.

126. **Saada, A., S. Edvardson, A. Shaag, W. K. Chung, R. Segel, C. Miller, C. Jalas, and O. Elpeleg**. 2011. Combined OXPHOS complex I and IV defect, due to mutated complex I assembly factor C20ORF7. J Inherit Metab Dis.
127. **Saada, A., R. O. Vogel, S. J. Hoefs, M. A. van den Brand, H. J. Wessels, P. H. Willems, H. Venselaar, A. Shaag, F. Barghuti, O. Reish, et al.** 2009. Mutations in NDUFAF3 (C3ORF60), encoding an NDUFAF4 (C6ORF66)-interacting complex I assembly protein, cause fatal neonatal mitochondrial disease. Am J Hum Genet **84**:718-727.
128. **Sadreyev, R. I., D. Baker, and N. V. Grishin**. 2003. Profile-profile comparisons by COMPASS predict intricate homologies between protein families. Protein Sci **12**:2262-2272.
129. **Schnitzler, G. R., W. H. Fischer, and R. A. Firtel**. 1994. Cloning and characterization of the G-box binding factor, an essential component of the developmental switch between early and late development in Dictyostelium. Genes Devel. **8**:502-514.
130. **Schubert, H. L., R. M. Blumenthal, and X. Cheng**. 2003. Many paths to methyltransfer: a chronicle of convergence. Trends in biochemical sciences **28**:329-335.
131. **Sharma, L. K., J. Lu, and Y. Bai**. 2009. Mitochondrial respiratory complex I: structure, function and implication in human diseases. Curr Med Chem **16**:1266-1277.
132. **Shaulsky, G., and W. F. Loomis**. 1993. Cell type regulation in response to expression of ricin-A in Dictyostelium. Dev. Biol. **160**:85-98.
133. **Sheftel, A. D., O. Stehling, A. J. Pierik, D. J. Netz, S. Kerscher, H. P. Elsasser, I. Wittig, J. Balk, U. Brandt, and R. Lill**. 2009. Human ind1, an iron-sulfur cluster assembly factor for respiratory complex I. Mol Cell Biol **29**:6059-6073.
134. **Shoubridge, E. A., and T. Wai**. 2007. Mitochondrial DNA and the mammalian oocyte. Current topics in developmental biology **77**:87-111.
135. **Shutt, T. E., and G. S. Shadel**. 2010. A compendium of human mitochondrial gene expression machinery with links to disease. Environ Mol Mutagen **51**:360-379.
136. **Steinert, M.** 2010. Pathogen-host interactions in Dictyostelium, Legionella, Mycobacterium and other pathogens. Semin Cell Dev Biol **22**:70-76.
137. **Sugiana, C., D. J. Pagliarini, M. McKenzie, D. M. Kirby, R. Salemi, K. K. Abu-Amero, H. H. Dahl, W. M. Hutchison, K. A. Vascotto, S. M. Smith, et al.** 2008. Mutation of C20orf7 disrupts complex I assembly and causes lethal neonatal mitochondrial disease. Am J Hum Genet **83**:468-478.
138. **Sussman, M.** 1987. Cultivation and synchronous morphogenesis of Dictyostelium under controlled experimental conditions. Meth. Cell Biol. **28**:9-29.
139. **Svoboda, A., and I. Slaninova**. 1997. Colocalization of microtubules and mitochondria in the yeast Schizosaccharomyces japonicus var. versatilis. Can J Microbiol **43**:945-953.
140. **Tiranti, V., P. Chariot, F. Carella, A. Toscano, P. Soliveri, P. Girlanda, F. Carrara, G. M. Fratta, F. M. Reid, C. Mariotti, et al.** 1995. Maternally inherited hearing loss, ataxia and myoclonus associated with a novel point mutation in mitochondrial tRNASer(UCN) gene. Hum Mol Genet **4**:1421-1427.
141. **Torija, P., A. Robles, and R. Escalante**. 2006. Optimization of a large-scale gene disruption protocol in Dictyostelium and analysis of conserved genes of unknown function. BMC Microbiol **6**:75.
142. **Torija, P., J. J. Vicente, T. B. Rodrigues, A. Robles, S. Cerdan, L. Sastre, R. M. Calvo, and R. Escalante**. 2006. Functional genomics in Dictyostelium: MidA, a new conserved protein, is required for mitochondrial function and development. J Cell Sci **119**:1154-1164.
143. **Tuppen, H. A., V. E. Hogan, L. He, E. L. Blakely, L. Worgan, M. Al-Dosary, G. Saretzki, C. L. Alston, A. A. Morris, M. Clarke, et al.** 2010. The p.M292T NDUFS2 mutation causes complex I-deficient Leigh syndrome in multiple families. Brain **133**:2952-2963.
144. **Ugalde, C., R. J. Janssen, L. P. van den Heuvel, J. A. Smeitink, and L. G. Nijtmans**. 2004. Differences in assembly or stability of complex I and other mitochondrial OXPHOS complexes in inherited complex I deficiency. Hum Mol Genet **13**:659-667.
145. **Vahsen, N., C. Cande, J. J. Briere, P. Benit, N. Joza, N. Larochette, P. G. Mastroberardino, M. O. Pequignot, N. Casares, V. Lazar, et al.** 2004. AIF deficiency compromises oxidative phosphorylation. EMBO J **23**:4679-4689.

146. **van Es, S., D. Wessels, D. R. Soll, J. Borleis, and P. N. Devreotes**. 2001. Tortoise, a novel mitochondrial protein, is required for directional responses of Dictyostelium in chemotactic gradients. J Cell Biol **152**:621-632.
147. **Van Gestel, K., R. H. Kohler, and J. P. Verbelen**. 2002. Plant mitochondria move on F-actin, but their positioning in the cortical cytoplasm depends on both F-actin and microtubules. J Exp Bot **53**:659-667.
148. **Varnum, B., and D. R. Soll**. 1984. Effects of cAMP on single cell motility in Dictyostelium. J. Cell Biol. **99**:1151-1155.
149. **Viana, R., C. Aguado, I. Esteban, D. Moreno, B. Viollet, E. Knecht, and P. Sanz**. 2008. Role of AMP-activated protein kinase in autophagy and proteasome function. Biochem Biophys Res Commun **369**:964-968.
150. **Vogel, R. O., R. J. Janssen, C. Ugalde, M. Grovenstein, R. J. Huijbens, H. J. Visch, L. P. van den Heuvel, P. H. Willems, M. Zeviani, J. A. Smeitink, et al.** 2005. Human mitochondrial complex I assembly is mediated by NDUFAF1. The FEBS journal **272**:5317-5326.
151. **Vogel, R. O., R. J. Janssen, M. A. van den Brand, C. E. Dieteren, S. Verkaart, W. J. Koopman, P. H. Willems, W. Pluk, L. P. van den Heuvel, J. A. Smeitink, et al.** 2007. Cytosolic signaling protein Ecsit also localizes to mitochondria where it interacts with chaperone NDUFAF1 and functions in complex I assembly. Genes & development **21**:615-624.
152. **Wallace, A. C., R. A. Laskowski, and J. M. Thornton**. 1995. LIGPLOT: a program to generate schematic diagrams of protein-ligand interactions. Prot. Eng.:127-134.
153. **Wallace, D. C., and W. Fan**. 2010. Energetics, epigenetics, mitochondrial genetics. Mitochondrion **10**:12-31.
154. **West, C. M.** 2003. Comparative analysis of spore coat formation, structure, and function in Dictyostelium. Int. Rev. Cyotol. **222**:237-293.
155. **Westermann, B.** 2010. Mitochondrial dynamics in model organisms: what yeasts, worms and flies have taught us about fusion and fission of mitochondria. Semin Cell Dev Biol **21**:542-549.
156. **Westermann, B.** 2010. Mitochondrial fusion and fission in cell life and death. Nature reviews **11**:872-884.
157. **Wienke, D. C., M. L. Knetsch, E. M. Neuhaus, M. C. Reedy, and D. J. Manstein**. 1999. Disruption of a dynamin homologue affects endocytosis, organelle morphology, and cytokinesis in Dictyostelium discoideum. Mol Biol Cell **10**:225-243.
158. **Wilczynska, Z., C. Barth, and P. R. Fisher**. 1997. Mitochondrial mutations impair signal transduction in Dictyostelium discoideum slugs. Biochem. Biophys. Res. Commun. **234**:39-43.
159. **Woods, A., S. R. Johnstone, K. Dickerson, F. C. Leiper, L. G. Fryer, D. Neumann, U. Schlattner, T. Wallimann, M. Carlson, and D. Carling**. 2003. LKB1 is the upstream kinase in the AMP-activated protein kinase cascade. Curr Biol **13**:2004-2008.
160. **Wu, C. C., M. J. MacCoss, K. E. Howell, and J. R. Yates, 3rd**. 2003. A method for the comprehensive proteomic analysis of membrane proteins. Nat Biotechnol **21**:532-538.
161. **Yamada, Y., and K. Okamoto**. 1992. Cell-type-specific responsiveness to cAMP in cell differentiation of Dictyostelium discoideum. Dev. Biol. **149**:235-237.
162. **Yang, W., and S. Hekimi**. 2010. Two modes of mitochondrial dysfunction lead independently to lifespan extension in Caenorhabditis elegans. Aging Cell **9**:433-447.
163. **Zemla, A.** 2003. LGA: A method for finding 3D similarities in protein structures. Nucleic Acids Res **31**:3370-3374.
164. **Zhu, J. H., C. Horbinski, F. Guo, S. Watkins, Y. Uchiyama, and C. T. Chu**. 2007. Regulation of autophagy by extracellular signal-regulated protein kinases during 1-methyl-4-phenylpyridinium-induced cell death. Am J Pathol **170**:75-86.
165. **Zhu, Q., D. Hulen, T. Liu, and M. Clarke**. 1997. The cluA- mutant of Dictyostelium identifies a novel class of proteins required for dispersion of mitochondria. Proc Natl Acad Sci U S A **94**:7308-7313.
166. **Zong, H., J. M. Ren, L. H. Young, M. Pypaert, J. Mu, M. J. Birnbaum, and G. I. Shulman**. 2002. AMP kinase is required for mitochondrial biogenesis in skeletal muscle in response to chronic energy deprivation. Proc Natl Acad Sci U S A **99**:15983-15987.

ANEXO

Artículos que forman parte de la Tesis:

MidA is a putative methyltransferase that is required for mitochondrial complex I function. Carilla-Latorre S, Gallardo ME, Annesley SJ, Calvo-Garrido J, Graña O, Accari SL, Smith PK, Valencia A, Garesse R, Fisher PR, Escalante R. J Cell Sci. 2010 May 15;123(Pt 10):1674-83. Epub 2010 Apr 20.

The *Dictyostelium* model for mitochondrial disease.
Francione LM, Annesley SJ, **Carilla-Latorre S**, Escalante R, Fisher PR.
Semin Cell Dev Biol. 2011 Feb;22(1):120-30. Epub 2010 Dec 1.

Artículos relacionados:

***Dictyostelium* transcriptional responses to *Pseudomonas aeruginosa*: common and specific effects from PAO1 and PA14 strains**. **Carilla-Latorre S**, Calvo-Garrido J, Bloomfield G, Skelton J, Kay RR, Ivens A, Martinez JL, Escalante R. BMC Microbiol. 2008 Jun 30;8:109.

Vacuole membrane protein 1 is an endoplasmic reticulum protein required for organelle biogenesis, protein secretion, and development. Calvo-Garrido J, **Carilla-Latorre S**, Lázaro-Diéguez F, Egea G, Escalante R. Mol Biol Cell. 2008 Aug;19(8):3442-53. Epub 2008 Jun 11.

Vacuole membrane protein 1, autophagy and much more. Calvo-Garrido J, **Carilla-Latorre S**, Escalante R. Autophagy. 2008 Aug 16;4(6):835-7. Epub 2008 Jul 9.

Autophagy in *Dictyostelium*: genes and pathways, cell death and infection.
Calvo-Garrido J, **Carilla-Latorre S**, Kubohara Y, Santos-Rodrigo N, Mesquita A, Soldati T, Golstein P, Escalante R. Autophagy. 2010 Aug 16;6(6):686-701. Epub 2010 Aug 28. Review.

A proteolytic cleavage assay to monitor autophagy in *Dictyostelium discoideum*.
Javier Calvo-Garrido, **Sergio Carilla-Latorre**, Ana Mesquita and Ricardo Escalante. Autophagy. 2011. In press.

MidA is a putative methyltransferase that is required for mitochondrial complex I function

Sergio Carilla-Latorre[1], M. Esther Gallardo[1,2], Sarah J. Annesley[3], Javier Calvo-Garrido[1], Osvaldo Graña[4], Sandra L. Accari[3], Paige K. Smith[3], Alfonso Valencia[4], Rafael Garesse[1,2], Paul R. Fisher[3] and Ricardo Escalante[1,*]

[1]Instituto de Investigaciones Biomédicas "Alberto Sols" (CSIC-UAM), Arturo Duperier 4, 28029 Madrid, Spain
[2]CIBERER, ISCIII, Madrid, Spain
[3]Department of Microbiology, La Trobe University, Melbourne, Victoria 3086, Australia
[4]O. G., Bioinformatics Unit, Structural Biology and Biocomputing Program, A. V., Structural Computational Biology Group, Structural Biology and Biocomputing Program, Centro Nacional de Investigaciones Oncológicas, C/ Melchor Fernández Almagro, 3, 28029 Madrid, Spain
*Author for correspondence (rescalante@iib.uam.es)

Accepted 22 February 2010
Journal of Cell Science 123, 1674-1683

doi:10.1242/jcs.066076

Summary

Dictyostelium and human MidA are homologous proteins that belong to a family of proteins of unknown function called DUF185. Using yeast two-hybrid screening and pull-down experiments, we showed that both proteins interact with the mitochondrial complex I subunit NDUFS2. Consistent with this, *Dictyostelium* cells lacking MidA showed a specific defect in complex I activity, and knockdown of human MidA in HEK293T cells resulted in reduced levels of assembled complex I. These results indicate a role for MidA in complex I assembly or stability. A structural bioinformatics analysis suggested the presence of a methyltransferase domain; this was further supported by site-directed mutagenesis of specific residues from the putative catalytic site. Interestingly, this complex I deficiency in a *Dictyostelium midA*$^{-}$ mutant causes a complex phenotypic outcome, which includes phototaxis and thermotaxis defects. We found that these aspects of the phenotype are mediated by a chronic activation of AMPK, revealing a possible role of AMPK signaling in complex I cytopathology.

Key words: *Dictyostelium*, Complex I, MidA, PRO1853, *C2orf56*, LOC55471, DUF185

Introduction

Mitochondrial diseases are caused by mutations that affect genes encoded in both the mitochondrial and nuclear genomes. The pathological phenotypic outcomes of mitochondrial diseases are very complex and include blindness, deafness, epilepsy, heart disease, and muscle and neurological disorders. Although much is known about the associated mutations, the relationship between genotype and phenotype is complicated and poorly understood. Surprisingly, the same genetic defect can result in different symptoms, and conversely, similar outcomes can be caused by different genetic lesions (Debray et al., 2008; DiMauro and Schon, 2008).

Among mitochondrial diseases, deficiencies in complex I (CI) are very relevant in human pathology because about 40% of mitochondrial OXPHOS diseases involve complex I defects, and the molecular cause of this deficiency is unknown in many patients (Janssen et al., 2006; Lazarou et al., 2009). Most cellular ATP is generated by the mitochondria through aerobic respiration. Together with complex III and complex IV, CI contributes to the generation of a proton gradient across the mitochondrial inner membrane. This proton gradient is used by the ATP synthase (complex V) for ATP production. Mitochondrial CI (NADH: ubiquinone oxidoreductase, EC 1.6.5.3) is a huge multiprotein complex of 45 subunits in mammals. Of the five major respiratory complexes, CI is the least understood, partly because of its large size and complexity. Accordingly, it is believed that new components involved in the assembly, stability and/or activity of CI still remain to be identified (Koopman et al., 2010; Remacle et al., 2008).

Extensive post-translational modifications of complex I subunits have been described, most of which affect the N-termini. Examples include the loss of mitochondrial import sequences and N-alpha-acetylation. Phosphorylation in several CI subunits has also been described to affect CI function. Mutational analysis of the phosphorylation sites of NDUFA1 and NDUFB11 revealed defects in CI assembly (Koopman et al., 2010). The presence of methylation in two CI subunits has also been previously described, although the functional relevance and the methyltransferase responsible are not yet known (Carroll et al., 2005; Fearnley et al., 2007; Wu et al., 2003). In contrast to N-alpha-acetylation, which appears to be a permanent modification, and similarly to phosphorylation, protein methylation might be reversible by demethylases and might have a regulatory role.

The social amoeba *Dictyostelium discoideum* is a useful model for the study of biological issues that are relevant to human disease, including mitochondrial dysfunction (Annesley and Fisher, 2009a; Barth et al., 2007; Bokko et al., 2007; Chida et al., 2004; Kotsifas et al., 2002; Torija et al., 2006b; Williams et al., 2006). *Dictyostelium* cells feed on bacteria and remain in the form of individual cells while food is present. However, when the supply of bacteria is exhausted, starvation triggers a remarkable process of cellular chemotaxis, allowing the formation of cell aggregates. These aggregates differentiate to form phototactic migrating slugs that eventually give rise to fruiting bodies containing spores that allow *Dictyostelium* to survive (Escalante and Vicente, 2000). This developmental program is sensitive to mitochondrial dysfunction, and slug phototaxis and thermotaxis in particular are affected by diverse mitochondrial defects (Annesley and Fisher, 2009b;

Journal of Cell Science

Wilczynska et al., 1997). Moreover, *Dictyostelium*, as opposed to the yeast model *Saccharomyces cerevisiae*, contains all the essential CI subunits (Eichinger et al., 2005; Ogawa et al., 2000).

Traditionally, it has been assumed that mitochondrial diseases mediate their effects on the phenotype through the reduced availability of ATP. However, recent studies in *Dictyostelium* suggest that some symptoms might be the consequence of abnormal regulation of signaling pathways. The relationship between AMP-activated protein kinase (AMPK), a master regulator of the energy status of the cell, and mitochondrial diseases has been recognized recently using *Dictyostelium* as an experimental model (Bokko et al., 2007). Previous studies suggest that a chronic activation of AMPK might be a key element in some of the observed phenotypes that are present in mitochondrial dysfunction (Barth et al., 2007).

Recently, we described the identification and initial characterization of a new mitochondrial protein conserved between *Dictyostelium* and humans that we named MidA (for mitochondrial dysfunction protein A) (Torija et al., 2006a; Torija et al., 2006b). This protein belongs to an uncharacterized conserved protein family (DUF185 or COG1565). It shows high similarity to the human protein of unknown function LOC55471 encoded on chromosome 2 (C2orf56 or PRO1853).

Dictyostelium midA^{-} cells showed reduced levels of ATP and a wide array of phenotypes, including slow growth and abnormal development. In this report, we have further analyzed the function of this mitochondrial protein using an integrated approach of bioinformatics and molecular genetics in *Dictyostelium* and human cell culture. The loss of MidA generated a mitochondrial dysfunction that specifically affected CI activity and the levels of the fully assembled complex. Moreover, both *Dictyostelium* and human MidA proteins interact with NDUFS2, an essential CI core subunit. The molecular function of MidA was studied by bioinformatics and site-directed mutagenesis. The results indicate the presence in this protein family (DUF185) of a methyltransferase fold, suggesting that methylation has an important role in CI function. The phenotypic outcome observed in the *Dictyostelium midA*$^{-}$ null mutant reveals the complexity of CI mitochondrial disease and the contribution of AMPK signaling.

Results

Dictyostelium and human MidA mitochondrial proteins are required for complex I activity

Dictyostelium and human MidA are highly homologous proteins. Our previous studies in *Dictyostelium* showed that MidA is a mitochondrial protein involved in bioenergetics and its high sequence homology among species suggested the possibility of functional conservation between humans and *Dictyostelium* (Torija et al., 2006b). We wanted to test this hypothesis and extend our knowledge of the function of these proteins. Consequently, our first aim was to determine the subcellular localization of MidA in human cells. A construct expressing the human protein fused to GFP was transiently transfected into HeLa and HEK293T cells, which were then stained with the mitochondria-specific dye Mitotracker Red. As shown in supplementary material Fig. S1, human MidA was also localized in mitochondria.

We next took advantage of comparative genomic tools to design working hypotheses about MidA function. There are homologues of MidA in many organisms but it seems to be absent in others and this phylogenetic profile might provide important functional clues. It is expected that proteins working together in a given function will have the same phylogenetic profile. Using the String server (http://string.embl.de/), we obtained very similar phylogenetic profiles for CI subunits, well known CI assembly factors and MidA. A more detailed analysis using a wide array of species is shown in supplementary material Table S1. There is a clear correlation between the presence of MidA and a representative complex I subunit (NDUFS7). It is well known that CI is not present in all eukaryotes (such as fermentative yeasts *S. cerevisiae* and *S. pombe*) but it is present in higher eukaryotes and *Dictyostelium* where it has a key role in ATP generation. As expected, MidA has no homologues in *S. cerevisiae* and *S. pombe*. Interestingly, MidA homologues are also found in α-proteobacteria, the closest living organisms to the putative precursors of eukaryote mitochondria.

To test the hypothesis of a functional connection between MidA and CI, we measured the activity of the OXPHOS complexes (I, II, III and IV) in *Dictyostelium midA*$^{-}$ null cells. A 50% decrease in the activity of CI in *Dictyostelium* was observed (Fig. 1A). Interestingly, the activity of the other complexes was either unaffected or was significantly higher in the mutant. This might be explained by a compensatory response to the loss of CI activity.

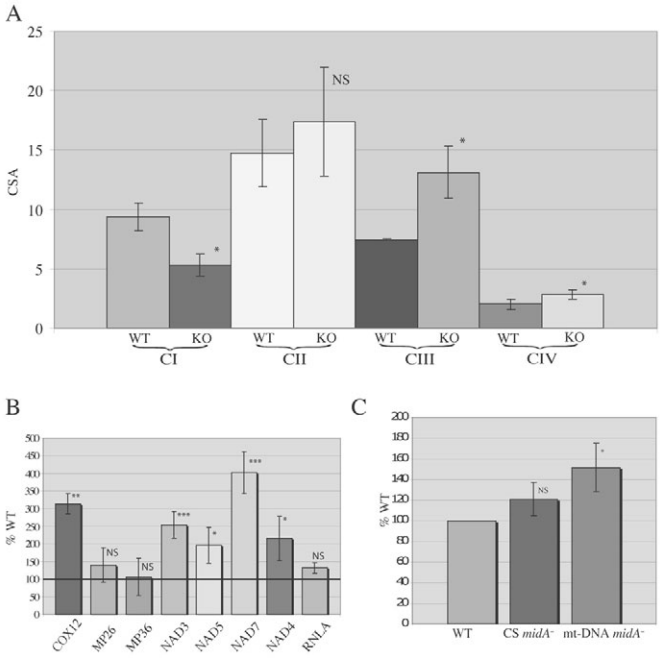

Fig. 1. The activity of complex I is reduced in cells lacking MidA. (**A**) Spectrophotometric analysis of the activity of complexes I, II, III and IV in *Dictyostelium* WT and *midA*$^{-}$ mutant cells. At least three independent experiments for each complex were performed and the bars represent mean ± s.d. Significance of differences were determined by Student's *t*-test; **P*<0.05; ***P*<0.01; ****P*<0.001; n.s., non-significant difference. Reduced activities of complex I were observed in *midA*$^{-}$ *Dictyostelium* cells. CSA, complex specific activity, corrected by citrate synthase. (**B**) The steady-state levels of expression of representative genes from the eight major polycistronic transcripts from mitochondrial RNA were measured and compared with the levels found in wild-type control cells. Five of them showed significant increases compared with wild-type cells. Three independent experiments were performed and the bars represent the mean ± s.d. Significance of differences were determined by Student's *t*-test and indicated by the *P* value, as described above. (**C**) The level of the activity of the mitochondrial enzyme citrate synthase (CS) and amount of mtDNA was measured and compared with the wild type (adjusted to 100%). Three independent experiments were performed and the statistical analysis was carried out as described above.

Consistent with this possible compensatory response, increases were also observed in the mutant in the steady state levels of mtDNA and most mtRNA transcripts (Fig. 1B,C). There also appeared to be a small, albeit statistically insignificant, increase in the activity of citrate synthase (Fig. 1C).

The level of assembled complex I is reduced in HEK293T cells where MidA is downregulated

We next wanted to study the level of assembled complex I by blue native (BN)-PAGE. We were unable to use *Dictyostelium* cells in these analyses owing to the lack of available antibodies to detect the different complexes and the low signal obtained by BN-PAGE. Therefore we used stable transfectants of HEK293T cells in which human MidA was downregulated by shRNAmir technology. Two different clones (S1 and S19) were obtained with a level of *MidA* mRNA downregulation of 93% and 87%, respectively. A control clone transformed with a scrambled vector showed no reduction in *MidA* mRNA. Fig. 2A shows representative gels and Fig. 2B a quantification by densitometry of three independent experiments where the level of CI had been normalized using the signal of complex III. Similar results were obtained when we normalized for complex II, complex IV and complex V (data not shown). We found a modest effect in fully assembled CI that ranged from 60% to 80% with respect to the control, which was treated with scrambled shRNA. The activity of CI was also measured by spectrophotometric analysis. A reduction in CI activity was only detected in clone S1, which had higher levels of mRNA inhibition. This clone showed an average CI activity that was 75% of that in control cells (data not shown). Together, these results suggest that both *Dictyostelium* and human MidA are involved in complex I assembly or stability.

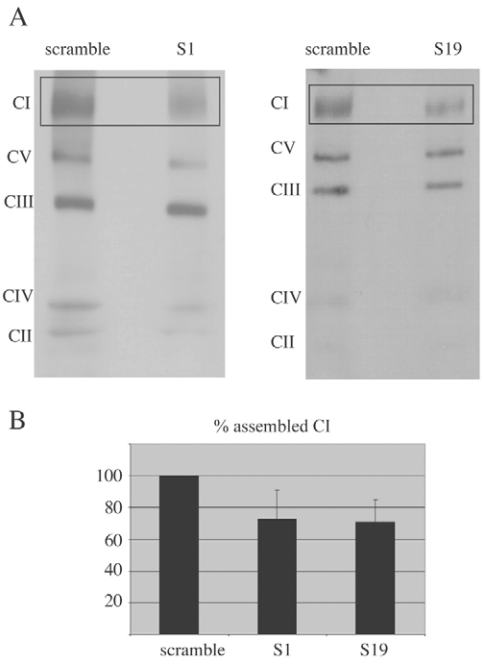

Fig. 2. Reduction of fully assembled complex I in human cells with downregulated MidA. (**A**) Mitochondrial complexes from human HEK293T clones S1 and S19, and control cells were extracted with N-dodecyl β-D-maltoside for BN-PAGE analysis. The gel was transferred to PVDF membrane and incubated with a cocktail of antibodies for complex detection. The different bands were assigned by the expected pattern and their approximate size calculated using a protein size standard. A significant reduction in CI levels (indicated by rectangle) was observed. (**B**) Densitometric quantification of three different BN-PAGE western blots showed a reduction of assembled CI to approximately 70-80% of that found in a clone harboring a scrambled vector. Densitometry was performed with ImageJ 1.33u (NIH, USA), and the values for CI were normalized to those of complex III. The bars represent mean ± s.d. P=0.060 for S1 and P=0.033 for S19 (Student's t-test).

MidA interacts with complex I subunit NDUFS2

In a parallel approach to elucidate the function of MidA, we performed a yeast two-hybrid screening to identify possible interactors. As bait we used the whole *Dictyostelium* MidA protein, except for the first 21 amino acids, which correspond to the putative mitochondrial targeting sequence. The vector used was pB29, which contains an N-bait-LexA-C fusion, and 57.4 million interactions were analyzed. Interestingly, ten independent positive clones were obtained that encode *Dictyostelium* NADH-ubiquinone oxidoreductase-chain 49 (DDB_G0294030), a homologue of the human complex I subunit NDUFS2. Fig. 3A shows the common region contained in the different clones that allowed us to restrain the minimal interaction region to 40 amino acids. This interaction was ranked with high confidence by a computer program (Global PBS®, Predicted Biological Score from Hybrigenics) that represents the probability of an interaction to be non-specific (Rain et al., 2001). Nevertheless, a further validation was performed using pull-down assays. The N-terminal fragment of *Dictyostelium* NDUFS2, which contains the minimal region of interaction, was fused to GST, purified from bacteria and incubated with cell extracts from *Dictyostelium* expressing MidA fused with GFP. As shown in Fig. 3B, MidA-GFP was pulled down by GST-NDUFS2 but not by GST alone, which was used as a control. We also wanted to validate this interaction using human MidA, expressed in HEK293T cells fused with GFP. The bacterially expressed N-terminus of human NDUFS2 was used in the assay (Fig. 3B). A positive pull-down was observed, again suggesting a functional conservation between *Dictyostelium* and human MidA proteins.

We next asked whether the observed interaction requires the functional methyltransferase domain identified in the MidA sequence (see below). We performed pull-down assays using *Dictyostelium* cell extracts expressing wild-type and mutated MidA (G170V) in which the methyltransferase domain is presumed to be inactivated (see below). As shown in Fig. 3C, both proteins were pulled down by the bacterially expressed *Dictyostelium* NDUFS2, suggesting that a functional methyltransferase domain is not required for the interaction.

Is MidA stably bound to CI or any other large subcomplex? To answer this question, we used the same *Dictyostelium* rescued strain used in the pull-down experiments that stably expressed MidA-GFP to perform a second-dimension analysis. After BN-PAGE, the lane was cut and resolved in a second SDS-denaturing dimension and MidA-GFP was detected by western blot analysis (supplementary material Fig. 2B). MidA had an apparent molecular size in the first dimension that was compatible with it being a homodimer (approximately 200 kDa, after taking into account the size of the GFP and TAP tags). Although most of the MidA protein is present as a dimer, a signal was also detected at higher molecular sizes (ranging from 450 to 750 kDa) (supplementary material Fig. S2B). *Dictyostelium* CI has an approximate molecular weight of 880 kDa, as determined previously by MALDI-TOF analysis of the corresponding band from BN-PAGE gels (supplementary material Fig. S2A). Therefore, *Dictyostelium* MidA does not seem

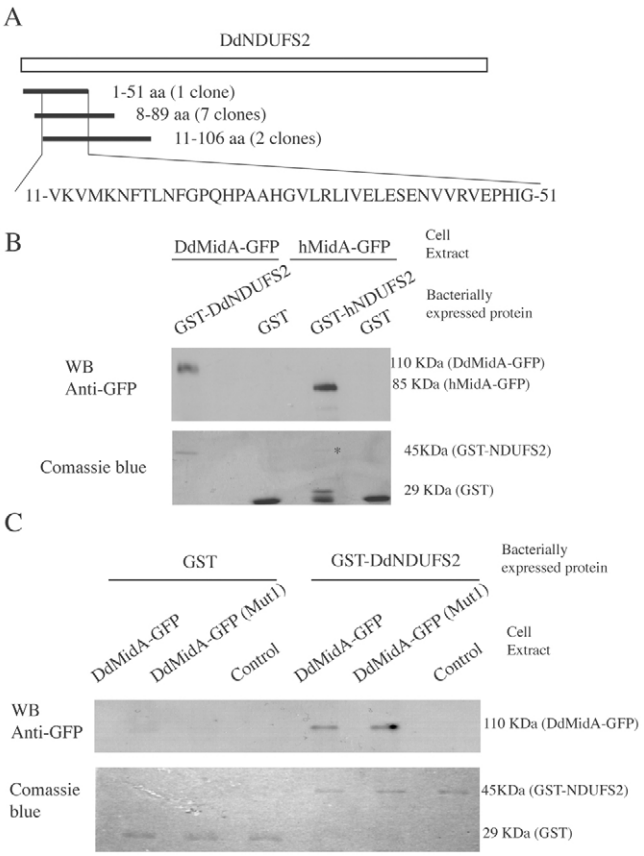

Fig. 3. MidA interacts with NDUFS2. (**A**) A yeast two-hybrid screening using *Dictyostelium* MidA as bait rendered a possible interaction with the N-terminus of the complex I core subunit NDUFS2. The open rectangle represents the complete amino acid sequence of *Dictyostelium* NDUFS2 and the lines below mark the position and the number of the different clones that gave a positive interaction in the screening. The amino acid sequence of the overlapping minimal region is also shown. (**B**) The interaction was validated by pull-down assay using bacterially expressed NDUFS2 fused with GST and cell extracts expressing *Dictyostelium* MidA and human MidA fused to GFP. A fraction of the bacterially expressed proteins used in the assay are shown by Coomassie blue staining after SDS-PAGE electrophoresis. Human NDUFS2 was sensitive to degradation and little protein was obtained (labeled with an asterisk). After incubation with the indicated cell extracts and subsequent washes, the samples were separated by SDS-PAGE, transferred and incubated with anti-GFP antibody. Both *Dictyostelium* and human MidA-GFP were efficiently pulled down and showed the expected molecular size. (**C**) Similar pull-down assays were performed using *Dictyostelium* cell extracts expressing MidA-GFP as before, or a mutated form (G170V), indicated as MidA-GFP (Mut1). A wild-type extract was used as an additional negative control. The lower blot shows the bacterially expressed proteins used in the assay stained with Coomassie blue. The upper blot shows both proteins interacting with NDUFS2.

to be stably bound to CI, but might be present in high molecular mass CI subcomplexes. This is in agreement with previous proteomic studies that have not detected MidA as part of CI (Fearnley et al., 2007). A similar experiment was performed with HEK293T expressing human MidA-GFP and we found no stable association of the human protein with subcomplexes, although its size suggested that it is also a homodimer (data not shown). Perhaps the interaction of the *Dictyostelium* protein in large complexes is more stable than that of the human homologue, allowing its detection by this technique, or there might be functional differences between species that we do not yet understand.

MidA has a conserved methyltransferase fold

The lack of obvious functional motifs in MidA amino acid sequences prevented us from speculating about the possible molecular function (Torija et al., 2006b). We have now searched for structural similarities with other proteins whose function is known and carried out bioinformatics modeling. To obtain a structural model for MidA, we performed an initial Blast search against PDB, the database of protein structures, to find a homologous protein of known structure (Altschul et al., 1997; Kirchmair et al., 2008). We found a highly similar candidate with 32% sequence identity with MidA and a Blast E-value of 2e-52. This protein belongs to *Rhodopseudomonas palustris* and is a target of a structural genomics consortium (Uniprot code Q6N1P6, PDB code: 1zkd). Its function is still unknown, as shown by its placement in the PFAM database of conserved domains as a DUF185 member, a family of proteins of unknown function (Finn et al., 2008). However, in the SCOP database of the structural classification of proteins (Andreeva et al., 2008), 1zkd was classified as a possible member of the S-adenosyl-L-methionine (SAM)-dependent methyltransferases, a large superfamily of proteins that is comprised of 52 protein families.

Using 1zkd as a template, a 3D model of MidA was built using the Phyre server (Kelley and Sternberg, 2009). From the set of models returned by this server, the one at the top of the list uses 1zkd as template, reflecting once more the relatedness of the two proteins. The sequence-to-structure alignment between MidA and 1zkd covered most of the MidA sequence (Fig. 4A). Of course, the MidA N-terminal sequence corresponding to the putative mitochondrial-targeting peptide, is totally excluded in the model.

We next wanted to define the functional residues that might occur in the catalytic site using FireStar (Lopez et al., 2007), a web server that predicts functionally important residues using FireDB (Lopez et al., 2007). FireDB is a database of PDB structures and their associated ligands, and contains the largest set of reliably annotated functionally important residues. These annotations are extracted from protein-ligand atom contacts and are also derived from the catalytic-site atlas (CSA) (Porter et al., 2004). Interestingly, the information obtained from FireStar indicated a relationship between the sequence of MidA and a human dimethyladenosine transferase (PDB code 1zq9, chain A). Following the FireStar annotations derived from the CSA, the catalytic site of 1zq9 contains three relevant residues: G64, E85 and N128. The two first are conserved in MidA (G170 and E200), whereas the third is replaced by a glutamine (Q257). The structure of the human dimethyladenosine transferase (1zq9) is available (PDB code 1zq9, chain A) and lzq9 was crystallized with S-adenosylmethionine (SAM), the methyl donor, that was in contact with these three residues. We superimposed our MidA 3D model with the region that contains the 1zq9 catalytic site (residues 64-128) using local-global alignment (LGA) (Zemla, 2003), and found that they superimposed fairly well, as shown in Fig. 4B.

To determine whether the SAM ligand can be accommodated in our MidA model in the proper manner, a docking was performed using the Haddock biomolecular docking software by searching 1000 models. The only spatial restriction imposed on Haddock was to keep SAM close to the equivalent three residues in our model. We obtained several clusters of models, and finally selected the first ten models of the best cluster. These models had good

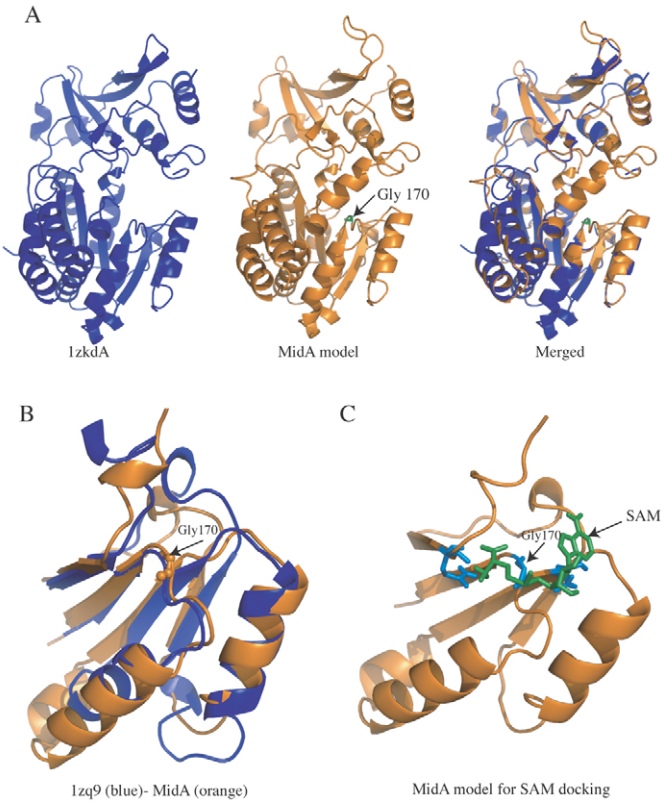

Fig. 4. MidA contains a methyltransferase domain. (**A**) A 3D model of MidA was built using as a template 1zkd, a *Rhodopseudomonas palustris* protein that belongs to DUF185 family. The blue diagram represents 1zkd, chain A from PDB (this protein is a homodimer and chain B is not displayed). The orange diagram shows the MidA model. The structural alignment between MidA and 1zkd is shown on the right and covers most of the MidA sequence. (**B**) Detail of the alignment of the MidA model and 1zq9. The catalytic region of the 3D model of MidA (orange) superimposes fairly well with that of 1zq9 (blue), a human dimethyladenosine transferase whose structure is known, showing a characteristic fold exposing a loop where several conserved residues reside. Among them, Gly170, was chosen for functional analysis. (**C**) The methyl donor SAM fits in the MidA model. Docking was performed running Haddock. SAM maintains the correct distances to the equivalent critical residues of the methyltransferase 1zq9. Residues G170, E200 and Q257 are blue and SAM is colored in green.

Haddock scores and were very similar, with a maximum interface ligand RMSD of 1.5 Å. The first ranked model is shown in Fig. 4C. The network of contacts between MidA and SAM remained, as shown with Ligplot (Wallace et al., 1995) in supplementary material Fig. S3, keeping the three aforementioned residues in contact with SAM.

The next step was to simulate the effect of the mutation G170V. We first replaced G170 with a valine with PyMol over the docking model (The PyMol Molecular Graphics System, DeLano Scientific, Palo Alto, CA) by selecting the rotamer that appears to be more frequent in proteins. Obviously, the effect of this mutation produced new clashes and so required a new docking of SAM with respect to the mutated model. We ran Haddock again to better accommodate the SAM molecule. Once more, we picked the first ten models of the best cluster, and checked the level of conservation of the spatial distance with respect to the three aforementioned residues in the mutation model. The new docking model allowed us to determine that the initial network of contacts was lost, and that SAM was now accommodated towards the exterior of the protein, presumably causing a loss of the function of the enzyme. This was confirmed experimentally by site-directed mutagenesis, as described below.

The crystal structure of 1zq9 indicates that the protein is homodimeric, as described for other methyltransferases. It should be noted that the BN- and SDS-PAGE analysis described above suggested that MidA is also a dimer (supplementary material Fig. S2).

The methyltransferase domain is required for MidA function

The structural model shown above strongly suggested the presence of a SAM-binding motif, which is characteristic of methyltransferases. To confirm this hypothesis, we performed site-directed mutagenesis to change residue G170, which is present in the conserved folding and whose change to valine was predicted to have a deleterious effect on the binding of SAM. A double mutation was also performed to change both G170 and G172 to valines. Both residues have been previously suggested to be important for SAM binding, and are well conserved among methyltransferases (Niewmierzycka and Clarke, 1999). The WT and mutated forms of MidA were fused to GFP to monitor their expression and localization in the cells and transformed into the *Dictyostelium midA*$^{-}$ null mutant (Fig. 5A). As described previously, *midA*$^{-}$ cells show defects in growth both in axenic medium and in association with bacteria, as a consequence of the mitochondrial dysfunction (Torija et al., 2006b). Although the WT protein complemented the phenotype completely, the G170 mutated protein was not able to complement the phenotype (Fig. 5C). A similar result was obtained for the G170 and G172 double mutation (data not shown). To exclude the possibility that the lack of complementation was a result of failed targeting to the mitochondria, we checked and showed that the proteins were localized in the mitochondria (Fig. 5B shows the result for the G170V mutant as an example). The lack of reversion of the phenotype strongly suggests that a single mutation in G170 from the methyltransferase domain is sufficient to render the protein inactive. These results also suggest that the putative methyltransferase domain is required for MidA function in *Dictyostelium*.

Characterization of MidA complex I deficiency and its relationship with AMPK signaling

To gain a better understanding of the genotype-phenotype relationship in mitochondrial dysfunction, we made use of *Dictyostelium* cells lacking MidA (*midA*$^{-}$ null mutant) as a cellular model for CI disease. We wanted to characterize in detail the phenotype of the null mutant and to study the relationship with AMPK signaling. *Dictyostelium* cells aggregate upon starvation to form a multicellular organism. At the slug stage, these structures show a remarkable capacity to move towards light and thermal gradients. This phototaxis and thermotaxis ability was shown to be more sensitive to mitochondrial dysfunction than other cellular functions (Kotsifas et al., 2002; Wilczynska et al., 1997). The *midA*$^{-}$ mutant showed a strong defect in phototaxis, as observed by the slug-trail assay (Fig. 6A, upper panel) and quantification of the accuracy of phototaxis (κ) (Fig. 6A, lower panel). κ measures how concentrated the trails are around the direction of the light source. It ranges from 0 when there is no orientation in any preferential

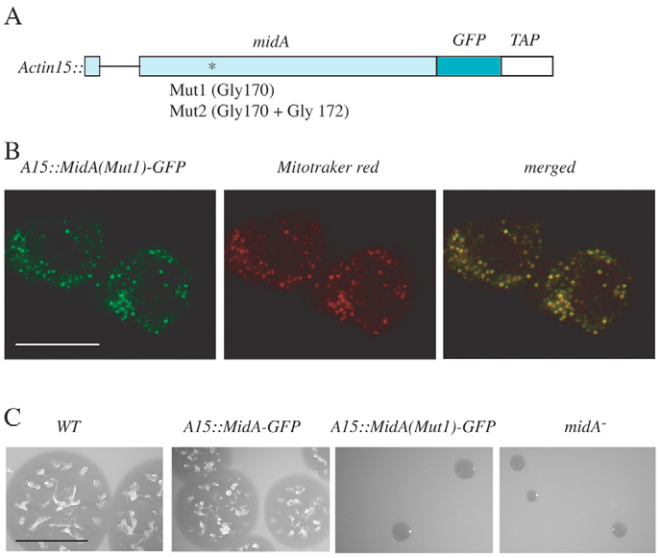

Fig. 5. Site-directed mutagenesis supports the presence of a methyltransferase domain. (**A**) Scheme of the expression constructs used for complementation studies. The coding region of the *midA* gene, fused to GFP and TAP (tandem affinity purification tag), is directed by the Actin15 (A15) promoter and is depicted as open boxes. A thin line represents an intron near the N-terminus. Site-directed mutagenesis was performed at the indicated residues (asterisk). (**B**) The wild-type and mutated constructs were transformed in the *midA*$^{-}$ mutant and stable transformant clones were checked for expression and localization of MidA in mitochondria. All the constructs showed mitochondrial localization of the protein. A representative analysis is shown for the mutated construct (G170V). Colocalization was observed between MidA-GFP (green) and mitotracker (red), indicating mitochondrial localization. Scale bar: 10 µm. (**C**) Analysis of growth in association with bacteria of transformant clones with WT and the mutated forms of MidA. The WT construct complemented the growth phenotype and other aspects of the phenotype (not shown). However, the constructs containing the indicated mutations were not able to complement the phenotype, giving rise to the small colony phenotype that is characteristic of *midA*$^{-}$ mutant. A representative analysis is shown for the mutation G170V. Scale bar: 1 cm.

direction to infinity in the case of a perfect orientation. The defect in phototaxis was restored in a *midA*$^{-}$ mutant strain where *Dictyostelium* MidA had been transformed with an expression vector under the control of an actin promoter (rescued strain). Similarly, a defect in thermotaxis was also observed, as shown in Fig. 6B where κ was measured in the wild type, the *midA*$^{-}$ mutant strain and the rescued strain during thermotaxis at different temperatures (Fig. 6B). Thermotaxis was also complemented in the rescued strain. Additionally, *midA*$^{-}$ mutants showed a growth defect that is accompanied by a phagocytosis and macropinocytosis defect, as previously described (Torija et al., 2006b) and shown in supplementary material Fig. S6. These defects in phagocytosis and macropinocytosis have not been observed previously in other mitochondrial *Dictyostelium* mutants, suggesting a more complex scenario, which will be discussed below (Barth et al., 2007).

We next explored the contribution of AMPK signaling in the complex phenotype of *midA*$^{-}$ cells. Overexpression of an AMPK antisense construct has been previously shown to inhibit the expression of AMPK and to restore phototaxis in several *Dictyostelium* mutants. As expected, we found that phototaxis and partly thermotaxis were restored in the *midA*$^{-}$ mutant when AMPK was downregulated suggesting that this phenotype is mediated by

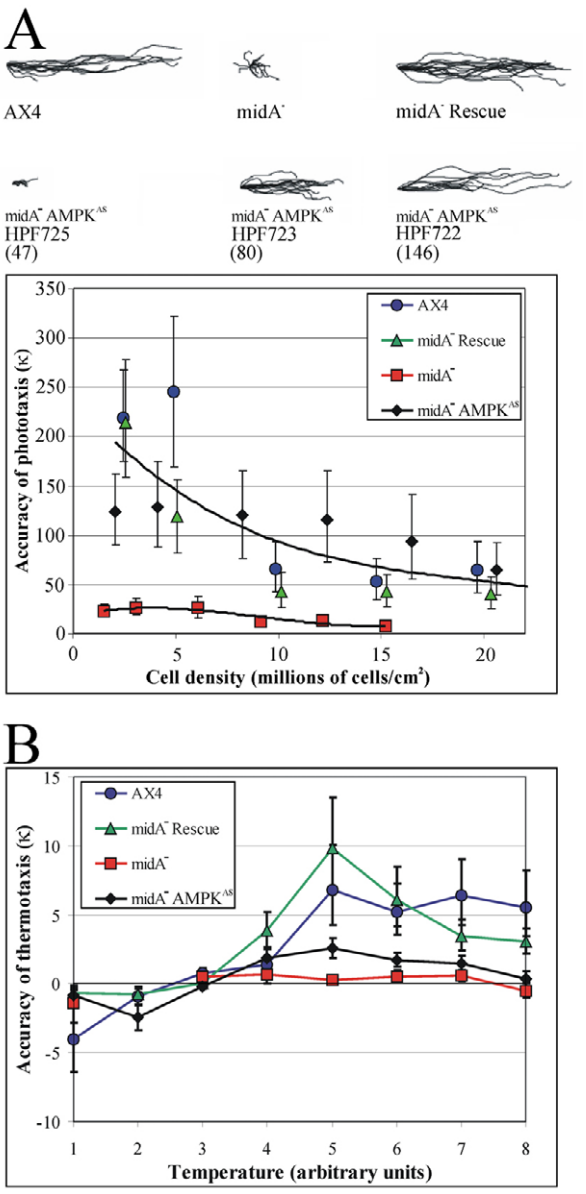

Fig. 6. Phototaxis defects in *Dictyostelium* MidA mutant can be rescued by AMPK inhibition. (**A**) Different *Dictyostelium* strains were allowed to form migrating slugs and exposed to lateral light to determine their phototaxis capabilities. The strains used were the following: wild-type *Dictyostelium* cells (AX4), the *midA*-null mutant (*midA*$^{-}$), a complemented strain ectopically expressing the complete *midA* gene (*midA*$^{-}$ Rescue) and several independent transformants (strain designations beginning with HPF) of the MidA mutant expressing different numbers of copies of an AMPK antisense construct (*midA*$^{-}$ AMPK^{AS}). The copy number for the AMPK antisense construct (pPROF362) is indicated within brackets. The phototaxis and migration (short trails) defects of the *midA*$^{-}$ mutant were suppressed in a copy number-dependent manner. In the lower panel, the accuracy of phototaxis (κ) was measured for the indicated strains at different cell densities. In this experiment, the *midA*$^{-}$ AMPK^{AS} strain was HPF722. (**B**) Defective thermotaxis in the *midA*$^{-}$ mutant is complemented by ectopic expression of MidA and suppressed by AMPK antisense inhibition. The accuracy of thermotaxis in a 0.2°C/cm gradient was measured for slugs formed at a density of 3×10^{6} cells/cm^{2} and migrating at temperatures ranging from 1 to 8 (arbitrary units corresponding in separate calibration experiments to 14°C to 28°C). The *midA*$^{-}$ AMPK^{AS} strain was HPF723 and it exhibited substantial (but not complete) suppression of the thermotaxis defect. Other details are as for A.

a chronic activation of the kinase (Fig. 6A). This is the first report that a phenotypic defect caused by a specific CI deficiency in a model system can be rescued by AMPK downregulation. Interestingly, the defects in growth, phagocytosis and macropinocytosis were not rescued by the same experimental manipulation, suggesting that these defects are independent of AMPK signaling in the *midA*$^{-}$ mutant (supplementary material Fig. S4).

Discussion

We used bioinformatics and experimental comparative analysis in *Dictyostelium* and human cells to shed light on the function of MidA, a protein that is conserved from bacteria to humans and contains a characteristic DUF185 motif of unknown function. The functional similarities between *Dictyostelium* MidA and its human homologue strongly suggest that both proteins are orthologous proteins that contain a methyltransferase domain and required for mitochondrial CI function. Another putative methyltransferase has recently been described to function in CI assembly or stability (Gerards et al., 2009; Sugiana et al., 2008), highlighting the potentially important but poorly understood role of methylation in CI function.

About 40% of inherited disorders of the OXPHOS system involve isolated or combined deficiencies in CI, the largest complex of the OXPHOS system. The genetic cause of many cases of CI deficiencies is still unknown, which is due in part to insufficient understanding of the CI assembly process and the factors involved. We do not know yet whether MidA is involved in human mitochondrial disorders, but it should definitely be considered a strong candidate. The loss of function of this protein in the model *Dictyostelium* generates a complex phenotypic outcome, including growth and developmental defects. In humans, disorders associated with CI dysfunction are also complex, and usually lead to multisystem failure that affects the brain, skeletal muscle and heart.

Dictyostelium midA^{-} null cells showed a decreased activity of CI, and BN-PAGE studies in human cells where MidA is downregulated also showed lower amounts of fully assembled complex, suggesting a role for MidA as an assembly or stability factor. The level of the assembly and activity of human CI in the knockdown cells was around 70% of the control values, a moderate effect but near the threshold that could have an impact in cellular bioenergetics (Pathak and Davey, 2008), or even cause human disease (Loeffen et al., 2001). CI is formed by a large number of subunits (up to 45 subunits in humans). The assembly and stability of such a large multiprotein complex requires specific chaperone and assembly factors, six of which have been implicated in human CI deficiency, including NDUFAF1-NDUFAF4 (Hoefs et al., 2009; Ogilvie et al., 2005; Saada et al., 2009; Vogel et al., 2005), C8ORF38 (Pagliarini et al., 2008) and C20ORF7 (Gerards et al., 2009; Sugiana et al., 2008). Others such as Ecsit (Vogel et al., 2007), AIF (Vahsen et al., 2004) and IndI (Bych et al., 2008) are required for CI assembly, but have not yet been implicated in human disease.

In spite of its large size, CI has a basic catalytic core formed by only 14 proteins that are evolutionarily conserved from prokaryotes to humans. All have been implicated in human CI disorders, including NDUFS2 (Loeffen et al., 2001; Ugalde et al., 2004), an iron-sulfur protein that we have shown to interact with MidA/PRO1853. NDUFS2 is encoded by the nuclear genome of human cells but it is encoded by the mitochondrial genome in *Dictyostelium* revealing its ancient origin as an endosymbiont protein. Interestingly, MidA homologues also exist in α-proteobacteria, suggesting that the interplay between MidA protein and the catalytic CI is of ancient origin and conserved from bacteria to humans.

The SAM-dependent methyltransferase enzymes share little sequence identity, but do contain a highly conserved structural fold that is involved in SAM binding. Surprisingly, the precise residues that bind the SAM cofactor are poorly conserved (Loenen, 2006; Schubert et al., 2003). We have shown by bioinformatics modeling and site-directed mutagenesis that DUF185 might have a methyltransferase domain. At the level of amino acid sequence, only a short region of homology can be detected between DUF185 proteins and methyltranferases, the so-called motif I, corresponding to a loop of the catalytic core involved in SAM binding (Niewmierzycka and Clarke, 1999). The consensus sequence was defined as a nine-residue block, hh(D/E)hGxGxG, where h represents a hydrophobic residue and x can be any residue (Kakebeeke et al., 1979; Niewmierzycka and Clarke, 1999). In previous studies based on multiple protein alignments, this short sequence was revealed and led to the proposal that DUF185 is a methyltransferase (Sadreyev et al., 2003). Our site-directed mutagenesis studies targeted the first two conserved glycines present in this sequence and showed that the first and possibly both of these residues are required for the protein function. Five different structural folds have been described to bind SAM and perform a methyl transfer. Our model fits with class I, the most abundant, which is composed of alternating β-strands and α-helices (Martin and McMillan, 2002; Schubert et al., 2003). Taken together, these studies strongly suggest that MidA proteins contain a methyltransferase domain. The characterization of its biochemical activity and the identification of the possible targets are of great interest and will warrant further investigation.

Methyltranferases are a large family of proteins that are involved in methylation of a wide variety of substrates including DNA, RNA and proteins and the atomic targets can be carbon, oxygen, nitrogen and sulfur. However, in most cases, no specific traits in the sequence or the structure can be reliably used to predict the substrate of the modification. Indeed, motif I is present in DNA, RNA, protein and small molecule methyltransferases (Kagan and Clarke, 1994). In mitochondria, methylation has an essential role. Mitochondrial DNA, tRNA and rRNA are all targets of specific methylation events (Helm et al., 1998; Pintard et al., 2002) and specific carriers transport SAM into the mitochondria (Agrimi et al., 2004). As far as protein methylation is concerned, only two methylated subunits have been detected in complex I subunits. One of them is the bovine NDUFB3 (B12), which is methylated at conserved His residues. Interestingly, the other one is the human NDUFS2, which harbors a methylated arginine, R323. Of course, the interaction of MidA with NDUFS2 and subsequent methylation of the subunit is an attractive hypothesis that remains to be investigated. The possible functional relevance of NDUFS2 methylation is not known but it is likely that this post-translational modification in such an important core subunit alters the assembly or the stability of the whole complex. In fact mutations in Arg228, Ser413 and Pro229 of NDUFS2 have been described to be involved in CI disease (Loeffen et al., 2001). However, we should also consider the possibility that MidA has a dual function as a chaperone and as a methyltransferase. MidA is not stably bound to CI, as suggested by our results using BN-PAGE. Therefore, it is possible that the interaction with NDUFS2 occurs during the assembly process of

the complex, thus functioning as a transitory step that is required for correct CI stability.

The complex phenotypes of *Dictyostelium* cells deficient in MidA show similarities with other strains with mitochondrial disease, but there are also differences. Defects in phototaxis and thermotaxis have been described previously in other *Dictyostelium* mitochondrial dysfunctions that affect respiration, such as ethidium-bromide-mediated mtDNA depletion and the antisense inhibition of Chaperonin 60 (Cpn60) (Bokko et al., 2007; Chida et al., 2004; Kotsifas et al., 2002; Wilczynska et al., 1997). Interestingly, the phototaxis impairment in the MidA mutant can be rescued by AMPK inhibition, similarly to the other described mitochondrial mutants. However, *midA*$^{-}$ cells showed a severe defect in phagocytosis and macropinocytosis: a phenotype that is not rescued by AMPK antisense inhibition and is not even present in the other described mitochondrial mutants. This defect would, in turn, explain the AMPK-independent impairment of growth that we observe in the MidA-null mutant. The results suggest that either MidA itself or CI activity are specifically required for normal phagocytosis and pinocytosis.

We observed compensatory responses that increased the expression and level of activity of other respiratory chain complexes and the amount of mtDNA in the cells. This suggests a feedback that stimulates mitochondrial biogenesis and ATP production, but fails to correct the specific CI deficiency caused by the absence of MidA. AMPK might participate in this feedback, because it stimulates mitochondrial biogenesis and ATP production in *Dictyostelium*, as in other organisms (Bokko et al., 2007). The pattern of phenotypic outcomes in the MidA-null mutant thus results from both chronic AMPK activity and a specific failure of the associated feedbacks to correct the CI deficiency. This reveals once more the complexity of mitochondrial cytopathology and specifically in CI diseases. The observation of the role played by AMPK signaling in complex I pathology in *Dictyostelium* suggests that in humans some of the associated phenotypes might also be mediated by chronic activation of this signaling pathway. If so, treatment aimed to regulate AMPK signaling might be beneficial.

Materials and Methods

Dictyostelium growth, transformation and development

Dictyostelium AX4 cells were grown axenically in HL-5 medium or in association with *Klebsiella aerogenes* in SM plates (Sussman, 1987). Transformations were carried out by electroporation, as described previously (Pang et al., 1999). For synchronous development, axenically growing cells were washed from culture medium by centrifugation, resuspended in water or PDF buffer and deposited on nitrocellulose filters (Shaulsky and Loomis, 1993).

Human cell culture and RNA interference

HEK293T and HeLa cell lines were obtained from the American Type Culture Collection (ATCC) (Manassas, VA) and were grown following the specifications of the repository. Two different micro RNA adapted short-hairpin RNAs (shRNAmir) cloned into pGIPZ vector (V2HLS_31857 and V2HLS_31862; Open Biosystems) were used to stably knockdown the human gene encoding MidA (*C2orf56*). Lipofectamine 2000 (Invitrogen) was used for transfection of the constructs according to the manufacturer's protocol. For selecting stable cell lines, the puromycin drug-resistance marker was used. Relative quantitative real-time PCR was carried out to estimate the knockdown levels of the human gene in a 7900HT Fast Real Time PCR system (Applied Biosystems). For this purpose, two different TaqMan assays were used. One specifically detected the levels of mRNA encoding MidA (Hs00218600; Applied Biosystems). The other was a TaqMan ribosomal RNA control designed to detect the 18S ribosomal RNA gene as endogenous control (4308329; Applied Biosystems).

Mitochondrial localization

Mitochondrial localization with Mitotracker Red (Molecular Probes) was performed as previously described (Torija et al., 2006b). Confocal analysis was performed in a Leica TCS SP5 using a PL APO 63×/1.4-0.6 objective and LAS-AF (Leica Application Suite) software.

Spectrophotometric analysis of the OXPHOS complexes and BN-PAGE

For spectrophotometric analysis, 5×10^7 growing cells were centrifuged and washed once with PBS. The pellet was resuspended in 2 ml SETH buffer (250 mM sucrose, 2 mM EDTA, 10 mM Tris-HCl, 100 U/l heparin, pH 7.4) and then sonicated three times in ice-cold water for 10 seconds with 30 second rests in between. To eliminate cell debris, the sample was centrifuged and the supernatant was used as reaction sample for spectrometric analysis, as previously described (Tiranti et al., 1995).

BN-PAGE analysis was basically performed as previously reported (Calvaruso et al., 2008) with small changes. Briefly, 1×10^7 cells were resuspended in 3× gel buffer (750 mM aminocaproic acid, 150 mM Bis-Tris pH 7.0) and the amount of protein quantified with the Bradford assay. N-dodecyl β-D-maltoside (Sigma) was added to a ratio 20 µg per µg total protein and made up to 40 µl with 3× gel buffer. 40 µg were loaded per lane for the CI detection, whereas 10 µg were loaded for MidA detection. For western blot analysis, the gel was transferred overnight at room temperature to a 0.45 µm PVDF membrane (PALL life sciences) at 30 V with 1× Tris-Gly, 20% methanol and 0.02% SDS buffer. Then, the membrane was stripped with 2% SDS, 62.5 mM Tris-HCl, pH 6.8, for 90 minutes. The western blot was carried out with total OXPHOS Human WB Antibody Cocktail (Mitosciences) to assay CI stability. A protein standard (Invitrogene) was used to estimate the size of the complexes. Secondary antibody goat anti-mouse IgG-HRP was provided by Santa Cruz Biotechnology. For MidA dimer experiments, the second dimension was made as previously described (Calvaruso et al., 2008). Anti-GFP (SIGMA) and goat anti-rabbit IgG-HRP (Santa Cruz) antibodies were used.

Site-directed mutagenesis

Site-directed mutagenesis of G170V and G172V was performed by PCR using as template the complete MidA gene cloned in pGEMt. Two complementary oligonucleotides containing the desired mutations were used. For G170V: oligo 1, CAA ATA GTT GAA ATG GTT CCA GGT AGA GGC ACA CTA ATG; oligo 2, CAT TAG TGT GCC TCT ACC TGG AAC CAT TTC AAC TAT TTG. For double mutation G170V and G172V: oligo 3, CAA ATA GTT GAA ATG GTT CCA GTT AGA GGC ACA CTA ATG. Oligo 4, CAT TAG TGT GCC TCT AAC TGG AAC CAT TTC AAC TAT TTG. The PCR reaction was digested with *Dpn*I and transformed into *E. coli* DH5α for plasmid amplification. The constructs were fully sequenced to confirm the mutations and cloned in-frame with GFP in the vector pDV-CGFP-CTAP, kindly provided by Pauline Shaap (University of Dundee, Dundee, UK). A similar construct was used with a complete wild-type sequence of MidA.

Pull-down assays

The N-terminus of *Dictyostelium* and human genes encoding NDUFS2 were expanded by PCR and cloned in PGEX plasmid (Pharmacia-Biotech) for bacterial expression and subsequent purification by the GST system according to the manufacturer's instructions. The *Dictyostelium* NDUFS2 construct spanned amino acids 8-176 and human NDUFS2 amino acids 38-234. GST alone was used as a control. The isolated proteins were kept associated with the Sepharose beads until used in the pull-down assay. 5×10^6 *Dictyostelium* and HEK293T cells expressing *Dictyostelium* or human MidA fused to GFP were resuspended in 500 µl STE+T buffer (10 mM Tris-HCl, pH 8, 1 mM EDTA pH 8, 150 mM NaCl, 5 mM DTT, 1% Triton X-100, 1× protease inhibitor cocktail) and shaken for 30 minutes at 4°C. After centrifugation, the supernatant was incubated with 30 µl of previously isolated proteins bound to the Sepharose beads for 1 hour at 4°C. Beads were washed three times with STE+T and finally resuspended in 30 µl protein loading buffer. The sample was split in two SDS-PAGE gels. One was stained with Coomassie Blue as a control and the other was transferred to PVDF for western blotting using anti-GFP antibody.

mtDNA and mtRNA quantification

For mtDNA quantification *Dictyostelium* cells were grown in HL-5 medium to log phase. Genomic DNA from 6×10^6 cells was extracted with 300 µl Quick Extract DNA Extraction Solution 1.0 (Epicentre). 1:50 dilution was used as a template in the PCR reaction carried out in 7900 HT Fast Real-Time PCR System, using Power Sybrgreen PCR Master Mix 2 with 300 nM oligonucleotides in a final volume of 10 µl. Results were acquired with SDS 2.3 software by Applied Biosystems and handled with Excel software by Microsoft. Two pairs of oligonucleotides were used: One for detection of mtDNA (DDB_G0294054), oligo1, AAC AAT CAT GTG GCT TTA GTA CGT AAA; oligo2, TCG GCC CTG CAT TTC GT and another for normalization with a nuclear gene (DDB_G0277273). Oligo 1, CCG TTG CCC TAA CTT ACT TCC A; oligo 2, GCC GCC ATT GAT GAA ACT ATT C. For mtRNA quantification, RNA from 1×10^7 cells growing to log phase in HL-5 medium was isolated with Tri-Reagent (Sigma) and adjusted to 2 µg/µl final concentration. DNA contamination was removed by adding 50 U DNase (New England Biolabs) to 10 µg RNA in a final volume of 10 µl. The reaction was incubated for 30 minutes at 37° C following an incubation at 70°C for 5 minutes to destroy DNase activity. The RNA was then adjusted with DEPC water to 100 ng/µl final concentration. 250 ng (2.5 µl) of this RNA was used as a template for RT-PCR with high capacity cDNA reverse transcription kit (Applied Biosystems) in a final volume of 20 µl. The cDNAs served as template in the PCR reaction carried out as described above. Eight genes

representative of the previously described eight major polycistronic transcripts (Barth et al., 2001) were studied for each sample, normalized to the nuclear gene DDB_G0277273 and referred to the wild-type levels. The oligonucleotides used are listed in supplementary material Table S2.

Phototaxis and thermotaxis assays

Qualitative phototaxis tests were performed as described (Darcy et al., 1994) by transferring a toothpick scraping of amoebae from a colony growing on a *K. aerogenes* lawn to the center of charcoal agar plates (5% activated charcoal, 1% agar). Phototaxis was scored after a 48 hour incubation at 21°C with a lateral light source. Quantitative phototaxis tests involved the harvesting of amoebae from mass plates, thoroughly washing them free of bacteria, suspending them in saline at the appropriate dilutions and inoculating 20 µl onto a 1 cm^2 area in the center of each charcoal agar plate. The resulting cell densities ranged from about 1.5×10^6 to 3.7×10^7 cells/cm^2. The phototaxis was again scored after a 48 hour incubation at 21°C with a lateral light source. Quantitative thermotaxis used washed amoebae prepared as for quantitative phototaxis and plated at a density of 3×10^6 amoebae/cm^2. A 20 µl aliquot of cells at this dilution was plated on a 1 cm^2 area in the center of water agar plates (1% agar) and incubated for 72 hours in darkness on a heat bar producing a 0.2°C/cm gradient at the agar surface. The arbitrary temperature units correspond to the temperatures 14°C at T1 and increasing in 2°C increments to 28°C at T8, as measured at the center of plates in separate calibration experiments. Slug trails were transferred to PVC discs, stained with Coomassie blue and digitized. The orientation of the slug migration was analysed using directional statistics (Fisher, 1981).

Phagocytosis and pinocytosis assays

All *Dictyostelium* strains (wild type AX2, midA null mutant and the midA rescued strain) were grown in HL-5 medium with no antibiotics to exponential phase before use in the pinocytosis and phagocytosis experiments. Bacterial uptake by *Dictyostelium* strains was determined by using as prey an *E. coli* strain expressing fluorescent protein DsRed (Maselli et al., 2002) as previously described (Bokko et al., 2007).

Pinocytosis assays (Klein and Satre, 1986) were performed by measuring the uptake of medium containing a fluorescent indicator, fluorescein isothiocyanate (FITC)-dextran (Sigma, average mol. mass 70 kDa), as previously described (Bokko et al., 2007).

This work was supported by grants BMC2006-00394 and BMC2009-09050 to R.E. from the Spanish Ministerio de Ciencia e Innovación; to P.R.F. from the Thyne Reid Memorial Trusts and the Australian Research Council; to A.V. and O.G. from the Spanish National Bioinformatics Institute (www.inab.org), a platform of Genome Spain; to R.G. from the Fondo de Investigaciones Sanitarias, Instituto de Salud Carlos III, Spain (PI070167) and from the Comunidad de Madrid (GEN-0269/2006). S.C. is supported by a research contract from Consejería de Educación de la Comunidad de Madrid y del Fondo Social Europeo (FSE). Sequence data for *Dictyostelium* were obtained from the Genome Sequencing Centers of the University of Cologne, Germany; the Institute of Molecular Biotechnology, Department of Genome Analysis, Jena; Baylor Collage of Medicine in Houston, Texas, USA; and the Sanger Center in Hinxton, Cambridge, UK. Y2H screening was performed by Hybrigenics (Paris, France). We thank Rosa M. Calvo for help with several experiments, Susana Peralta for advice on BN-PAGE, Gloria Fuentes for all the help with Haddock and Ana Rojas, Gonzalo López and Michael L. Tress for their interesting suggestions.

Supplementary material available online at
http://jcs.biologists.org/cgi/content/full/123/10/1674/DC1

References

Agrimi, G., Di Noia, M. A., Marobbio, C. M., Fiermonte, G., Lasorsa, F. M. and Palmieri, F. (2004). Identification of the human mitochondrial S-adenosylmethionine transporter: bacterial expression, reconstitution, functional characterization and tissue distribution. *Biochem. J.* **379**, 183-190.

Altschul, S. F., Madden, T. L., Schaffer, A. A., Zhang, J., Zhang, Z., Miller, W. and Lipman, D. J. (1997). Gapped BLAST and PSI-BLAST: a new generation of protein database search programs. *Nucleic Acids Res.* **25**, 3389-3402.

Andreeva, A., Howorth, D., Chandonia, J. M., Brenner, S. E., Hubbard, T. J., Chothia, C. and Murzin, A. G. (2008). Data growth and its impact on the SCOP database: new developments. *Nucleic Acids Res.* **36**, D419-D425.

Annesley, S. J. and Fisher, P. R. (2009a). *Dictyostelium discoideum*-a model for many reasons. *Mol. Cell Biochem.* **329**, 73-91.

Annesley, S. J. and Fisher, P. R. (2009b). *Dictyostelium* slug phototaxis. *Methods Mol. Biol.* **571**, 67-76.

Barth, C., Greferath, U., Kotsifas, M., Tanaka, Y., Alexander, S., Alexander, H. and Fisher, P. R. (2001). Transcript mapping and processing of mitochondrial RNA in *Dictyostelium discoideum*. *Curr. Genet.* **39**, 355-364.

Barth, C., Le P. and Fisher, P. R. (2007). Mitochondrial biology and disease in *Dictyostelium*. *Int. Rev. Cytol.* **263**, 207-252.

Bokko, P. B., Francione, L., Bandala-Sanchez, E., Ahmed, A. U., Annesley, S. J., Huang, X., Khurana, T., Kimmel, A. R. and Fisher, P. R. (2007). Diverse cytopathologies in mitochondrial disease are caused by AMP-activated protein kinase signaling. *Mol. Biol. Cell* **18**, 1874-1886.

Bych, K., Kerscher, S., Netz, D. J., Pierik, A. J., Zwicker, K., Huynen, M. A., Lill, R., Brandt, U. and Balk, J. (2008). The iron-sulphur protein Ind1 is required for effective complex I assembly. *EMBO J.* **27**, 1736-1746.

Calvaruso, M. A., Smeitink, J. and Nijtmans, L. (2008). Electrophoresis techniques to investigate defects in oxidative phosphorylation. *Methods* **46**, 281-287.

Carroll, J., Fearnley, I. M., Skehel, J. M., Runswick, M. J., Shannon, R. J., Hirst, J. and Walker, J. E. (2005). The post-translational modifications of the nuclear encoded subunits of complex I from bovine heart mitochondria. *Mol. Cell Proteomics* **4**, 693-699.

Chida, J., Yamaguchi, H., Amagai, A. and Maeda, Y. (2004). The necessity of mitochondrial genome DNA for normal development of *Dictyostelium* cells. *J. Cell Sci.* **117**, 3141-3152.

Darcy, P. K., Wilczynska, Z. and Fisher, P. R. (1994). Genetic analysis of *Dictyostelium* slug phototaxis mutants. *Genetics* **137**, 977-985.

Debray, F. G., Lambert, M. and Mitchell, G. A. (2008). Disorders of mitochondrial function. *Curr. Opin. Pediatr.* **20**, 471-482.

DiMauro, S. and Schon, E. A. (2008). Mitochondrial disorders in the nervous system. *Annu. Rev. Neurosci.* **31**, 91-123.

Eichinger, L., Pachebat, J. A., Glockner, G., Rajandream, M. A., Sucgang, R., Berriman, M., Song, J., Olsen, R., Szafranski, K., Xu, Q. et al. (2005). The genome of the social amoeba *Dictyostelium discoideum*. *Nature* **435**, 43-57.

Escalante, R. and Vicente, J. J. (2000). *Dictyostelium discoideum*: a model system for differentiation and patterning. *Int. J. Dev. Biol.* **44**, 819-835.

Fearnley, I. M., Carroll, J. and Walker, J. E. (2007). Proteomic analysis of the subunit composition of complex I (NADH:ubiquinone oxidoreductase) from bovine heart mitochondria. *Methods. Mol. Biol.* **357**, 103-125.

Finn, R. D., Tate, J., Mistry, J., Coggill, P. C., Sammut, S. J., Hotz, H. R., Ceric, G., Forslund, K., Eddy, S. R., Sonnhammer, E. L. et al. (2008). The Pfam protein families database. *Nucleic Acids Res.* **36**, D281-D288.

Fisher, P. R., Smith, E. and Williams, K. L. (1981). An extracellular chemical signal controlling phototactic behavior by *D. discoideum* slugs. *Cell* **23**, 799-807.

Gerards, M., Sluiter, W., van den Bosch, B. J., de Wit, E., Calis, C. M., Frentzen, M., Akbari, H., Schoonderwoerd, K., Scholte, H. R., Jongbloed, R. J. et al. (2009). Defective complex I assembly due to C20orf7 mutations as a new cause of Leigh syndrome. *J. Med. Genet*. PMID: 19452079.

Helm, M., Brule, H., Degoul, F., Cepanec, C., Leroux, J. P., Giege, R. and Florentz, C. (1998). The presence of modified nucleotides is required for cloverleaf folding of a human mitochondrial tRNA. *Nucleic Acids Res.* **26**, 1636-1643.

Hoefs, S. J., Dieteren, C. E., Rodenburg, R. J., Naess, K., Bruhn, H., Wibom, R., Wagena, E., Willems, P. H., Smeitink, J. A., Nijtmans, L. G. et al. (2009). Baculovirus complementation restores a novel NDUFAF2 mutation causing complex I deficiency. *Hum. Mutat.* **30**, E728-E736.

Janssen, R. J., Nijtmans, L. G., van den Heuvel, L. P. and Smeitink, J. A. (2006). Mitochondrial complex I: structure, function and pathology. *J. Inherit. Metab. Dis.* **29**, 499-515.

Kagan, R. M. and Clarke, S. (1994). Widespread occurrence of three sequence motifs in diverse S-adenosylmethionine-dependent methyltransferases suggests a common structure for these enzymes. *Arch. Biochem. Biophys.* **310**, 417-427.

Kakebeeke, P. I. J., de Wit, R. J. W., Kohtz, S. D. and Konijn, T. M. (1979). Negative chemotaxis in *Dictyostelium* and *Polysphondylium*. *Exp. Cell Res.* **124**, 429-433.

Kelley, L. A. and Sternberg, M. J. (2009). Protein structure prediction on the Web: a case study using the Phyre server. *Nat. Protoc.* **4**, 363-371.

Kirchmair, J., Markt, P., Distinto, S., Schuster, D., Spitzer, G. M., Liedl, K. R., Langer, T. and Wolber, G. (2008). The Protein Data Bank (PDB), its related services and software tools as key components for in silico guided drug discovery. *J. Med. Chem.* **51**, 7021-7040.

Klein, G. and Satre, M. (1986). Kinetics of fluid-phase pinocytosis in *Dictyostelium discoideum* amoebae. *Biochem. Biophys. Res. Commun.* **138**, 1146-1152.

Koopman, W. J., Nijtmans, L. G., Dieteren, C. E., Roestenberg, P., Valsecchi, F., Smeitink, J. A. and Willems, P. H. (2010). Mammalian mitochondrial complex I: biogenesis, regulation and reactive oxygen species generation. *Antioxid. Redox Signal*. PMID: 19803744.

Kotsifas, M., Barth, C., De Lozanne, A., Lay, S. T. and Fisher, P. R. (2002). Chaperonin 60 and mitochondrial disease in *Dictyostelium*. *J. Muscle Res. Cell Motil.* **23**, 839-852.

Lazarou, M., Thorburn, D. R., Ryan, M. T. and McKenzie, M. (2009). Assembly of mitochondrial complex I and defects in disease. *Biochim. Biophys. Acta*. **1793**, 78-88.

Loeffen, J., Elpeleg, O., Smeitink, J., Smeets, R., Stockler-Ipsiroglu, S., Mandel, H., Sengers, R., Trijbels, F. and van den Heuvel, L. (2001). Mutations in the complex I NDUFS2 gene of patients with cardiomyopathy and encephalomyopathy. *Ann. Neurol.* **49**, 195-201.

Loenen, W. A. (2006). S-adenosylmethionine: jack of all trades and master of everything? *Biochem. Soc. Trans.* **34**, 330-333.

Lopez, G., Valencia, A. and Tress, M. L. (2007). firestar-prediction of functionally important residues using structural templates and alignment reliability. *Nucleic Acids Res.* **35**, W573-W577.

Martin, J. L. and McMillan, F. M. (2002). SAM (dependent) I AM: the S-adenosylmethionine-dependent methyltransferase fold. *Curr. Opin. Struct. Biol.* **12**, 783-793.

Maselli, A., Laevsky, G. and Knecht, D. A. (2002). Kinetics of binding, uptake and degradation of live fluorescent (DsRed) bacteria by *Dictyostelium discoideum*. *Microbiology* **148**, 413-420.

Niewmierzycka, A. and Clarke, S. (1999). S-Adenosylmethionine-dependent methylation in *Saccharomyces cerevisiae*. Identification of a novel protein arginine methyltransferase. *J. Biol. Chem.* **274**, 814-824.

Ogawa, S., Yoshino, R., Angata, K., Iwamoto, M., Pi, M., Kuroe, K., Matsuo, K., Morio, T., Urushihara, H., Yanagisawa, K. et al. (2000). The mitochondrial DNA of *Dictyostelium discoideum*: complete sequence, gene content and genome organization. *Mol. Gen. Genet.* **263**, 514-519.

Ogilvie, I., Kennaway, N. G. and Shoubridge, E. A. (2005). A molecular chaperone for mitochondrial complex I assembly is mutated in a progressive encephalopathy. *J. Clin. Invest.* **115**, 2784-2792.

Pagliarini, D. J., Calvo, S. E., Chang, B., Sheth, S. A., Vafai, S. B., Ong, S. E., Walford, G. A., Sugiana, C., Boneh, A., Chen, W. K. et al. (2008). A mitochondrial protein compendium elucidates complex I disease biology. *Cell* **134**, 112-123.

Pang, K. M., Lynes, M. A. and Knecht, D. A. (1999). Variables controlling the expression level of exogenous genes in *Dictyostelium*. *Plasmid* **41**, 187-197.

Pathak, R. U. and Davey, G. P. (2008). Complex I and energy thresholds in the brain. *Biochim. Biophys. Acta* **1777**, 777-782.

Pintard, L., Bujnicki, J. M., Lapeyre, B. and Bonnerot, C. (2002). MRM2 encodes a novel yeast mitochondrial 21S rRNA methyltransferase. *EMBO J.* **21**, 1139-1147.

Porter, C. T., Bartlett, G. J. and Thornton, J. M. (2004). The Catalytic Site Atlas: a resource of catalytic sites and residues identified in enzymes using structural data. *Nucleic Acids Res.* **32**, D129-D133.

Rain, J. C., Selig, L., De Reuse, H., Battaglia, V., Reverdy, C., Simon, S., Lenzen, G., Petel, F., Wojcik, J., Schachter, V. et al. (2001). The protein-protein interaction map of *Helicobacter pylori*. *Nature* **409**, 211-215.

Remacle, C., Barbieri, M. R., Cardol, P. and Hamel, P. P. (2008). Eukaryotic complex I: functional diversity and experimental systems to unravel the assembly process. *Mol. Genet. Genomics* **280**, 93-110.

Saada, A., Vogel, R. O., Hoefs, S. J., van den Brand, M. A., Wessels, H. J., Willems, P. H., Venselaar, H., Shaag, A., Barghuti, F., Reish, O. et al. (2009). Mutations in NDUFAF3 (C3ORF60), encoding an NDUFAF4 (C6ORF66)-interacting complex I assembly protein, cause fatal neonatal mitochondrial disease. *Am. J. Hum. Genet.* **84**, 718-727.

Sadreyev, R. I., Baker, D. and Grishin, N. V. (2003). Profile-profile comparisons by COMPASS predict intricate homologies between protein families. *Protein Sci.* **12**, 2262-2272.

Schubert, H. L., Blumenthal, R. M. and Cheng, X. (2003). Many paths to methyltransfer: a chronicle of convergence. *Trends Biochem. Sci.* **28**, 329-335.

Shaulsky, G. and Loomis, W. F. (1993). Cell type regulation in response to expression of ricin-A in *Dictyostelium*. *Dev. Biol.* **160**, 85-98.

Sugiana, C., Pagliarini, D. J., McKenzie, M., Kirby, D. M., Salemi, R., Abu-Amero, K. K., Dahl, H. H., Hutchison, W. M., Vascotto, K. A., Smith, S. M. et al. (2008). Mutation of C20orf7 disrupts complex I assembly and causes lethal neonatal mitochondrial disease. *Am. J. Hum. Genet.* **83**, 468-478.

Sussman, M. (1987). Cultivation and synchronous morphogenesis of *Dictyostelium* under controlled experimental conditions. *Meth. Cell Biol.* **28**, 9-29.

Tiranti, V., Chariot, P., Carella, F., Toscano, A., Soliveri, P., Girlanda, P., Carrara, F., Fratta, G. M., Reid, F. M., Mariotti, C. et al. (1995). Maternally inherited hearing loss, ataxia and myoclonus associated with a novel point mutation in mitochondrial tRNASer(UCN) gene. *Hum. Mol. Genet.* **4**, 1421-1427.

Torija, P., Robles, A. and Escalante, R. (2006a). Optimization of a large-scale gene disruption protocol in *Dictyostelium* and analysis of conserved genes of unknown function. *BMC Microbiol.* **6**, 75.

Torija, P., Vicente, J. J., Rodrigues, T. B., Robles, A., Cerdan, S., Sastre, L., Calvo, R. M. and Escalante, R. (2006b). Functional genomics in *Dictyostelium*: MidA, a new conserved protein, is required for mitochondrial function and development. *J. Cell Sci.* **119**, 1154-1164.

Ugalde, C., Janssen, R. J., van den Heuvel, L. P., Smeitink, J. A. and Nijtmans, L. G. (2004). Differences in assembly or stability of complex I and other mitochondrial OXPHOS complexes in inherited complex I deficiency. *Hum. Mol. Genet.* **13**, 659-667.

Vahsen, N., Cande, C., Briere, J. J., Benit, P., Joza, N., Larochette, N., Mastroberardino, P. G., Pequignot, M. O., Casares, N., Lazar, V. et al. (2004). AIF deficiency compromises oxidative phosphorylation. *EMBO J.* **23**, 4679-4689.

Vogel, R. O., Janssen, R. J., Ugalde, C., Grovenstein, M., Huijbens, R. J., Visch, H. J., van den Heuvel, L. P., Willems, P. H., Zeviani, M., Smeitink, J. A. et al. (2005). Human mitochondrial complex I assembly is mediated by NDUFAF1. *FEBS J.* **272**, 5317-5326.

Vogel, R. O., Janssen, R. J., van den Brand, M. A., Dieteren, C. E., Verkaart, S., Koopman, W. J., Willems, P. H., Pluk, W., van den Heuvel, L. P., Smeitink, J. A. et al. (2007). Cytosolic signaling protein Ecsit also localizes to mitochondria where it interacts with chaperone NDUFAF1 and functions in complex I assembly. *Genes Dev.* **21**, 615-624.

Wallace, A. C., Laskowski, R. A. and Thornton, J. M. (1995). LIGPLOT: a program to generate schematic diagrams of protein-ligand interactions. *Prot. Eng.* **8**, 127-134.

Wilczynska, Z., Barth, C. and Fisher, P. R. (1997). Mitochondrial mutations impair signal transduction in *Dictyostelium discoideum* slugs. *Biochem. Biophys. Res. Commun.* **234**, 39-43.

Williams, R. S., Boeckeler, K., Graf, R., Muller-Taubenberger, A., Li, Z., Isberg, R. R., Wessels, D., Soll, D. R., Alexander, H. and Alexander, S. (2006). Towards a molecular understanding of human diseases using *Dictyostelium discoideum*. *Trends Mol. Med.* **12**, 415-424.

Wu, C. C., MacCoss, M. J., Howell, K. E. and Yates, J. R., 3rd. (2003). A method for the comprehensive proteomic analysis of membrane proteins. *Nat. Biotechnol.* **21**, 532-538.

Zemla, A. (2003). LGA: a method for finding 3D similarities in protein structures. *Nucleic Acids Res.* **31**, 3370-3374.

Seminars in Cell & Developmental Biology 22 (2011) 120–130

Contents lists available at ScienceDirect

Seminars in Cell & Developmental Biology

journal homepage: www.elsevier.com/locate/semcdb

Review

The *Dictyostelium* model for mitochondrial disease

Lisa M. Francione[a], Sarah J. Annesley[a], Sergio Carilla-Latorre[b], Ricardo Escalante[b], Paul R. Fisher[a,*]

[a] *Department of Microbiology, La Trobe University, VIC 3086, Australia*
[b] *Instituto de Investigaciones Biomédicas Alberto Sols, CSIC-UAM, Arturo Duperier 4, 28029 Madrid, Spain*

ARTICLE INFO

Article history:
Available online 1 December 2010

Key words:
Mitochondrial disease
Dictyostelium
Oxidative phosporylation
AMPK
ROS
Complex I
Phototaxis
Thermotaxis
Phagocytosis
Pinocytosis
Cell growth
Legionella
Mitochondrial biogenesis

ABSTRACT

Mitochondrial diseases are a diverse family of genetic disorders caused by mutations affecting mitochondrial proteins encoded in either the nuclear or the mitochondrial genome. By impairing mitochondrial oxidative phosphorylation, they compromise cellular energy production and the downstream consequences in humans are a bewilderingly complex array of signs and symptoms that can affect any of the major organ systems in unpredictable combinations. This complexity and unpredictability has limited our understanding of the cytopathological consequences of mitochondrial dysfunction. By contrast, in *Dictyostelium* the mitochondrial disease phenotypes are consistent, measurable "readouts" of dysregulated intracellular signalling pathways. When the underlying genetic defects would produce coordinate, generalized deficiencies in multiple mitochondrial respiratory complexes, the disease phenotypes are mediated by chronic activation of an energy-sensing protein kinase, AMP-activated protein kinase (AMPK). This chronic AMPK hyperactivity maintains mitochondrial mass and cellular ATP concentrations at normal levels, but chronically impairs growth, cell cycle progression, multicellular development, photosensory and thermosensory signal transduction. It also causes the cells to support greater proliferation of the intracellular bacterial pathogen, *Legionella pneumophila*. Notably however, phagocytic and macropinocytic nutrient uptake are impervious both to AMPK signalling and to these types of mitochondrial dysfunction. Surprisingly, a Complex I-specific deficiency (*midA* knockout) not only causes the foregoing AMPK-mediated defects, but also produces a dramatic deficit in endocytic nutrient uptake accompanied by an additional secondary defect in growth. More restricted and specific phenotypic outcomes are produced by knocking out genes for nuclear-encoded mitochondrial proteins that are not required for respiration. The *Dictyostelium* model for mitochondrial disease has thus revealed consistent patterns of sublethal dysregulation of intracellular signalling pathways that are produced by different types of underlying mitochondrial dysfunction.

Contents

* Corresponding author. Tel.: +61 3 9479 2229; fax: +61 3 9479 1222.
E-mail address: P.Fisher@latrobe.edu.au (P.R. Fisher).

1084-9521/$ – see front matter © 2010 Elsevier Ltd. All rights reserved.
doi:10.1016/j.semcdb.2010.11.004

1. Introduction

Mitochondrial diseases are complex degenerative disorders caused by mutations affecting nuclear genes for mitochondrial proteins or mitochondrial genes that encode subunits of the oxidative complexes or translational machinery [1]. In humans, the pathological outcomes include blindness, deafness, epilepsy, heart disease, stroke-like episodes, ataxia, muscle weakness, exercise intolerance, diabetes and kidney disease [2,3]. Mitochondrial dysfunction also plays pathological roles in neurological disorders such as Parkinson's disease and Alzheimer's disease [3–6].

Although much is known about the mtDNA mutations associated with human mitochondrial diseases, the relationship between genotype and phenotype is complicated and poorly understood. To gain further insight into this relationship, *Dictyostelium discoideum* has been employed as a model organism to study mitochondrial biogenesis and disease [7–11]. The mitochondrial genome of *Dictyostelium* has been fully sequenced [12], while mitochondrial transcription and RNA processing in this organism have been thoroughly examined [13–15]. Mitochondrial disease has been created in *Dictyostelium* by a variety of methods and the pathological consequences studied. Since *Dictyostelium* has motile unicellular and multicellular stages with multiple cell types, many phenotypes can be examined including phototaxis, thermotaxis, macropinocytosis, phagocytosis, cell cycle progression and growth, amoeboid motility and chemotaxis, morphogenesis and intracellular growth of pathogens such as *Legionella pneumophila*. These varied phenotypes represent measurable, reproducible "readouts" of the intracellular signaling pathways that regulate them. By assaying them in mitochondrially diseased *Dictyostelium* lines, we can gain a better understanding of genotype–phenotype relationships in mitochondrial disease, without the overlaid complexities associated with mammalian systems.

To understand the cytopathological pathways involved in mitochondrial diseases it is important to identify and study proteins that play roles in these pathways. One such protein is AMP-activated protein kinase (AMPK), a ubiquitous, highly conserved protein kinase that maintains cellular energy homeostasis in healthy and diseased cells [9,16]. Bokko et al. [9] and Francione et al. [11] have shown that signalling by this protein is responsible for diverse cytopathologies seen in *Dictyostelium* mitochondrial disease. However, Carilla-Latorre et al. [17] reported recently that, in Complex I-specific disease, additional aberrant signalling pathways become involved so that additional AMPK-independent phenotypes are also observed. This review will highlight the contributions made by the *Dictyostelium* model to our understanding of mitochondrial biology and disease. The genetic manipulation strategies that have been brought to bear and the associated phenotypes in *D. discoideum* are discussed, the role of AMPK is featured and our emerging understanding of Complex I-specific disease is described.

2. Mitochondrial biology

Mitochondria are ubiquitous in eukaryotic cells where they are central to the maintenance of cell function and viability. These organelles, numbering from one to thousands depending on the cell type, are responsible for generating most of the cell's ATP which constitutes the direct or indirect energy source for most cellular functions. ATP is generated by oxidative phosphorylation (OXPHOS) at the inner mitochondrial membrane. The proteins involved in OXPHOS are encoded by genes of both the mitochondrial and nuclear genomes (see Supplementary Table 1). Mutations in these or other genes that affect OXPHOS lead to an array of mitochondrial diseases [18].

2.1. The mitochondrial genome of humans and D. discoideum

Each *D. discoideum* cell contains about 200 copies of the mitochondrial genome which, like that of humans, is a circular molecule. The mitochondrial genome of humans is 16,569 bp [19] whereas in *D. discoideum* it is larger at 55,564 bp [12]. The average coding capacity of the mitochondrial genome in eukaryotes is 40–50 genes. The mitochondrial gene products are mainly required for five processes: respiration and/or OXPHOS, translation and in some organisms also transcription, RNA maturation and protein import [1,20]. In mammals, the majority of protein subunits (>80) of the respiratory chain are encoded in the nucleus whereas only 13 subunits are encoded in the mitochondrial genome [18,20]. Production of these mitochondrially encoded proteins requires the import of a variety of nuclear encoded proteins such as the single subunit mitochondrial RNA polymerase, amino acyl tRNA synthetases and the mitochondrial transcription factor A. Molecules required for mitochondrial protein synthesis which are encoded by the human and *D. discoideum* mitochondrial genomes are shown in Supplementary Table 2.

The mitochondrial genes and ORFs in *Dictyostelium* are all transcribed in the same orientation [12] (Fig. 1). Some overlapping of genes is evident in the tightly packed genome, which also exhibits intergenic spacing from several nucleotides to greater than 2 kb. The genome also encodes several ORFs that do not exist in most other organisms and presumably do not play essential universal roles.

All of the genes in the *Dictyostelium* mitochondrial genome are transcribed to one of eight large polycistronic mRNA transcripts which are further processed to form a variety of smaller monocistronic, dicistronic or tricistronic mature RNA molecules [14]. Recently these eight transcripts were shown to be derived from processing of a single primary RNA transcript [15,21]. The transcription initiation site in the *Dictyostelium* mitochondrial genome is located in a noncoding region upstream of *rnl* which encodes the large ribosomal subunit RNA (Fig. 1) [15].

2.2. The mitochondrial protein import machinery

The majority of the *ca.* 1500 resident mitochondrial proteins are encoded by nuclear DNA, translated by cytoplasmic ribosomes and imported by the mitochondrial protein import machinery [20,22]. These include not only the other metabolic enzymes and "housekeeping" proteins, but also the remaining 70 subunits of the OXPHOS complexes (that assemble with those encoded by mtDNA) as well as factors required for expression and replication of the mitochondrial genome [23]. Defective protein import may

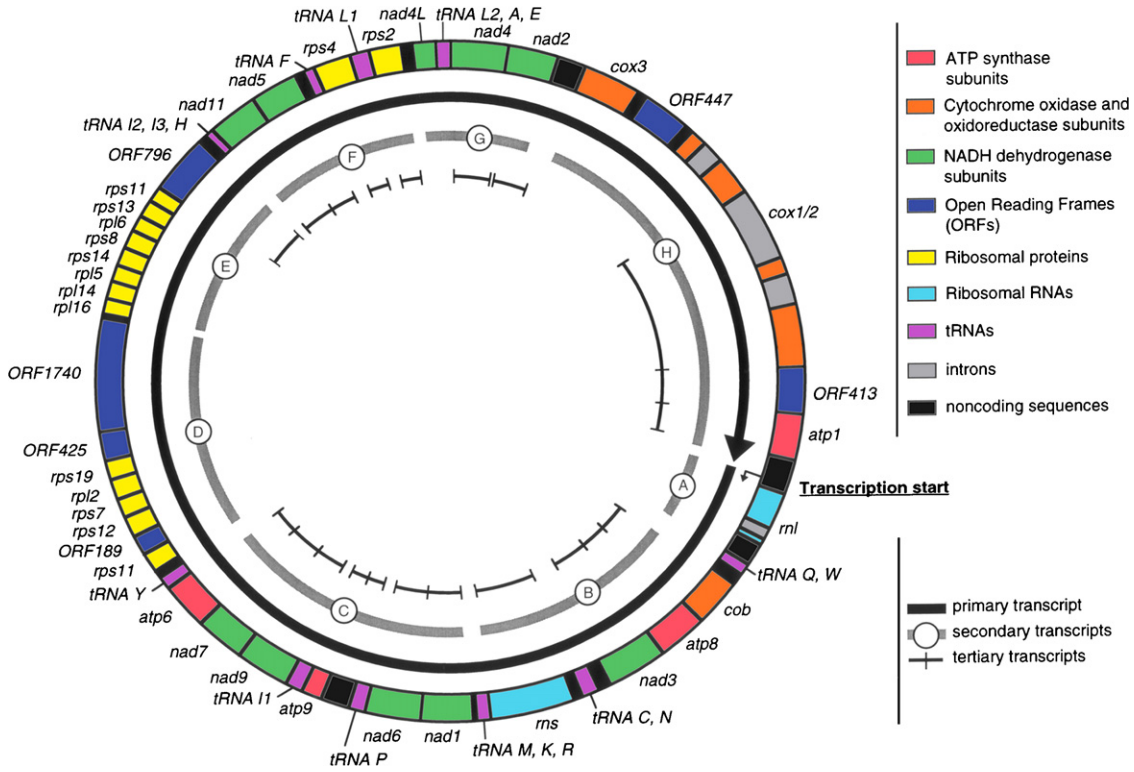

Fig. 1. Organization, transcription and transcript processing of the *Dictyostelium* mitochondrial genome. The *Dictyostelium* mitochondrial genes as well as introns and noncoding regions are shown. The genome is transcribed from a single start site as indicated by "Transcription start" [15]. The primary transcript may be rapidly and cotranscriptionally processed into smaller mature transcripts. Only the secondary transcripts A (3.1 kb), B (4.6 kb), C (5.6 kb), D (9.5 kb), E (6.0 kb), F (6.5 kb), G (3.7 kb), H (8.7 kb) and their smaller derivatives (tertiary transcripts) have been detected in northern hybridisation studies (Barth et al. [14]). From Fig. 1 of Barth et al. [21].

lead to mitochondrial respiratory dysfunction, reduced ATP production and mitochondrial disease (e.g. Human Deafness Dystonia Syndrome [24]). In turn impairment of respiration can inhibit mitochondrial protein import, since import is energized both directly by the mitochondrial membrane potential ($\Delta\psi_m$) and by ATP hydrolysis involving proteins such as the mitochondrial heat-shock protein (Hsp) 70 (mtHsp70) and mitochondrial import stimulation factor (MSF) [25,26]. The mitochondrial protein import machinery also assists in the correct sorting and translocation of proteins to the correct mitochondrial compartments – the matrix, the inner membrane, the intermembrane space and the outer membrane [22].

Although our knowledge of protein import into mitochondria is based mostly on research in *Saccharomyces cerevisiae* and *Neurospora crassa*, similar processes are likely to occur in other species. Tom40, Tom70 and Tom22 were found to be common elements of the mitochondrial protein machinery amongst eukaryotic genome sequences and orthologues are also encoded in the *Dictyostelium* genome [27].

Interestingly Ahmed et al. [28] reported that import of some mitochondrial proteins in *Dictyostelium* occurs cotranslationally *in vivo*. Cotranslational import of mitochondrial proteins has also been observed in yeast [29,30]. Current evidence suggest that it occurs as a result of transport and binding of the mRNA to the mitochondrial surface in a manner that depends on secondary stem-loop structures in the mRNA, often in untranslated regions of the transcript [29].

3. Human mitochondrial diseases

Mutations in mitochondrial or nuclear genes that encode components of the translational machinery or the OXPHOS complexes have been associated with human mitochondrial diseases. Due to the presence of mitochondria in all cells of the human body, every tissue can be adversely affected by mutations in the mitochondrial genome. However, there is tissue-specific variation in the numbers of mitochondria, the proportion of mutant mitochondrial genomes, the energy demands of the cell, the isoforms of nuclear-encoded mitochondrial proteins that are expressed and the extent of cellular and mitochondrial proliferation. Depending on which tissues are affected most in a given individual, this leads to a bewildering complexity in mitochondrial diseases which exhibit a very broad range of possible symptoms (Supplementary Tables 3 and 4). Individuals with the same mitochondrial disease mutation can exhibit huge variation in clinical symptoms while different mutations can result in similar clinical manifestations. Thus phenotypes associated with human mitochondrial diseases are unpredictable from specific genetic defects.

In mitochondrial diseases, pathogenic mutations in mitochondrial genes usually affect only a subset of the genomes (a state referred to as heteroplasmy) and the extent of the phenotypic outcomes is sometimes related to how large this subset is (the mutant load). This can contribute to a phenomenon whereby a particular pathological outcome is only observed when the mutant load exceeds a particular threshold. A good example of such a threshold is shown by NARP (Neuropathy, Ataxia and Retinitis Pigmentosa) and LS (Leigh Syndrome) which can result from the same mutation. NARP is caused by 70–90% of mutated mtDNA whereas LS develops if the mutation load is above 90–95% [31,32]. In some cases, mtDNA mutations must be above a particular threshold for significant ATP depletion and/or symptoms of the disease to occur [33]. Biochemical thresholds that influence the extent to which ATP levels are reduced as a consequence of gene mutations, have been described in detail by Rossignol et al. [34].

4. *D. discoideum* as a model organism for mitochondrial disease

The genetics, biochemistry and signal transduction processes of *D. discoideum* have been studied extensively and are well understood. With fully sequenced mitochondrial [12] and nuclear [35] genomes, the organism is one of a small number of nonmammalian model organisms recognized by the National Institute of Health (NIH) in the U.S.A. for their importance in biomedical research (http://www.nih.gov/science/models/). Many *Dictyostelium* genes are orthologues of disease-related genes [35] and this has facilitated the establishment of *Dictyostelium* models for investigating a variety of human diseases [10,36,37,39,40], including mitochondrial disease [21]. In those cases where the relevant experiments have been done, heterologous expression and study of *Dictyostelium* genes in other organisms, or *vice versa*, has confirmed directly that the functions of orthologous proteins have been conserved during evolution [10].

4.1. Life cycle and phenotypes

What makes *Dictyostelium* so valuable a model organism is that it combines genetic, biochemical and cell biological tractability with a unique life cycle providing a great variety of readily assayed, reproducible disease phenotypes. The organism grows as isolated amoeboid cells that divide mitotically and obtain nutrients either by phagocytic consumption of bacteria or by macropinocytosis of liquid medium. Starvation induces a developmental programme in which the amoebae differentiate and consequently become responsive to an attractant, cAMP, which they now synthesize and secrete. The resulting aggregation process leads to formation of a motile, multicellular organism (the "slug") containing multiple cell types organized in a well-defined spatial pattern. The migratory slug exhibits highly sensitive phototactic and thermotactic responses under control of its specialized anterior cells. After a variable period of migration it forms a fruiting body by a combination of morphogenetic movements and further cell differentiation. This life cycle, with its motile unicellular and multicellular stages, offers diverse phenotypic "readouts" of the signaling pathways that regulate them. These include cell growth and division [38]; amoeboid motility and chemotaxis [39]; phagocytosis and macropinocytosis [40]; phototaxis and thermotaxis [41,42]; cell and tissue differentiation and pattern formation [43]; autophagic cell death [44]; multicellular tissue movement and morphogenesis [45,46]. *Dictyostelium* has also been used to study the interactions between microbial pathogens, such as *L. pneumophila*, and their hosts [47]. The molecular mechanisms of *Legionella* pathogenesis in *D. discoideum* are similar to those in human cells [48,49]. Despite this phenotypic richness, many of the complexities associated with mammalian systems are eliminated in the *Dictyostelium* model, since all stages of the life cycle can be readily studied in clonally derived, genetically identical cell lines. The study of mitochondrially diseased *Dictyostelium* strains has accordingly revealed consistent, reproducible outcomes that contrast with the unpredictability of mitochondrial disease in humans.

As mentioned previously human mitochondrial diseases are characterized by pathological or biochemical thresholds. Mitochondrial disease in *Dictyostelium* has exhibited similar thresholds in that some phenotypes appear more sensitive to mitochondrial dysfunction than others [7,8,50]. Although genetic manipulations that would impair respiration resulted in similar phenotypic outcomes, the severity of the phenotypes varied amongst the mitochondrially diseased strains so that particular defects such as slow growth were not observed in every strain [7–9,50]. Much of this variation in the severity of the phenotypic aberrations in mitochondrially diseased *Dictyostelium* was shown to be caused by differences in the severity of the underlying genetic defect. As described in the next section, such differences are readily created and quantitatively measured in *Dictyostelium*.

4.2. Genetic manipulation to produce mitochondrial disease in *Dictyostelium*

In order to study mitochondrial disease in *Dictyostelium* various methods have been employed to create sublethal mitochondrial dysfunction. These include RNA_i (interfering RNA) [51] or antisense inhibition of expression of specific mitochondrial proteins [8,9], heteroplasmic disruption of mitochondrial genes [7,11,52] and knockout of nuclear genes encoding nonessential mitochondrial proteins [53–56]. Mitochondrial defects in *Dictyostelium* have also been generated pharmacologically through the use of ethidium bromide to deplete the cells of mitochondrial DNA [57].

4.2.1. Heteroplasmic targeted disruption

The first *Dictyostelium* mitochondrial gene targeted for heteroplasmic disruption was *rnl*, the mitochondrial large ribosomal subunit RNA gene [7]. The original disruption of this gene was a result of a nontargeted insertion into a gene important for phototaxis. Subsequent targeted disruptions confirmed the effect on phototaxis and initiated the study of mitochondrial disease in *Dictyostelium* [7]. Another *Dictyostelium* mitochondrial gene *rps4*, encoding a ribosomal protein, was targeted for heteroplasmic disruption by Inazu et al. [52]. Apart from *rnl* and *rps4*, 8 other mitochondrial genes have been disrupted and regardless of which gene was targeted, the expression of the entire mitochondrial genome was reduced [50]. The strength of signals in Southern blots of the mitochondrial DNA indicates that only a subset of the mitochondrial genomes is affected in these strains *i.e.* the disruptions are heteroplasmic [7,50] allowing *Dictyostelium* to be used as a model for human heteroplasmic mitochondrial disease.

4.2.2. Antisense and RNAi inhibition of nuclear genes encoding essential mitochondrial proteins

Mitochondrial disease can also be caused by mutations affecting nuclear genes that encode mitochondrial proteins. An example is *hspA*, which encodes chaperonin 60 (Cpn60), a protein located in the mitochondrial matrix. Cpn60 is required for correctly folding proteins newly imported into the mitochondrial matrix. A deficiency of Cpn60 is linked to a mitochondrial disease in humans, the symptoms of which include severe neurological and developmental defects and depletion of many respiratory enzymes [58–60]. In *D. discoideum* a Cpn60 insufficiency was created by antisense inhibition of expression of the protein [8,9]. Transformation of *Dictyostelium* with an antisense-inhibition construct produces transformants in each of which a different number of copies of the plasmid are integrated into the nuclear genome. The copy number is stable, easily determined using several techniques [61,62] and correlates with the reduction of expression of the target gene and the phenotypic outcomes [8,9]. RNAi constructs have been used similarly to reduce the expression of the catalytic subunit of mitochondrial succinate dehydrogenase (respiratory Complex II) (Lay and Fisher, unpublished results) and Dd-TRAP1 (*D. discoideum* Tumor necrosis factor receptor-associated protein), a Hsp90 homologue which translocates to the mitochondria in early differentiation [51]. By analogy with Hsp90 in other organisms, it may play a role in chaperoning some proteins *en route* to the mitochondria.

4.2.3. Targeted disruption of nuclear genes encoding nonessential mitochondrial proteins

While the heteroplasmic disruption of essential mitochondrial genes is possible, it is lethal to disrupt a nuclear gene in

Table 1
Phenotypes associated with mitochondrial dysfunction in *Dictyostelium*.

Method of generating mitochondrial dysfunction	Phenotype										
	Growth on bacteria	Growth in broth	Phagocytosis	Pinocytosis	Phototaxis	Thermotaxis	Morphogenesis	Aggregation	Chemotaxis	*Legionella* susceptibility	Reference
Pharmacological, expected to affect respiration											
Ethidium bromide inhibition of mtDNA replication		–			–		– (Stalky)	–			57
Genetic, expected to affect respiration											
Heteroplasmic mitochondrial gene disruption (*rnl*, *nad5*, *cob*, *nad2*, *atp6*, *atp1*, *cox3*, *ORF1740*, *ORF796*)	–	–	+	+	–	–	– (Stalky)	–		–	7,11,50
Heteroplasmic *rps4* disruption		±			–			–			52, Fisher (unpublished)
Chaperonin 60 antisense inhibition	–	–	+	+	–	–	– (Stalky)	–		–	8,9,11
Genetic, respiratory complex–specific defect in respiration											
MidA knockout producing specific Complex I deficiency	–	–	–	–	–	–	± (Stalky)	+			63,17
Genetic, not known to affect respiration											
Nuclear *fszA*, *fszB* disruption	+ (fszA$^-$); – (fszB$^-$)	+ (fszA$^-$); – (fszB$^-$)			+		+	+			55, Fisher (unpublished)
Nuclear *cluA* disruption	– (Defective cytokinesis)	– (Defective cytokinesis)					+	+			54
Nuclear *torA* disruption	–		+					–	–		53
Nuclear Dd–TRAP1 RNAi inhibition		–						–			56
Nuclear *aoxA* disruption		+					+	+			64

+, Wild type phenotype; –, aberrant phenotype; ±, mildly aberrant phenotype; Empty cells, Phenotype not reported.

Dictyostelium's haploid genome if it encodes an essential mitochondrial protein. Such a gene must supply its encoded protein to every mitochondrion in the cell. However some mitochondrial proteins are not essential for viability. Genes encoding these proteins can be disrupted through homologous recombination and the associated phenotypes examined. Such genes include *cluA* [54], *torA* (Tortoise) [53], *fszA* and *fszB* [55], *midA* [17,63] and *aoxA* [64].

4.3. Dictyostelium mitochondrial disease pathology

Several broad categories of mitochondrial dysfunction have been studied in the *Dictyostelium* model (Table 1). The first is generalized oxidative phosphorylation (OXPHOS) defects that are expected to impair multiple respiratory complex deficiencies. Such defects have been studied by sublethal genetic or pharmacological manipulations that reduce but do not eliminate the oxidative phosphorylation (OXPHOS) capacity of the mitochondria. The second category of mitochondrial defects studied in *Dictyostelium* are those that affect mitochondrial functions other than OXPHOS. Finally, in very recent work, a class of mutant has been found that produces a specific reduction in the activity of only one of the respiratory complexes (Complex I). Each of these categories of mitochondrial dysfunction has contributed to our growing understanding of the cytopathological pathways underlying mitochondrial disease.

4.3.1. Generalized OXPHOS defects

The most obvious biochemical consequence of a generalized deficiency in oxidative phosphorylation is a reduced capacity to synthesize ATP. In humans the phenotypic outcomes of mitochondrial disease were thought accordingly to result from a depletion of ATP and the different energy requirements of cellular functions. However, in *Dictyostelium* it has been shown that mitochondrial disease phenotypes arising from generalized OXPHOS defects (Table 1) do not result simply from a depletion of ATP but from disturbances in intracellular signalling networks. In mitochondrial disease the energy generating capacity of the mitochondria is compromised which results in activation of intracellular energy stress signals. These signals are relayed into various signalling pathways to produce phenotypic affects, some of which are more sensitive to mitochondrial dysfunction than others.

The first mitochondrial disease phenotype to be discovered in *Dictyostelium* was impaired phototaxis and thermotaxis in the multicellular slug stage of the life cycle [7]. *Dictyostelium* slugs display extremely sensitive, accurate orientation towards light and in temperature gradients [47,48]. Phototaxis and thermotaxis pathways converge early so that almost all of the proteins involved are required for both processes. The photo/thermosensory transduction pathways in *Dictyostelium* are not completely understood, but many participating molecules have been identified which could be downstream targets of energy stress signalling. These include heterotrimeric G proteins [47,48]; the second messengers cAMP, cGMP, IP_3 and Ca^{2+} [47,48]; signalling proteins such as RasD [65], GefE and GefL [66]; protein kinases such as PKB and ErkB [67]; and cytoskeletal proteins such as GRP125 [68], villidin [69], CAP [70], filamin [71] and FIP [72]. A number of the proteins involved form a photosensory signalling complex that is assembled on the scaffolding protein filamin [67,73]. The phototaxis and thermotaxis signalling pathways were impaired by mitochondrial disease in all cases tested, regardless of how the mitochondrial dysfunction was caused. Thus heteroplasmic disruption of any of 10 different mitochondrial genes and down regulation of chaperonin 60 all resulted in phototaxis and thermotaxis defects [7,8,11,50,52]. Likewise phototaxis was impaired by depletion of mitochondrial DNA using ethidium bromide treatment [57].

The second phenotype to be affected by mitochondrial disease is growth. *Dictyostelium* cells can grow either on bacterial lawns (obtaining nutrients by phagocytosis) or axenically in liquid medium (obtaining nutrients by macropinocytosis). Mitochondrially diseased *Dictyostelium* cells showed impaired growth in liquid and on bacterial lawns [7–9]. However these growth defects were not a result of altered phagocytosis or macropinocytosis [9], nor did the cells show alterations to their size, implying a coordinate inhibition of both cell growth and cell cycle progression (Ahmed and Fisher, unpublished data).

The proteins controlling the cell cycle that could be dysregulated in mitochondrial disease include seven cyclins, six cyclin-dependent kinases identified in *Dictyostelium* and homologues of inhibitors of cell cycle progression such as the retinoblastoma protein Rb, a homologue of which is encoded by *rblA* [35]. The major signalling pathway controlling cell growth in metazoans involves the protein kinase TOR in a multiprotein complex called TORC1. Inhibition of this pathway involves activation of TSC2 which in turn inactivates Rheb and thereby inactivates TOR [38,74]. These proteins are conserved in *Dictyostelium* [35] but their functional roles in signalling pathways involved in growth control or mitochondrial disease have not been determined. In mammals AMPK inhibits TORC1 directly through the RapTOR subunit [75] and indirectly by activating TSC2 [74]. Because mitochondrial dysfunction compromises ATP generation, AMPK should be chronically activated in mitochondrially diseased cells. This indeed appears to be the case for mitochondrially diseased *Dictyostelium* cells [9] as well as Parkinson's [76], Alzheimer's [77] and Huntington's [78] disease neurons. As described in greater detail in later sections, chronic AMPK signalling was found to be responsible for the slow growth of mitochondrially diseased *Dictyostelium* cells [9].

The third phenotype which is consistently affected by mitochondrial dysfunction is the differentiation of cells into stalk and spore cells, with mitochondrially diseased cells showing an increased number of cells directed into the stalk differentiation pathway and mislocalisation of these cells in the multicellular slug. At culmination this results in fruiting bodies with thick short stalks. This effect was seen in mitochondrially diseased cells created either by genetic manipulation [8,9] or by treatment with ethidium bromide [57]. In addition, almost all cells were directed into the stalk differentiation pathway by inhibitors of cyanide-resistant respiration that also impaired the mitochondrial membrane potential, loss of which is known to stimulate autophagy [79]. Stalk cell differentiation in *Dictyostelium* involves a programmed cell death accompanied by the accumulation of autophagic vacuoles. Mitochondrial dysfunction in *Dictyostelium* thus appears to direct cells into an autophagic cell death pathway that may be analogous to the autophagic cell death implicated in neurodegeneration in humans [44].

The last phenotype to be associated with mitochondrial disease in *Dictyostelium* is altered transition from growth to development and subsequent chemotactic aggregation. Inazu et al. [52] showed that knock down of the mitochondrial *rps4* gene resulted in greatly impaired cell aggregation and significantly lower levels of *car1*, an early developmental gene. Depletion of mitochondrial DNA by ethidium bromide treatment impaired aggregation significantly and reduced the expression of early developmental genes including *carA* [57]. Aggregation was also impaired in chaperonin 60 or succinate dehydrogenase antisense-inhibited cells resulting in fewer, smaller aggregates [8,9,Lay and Fisher, unpublished].

4.3.2. Defects not known to affect OXPHOS

Mutations affecting the mitochondria have been created which do not damage the energy generating capability of the mitochondria (Table 1). One example is knockout of the mitochondrial fission proteins FszA and FszB [55], whose closest homologues are FtsZ proteins that mediate binary fission in the α-proteobacteria, the presumed ancestors of mitochondria. In some eukaryotic lineages such as fungi, animals and plants, no mitochondrial FtsZ proteins

have been identified and mitochondrial division is primarily undertaken by FIS1 and DNM1L (dynamin-like protein also known as DRP1) [80]. Mitochondrial fission in *Dictyostelium* involves both dynamin-like proteins [81] and FtsZ proteins [55], indicating that the latter were retained in the amoebozoan lineage but discarded in some others. Disruption of FszA or FszB impaired mitochondrial division, producing more elongated mitochondria, while disruption of FszB but not FszA also caused growth defects [55]. However, none of the other characteristic mitochondrial disease phenotypes described in the preceding section were observed.

FszB was found localised to submitochondrial bodies of unknown function [55] which are also enriched in another mitochondrial protein TorA (tortoise) [53]. TorA null amoebae move slowly and fail to suppress inappropriate lateral pseudopod formation during chemotaxis, defects which may explain why they grow slowly on bacterial lawns. The specificity of the motility and chemotaxis defects suggests that TorA null cells still produce wild type levels of ATP [53]. There is no human homologue for TorA and it is unknown whether TorA mutant cells display any of the phenotypes typically associated with mitochondrial respiratory dysfunction in *Dictyostelium*.

A nuclear gene required for normal subcellular localisation of mitochondria is *cluA*. First discovered and functionally characterized in *Dictyostelium*, *cluA* has homologues in all eukaryotes whose genomes have been sequenced. CluA null mutants exhibit pronounced perinuclear clustering of the mitochondria in mutant cells [54]. CluA is also involved in cytokinesis since mutant cells were multinucleate and slightly impaired in growth [54]. The involvement in cytokinesis is likely to be an indirect result of the contractile ring being physically occluded by large aggregates of mitochondria that block completion of cleavage [82].

Another mitochondrial protein that has been studied genetically is TRAP1, a homologue of mammalian Tumor Necrosis Factor Receptor-Associated Protein 1 (TRAP1). TRAP1 belongs to the Hsp90 molecular chaperone family and localises to the mitochondria as well as to extramitochondrial sites such as the nucleus, secretory granules and cell membranes [83–85]. The protein is localised to the cell cortex of cells growing at low cell densities and translocates to the mitochondria as the cell density of growing cells increases [56]. RNAi inhibition of TRAP1 expression resulted in slow vegetative growth and delayed aggregation, while overexpression resulted in premature aggregation.

The alternative oxidase encoded by *aoxA* in *Dictyostelium* is a mitochondrial protein with homologues in animals, plants, fungi and bacteria [86]. It can accept electrons from ubiquinone in place of Complex III and pass them directly to molecular oxygen, thus providing an alternative pathway for electron flow in which protons are pumped across the mitochondrial inner membrane only at Complex I. This process of cyanide-resistant respiration appears to serve primarily as an electron sink that prevents leakage of electrons in single electron transfers to oxygen that would form superoxide anions and thence other reactive oxygen species (ROS). Kimura et al. [64] knocked out *aoxA* in *Dictyostelium* and found no obvious phenotypic changes in growth or development under normal conditions. However development in the mutant was completely blocked by millimolar concentrations of KCN that merely delayed development in the wild type.

4.3.3. The role of AMPK

It was first proposed by Wilzcynska et al. [7] that a cytopathological effect of mitochondrial disease is impairment of signal transduction pathways with some pathways being more sensitive than others. Recently a molecular link between mitochondrial disease and cellular signalling was identified in *Dictyostelium* in the form of AMP-activated protein kinase (AMPK) [9]. AMPK is an essential sensor and homeostatic regulator of cellular energy status [87]. The serine/threonine protein kinase is a heterotrimer composed of a catalytic α subunit, a regulatory γ subunit and a β subunit which acts as a scaffold for the other subunits. In mammalian cells there are three genes encoding isoforms of the γ subunit and two for each of the α and β subunits, whereas in *Dictyostelium* only one of each subunit is encoded in the genome.

Activation of AMPK occurs when AMP binds to the two Bateman domains on the γ subunit relieving its inhibition of the catalytic α subunit. The α subunit is now able to be phosphorylated at a threonine residue by an upstream kinase and is also resistant to dephosphorylation by phosphatases. Because of competition between AMP and ATP for binding to the Bateman domains, AMPK activation is very sensitively regulated by AMP/ATP ratios with high ATP levels producing the inactive heterotrimer. Several upstream AMPK kinases have been identified to date – LKB1 [88,89], CaMKKα and β [90,91] and TAK1 [92]. Of these, LKB1 is reported to be the major activator [89].

Once activated, AMPK homeostatically rectifies low cellular energy levels by activating pathways that produce ATP while inhibiting others that consume it. These effects are exerted by inhibiting key enzymes in biosynthetic pathways (e.g. acyl CoA carboxylase in fatty acid synthesis and 3-hydroxy-3-methylglutaryl-CoA reductase in cholesterol biosynthesis), activating protein translocation (e.g. the GLUT4 glucose transporter to the plasma membrane, increasing glucose uptake) [93], and altering gene expression (e.g. repression of glucose responsive genes and protein synthesis [94,95], induction of mitochondrial biogenesis [96,97]). These actions enable AMPK to regulate the AMP/ATP ratio and maintain healthy energy levels within the cell.

Because of its exquisite sensitivity to AMP/ATP ratios, AMPK exerts its effects prior to a serious depletion in energy. Bokko et al. [9] provided molecular genetic evidence that AMPK is chronically activated in mitochondrial disease. Mitochondrial disease was created in *Dictyostelium* by antisense inhibition of chaperonin 60 to produce the defective phenotypes discussed earlier, including defective photo/thermotaxis, growth and morphogenesis. These defective phenotypes were phenocopied by overexpressing a constitutively activated form of AMPK (AMPKαT). Conversely, when AMPKα expression was knocked down in mitochondrially diseased cells (chaperonin 60 antisense inhibition), the defective phenotypes were suppressed. AMPKαT-expressing strains also exhibited increased mitochondrial mass and higher ATP levels, as expected since AMPK stimulates biogenesis and ATP production in mammalian cells. Mitochondrially diseased cells did not show changes in mitochondrial mass or steady state ATP levels presumably due to a balance between reduced biogenesis and ATP production caused by antisense inhibition of chaperonin 60 and increases due to chronic activation of AMPK. However this chronic AMPK hyperactivity in mitochondrially diseased cells leads to permanent dysregulation of the downstream energy-consuming pathways under AMPK's control (Fig. 2).

4.3.4. Dictyostelium and Complex I dysfunction

NADH:ubiquinone oxidoreductase or Complex I (CI) is the first and the largest complex of the respiratory chain and couples the oxidation of NADH to reduction of ubiquinone and the transport of protons. It is formed by 45 protein subunits in mammalian cells that assemble together into a structure of approximately 1 Mda [98]. CI has important implications in human pathology due to its role in the generation of reactive oxygen species and the increasing number of diseases whose cause is directly or indirectly associated with CI function. About 40% of inherited disorders of the OXPHOS system involve isolated or combined deficiencies in CI. As described previously these deficiencies present diverse combinations of clinical manifestations, including fatal childhood disorders such as Leigh syndrome. Complex I dysfunction has also been linked to neurode-

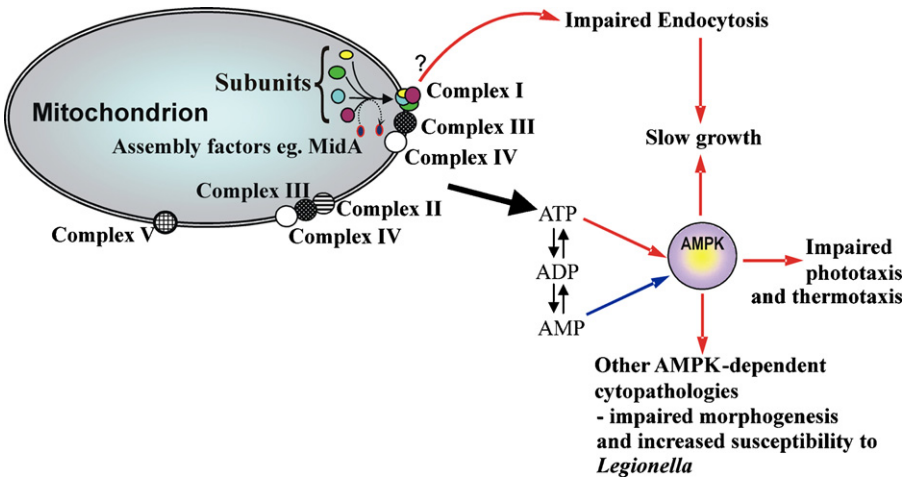

Fig. 2. Cytopathological pathways in *Dictyostelium* mitochondrial disease. Two pathways are shown. 1. Generalized mitochondrial respiratory dysfunction affecting multiple oxidative phosphorylation complexes compromises mitochondrial ATP generation, leading to chronic AMPK activation. The resulting dysregulation of intracellular signalling produces multiple cytopathological outcomes. Not shown is the homeostatic feedback by which AMPK stimulates mitochondrial biogenesis and ATP production. In mitochondrially diseased cells chronic AMPK activation can thereby maintain ATP at normal levels while at the same time causing chronic downstream cytopathologies. 2. In addition to AMPK-dependent pathways, a MidA-dependent dysfunction (possibly through Complex I-specific deficiency indicated by the question mark) impairs endocytic pathways (phagocytosis and macropinocytosis) in an AMPK-independent manner. Different, more limited cytopathologies may be caused by mutations that affect other aspects of mitochondrial biology without impairing ATP production.

generative disorders such as Parkinson's and Alzheimer's diseases [99–101]. Despite its importance in human pathology many aspects of CI function, including its regulation, assembly and structure are poorly understood.

CI is present in prokaryotes in its minimal version formed by the so-called core subunits. This bacterial complex is able to perform the essential redox reactions required for its function. However eukaryotic CI contains additional subunits (known as accessory subunits) that might have been acquired during evolution to enrich CI with new functions and regulatory properties. Interestingly CI has been lost in certain eukaryote lineages such as the one leading to the yeast *Saccharomyces cerevisiae*. However, other fungi such as *Yarrowia lipolytica* and *N. crassa* do contain CI and have been used as simple models for its study [102,103].

Like *Yarrowia* and *Neurospora*, *Dictyostelium* possesses CI and homologous genes encoding Complex I subunits can be recognized in the mitochondrial and nuclear genomes. Also like them, *Dictyostelium* has proteins similar to all core subunits and a subset of accessory proteins (Supplementary Table 5). Interestingly the *Dictyostelium* mitochondrial genome codes for three CI subunits that are nuclear encoded in other organisms [104]. This is consistent with divergence of major eukaryotic lineages before the process of transferring mitochondrial genes to the nuclear genome had been completed.

Despite its complexity only few assembly factors have been described to be required for the correct assembly and stability of this huge multiprotein complex. Six have been described to be involved in human CI deficiency: NDUFAF1, NDUFAF2, NDUFAF3 and NDUFAF4 [105–108], C8orf38 [109] and C20orf7 [110,111]. Others are required for CI assembly but have not yet been implicated in human disease such as Ecsit [112], AIF [113], IndI [114,115] and MidA/C2orf56 [17]. Interestingly, two (C20orf7 and MidA) are putative methyltransferases suggesting that methylation might play a relevant role in CI function.

MidA is a conserved protein that was described for the first time in *Dictyostelium* as a mitochondrial protein required for cellular bioenergetics since null mutants have reduced ATP levels and are compromised in growth and development [63]. Bioinformatics modeling and site directed mutagenesis suggested that MidA contains a methyltransferase domain required for its function. The protein's ability to complement the mutant phenotype is abolished by mutations in a critical glycine in the catalytic core that is predicted to interact with the methyl donor S-adenosyl methionine (SAM) [17]. *Dictyostelium* cells lacking MidA show a specific defect in Complex I activity and this role has also been confirmed in mammalian cells since the knock-down of human MidA in HEK293T cells results in an isolated defect in the activity and assembly of Complex I. Both *Dictyostelium* and human MidA interact with the CI core subunit NDUFS2, but the consequences of this interaction and whether or not MidA is involved in Ndufs2 methylation remain open questions [17]. Only two protein methylation modifications have been detected in Complex I subunits. One of them is in the bovine NDUFB3 (B12) subunit that is methylated at conserved His residues but has no homologue in *Dictyostelium*. Interestingly, the other one is the human NDUFS2 subunit that harbors a methylated arginine, R323 [116].

MidA knockout in *Dictyostelium* causes a complex phenotype that shows similarities but also differences with that of other mitochondrially diseased strains (Table 1 and Fig. 2). Defects in phototaxis and thermotaxis, a hallmark of *Dictyostelium* mitochondrial defects, are present in the MidA mutant and can be rescued by AMPK antisense inhibition, similarly to the other described mitochondrial mutants [9,17]. However, *midA*$^-$ cells are also defective in phagocytosis and macropinocytosis, a phenotype that is not rescued by AMPK antisense inhibition and is not even present in the other described mitochondrial mutants. These results suggest that isolated defects in CI might cause abnormal phagocytosis and pinocytosis. Alternatively, MidA might have additional functions beyond CI that could affect these cellular activities. The study of other CI-specific mutants in *Dictyostelium* is necessary to distinguish between these possibilities and to clarify the complex cytopathology associated with CI disease.

5. Conclusion

The *Dictyostelium* model for mitochondrial disease is proving to be a rich field for investigation. It is simple and tractable enough to yield consistent, reproducible phenotypes in clonally derived mutants, yet has a sufficiently complex life cycle with unicellular and multicellular motile forms to provide a rich lode of phenotypic readouts of varied intracellular signalling pathways. It has taught us that sublethal mitochondrial dysfunction at the cellular level pro-

duces phenotypic outcomes from disturbed intracellular signalling networks not merely ATP depletion, cumulative oxidative damage and cell death. The implication is that whole organism pathology may arise earlier and be more nuanced than is often supposed – an outcome of sublethal cellular dysfunction not simply the result of cell death. It is to be hoped that with this insight and greater understanding of the nature of the cellular disturbances produced by mitochondrial disease, new treatment strategies will present themselves for these currently untreatable disorders.

Acknowledgements

This work was supported by grants BMC2006-00394 and BMC2009-09050 to R.E. from the Spanish Ministerio de Ciencia e Innovación and to P.R.F. from the Thyne Reid Memorial Trusts and the Australian Research Council.

Appendix A. Supplementary data

Supplementary data associated with this article can be found, in the online version, at doi:10.1016/j.semcdb.2010.11.004.

References

[1] Wallace DC. Mitochondrial DNA mutations in disease and aging. Environ Mol Mutagen 2010;51(5):440–50.
[2] Francione L, Fisher PR. Cytopathological mechanisms in mitochondrial disease. Curr Chem Biol 2010;4:32–48.
[3] Zeviani M, Carelli V. Mitochondrial disorders. Curr Opin Neurol 2007;20(5):564–71.
[4] Bender A, Krishnan KJ, Morris CM, Taylor GA, Reeve AK, Perry RH, et al. High levels of mitochondrial DNA deletions in *substantia nigra* neurons in aging and Parkinson disease. Nat Genet 2006;38:515–7.
[5] Coskun PE, Beal MF, Wallace DC. Alzheimer's brains harbor somatic mtDNA control-region mutations that suppress mitochondrial transcription and replication. Proc Natl Acad Sci USA 2004;101:10726–31.
[6] Kraytsberg Y, Kudryavtseva E, McKee AC, Geula C, Kowall NW, Khrapko K. Mitochondrial DNA deletions are abundant and cause functional impairment in aged human substantia nigra neurons. Nat Genet 2006;38:518–20.
[7] Wilczynska Z, Barth C, Fisher PR. Mitochondrial mutations impair signal transduction in *Dictyostelium discoideum* slugs. Biochem Biophys Res Commun 1997;234:39–43.
[8] Kotsifas M, Barth C, Lay ST, de Lozanne A, Fisher PR. Chaperonin 60 and mitochondrial disease in *Dictyostelium*. J Muscle Res Cell Motil 2002;23:839–52.
[9] Bokko PB, Francione L, Bandala-Sanchez E, Ahmed AU, Annesley SJ, Huang X, et al. Diverse cytopathologies in mitochondrial disease are caused by AMP-activated protein kinase signaling. Mol Biol Cell 2007;18:1874–86.
[10] Annesley SJ, Fisher PR. *Dictyostelium discoideum*—a model for many reasons. Mol Cell Biochem 2009;329:73–91.
[11] Francione L, Smith PK, Accari SL, Taylor PE, Bokko PB, Bozzaro S, et al. *Legionella pneumophila* multiplication is enhanced by chronic AMPK signalling in mitochondrially diseased *Dictyostelium* cells. Dis Model Mech 2009;2:479–89.
[12] Ogawa S, Yoshino R, Angata K, Iwamoto M, Pi M, Kuroe K, et al. The mitochondrial DNA of *Dictyostelium discoideum*: complete sequence, gene content and genome organisation. Mol Gen Genet 2000;263:514–9.
[13] Barth C, Greferath U, Kotsifas M, Fisher PR. Polycistronic transcription and editing of the mitochondrial small subunit (*SSU*) ribosomal RNA in *Dictyostelium discoideum*. Curr Genet 1999;36:55–61.
[14] Barth C, Greferath U, Kotsifas M, Tanaka Y, Alexander S, Alexander H, et al. Transcript mapping and processing of mitochondrial RNA in *Dictyostelium discoideum*. Curr Genet 2001;39:355–64.
[15] Le P, Fisher PR, Barth C. Transcription of the *Dictyostelium discoideum* mitochondrial genome occurs from a single initiation site. RNA 2009;15:2321–30.
[16] Ruderman NB, Xu XJ, Nelson L, Cacicedo JM, Saha AK, Lan F, et al. AMPK and SIRT1: a long-standing partnership? Am J Physiol Endocrinol Metab 2010;298(4):E751–60.
[17] Carilla-Latorre S, Gallardo ME, Annesley SJ, Calvo-Garrido J, Grana O, Accari SL, et al. MidA is a putative methyltransferase that is required for mitochondrial complex I function. J Cell Sci 2010;123:1674–83.
[18] Wallace DC, Fan WW. Energetics epigenetics, mitochondrial genetics. Mitochondrion 2010;10(1):12–31.
[19] Leonard JV, Schapira AHV. Mitochondrial respiratory chain disorders. I. Mitochondrial DNA defects. Lancet 2000;355:299–304.
[20] Shutt TE, Shadel GS. A compendium of human mitochondrial gene expression machinery with links to disease. Environ Mol Mutagen 2010;51(5):360–79.
[21] Barth C, Le P, Fisher PR. Mitochondrial biology and disease in *Dictyostelium*. Intern Rev Cytol 2007;263:207–52.
[22] Bolender N, Sickmann A, Wagner R, Meisinger C, Pfanner N. Multiple pathways for sorting mitochondrial precursor proteins. EMBO Rep 2008;9:42–9.
[23] Bonawitz ND, Clayton DA, Shadel GS. Initiation and beyond: multiple functions of the human mitochondrial transcription machinery. Mol Cell 2006;24:813–25.
[24] Koehler CM, Leuenberger D, Merchant S, Renold A, Junne T, Schatz G. Human Deafness Dystonia Syndrome is a mitochondrial disease. Proc Natl Acad Sci USA 1999;96:2141–6.
[25] Hood DA, Joseph AM. Mitochondrial assembly: protein import. Proc Nutr Soc 2004;63:293–300.
[26] Baker MJ, Frazier AE, Gulbis JM, Ryan MT. Mitochondrial protein-import machinery: correlating structure with function. Trends Cell Biol 2007;17:456–64.
[27] Macasev D, Whelan J, Newbigin E, Silva-Filho MC, Mulhern TD, Lithgow T. Tom22′, an 8-kDa trans-site receptor in plants and protozoans, is a conserved feature of the TOM complex that appeared early in the evolution of eukaryotes. Mol Biol Evol 2004;21:1557–64.
[28] Ahmed AU, Beech PL, Lay ST, Gilson PR, Fisher PR. Import-associated translational inhibition-novel *in vivo* evidence for cotranslational protein import into *Dictyostelium* mitochondria. Eukaryot Cell 2006;5:1314–27.
[29] Ahmed AU, Fisher PR. Import of nuclear-encoded mitochondrial proteins: a cotranslational perspective. Int Rev Cell Mol Biol 2009;273:49–68.
[30] Holt IJ, Harding AE, Petty RK, Morgan-Hughes JA. A new mitochondrial disease associated with mitochondrial DNA heteroplasmy. Am J Hum Genet 1990;46:428–33.
[31] Lithgow T. Targeting of proteins to mitochondria. FEBS Lett 2000;476:22–6.
[32] Tatuch Y, Christodoulou J, Feigenbaum A, Clarke JT, Wherret J, Smith C, et al. Heteroplasmic mtDNA mutation (T-G) at 8993 can cause Leigh disease when the percentage of abnormal DNA is high. Am J Hum Genet 1992;50:852–8.
[33] Kraytsberg Y, Kudryavtseva E, McKee AC, Geula C, Kowall NW, Kharpko K. Mitochondrial DNA deletions are abundant and cause functional impairment in aged human substantia nigra neurons. Nat Genet 2006;38:518–20.
[34] Rossignol R, Faustin B, Rocher C, Malgat M, Mazat J, Letellier T. Mitochondrial threshold effects. Biochem J 2003;370:751–62.
[35] Eichinger L, Pachebat JA, Glöckner G, Rajandream M-A, Sucgang R, Berriman M, et al. The genome of the social amoeba *Dictyostelium discoideum*. Nature 2005;435:43–57.
[36] Williams RS, Boeckeler K, Gräf R, Müller-Taubenberger A, Li Z, Isberg RR, et al. Towards a molecular understanding of human diseases using *Dictyostelium discoideum*. Trends Mol Med 2006;12:415–24.
[37] Jin T, Xu X, Hereld D. Chemotaxis, chemokine receptors and human disease. Cytokine 2008;44:1–8.
[38] Liao XH, Majithia A, Huang X, Kimmel AR. Growth control via TOR kinase signaling, an intracellular sensor of amino acid and energy availability, with crosstalk potential to proline metabolism. Amino Acids 2008;35:761–70.
[39] Swaney KF, Huang CH, Devreoted PN. Eukaryotic chemotaxis: a network of signaling pathways controls motility, directional sensing, and polarity. Annu Rev Biophys 2010;39:265–89.
[40] Cosson P, Soldati T. Eat, kill or die: when amoeba meets bacteria. Curr Opin Microbiol 2008;11:271–6.
[41] Fisher PR. Genetics of phototaxis in a model eukaryote, *Dictyostelium discoideum*. Bioessays 1997;19:397–408.
[42] Fisher PR. Genetic analysis of phototaxis in *Dictyostelium*. In: Hader D-P, Lebert V, editors. Photomovement. ESP Comprehensive Series in Photosciences, vol.1. Amsterdam: Elsevier Science Ltd.; 2001. p. 519–59.
[43] Williams JG. Transcriptional regulation of *Dictyostelium* pattern formation. EMBO Rep 2006;7:694–8.
[44] Calvo-Garrido J, Carilla-Latorre S, Kubohara Y, Santos-Rodrigo N, Mesquita A, Soldati T, et al. Autophagy in *Dictyostelium*: genes and pathways, cell death and infection. Autophagy 2010;16:686–701.
[45] Weijer CJ. Collective cell migration in development. J Cell Sci 2009;122:3215–23.
[46] Dormann D, Weijer CJ. Chemotactic cell movement during *Dictyostelium* development and gastrulation. Curr Opin Genet Dev 2006;16:367–73.
[47] Clarke M. Recent insights into host-pathogen interactions from Dictyostelium. Cell Microbiol 2010;12:283–91.
[48] Albert-Weissenberger C, Cazalet C, Buchrieser C. Legionella pneumophila – a human pathogen that co-evolved with fresh water protozoa. Cell Mol Life Sci 2007;64:432–48.
[49] Hilbi H, Weber SS, Ragaz C, Nyfeler Y, Urwyler S. Environmental predators as models for bacterial pathogenesis. Environ Microbiol 2007;9:563–75.
[50] Francione L. Mitochondrial disease in *Dictyostelium discoideum*. PhD Thesis. La Trobe University; 2008.
[51] Morita T, Yamaguchi H, Amagai A, Maeda Y. Involvement of the TRAP-1 homologue, Dd-TRAP1, in spore differentiation during *Dictyostelium* development. Exp Cell Res 2005;303:425–31.
[52] Inazu Y, Chae SC, Maeda Y. Transient expression of a mitochondrial gene cluster including *rps4* is essential for the phase-shift of *Dictyostelium* cells from growth to differentiation. Dev Genet 1999;25:339–52.
[53] van Es S, Wessels D, Soll DR, Borleis J, Devreotes PN. Tortoise, a novel mitochondrial protein, is required for directional responses of Dictyostelium in chemotactic gradients. J Cell Biol 2001;152:621–32.
[54] Zhu Q, Hulen D, Liu T, Clarke M. The *cluA*$^-$ mutant of *Dictyostelium* identifies a novel class of proteins required for dispersion of mitochondria. Proc Natl Acad Sci USA 1997;94:7308–13.
[55] Gilson PR, Yu X-C, Hereld D, Barth C, Savage A, Kiefel BR, et al. Two *Dictyostelium* orthologs of the prokaryotic cell division protein FtsZ localize to

mitochondria and are required for the maintenance of normal mitochondrial morphology. Eukaryot Cell 2003;2:1315–26.
[56] Morita T, Amagai A, Maeda Y. Translocation of the *Dictyostelium* TRAP1 homologue to mitochondria induces a novel prestarvation response. J Cell Sci 2004;117:5759–70.
[57] Chida J, Yamaguchi H, Amagai A, Maeda Y. The necessity of mitochondrial genome DNA for normal development of *Dictyostelium* cells. J Cell Sci 2004;117:3141–52.
[58] Agsteribbe E, Huckriede A, Veenhuis M, Ruiters MHJ, Niezen-Koning KE, Skjeidal OH, et al. A fatal, systemic mitochondrial disease with decreased mitochondrial enzyme activities, abnormal ultrastructure of the mitochondria and deficiency of heat shock protein 60. Biochem Biophys Res Commun 1993;193:146–54.
[59] Huckriede A, Agsteribbe E. Decreased synthesis and inefficient mitochondiral import of Hsp60 in a patient with a mitochondrial encephalomyopathy. Biochim Biophy Acta 1994;1227:200–6.
[60] Briones P, Vilaseca MA, Ribes A, Vernet A, Lluch M, Cusi V, et al. A new case of multiple mitochondrial enzyme deficiencies with decreased amount of heat shock protein. J Inherit Metab Dis 1997;20:569–77.
[61] Barth C, Fraser DJ, Fisher PR. Co-insertional replication is responsible for tandem multiple formation during plasmid integration into the *Dictyostelium* genome. Plasmid 1998;39:141–53.
[62] Barth C, Fraser DJ, Fisher PR. A rapid, small scale method for characterization of plasmid insertions in the *Dictyostelium* genome. Nucl Acids Res 1998;26:3317–8.
[63] Torija P, Vicente JJ, Rodrigues TB, Robles A, Cerdan S, Sastre L, et al. Functional genomics in Dictyostelium: MidA, a new conserved protein, is required for mitochondrial function and development. J Cell Sci 2006;119(Pt 6):1154–64.
[64] Kimura K, Kuwayama H, Amagai A, Maeda S. Developmental significance of cyanide-resistant respiration under stressed conditions: experiments in *Dictyostelium* cells. Dev Growth Differ 2010;52:645–56.
[65] Wilkins A, Khosla M, Fraser DJ, Spiegelman GB, Fisher PR, Weeks G, et al. *Dictyostelium* RasD is required for normal phototaxis, but not differentiation. Genes Dev 2000;14:1407–13.
[66] Wilkins A, Szafranski K, Fraser DJ, Bakthavatsalam D, Muller R, Fisher PR, et al. The *Dictyostelium* genome encodes numerous RasGEFs with multiple biological roles. BMC Genome Biol 2005;6:R68.
[67] Bandala-Sanchez E, Annesley SJ, Fisher PR. A phototaxis signalling complex in *Dictyostelium discoideum*. Eur J Cell Biol 2006;85:1099–106.
[68] Stocker S, Hiery M, Marriot G. Phototactic migration of *Dictyostelium* cells is linked to a new type of gelsolin-related protein. Mol Biol Cell 1999;10:161–78.
[69] Gloss A, Rivero F, Khaire N, Muler R, Loomis WF, Schleicher M, et al. Villidin, a novel WD-repeat and villin-related protein from *Dictyostelium*, is associated with membranes and the cytoskeleton. Mol Biol Cell 2003;14:2716–27.
[70] Noegel AA, Blau-Wasser R, Sultana H, Israel L, Schleicher M, Patel H, et al. The cyclase-associated protein CAP as regulator of cell polarity and cAMP signalling in *Dictyostelium*. Mol Biol Cell 2004;15:934–45.
[71] Fisher PR, Noegel AA, Fechheimer M, Rivero F, Prassler J, Gerisch G. Photosensory and thermosensory responses in *Dictyostelium* slugs are specifically impaired by absence of the F-actin cross-linking gelation factor (ABP-120). Curr Biol 1997;7:889–92.
[72] Knuth M, Khaire N, Kuspa A, Lu SJ, Schleicher M, Noegel AA. A novel partner for *Dictyostelium* filamin is an α-helical developmentally regulated protein. J Cell Sci 2004;117:5013–22.
[73] Annesley SJ, Bandala-Sanchez E, Ahmed AU, Fisher PR. Filamin repeat segments required for photosensory signalling in *Dictyostelium discoideum*. BMC Cell Biol 2007;8:48.
[74] Inoki K, Corradetti MN, Guan KL. Dysregulation of the TSC-mTOR pathway in human disease. Nat Genet 2005;37:19–24.
[75] Gwinn DM, Shackelford DB, Egan DF, Mihaylova MM, Mery A, Vasquez DS, et al. AMPK phosphorylation of RapTOR mediates a metabolic checkpoint. Mol Cell 2008;30:214–26.
[76] Choi JS, Park C, Jeong JW. AMP-activated protein kinase is activated in Parkinson's disease models mediated by 1-methyl-4-phenyl-1,2,3,6-tetrahydropyridine. Biochem Biophys Res Commun 2010;39:1147–51.
[77] Lopez-Lopez C, Dietrich MO, Metzger F, Loetscher H, Torres-Aleman I. Disturbed cross talk between insulin-like growth factor I and AMP-activated protein kinase as a possible cause of vascular dysfunction in the amyloid precursor protein/presenilin 2 mouse model of Alzheimer's disease. J Neurosci 2007;27:824–31.
[78] Chou SY, Lee YC, Chen HM, Chiang MC, Lai HL, Chang HH, et al. CGS21680 attenuates symptoms of Huntington's disease in a transgenic mouse model. J Neurochem 2005;93(2):310–20.
[79] Matsuyuma S, Maeda Y. Involvement of cyanide-resistant respiration in cell-type proportioning during *Dictyostelium* development. Dev Biol 1995;172:182–91.
[80] Liesa M, Palacin M, Zorzano A. Mitochondrial dynamics in health and disease. Physiol Rev 2009;89:799–845.
[81] Wienke DC, Knetsch MLW, Neuhais EM, Reedy MC, Manstein DJ. Disruption of a dynamin homologue affects endocytosis, organelle morphology and cytokinesis in *Dictyostelium discoideum*. Mol Biol Cell 1999;10:225–43.
[82] Fields SD, Conrad MN, Clarke M. The *S. cerevisiae* CLU1 and *D. discoideum cluA* genes are functional homologues that influence mitochondrial morphology and distribution. J Cell Sci 1998;111:1717–27.
[83] Cechetto JD, Gupta RS. Immunoelectron microscopy provides evidence that tumor necrosis factor receptor-associated protein 1 (TRAP1) is a mitochondrial protein which also localises at specific extramitochondrial sites. Exp Cell Res 2000;260:30–9.
[84] Morita T, Amagai A, Maeda Y. Unique behavior of a *Dictyostelium* homologue of TRAP-1, coupling with differentiation of *D. discoideum* cells. Exp Cell Res 2002;208:45–54.
[85] Yamaguchi H, Morita T, Amagai A, Maeda Y. Changes in spatial and temporal localization of *Dictyostelium* homologues of TRAP1 and GRP94 revealed by immnunoelectron microscopy. Exp Cell Res 2005;303:415–24.
[86] Jarmuszkiewicz W, Behrendt M, Navet R, Sluse FE. Uncoupling protein and alternative oxidase of *Dictyostelium discoideum*: occurrence, properties and protein expression during vegetative life and starvation-induced early development. FEBS Lett 2002;532:459–64.
[87] Hardie DG, Sakamoto K. AMPK a key sensor of fuel and energy status in skeletal muscle. Physiology 2006;21:48–60.
[88] Hong SP, Leiper FC, Woods A, Carling D, Carlson M. Activation of yeast Snf1 and mammalian AMP-activated protein kinase by upstream kinases. Proc Natl Acad Sci USA 2003;100:8839–43.
[89] Woods A, Johnstone SR, Dickerson K, Leiper FC, Fryer LG, Neumann D, et al. LKB1 is the upstream kinase in the AMP-activated protein kinase cascade. Curr Biol 2003;13:2004–8.
[90] Hong SP, Momcilovic M, Carlson M. Function of mammalian LKB1 and Ca^{2+}/calmodulin-dependent protein kinase kinase α as Snf1-activating kinases in yeast. J Biol Chem 2005;280:21804–9.
[91] Hurley RL, Anderson KA, Franzone JM, Kemp BE, Means AR, Witters LA. The Ca^{2+}/calmodulin-dependent protein kinase kinases are AMP-activated protein kinase kinases. J Biol Chem 2005;280:29060–6.
[92] Momcilovic M, Hong S-P, Carlson M. Mammalian TAK1 activates Snf1 protein kinase in yeast and phosphorylates AMP-activated protein kinase *in vitro*. J Biol Chem 2006;281:25336–43.
[93] Kurth-Kraczek EJ, Hirshman MF, Goodyear LJ, Winder WW. 5′ AMP-activated protein kinase activation causes GLUT4 trasnlocation in skeletal muscle. Diabetes 1999;48:1667–71.
[94] Inoki K, Zhu T, Guan KL. TSC2 mediates cellular energy response to control cell growth and survival. Cell 2003;115:577–90.
[95] Horman S, Browne G, Krause U, Patel J, Vertommen D, Bertrand L, et al. Activation of AMP-activated protein kinase leads to the phosphorylation of elongation factor 2 and an inhibition of protein synthesis. Curr Biol 2002;12:1419–23.
[96] Bergeron R, Ren JM, Cadman KS, Moore IK, Perret P, Pypaert M, et al. Chronic activation of AMP kinase results in NRF-1 activation and mitochondrial biogenesis. Am J Physiol Endocrinol Metab 2001;281:E1340–6.
[97] Zong H, Ren JM, Young LH, Pypaert M, Mu J, Birnbaum MJ, et al. AMP kinase is required for mitochondrial biogenesis in skeletal muscle in response to chronic energy deprivation. Proc Natl Acad Sci USA 2002;99:15983–7.
[98] Koopman WJ, Nijtmans LG, Dieteren CE, Roestenberg P, Valsecchi F, Smeitink JA, et al. Mammalian mitochondrial complex I: biogenesis, regulation, and reactive oxygen species generation. Antioxid Redox Signal 2010;12(12):1431–70.
[99] Janssen RJ, Nijtmans LG, van den Heuvel LP, Smeitink JA. Mitochondrial complex I: structure, function and pathology. J Inherit Metab Dis 2006;29(4):499–515.
[100] Lazarou M, Thorburn DR, Ryan MT, McKenzie M. Assembly of mitochondrial complex I and defects in disease. Biochim Biophys Acta 2009;1793:78–88.
[101] Sharma LK, Lu J, Bai Y. Mitochondrial respiratory complex I: structure, function and implication in human diseases. Curr Med Chem 2009;16(10):1266–77.
[102] Brandt U, Abdrakhmanova A, Zickermann V, Galkin A, Drose S, Zwicker K, et al. Structure-function relationships in mitochondrial complex I of the strictly aerobic yeast *Yarrowia lipolytica*. Biochem Soc Trans 2005;33(Pt 4):840–4.
[103] Videira A, Duarte M. From NADH to ubiquinone in Neurospora mitochondria. Biochim Biophys Acta 2002;1555(1–3):187–91.
[104] Cole RA, Slade MB, Williams KL. *Dictyostelium discoideum* mitochondrial DNA encodes a NADH: ubiquinone oxidoreductase subunit which is nuclear encoded in other eukaryotes. J Mol Evol 1995;40:616–21.
[105] Hoefs SJ, Dieteren CE, Rodenburg RJ, Naess K, Bruhn H, Wibom R, et al. Baculovirus complementation restores a novel NDUFAF2 mutation causing complex I deficiency. Hum Mutat 2009;30(7):E728–36.
[106] Ogilvie I, Kennaway NG, Shoubridge EA. A molecular chaperone for mitochondrial complex I assembly is mutated in a progressive encephalopathy. J Clin Invest 2005;115(10):2784–92.
[107] Saada A, Vogel RO, Hoefs SJ, van den Brand MA, Wessels HJ, Williams PH, et al. Mutations in NDUFAF3 (C3ORF60), encoding an NDUFAF4 (C6ORF66)-interacting complex I assembly protein, cause fatal neonatal mitochondrial disease. Am J Hum Genet 2009;84(6):718–27.
[108] Vogel RO, Janssen RJ, Ugalde C, Grovenstein M, Huijbens RJ, Visch HJ, et al. Human mitochondrial complex I assembly is mediated by NDUFAF1. FEBS 2005;272(20):5317–26.
[109] Pagliarini DJ, Calvo SE, Chang B, Sheth SA, Vafai SB, Ong SE, et al. A mitochondrial protein compendium elucidates Complex I disease biology. Cell 2008;134:112–23.
[110] Gerards M, Sluiter W, van den Bosch BJC, de Wit LEA, Calis CMH, Frentzen M, et al. Defective complex I assembly due to C20orf7 mutations as a new cause of Leigh syndrome. J Med Genet 2010;47:507–12.
[111] Sugiana C, Pagliarini DJ, McKenzie M, Kirby DM, Salemi R, Abu-Amero KK, et al. Mutation of C20orf7 disrupts complex I assembly and causes

lethal neonatal mitochondrial disease. Am J Hum Genet 2008;83(4):468–78.
[112] Vogel RO, Janssen RJ, van den Brand MA, Dieteren CE, Verkaart S, Koopman WJ, et al. Cytosolic signaling protein Ecsit also localizes to mitochondria where it interacts with chaperone NDUFAF1 and functions in complex I assembly. Genes Dev 2007;21(5):615–24.
[113] Vahsen N, Cande C, Briere JJ, Benit P, Joza N, Larochette N, et al. AIF deficiency compromises oxidative phosphorylation. EMBO J 2004;23(23): 4679–89.
[114] Bych K, Kerscher S, Netz DJ, Pierik AJ, Zwicker K, Huynen MA, et al. The iron-sulphur protein Ind1 is required for effective complex I assembly. EMBO J 2008;27(12):1736–46.
[115] Sheftel AD, Stehling O, Pierik AJ, Netz DJ, Kerscher S, Elsasser HP, et al. Human ind1, an iron-sulfur cluster assembly factor for respiratory complex I. Mol Cell Biol 2009;29(22):6059–73.
[116] Carroll J, Fearnley IM, Shannon RJ, Hirst J, Walker JE. Analysis of the subunit composition of complex I from bovine heart mitochondria. Mol Cell Proteom 2003;2(2):117–26.

BMC Microbiology

Research article

Dictyostelium transcriptional responses to *Pseudomonas aeruginosa*: common and specific effects from PAO1 and PA14 strains

Sergio Carilla-Latorre†[1], Javier Calvo-Garrido†[1], Gareth Bloomfield[2], Jason Skelton[3], Robert R Kay[2], Alasdair Ivens[3], José L Martinez[4] and Ricardo Escalante*[1]

Address: [1]Instituto de Investigaciones Biomédicas Alberto Sols, Universidad Autónoma de Madrid-Consejo Superior de Investigaciones Científicas, Madrid, Spain, [2]MRC Laboratory of Molecular Biology, Cambridge, UK, [3]Wellcome Trust Sanger Institute, Hinxton, UK and [4]Centro Nacional de Biotecnología, CSIC, Madrid and CIBERESP, Spain

Email: Sergio Carilla-Latorre - scarilla@iib.uam.es; Javier Calvo-Garrido - jcalvo@iib.uam.es; Gareth Bloomfield - garethb@mrc-lmb.cam.ac.uk; Jason Skelton - jps@sanger.ac.uk; Robert R Kay - rrk@mrc-lmb.cam.ac.uk; Alasdair Ivens - alicat@sanger.ac.uk; José L Martinez - jlmtnez@cnb.csic.es; Ricardo Escalante* - rescalante@iib.uam.es

* Corresponding author †Equal contributors

Published: 30 June 2008

BMC Microbiology 2008, **8**:109 doi:10.1186/1471-2180-8-109

Received: 6 March 2008
Accepted: 30 June 2008

This article is available from: http://www.biomedcentral.com/1471-2180/8/109

Abstract

Background: *Pseudomonas aeruginosa* is one of the most relevant human opportunistic bacterial pathogens. Two strains (PAO1 and PA14) have been mainly used as models for studying virulence of *P. aeruginosa*. The strain PA14 is more virulent than PAO1 in a wide range of hosts including insects, nematodes and plants. Whereas some of the differences might be attributable to concerted action of determinants encoded in pathogenicity islands present in the genome of PA14, a global analysis of the differential host responses to these *P. aeruginosa* strains has not been addressed. Little is known about the host response to infection with *P. aeruginosa* and whether or not the global host transcription is being affected as a defense mechanism or altered in the benefit of the pathogen. Since the social amoeba *Dictyostelium discoideum* is a suitable host to study virulence of *P. aeruginosa* and other pathogens, we used available genomic tools in this model system to study the transcriptional host response to *P. aeruginosa* infection.

Results: We have compared the virulence of the *P. aeruginosa* PAO1 and PA14 using *D. discoideum* and studied the transcriptional response of the amoeba upon infection. Our results showed that PA14 is more virulent in *Dictyostelium* than PA01using different plating assays. For studying the differential response of the host to infection by these model strains, *D. discoideum* cells were exposed to either *P. aeruginosa* PAO1 or *P. aeruginosa* PA14 (mixed with an excess of the non-pathogenic bacterium *Klebsiella aerogenes* as food supply) and after 4 hours, cellular RNA extracted. A three-way comparison was made using whole-genome *D. discoideum* microarrays between RNA samples from cells treated with the two different strains and control cells exposed only to *K. aerogenes*. The transcriptomic analyses have shown the existence of common and specific responses to infection. The expression of 364 genes changed in a similar way upon infection with one or another strain, whereas 169 genes were differentially regulated depending on whether the infecting strain was either *P. aeruginosa* PAO1 or PA14. Effects on metabolism, signalling, stress response and cell cycle can be inferred from the genes affected.

Conclusion: Our results show that pathogenic *Pseudomonas* strains invoke both a common transcriptional response from *Dictyostelium* and a strain specific one, indicating that the infective process of bacterial pathogens can be strain-specific and is more complex than previously thought.

Background

Nosocomial infections caused by opportunistic pathogens are one of the most important health problems in developed countries. Depending on the geographic location, *P. aeruginosa* is the first or second causative agent of nosocomial infections [1,2]. *P. aeruginosa* infects patients suffering from AIDS, people at intensive care units, and burned people among others, and is the major cause of morbidity and mortality in patients with cystic fibrosis, the most prevalent hereditary disease in Caucasian populations [3]. A successful infection by this type of pathogens depends on the interplay of multiple factors including the susceptibility of the host, the virulence of the strain and its resistance to antibiotics [4]. Previous work has shown that the physiological fitness and the virulence of *P. aeruginosa* and other opportunists are affected by the expression of antibiotic resistance mechanisms such as MDR-pumping systems [5-8].

The pathogenicity of *Pseudomonas aeruginosa* involves various components operating at different levels. The flagella and *pili* facilitate contact with the bacterium's cell target and play a role in its adhesion, which is a critical step in the infection [9,10]. After contact, the type III secretion system is able to inject into the cytoplasm of the target cell a series of cytotoxic molecules that act at various levels. The mechanism of action involves, in many cases, the presence of host cofactors still unidentified [11]. Other virulence factors involve products secreted into the extracellular medium by systems I and II such as elastase, alkaline phosphatase and exotoxin A among others. The expression of many of these virulence factors is regulated by a mechanism of bacteria-to-bacteria cell signalling known as quorum-sensing [12]. Despite the functional and genomic similarity among different *P. aeruginosa* strains [13,14], some differences in their pathogenicity have been observed [15]. For example, the clinical isolate PA14 is more virulent than PAO1 in a wide range of hosts [15-17]. It has been shown that the genome of PA14 contains two pathogenicity islands that are not present in PAO1 and it has been proposed that the virulence in this organism (and the difference between PA14 and PAO1) is the result of a pool of pathogenicity genes interacting in various combinations in different genetic backgrounds [15]. In spite of these suggestions, the cause of the different virulence behavior of PAO1 and PA14 is not yet fully understood.

Although most of the work on pathogenesis has been focused on understanding the bacterial factors that render a virulence phenotype, increasing attention is being paid to the host and those aspects connected to the susceptibility or resistance to infection. Understanding the host-pathogen relationship, at both the cellular and molecular level, is essential to identify new targets and develop new strategies to fight infection. Molecular analysis of host-pathogen interactions would benefit from the use of model systems allowing a systematic study of the factors involved. In this regard the social amoeba *D. discoideum* has proven particularly useful for its ease of handling, genetic tractability [18-22] and fully sequenced genome [23].

D. discoideum is a soil microorganism that feeds on bacteria by phagocytosis. The interaction between bacteria and their natural predators (*Dictyostelium*, other protists and worms) is believed to have shaped both predators [24] and bacterial evolution. As a consequence, some of the mechanisms developed by bacteria to avoid the activity of their natural predators in the environment might have been adapted later in evolution to allow the infection of higher organisms such as humans [25]. Specifically, it was found that the quorum-sensing mechanisms and type III secretion, which are essential factors in the infectivity to humans are also responsible for the infectivity of *P. aeruginosa* in *D. discoideum* [18,20,21].

Our previous studies have shown the utility of this model system of infection to analyze the virulence of other opportunistic pathogens like *Stenotrophomonas maltophilia* [7]. It has been also demonstrated the validity of *D. discoideum* as a model of infection by intracellular pathogens such as *Legionella, Cryptococcus and Mycobacterium* [19,22]. Consequently, the conservation of the mechanisms of infection needed to infect mammals and *D. discoideum* in a wide variety of pathogens reinforces the use of this system as a valid model to study host-pathogen relations. We have used whole-genome *D. discoideum* microarrays to study global host transcription upon infection with *Pseudomonas aeruginosa* PAO1 and PA14 to determine whether or not transcription is being affected as a defense mechanism or altered in the benefit of the pathogen.

Results

Pseudomonas aeruginosa *strains PAO1 and PA14 show a different virulence behavior in* D. discoideum

PAO1 and PA14 are two clinical isolates of *P. aeruginosa* frequently used as model strains to analyze the virulence of this bacterial pathogen. Since they behave differently in some aspects dealing with the expression of virulence determinants, we wanted to compare the differential response of the host to these strains. For this purpose, we made use of *D. discoideum* as a model for virulence. As a first step a plating assay of virulence was set up. Figure 1 shows a representative experiment of three independent assays in which *D. discoideum* cells were grown in association with bacteria on nutrient SM plates. *Klebsiella aerogenes*, a non -pathogenic bacteria, was used as an appropriate food supply and *P. aeruginosa* mixed at the indicated proportions. An effect in the size of the clearing

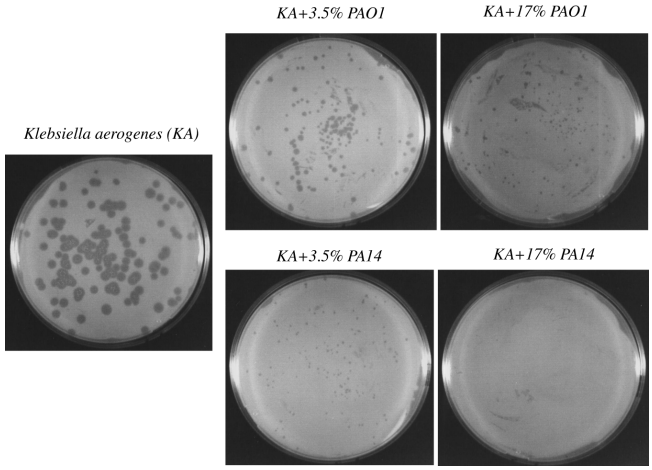

Figure 1
PA14 is more virulent than PAO1 in SM-plating assay. Approximately 100 *D. discoideum* cells were cultivated in SM-plates with the indicated proportion of *Klebsiella* and *Pseudomonas* strains (PAO1 or PA14) previously grown and adjusted to the same optical density. Plates were maintained at 22°C for 5 days. Growth of *D. discoideum* is severely affected by the presence of *Pseudomonas* but the inhibition is stronger when PA14 is used.

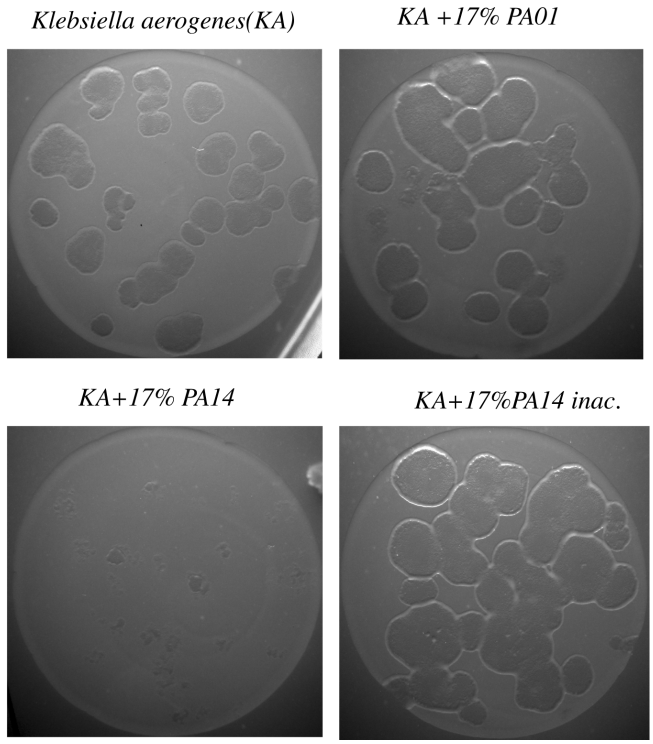

Figure 2
PA14 is more virulent than PAO1 in PDF-agar plating assay. *D. discoideum* cells were cultivated in non-nutrient agar on a lawn of *Klebsiella* and *Pseudomonas* (PAO1 and PA14) at the indicated proportion. Under these conditions PA14 maintain a high virulence as seen by the strong inhibition of *D. discoideum* growth. Heat inactivated PA14 is used as a control.

plaques could already be seen when only 3.5% of *P. aeruginosa* cells were mixed with 96.5% of *K. aerogenes* cells and this effect was even clearer using 17% of *P. aeruginosa* cells. When the behavior of the strains was analyzed in more detail, it was found that PAO1 is reproducibly more permissive than PA14 as observed by the higher growth of *D. discoideum* on PAO1. The differences in the area of the cleared bacterial lawn between PAO1 and PA14 were measured for the condition corresponding to the 3.5 % mixture. The average area and the standard deviation were 1.65 ± 1.2 mm^2 for PAO1 and 0.11 ± 0.07 mm^2 for PA14 (the number of clear plaques measured in each condition was 50). The significance of differences between groups as determined by Student's *t*-test was $p < 10^{-8}$. To further confirm these results a different plating assay was performed on non-nutrient agar. PAO1, PA14 and *K. aerogenes* were previously grown in LB overnight, washed out of the media by centrifugation and deposited with *D. discoideum* cells in agar plates at the indicated proportions. Under these conditions the difference in the virulence between PAO1 and PA14 was even more evident as shown in a representative experiment in Figure 2. Interestingly PAO1 is permissive to *D. discoideum* growth under these non-nutrient conditions. However, PA14 still shows a strong virulence against *D. discoideum*. All together these results suggest that PA14 is more virulent than PAO1 in the *D. discoideum* model of virulence.

Pseudomonas aeruginosa *induces a specific gene expression response in* Dictyostelium

Little is known about the interplay between the host and the pathogen in terms of gene expression responses. We wanted to determine if there is a specific gene expression response of *D. discoideum* to their interaction with *P. aeruginosa*. *D. discoideum* cells were exposed to *P. aeruginosa* strains PAO1 and PA14 mixed with an excess of *K. aerogenes* in HL5 for 4 hours. *K. aerogenes* alone was used as a control to which the gene expression levels were compared. RNA was extracted from *D. discoideum* and used to study the global pattern of gene expression using whole-genome *D. discoideum* microarrays (see Additional file 1 for the complete data). Using a $P < 0.05$ cutoff, there were 752 genes whose expression was significantly different between the PAO1-treated cells and the controls and 624 genes between PA14-treated cells and controls (Table 1 summarizes the results at different P values and log-ratios). The heat map shown in Figure 3 indicates that the responses were broadly comparable between the two strains with very few genes oppositely altered in the two

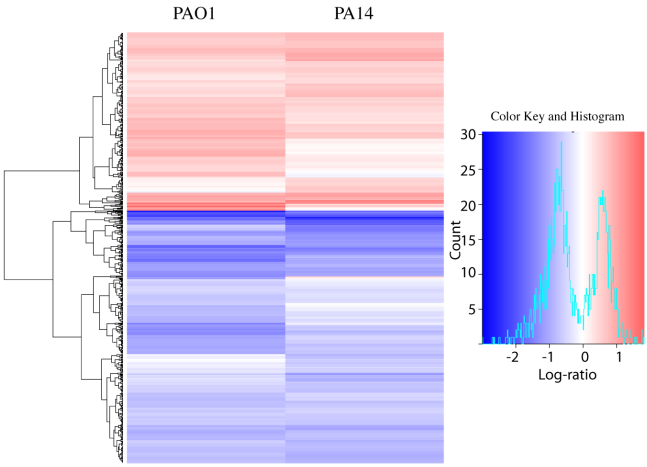

Figure 3
Pseudomonas aeruginosa* induces gene expression changes in *Dictyostelium. Heat map comparing the genes significantly altered ($p < 0.05$) between PAO1-treated cells versus control (975) and PA14-treated cells versus control (838). Each row of the plot is a gene and was colored according to the log2ratio of expression with red meaning up-regulation in relation to the controls and blue downregulation. The histogram shows the range of changes in a log2 scale. The data presented are for the three independent experiments combined. The heatmap was generated using the heatmap.2 function of the gplots package in R [47]. The dendrogram was generated using Euclidean distance and the "complete" agglomeration method.

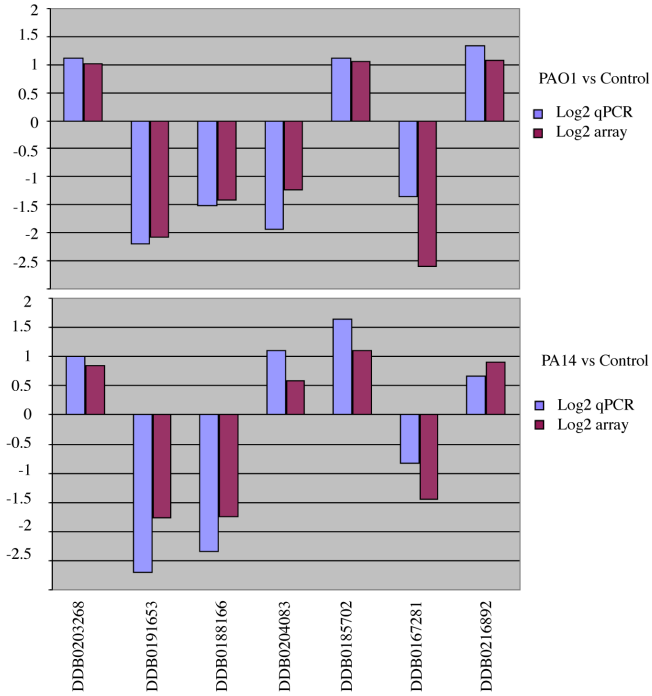

Figure 4
Correlation of microaray and real-time PCR. Real-time PCR measurements of the mRNA levels for seven representative genes whose expression were affected in the array. Upper panel shows a direct comparison of the changes in a log2 scale for PAO1 versus control and the lower panel shows the same genes for PA14 versus control. Blue bars corresponded to quantitative real time PCR and the purple bars to the array data. The array data and the real time PCR displayed are the combination of three independent biological experiments. The correlation coefficients were: $R^2 = 0.87$ for PAO1 and $R^2 = 0.91$ for PA14.

conditions. The differences in the gene expression are approximately in the range between four-fold repression and three-fold induction (log-ratios between of -2 to +1.5 as shown in the histogram of Figure 3). These results were validated by real time PCR of the same samples used for the transcriptomic assays, measuring the expression of 7 representative genes that were up-regulated or down-regulated in the different conditions. Figure 4 shows a good correlation between the data obtained from the microarray transcriptomic experiment as compared with that obtained by quantitative RT-PCR. Although the log-ratio changes in the gene expression showed some differences the overall trend were consistent, supporting the reliability of our data.

Common and specific responses of D. discoideum *to the infection with PAO1 and PA14 strains*

As shown in Table 1 there were 364 genes that showed similar differential regulation with both bacterial strains compared with the controls (labeled as PAO1+PA14 vs control). We have considered in the analysis those genes showing differences in log-ratios that are higher than +0.5 or lower than -0.5. Interestingly the expression of another group of 169 genes (labeled as PAO1 vs PA14) was different depending on whether the infecting strain was PAO1 or PA14. We have studied in detail both groups by manual annotation and categorizing using the extended categorization for *D. discoideum* previously described [26]. Genes of unknown function and those showing weak homologies were not included in the list. Table 2 contains the genes that were similarly regulated upon infection with any of both strains, and in Figure 5 the genes are categorized by function (see Additional file 2 for the complete data). The first interesting conclusion from this experiment is the existence of a common transcriptional response that affects many different genes that are involved in a wide range of functions. The proportion of the genes that were downregulated by the treatment with both strains of *P. aeruginosa* is higher (258 genes) compared to those upregulated (106 genes). This difference is more evident in categories such as stress response and transport (Figure 5).

Table 1: Differential genes at p < 0.05 and different Log 2 ratios

	PAO1 vs Control	PA14 vs Control	PAO1+PA14 vs Control	PAO1 vs PA14
Log 2 ratio	**752**	**623**	**364 (Table 2)**	**169 (Table 3)**
(>+0.5 or <-0.5)	461 down 291 up	396 down 227 up	258 down 106 up	60 down 109 up
Log 2 ratio	**150**	**125**	**70**	**35**
(>+1 or <-1)	126 down 24 up	105 down 20 up	66 down 4 up	14 down 21 up

Table 3 displays the D. discoideum genes whose expression changed differentially between PAO1 and PA14 infection and Figure 6 shows the number of genes in each category (see Additional file 3 for complete data). In general a higher proportion of the genes showed a higher level of expression by PAO1 infection (109 genes) when compared with the levels observed by PA14. On the other hand, 60 genes behaved oppositely showing lower levels of expression upon exposure to PAO1 compared to those levels obtained after PA14 infection. Interestingly, all the genes represented in the categories stress-response and protein targeting had a higher level of expression in the cells exposed to PAO1 compared to PA14. The behavior of these genes in comparison with the control is also displayed in Table 3.

Discussion

P. aeruginosa is able to infect *D. discoideum* cells using several virulence traits that are similar to those used to infect mammalian cells and other hosts [18]. The clinical *P. aeruginosa* isolates PA14 and PAO1 have been used independently to study the infection of *Dictyostelium* by *Pseudomonas* in two different laboratories [20,21]. However, no direct comparison had been reported so far between these strains in this pathogenicity model. We now report that PA14 is indeed more virulent in *D. discoideum* using different plating assays. Since *P. aeruginosa* is phagocytosed at much lower rate than the non-pathogenic *K. aerogenes* (commonly used to grow *Dictyostelium*) [20], the assays were designed to provide sufficient food to *D. discoideum* to avoid cell starvation. Thus, *K. aerogenes* was always used in excess together with the pathogenic strains. In the first assay (Figure 1) a nutrient plate was used to allow the growth of bacteria and *D. discoideum* simultaneously. Under these conditions the presence of PA14 inhibits *D. discoideum* growth to a greater extent than PAO1. To avoid differences in the growth rates between bacteria that might alter their final proportions, a non-nutrient assay was performed (Figure 2). In these experiments, *D. discoideum* feed on bacteria that have been previously grown and deposited at different proportions in non-nutrient agar. Interestingly, PAO1 is not virulent in this condition suggesting that bacterial growth is necessary for the expression of the virulence in this strain. However, even in these conditions PA14 is capable of inhibiting *D. discoideum* growth. Some studies have suggested that PA14 pathogenicity is multifactorial and required the action of multiple virulence mechanisms [15,27]. These differences between strains prompted us to study the transcriptional profile of *D. discoideum* upon infection with PAO1 and PA14 to gain insights not only into the possible common transcriptional response but also into any specific response that could explain the observed differences in their virulence. Pilot experiments showed that 4 hours of exposure of *D. discoideum* cells to either *Pseudomonas aeruginosa* strains did not result in any apparent cell death or change in cell morphology (data not shown). Since we wanted to study the early transcriptional response we chose this short time of exposure to avoid changes due to cell death. The existence of a rapid gene expression response between 1–6 hours upon exposure of *D. discoideum* cells to *Legionella*, an intracellular pathogen, has also been described [28].

Our results show the existence of a common transcriptional response to the infection with *P. aeruginoa* PAO1 or PA14 that affects 364 genes grouped in many different cellular functions. The complexity of the observed transcriptional changes could be the result of the induction of *D. discoideum* defensive responses or triggered by *P. aeruginosa* to make a less hostile cell environment that would support a better survival of the pathogen. In this scenario downregulation of genes involved in stress response might be beneficial for a successful infection. Interestingly, we have observed a clear down-regulation of genes dedicated to stress in the common response to PAO1 and PA14 but also in the specific response to the more virulent strain PA14. For example the gene coding for Strictosidine synthase (DDB0185428) which is involved in the synthesis of alkaloids related to defense mechanisms in plants [29], Trap1 (DDB0169033) that plays a central role in cell cycle regulation and differentiation [30] or the genes coding for lysozymes involved in bacterial degradation (DDB0167491) [31], to mention just a few.

Besides stress response other categories are affected by an overall downregulation such as metabolism, translation and transport facilitation. A subcategorization of the genes included in metabolism (see supplementary table 2) showed that all the genes coding for proteins involved in nucleotide metabolism were downregulated in the common response suggesting an effect on cell prolifera-

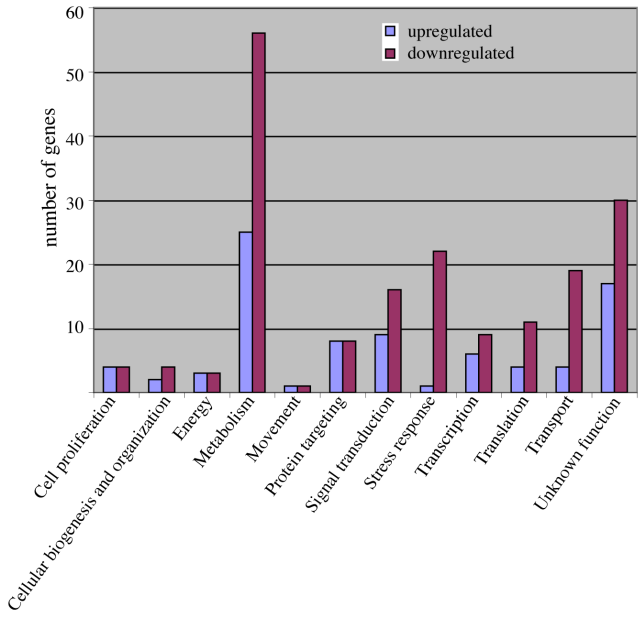

Figure 5
Functional categories of the genes affected similarly by the exposure with PAO1 and PA14. The genes whose expression was altered by PAO1 and PA14 were manually annotated (see Table 2) and grouped in functional categories. The size of the blue bars indicates the number of genes upregulated in each category related to the control and purple bars the number of genes downregulated.

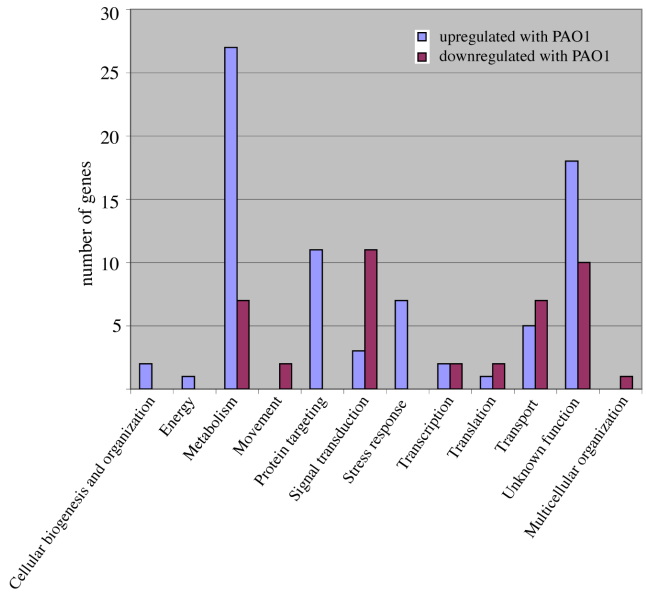

Figure 6
Functional categories of the genes differentially affected by the exposure to PAO1 and PA14. The genes whose expression was differentially altered in PAO1 versus PA14 were manually annotated (see Table 3) and grouped in functional categories. The size of the blue bars indicates the number of genes upregulated in PAO1 versus PA14 in each category and purple bars the number of genes downregulated in PAO1 versus PA14.

tion. Moreover, a number of other downregulated genes are directly involved in cell growth as demonstrated functionally in previous studies. This is the case for example of DDB0192001 (ppkA, polyphosphate kinase), whose disruption leads to reduced growth on bacteria [32,33], DDB0186120 (gcsA, glutamylcysteine synthetase), which is essential for cell growth as mutants in the gene are not viable in the absence of glutathione [34]. DDB0168860 (sgkA, sphingosine kinase) that is involved in cell proliferation [35], among others that have been annotated in Supplementary Table 2, 3.

Two different expression microarray analysis in mammals upon infection with *Pseudomonas aeruginosa* have been reported. In the first report epithelial cells were exposed to the pathogen for 3 hours, a short exposure similar to our experimental design. Unfortunately the number of genes represented in the array was very limited (1500 cDNAs) [36]. Only 22 genes were differentially regulated and we have not found any homologous gene in common. The other work reported the analysis of *Pseudomonas aeruginosa* corneal infection using an oligonucleotide microarray [37]. This experiment is not directly comparable to ours since a long exposure to the pathogen (1 day) was performed to assure an infection process. As a consequence most of the regulated genes were associated with the immune response and apoptosis, aspects that are not present in *Dictyostelium*.

D. discoideum is also susceptible to the infection by *Legionella pneumophila*, a facultative intracellular parasite, which uses different infective mechanisms from *P. aeruginosa*. It is important to note here that the transcriptional response of *D. discoideum* upon infection with *Legionella* [28] was essentially different to the one we report for *P. aeruginosa*. Only 8 genes were found to be altered in both experiments (DDB0186332, DDB0219578, DDB0167879, DDB0205386, DDB0185740, DDB0167345, DDB0201617, DDB0202615). This indicates that the host response is rather specific of the type of infection and the bacterial pathogen involved. Nevertheless, some responses can be also common. For instance, DDB0202615 (nramp1, natural resistance-associated macrophage protein) whose expression is downregulated in PAO1 and PA14, plays an important role in Legionella infection since the null mutant has increased sensitivity to the infection [38]. Nramp1 transports metal cations out of the phagolysosome in an ATP-dependent process. This

Table 2: Genes differentially expressed upon infection with PAO1 and PA14 versus *Klebsiella*

Gene ID	Gene function and name	Log 2 ratio: PAO1-C	PA14-C
Cell proliferation			
DDB0216882	Cyclin-dependent kinase regulatory	-0,89	-0,97
DDB0188449	cdc40, conserved splicing factor	0,68	0,78
DDB0205486	CDK family protein kinase	0,81	0,89
DDB0168249	cdk1, "cyclin-dependent_kinase, p34-cdc2_protein"	-0,78	-0,83
DDB0216532	cdk10;"putative_CDK_family_protein_kinase	0,91	1,08
DDB0185341	PP-loop family	-0,60	-0,70
DDB0205486	putative protein serine/threonine kinase, CDK family protein kinase	0,68	0,64
DDB0218360	PhoPQ-activated pathogenicity-related protein	-0,59	-0,57
Cellular biogenesis and organization			
DDB0189693	copA, coatomer protein complex alpha subunit	0,52	0,68
DDB0216892	lvsB;"BEACH_domain-containing_protein"	1,05	0,91
DDB0202609	Transport protein particle (TRAPP)	-0,77	-0,61
DDB0187558	putative mitochondrial import inner membrane translocase	-0,65	-0,65
DDB0186481	atg9, APG9, "autophagy_protein_9"	-0,88	-0,77
DDB0217942	Putative Mpv17/PMP22 family	-0,66	-0,93
Energy			
DDB0217090	Isocitrate lyase family	-0,80	-0,84
DDB0192001	ppkA, "poly_P_kinase, polyphosphate_kinase"	-0,65	-0,51
DDB0190821	sdhB, complex II, iron-sulfur protein (IP) subunit	0,74	0,53
DDB0190821	sdhB;"complex_II,(ubiquinone), succinic_dehydrogenase"	0,59	0,61
DDB0167662	similar to Coenzyme Q9	-0,71	-0,72
DDB0204006	AMPK beta-2 chain	0,52	0,73
Metabolism			
DDB0187528	cysteine dioxygenase	0,69	0,66
DDB0185702	hgd;"homogentisate_1,2-dioxygenase"	1,05	1,10
DDB0184361	Thiamine pyrophosphate enzyme	-0,57	-0,88
DDB0186120	gshA, "gamma_glutamylcysteine_synthetase, glutamate-cysteine_ligase"	-1,72	-0,94
DDB0167249	Aldehyde dehydrogenase	-0,77	-0,94
DDB0192169	alrA;"aldehyde_reductase, aldo-keto_reductase"	-0,54	-0,88
DDB0218652	alrB;"aldo-keto_reductase"	-0,60	-0,69
DDB0189745	alrC;"aldo-keto_reductase"	-0,84	-0,72
DDB0186332	alrE;"aldo-keto_reductase"	-1,23	-0,99
DDB0204015	D-Lactate dehydrogenase	0,92	0,65
DDB0187572	Endoglucanase_E_like	0,64	0,78
DDB0203268	glgB;"1,4-alpha-glucan_branching_enzyme, branching_enzyme"	1,02	0,85
DDB0187562	glk;glucokinase	0,69	0,56
DDB0217973	Gluconolactonase	0,85	0,82
DDB0202855	Glycoside hydrolase	-1,63	-1,45
DDB0202233	Glycosyl hydrolase family 7	-1,26	-1,38
DDB0167594	Glycosyl hydrolases family	0,60	0,56
DDB0204016	gpt10;"putative_glycophosphotransferase"	-0,69	-1,11
DDB0204037	Legume lectins beta-chain signature	-0,86	-1,16
DDB0206405	Mannosyl oligosaccharide glucosidase	-0,80	-0,68
DDB0205896	NAD-dependent epimerase/dehydratase family protein	-2,12	-1,73
DDB0204752	Phosphoglycerate mutase family	0,64	0,61
DDB0190464	Predicted kinase related to galactokinase and mevalonate kinase	0,52	1,02
DDB0186919	zinc-containing alcohol dehydrogenase	-2,09	-1,99
DDB0168737	zinc-containing alcohol dehydrogenase (ADH)	-1,35	-1,03
DDB0169356	carboxylic ester hydrolase	-1,03	-0,72
DDB0190523	CAS1;"cycloartenol_synthase"	0,85	0,88
DDB0185601	cutA;"fatty_acid_elongase_3-ketoacyl-CoA_synthase, long_chain_fatty_acid_elongase"	-0,93	-0,62
DDB0188166	delta-24-sterol methyltransferase	-1,42	-1,74
DDB0186908	eapA;"alkyl-dihydroxyacetonephosphate_synthase"	0,72	0,81
DDB0187604	enoyl-CoA hydratase/isomerase domain-containing protei	-0,65	-0,63
DDB0205302	Enoyl-CoA hydratase/isomerase family	-0,64	-0,68
DDB0205157	fadB, des5-2, "delta_5_fatty_acid_desaturase"	0,89	1,11
DDB0190288	fcsB, fatty acyl-CoA synthetase, long-chain-fatty-acid-CoA ligase	-1,45	-1,57
DDB0191679	GNS1/SUR4 family	-1,03	-0,59

Table 2: Genes differentially expressed upon infection with PAO1 and PA14 versus *Klebsiella* *(Continued)*

DDB0205505	mfeB;"hypothetical_peroxisomal_multifunctional_enzyme_2"	-1,06	-0,65
DDB0191653	patatin family protein	-2,07	-1,77
DDB0218187	Perilipin family	-1,35	-1,04
DDB0184443	Saposin (B) Domains	0,59	0,59
DDB0190553	Similar to sterol-C4-methyl oxidase-like	-0,71	-0,91
DDB0217332	stearoyl-CoA desaturase	0,90	1,02
DDB0206478	allC;"allantoate_amidinohydrolase, allantoicase"	-1,12	-1,25
DDB0205700	cysteine desulfurase	-1,31	-1,26
DDB0169540	MOSC domain	-1,00	-0,67
DDB0187599	5 prime nucleotidase family	-0,90	-0,70
DDB0187063	3-methyl-2-oxobutanoate hydroxymethyltransferase	-1,83	-1,41
DDB0190860	adenine phosphoribosyltransferase	-0,98	-0,75
DDB0203073	adenosine deaminase-related growth factor	-1,35	-0,74
DDB0215237	ATP:D-ribose_5-phosphotransferase, ribokinase	-0,56	-0,51
DDB0206047	CTP synthase	-1,01	-1,20
DDB0187738	Cytidine and deoxycytidylate deaminase zinc-binding region	-0,76	-0,73
DDB0191911	putative RNA methylase	-1,01	-1,21
DDB0185785	Putative RNA methylase family	-0,59	-0,63
DDB0219236	pyrK, cytidylate kinase	-0,98	-0,71
DDB0217423	rnrB_2, ribonucleotide reductase small subunit	-0,79	-0,84
DDB0215284	tRNA/rRNA methyltransferase SpoU family protein	-0,77	-0,93
DDB0186269	Thioredoxin family	-1,41	-1,91
DDB0206431	FAD binding domain	-1,63	-1,13
DDB0187958	gchA, "GTP_cyclohydrolase_I"	-0,91	-0,89
DDB0185963	Oxysterol-binding protein	-0,55	-0,75
DDB0205608	pks18, putative polyketide synthase	0,54	0,60
DDB0168380	pks5, putative polyketide synthase	0,57	0,99
DDB0219613	stlB, putative polyketide synthase	0,68	1,05
DDB0186173	Histidine acid phosphatase	-0,79	-0,80
DDB0184156	Acetyltransferase (GNAT) family	0,81	0,78
DDB0205937	Aldehyde dehydrogenase family	1,02	0,81
DDB0183800	dihydrolipoamide_dehydrogenase	-0,60	-0,57
DDB0188526	FAD binding domain	-1,14	-0,93
DDB0169374	haloacid dehalogenase-like hydrolase	-1,26	-1,45
DDB0204714	hemA, ALAS, "5-aminolevulinate_synthase, ALA_synthase"	1,00	0,99
DDB0187575	monooxygenase, FAD-binding	-1,30	-1,14
DDB0203608	NADH:flavin oxidoreductase/NADH oxidase domain-containing protein	-2,99	-2,49
DDB0186877	Predicted hydrolases or acyltransferases	-0,70	-0,83
DDB0203708	Putative dehydrogenase domain	0,60	0,66
DDB0186921	Putative quinone oxidoreductase	-0,68	-0,80
DDB0218378	selD, selenophosphate synthase	0,83	0,85
DDB0219578	short chain dehydrogenase	-0,56	-0,76
DDB0168766	short chain dehydrogenase	0,75	0,90
DDB0201995	Short-chain alcohol dehydrogenase	-0,64	-0,69
DDB0191047	Sucrolytic enzyme/ferredoxin homolog protei	-0,76	-0,55
DDB0205223	Ubiquinone biosynthesis protein	1,02	0,99
Movement			
DDB0190345	Actin	-0,62	-0,64
DDB0216677	tubB;"beta_tubulin"	0,78	0,66
Protein targeting			
DDB0189280	CLN3 protein;Major Facilitator Superfamily	-1,38	-0,81
DDB0186130	pigF, phosphatidylinositol glycan, class Fphosphoethanolamine N- methyltransferase family	-1,13	-1,33
DDB0187271	Protein prenyltransferase, alpha subunit	-0,69	-0,66
DDB0187195	Ubiquitin family protein	-0,68	-0,56
DDB0217546	vps13B, vacuolar protein sorting-associated protein	0,80	0,57
DDB0205767	Importin-beta N-terminal domain	-1,39	-0,91
DDB0219696	CSN3, COP9 signalosome complex subunit 3	0,86	0,56
DDB0188097	mppB;"mitochondrial_processing_peptidase_beta_subunit"	0,85	0,93
DDB0188792	npl4, nuclear protein localization 4	-1,46	-1,26
DDB0189322	Peptidase family M41	0,66	0,82
DDB0204548	putative E3 ubiquitin ligase	0,56	0,88
DDB0203213	Putative serine protease	0,57	0,64
DDB0190305	RING-finger-containing ubiquitin ligase	-1,71	-2,23

Table 2: Genes differentially expressed upon infection with PAO1 and PA14 versus *Klebsiella* *(Continued)*

DDB0191910	sigB, GP63, orfGP63", "leishmanolysin_family_protein, peptidase	-1,44	-1,19
DDB0219558	usp12, putative ubiquitin carboxyl-terminal hydrolase (UCH)	0,81	0,50
DDB0188490	usp40, putative ubiquitin carboxyl-terminal hydrolase (UCH)	0,83	0,60
Signal transduction			
DDB0167328	ArfGAP, Arf GTPase activating protein	0,58	0,67
DDB0187828	gacX, RacGAP	0,62	0,52
DDB0217797	gpaG, "G-protein_subunit_alpha_7"	-0,93	-0,77
DDB0205484	GTPase-activator protein for Ras-like	0,58	0,69
DDB0202545	rabX;"Rab_GTPase"	-0,59	-0,76
DDB0186244	abkD, AdckB2, "putative_ABC1_family_protein_kinase"	0,80	0,88
DDB0217600	nek3, putative protein serine/threonine kinase	0,55	0,56
DDB0203684	tyrosine kinase-like	0,53	0,56
DDB0189806	vwkA;"protein_serine/threonine_kinase"	-0,77	-0,67
DDB0205355	Calcineurin-like phosphoesterase	-1,27	-0,86
DDB0218779	pdsA, "PDE, pde1, pdeA", "cAMP_phosphodiesterase"	0,79	1,40
DDB0204820	rabS;"Rab_GTPase"	-0,80	-0,87
DDB0190872	NLI interacting factor-like phosphatase	-0,55	-0,60
DDB0185382	Protein phosphatase 5, catalytic subunit	-0,68	-0,62
DDB0186390	protein tyrosine phosphatase	-0,85	-0,74
DDB0218065	ptpB, DdPTPa, "phosphotyrosine_phosphatase_ptp2	-1,20	-1,01
DDB0189698	Tyrosine specific protein phosphatases family	-0,76	-0,89
DDB0203756	G-protein-coupled receptor (GPCR) family protein	0,69	0,99
DDB0189216	gacD, RacGAP	-0,63	-0,58
DDB0217433	Regulator of G protein signaling	0,90	0,72
DDB0169375	cGMP-specific phosphodiesterase	-0,83	-0,79
DDB0167494	plbF, PLB, "phospholipase_B-like"	-1,17	-1,01
DDB0168860	sgkA, "SK, SPHK", "sphingosine_kinase"	-0,97	-0,79
DDB0167227	Cytochrome b5-like Heme/Steroid binding domain	-0,71	-1,57
DDB0216720	Tetraspanin family	-0,73	-0,68
Stress response			
DDB0202483	AhpC/TSA family	-0,51	-0,68
DDB0203727	AhpC/TSA family protein. Thioredoxin-like	-1,25	-1,89
DDB0203727	AhpC/TSA family protein. Thioredoxin-like	-1,11	-2,00
DDB0205904	AhpC/TSA family protein. Thioredoxin-like	-1,10	-1,63
DDB0168230	Cytochrome P450	0,61	0,67
DDB0217979	cytochrome P450 family protein	-1,11	-1,24
DDB0187276	cytochrome P450 family protein	-0,73	-0,88
DDB0186118	cytochrome P450 family protein	-0,54	-0,51
DDB0167587	Glutathione S-transferase	-2,24	-2,02
DDB0218804	Glutathione S-transferase	-1,07	-0,86
DDB0185602	putative FMN-dependent NAD(P)H:quinone reductase	-0,66	-0,93
DDB0168563	putative glutathione S-transferase	-0,64	-1,23
DDB0201962	Ku70-binding family protein	-0,60	-0,51
DDB0191833	TFIIH4, "TFIIH_subunit, general_transcription_factor_IIH,_polypeptide_4"	-0,81	-0,90
DDB0204089	NUDIX hydrolase family	-0,89	-1,14
DDB0185428	Strictosidine synthase	-1,74	-1,01
DDB0169033	trap1, Dd-trap1, "TNF_receptor-associated_protein", member of the HSP90 fam	-1,93	-1,56
DDB0188234	Chaperone clpB	-1,00	-1,25
DDB0192088	heat shock cognate protein	-0,82	-0,99
DDB0192086	heat shock protein, 70 kDa heat shock protein	-0,94	-1,18
DDB0169051	Hsp20/alpha crystallin family	-1,13	-1,30
DDB0169044	Hsp20/alpha crystallin family	-1,07	-1,12
DDB0169207	hspG12, heat shock protein Hsp20 domain-containing protein	-0,72	-0,86
Transcription			
DDB0204405	CRTF;"transcription_factor"	0,97	1,15
DDB0167879	IWS1 C-terminus	0,70	0,69
DDB0205969	snd1, tudor domain-containing protein	0,66	0,79
DDB0188840	TFIIAL, "transcription_factor_IIA"	-0,79	-0,55
DDB0167865	ddx52, DEAD/DEAH box helicase	-0,55	-0,55
DDB0184074	ddx6, DEAD/DEAH box helicase	0,62	0,66
DDB0184228	DEAD/DEAH box helicase	-0,63	-0,60
DDB0206136	myb domain-containing protein	0,59	0,58
DDB0189583	rpmA;"DNA-dependent_RNA_polymerase"	-1,33	-1,17

Table 2: Genes differentially expressed upon infection with PAO1 and PA14 versus *Klebsiella* *(Continued)*

DDB0186101	pwp2, ortholog of H. sapiens and S. cerevisiae PWP2	-0,80	-0,88
DDB0192008	rpa2, RNA polymerase I, second largest subunit	-0,98	-1,13
DDB0218008	rpc4;"putative_RNA_polymerase_III_subunit"	-0,58	-0,55
DDB0216877	tRNA pseudouridine synthase	-0,56	-0,65
DDB0204724	DNA helicase TIP49, TBP-interacting protei	0,63	0,64
DDB0219410	pirin-like protein	-0,99	-0,81
Translation			
DDB0167043	Ribosomal protein L10	-0,86	-1,37
DDB0190639	Fibrillarin	-0,65	-0,84
DDB0184302	Mitochondrial small ribosomal subunit Rsm22	-0,70	-0,72
DDB0205674	MPP10, U3 small nucleolar ribonucleoprotein	-0,77	-0,66
DDB0201601	mrpl11, S60 ribosomal protein L11, mitochondrial	-0,91	-1,26
DDB0204554	Ribosomal protein L28	-0,50	-0,69
DDB0188692	Ribosomal protein S8e	-0,94	-0,79
DDB0183814	Ribosomal RNA processing protein 4	0,58	0,56
DDB0188661	rps9, "rp1024, v12", "40S_ribosomal_protein_S9	0,60	0,70
DDB0219852	u3 small nucleolar RNA interacting protein 2, putative	-0,75	-0,63
DDB0191852	eukaryotic translation initiation factor 3 subunit 5	0,59	0,54
DDB0203843	Eukaryotic translation initiation factor 6 (EIF-6)-like protein	-0,96	-0,64
DDB0189529	gfm2, mitochondrial translation elongation factor G	-0,59	-0,50
DDB0202851	NMD3 family	-0,95	-0,97
DDB0168814	aspartyl-tRNA_synthetase	0,70	0,98
Transport			
DDB0217304	ABC transporter AbcG17	-1,58	-1,44
DDB0167281	ABC transporter mdrA2	-2,65	-1,44
DDB0167281	ABC transporter mdrA2	-2,26	-1,45
DDB0191940	abcB2;"ABC_transporter_B_family_protein"	0,87	0,93
DDB0188931	abcE1;"RNaseL_inhibitor-like_protein, non-transporter_ABC_protein"	0,61	0,74
DDB0189332	amino acid permease family protein	-0,72	-0,87
DDB0168564	Amino acid/polyamine transporter	-1,28	-1,06
DDB0190286	mcfF, Mitochondrial carrier protein	-0,99	-0,86
DDB0216936	mftA;"carrier_protein_RIM"	-0,91	-1,05
DDB0188529	nucleoporin family protein	-0,94	-0,72
DDB0189222	ccsA, copper chaperone for superoxide dismutase	-0,69	-0,62
DDB0205129	Co/Zn/Cd efflux system component	-0,56	-0,71
DDB0202441	nhe1, DdNHE1, "Na-H_exchanger, sodium/hydrogen_exchanger"	-0,77	-0,59
DDB0168533	porA;porin	0,68	0,59
DDB0218156	P-type cation-transporting ATPase	-0,69	-0,57
DDB0189480	mcfT, mitochondrial substrate carrier family protein	-0,74	-0,86
DDB0202337	Nodulin, Major Facilitator Superfamily	-0,60	-0,68
DDB0185520	Nucleoside transporter	-0,53	-0,56
DDB0203447	Sugar (and other) transporter	1,01	0,71
DDB0168979	Sugar transport proteins signature 1	-0,78	-1,28
DDB0189650	sodium/potassium-transporting ATPase alpha chain 2	-1,48	-0,81
DDB0190036	Major Facilitator Superfamily	-1,13	-1,05
DDB0205693	Major Facilitator Superfamily	-1,33	-1,08

activity is believed to be necessary to avoid the growth of intracellular pathogens and might also contribute to the efficient killing of other bacterial pathogens.

The variety of genes whose expression is altered by *P. aeruginosa* infection suggests a complex scenario in which a combined downregulation of the expression of some of the mentioned genes might affect *D. discoideum* fitness thus favoring the infection. The precise role of these genes in the pathogenesis and the mechanisms that regulates their expression will promote further investigation.

Conclusion

Our results showed that *P. aeruginosa* PA14 is more virulent than PAO1 in the *D. discoideum* model using different plating assays. The transcriptional responses of *D. discoideum* infected by either *P. aeruginosa* PAO1 or PA14 were analyzed by whole-genome microarrays and the expression of 364 genes changed similarly upon infection with

Table 3: Genes differentially expressed upon infection with PAO1 versus PA14

Gene ID	Gene function and name	Log2 ratio: PAO1-14	PAO1-C	PA14-C
Cellular Biogenesis and organization				
DDB0187116	vps13A, vacuolar protein sorting-associated protein	0,81	0,67	-0,13
DDB0189855	vps46, Vacuolar Protein Sorting	0,83	0,59	-0,24
Energy				
DDB0204335	cxgE, "cox7E, coxVIIe", "cytochrome_c_oxidase_subunit_VII_E"	1, 20	0,80	-0,40
Metabolism				
DDB0190752	diaminopimelate epimerase	1,08	0,02	-1,06
DDB0204319	Hydroxymethyltransferase	0,63	0,43	-0,20
DDB0168738	putative arginine deiminase	-0,62	-0,78	-0,16
DDB0205389	acly, ATP citrate lyase	0,89	0,75	-0,15
DDB0169357	methylenetetrahydrofolate dehydrogenase	0,78	0,21	-0,57
DDB0187393	NAD-dependent epimerase/dehydratase family protein	-0,91	-1,18	-0,28
DDB0205386	putative ATP citrate synthase	0,96	0,79	-0,17
DDB0205339	rpe;"ribulose_phosphate_3-epimerase"	0,78	0,43	-0,35
DDB0187942	Short-chain alcohol dehydrogenase of unknown specificit	0,70	0,43	-0,27
DDB0187544	smlA	1,43	1,00	-0,43
DDB0217455	zinc-containing alcohol dehydrogenase (ADH)	-1,21	-1,16	0,06
DDB0217374	zinc-containing alcohol dehydrogenase (ADH)	-1,02	-1,37	-0,35
DDB0190948	acid ceramidase-like protein	-0,87	-0,31	0,56
DDB0188248	Acyltransferase	0,64	0,16	-0,48
DDB0219652	cinB, "esterase/lipase/thioesterase_domain-containing_protein	0,92	1,28	0,36
DDB0189754	esterase/lipase/thioesterase domain-containing protein	1,07	1,07	0,00
DDB0185740	esterase/lipase/thioesterase domain-containing protein	1,08	1,27	0,20
DDB0184141	Phosphate acyltransferases	0,55	-0,26	-0,82
DDB0167446	pks16, putative fatty acid synthase	1,19	1,81	0,63
DDB0189182	Putative esterase/lipase/thioesterase	0,99	1,43	0,44
DDB0191907	dUTP diphosphatase	0,61	0,14	-0,47
DDB0217901	purH, AICAR transformylase/IMP cyclohydrolase	0,89	0,34	-0,55
DDB0167009	pyr4;"dihydroorotate_dehydrogenase, dihydroorotate_oxidase"	0,68	0,18	-0,50
DDB0217842	rpiA;"ribose-5-phosphate_isomerase"	0,63	0,42	-0,21
DDB0189571	Sulfite reductase, alpha subunit (flavoprotein)	-0,89	-0,09	0,79
DDB0202318	Cyclopropyl sterol isomerase	0,73	0,31	-0,42
DDB0167227	Cytochrome b5-like Heme/Steroid binding domain	0,86	-0,71	-1,57
DDB0168923	dihydropteridine reductase	0,60	0,14	-0,47
DDB0185998	ERG24, Ergosterol biosynthesis	0,59	-0,02	-0,61
DDB0219255	Fe(II) oxygenase superfamily	1,14	0,91	-0,23
DDB0217308	Predicted iron-dependent peroxidase	-0,55	-0,12	0,43
DDB0192180	putative O-methyltransferase	0,56	0,71	0,15
DDB0202301	putative SAM dependent methyltransferase	0,88	0,94	0,05
DDB0167345	short-chain dehydrogenase/reductase (SDR) family protein	0,73	0,56	-0,17
Movement				
DDB0188280	myoB, "DMIB, abmB", "myosin_IB"	-0,85	-0,30	0,55
DDB0167337	myoD, DMID, "myosin_ID_heavy_chain"	-0,81	-0,76	0,05
Multicellular organization				
DDB0216906	comC;"FIBROSURFIN_PRECURSOR"	-0,65	-0,39	0,26
Protein destination				
DDB0189735	homolog to co-chaperone p23	0,56	0,45	-0,11
DDB0187409	Acetyltransferase (GNAT) family	0,57	0,33	-0,24
DDB0189799	SET domain-containing protein	0,52	0,33	-0,19
DDB0202482	26S proteasome non-ATPase regulatory subunit 9	0,78	1,25	0,47
DDB0219654	Cysteine proteinase 1 precursor	0,70	0,61	-0,09
DDB0167298	Dipeptidyl aminopeptidase	0,51	-0,07	-0,59
DDB0190542	Probable proteasome subunit beta type 3	0,57	-0,06	-0,63
DDB0216902	prtA, M3L, "proteosomal_alpha-subunit_M3"	0,93	0,94	0,01
DDB0216901	prtB, M3R, "proteosomal_alpha-subunit_7-1"	1,37	1,30	-0,06
DDB0186869	small ubiquitin-like protein	0,61	0,33	-0,28
DDB0217344	ubiquitin-like domain containing CTD phosphatase	0,52	0,29	-0,23
Signal transduction				
DDB0169410	gpaB, "Ga2, Galpha2, gpa2", "G-protein_subunit_alpha_2"	-0,82	-0,55	0,27

Table 3: Genes differentially expressed upon infection with PAO1 versus PA14 *(Continued)*

DDB0190318	rab1C;"Rab_GTPase"	0,87	0,76	-0,10
DDB0202066	pakC, STE20 family protein kinase	-0,61	-0,18	0,43
DDB0169250	putative protein serine/threonine kinase	-0,87	-0,58	0,29
DDB0205782	roco6;"putative_protein_serine/threonine_kinase	-0,61	-0,48	0,14
DDB0167076	sepA, putative protein serine/threonine kinase	-0,57	-0,31	0,26
DDB0217465	fslH, G-protein-coupled receptor (GPCR) family protein	0,71	0,24	-0,46
DDB0205174	grlF, GABA-B receptor-like protein	-1,41	-1,54	-0,12
DDB0168770	grlJ, GABA-B receptor-like protein	-0,63	-0,96	-0,32
DDB0204083	grlL, GABA-B receptor-like protein	-1,84	-1,25	0,60
DDB0229801	grlQ, G-protein-coupled receptor (GPCR) family protein	0,77	0,98	0,21
DDB0167432	gacFF, RacGAP	-0,57	0,08	0,66
DDB0167384	putative guanine nucleotide exchange factor (GEF)	-0,70	-0,01	0,70
DDB0167541	dpoA;"prolyl_oligopeptidase"	-0,66	-0,11	0,55
Stress response and cell rescue				
DDB0218719	AhpC/TSA family protein	0,82	0,76	-0,05
DDB0205882	AhpC/TSA family protein. Thioredoxin-like	0,75	0,57	-0,18
DDB0217383	Cytochrome P450	1,16	0,42	-0,74
DDB0168563	putative glutathione S-transferase	0,59	-0,64	-1,23
DDB0167491	alyA;lysozyme	0,63	0,73	0,10
DDB0167489	alyB;lysozyme	0,69	0,75	0,07
DDB0167490	alyC;lysozyme	0,71	0,87	0,16
Transcription				
DDB0206051	member of NOD protein family	1,05	0,90	-0,15
DDB0202276	srfC;"putative_MADS-box_transcription_factor"	-0,90	-0,30	0,60
DDB0217613	wrky1;"putative_WRKY_transcription_factor"	1,04	1,11	0,07
DDB0167422	putative histone acetyltransferase	-0,64	-0,55	0,09
Translation				
DDB0201621	mrps2, ribosomal protein S2, mitochondrial	0,75	0,49	-0,27
DDB0218535	Eukaryotic elongation factor 1 (EF1) alpha subfamily	-0,83	-0,18	0,65
DDB0167339	tRNA-ribosyltransferase	-0,52	-0,56	-0,04
Transport facilitation				
DDB0187089	abcC5;"ABC_transporter_C_family_protein"	-1,12	-0,68	0,44
DDB0218568	Copper-transporting P-type ATPase	-1,14	-0,60	0,54
DDB0204460	patA, PAT1, "Ca2+-ATPase, P-type_ATPase"	-0,93	-0,15	0,78
DDB0205031	potassium channel tetramerization domain-containing protein	0,92	0,84	-0,08
DDB0217251	P-type cation-transporting ATPase	-2,09	-1,46	0,63
DDB0186223	P-type cation-transporting ATPase	-0,69	-0,40	0,29
DDB0167361	vatE;"vacuolar_H+-ATPase_E_subunit"	0,54	0,47	-0,08
DDB0217699	phospholipid-translocating P-type ATPase family protein	-0,67	-0,63	0,04
DDB0187945	Sugar (and other) transporter	-0,90	-0,78	0,11
DDB0206579	mcfQ, mitochondrial substrate carrier family protein	0,65	0,78	0,13
DDB0192172	mcfZ, mitochondrial substrate carrier family protein	0,73	0,92	0,18
DDB0183815	Mitochondrial carrier protein	0,55	0,81	0,26

any of both strains as compared with the control. Effects on metabolism, signaling, stress response and cell cycle can be inferred from the genes affected. Interestingly there were 169 genes differentially regulated between PAO1 and PA14, and this differential response might contribute to the different virulence behavior displayed by these two model strains. This is a starting point to begin to understand the complex relationships between environmental opportunistic pathogens and their natural hosts. Besides, our data support the idea that the host responses to different isolates of the same bacterial pathogen are largely different, thus indicating that the crosstalk between the pathogen and its host is more specific and more complex than previously thought.

Methods

D. discoideum growth and plating assays

Dictyostelium AX4 cells were grown axenically in HL5 medium (14 g/l tryptone, 7 g/l yeast extract, 0.35 g/l Na_2HPO_4, 1.2 g/l KH_2PO_4, 14 g/l glucose, pH 6.5) or in association with *Klebsiella aerogenes* on SM plates (10 g/l glucose, 1 g/l yeast extract, 10 g/l peptone, 1 g/l $MgSO_4 \cdot 6H_20$, 1.9 g/l KH_2PO_4, 0.6 g/l K_2HPO_4, 20 g/l agar, pH 6.5) [39].

For the nutrient SM-plating assay *Pseudomonas aeruginosa* (PAO1 and PA14) and *Klebsiella aerogenes (KA)* were grown overnight in LB. After washing, bacteria were resuspended with PDF (20 mM KCl; 9 mM K_2HPO_4, 13 mM KH_2PO_4, 1 mM $CaCl_2$; 1 mM $MgSO_4$; pH: 6.4) and the

optical density (OD) determined at 600 nm. After adjusting to 0.5 OD units, 300 μl of *Klebsiella* and *Pseudomonas* at the indicated proportions were plated in SM-agar plates with approximately 100 *D. discoideum* cells.

For non-nutrient plating assay bacteria were grown as before, washed and resuspended in PDF (at an OD of 15 units at 600 nm. 100 μl of bacteria at the indicated proportions were mixed with *D. discoideum* cells and deposited in a drop over a PDF-based non-nutrient agar plates.

Microarrays

Dictyostelium cells (5×10^7 cells) were deposited in 10 ml of HL5 (without antibiotics) in shaking culture and exposed during 4 hours to 1.0 OD (approximate multiplicity of infection: 1000) of *Klebsiella aerogenes* as a control or to a mixture of *Pseudomonas aeruginosa* (PAO1 and PA14) and *Klebsiella* (used in excess to provide similar conditions of food supply). The proportion of *Klebsiella* to *Pseudomonas* (either PAO1 or PA14) was 7:3. Previous experiments showed that these proportions are adequate for a clear inhibition of *Dictyostelium* growth in plating assays (see the results section). *Dictyostelium* cells were separated from the bacteria by gentle centrifugation (twice at 1000 rpm, 5 minutes) and RNA isolated by Trizol (Life Technologies) according to manufacturer's instructions. Three independent biological experiments were performed making a total of three independent treatments for each condition (*Klebsiella* control, PAO1, and PA14). RNA from the three treatments were paired in all three combinations (Control/PAO1; Control/PA14 and PAO1/PA14) and hybridized to three different arrays. The same was performed for the other two biological replicates making a total of 9 microarrays hybridized. One of the three biological replicates was hybridized in the opposite dye orientation to the other two. The arrays, and protocols for labelling, hybridisation and scanning were as previously described [40]. Background fluorescence was subtracted [41], linear models were fitted and the significance of apparent changes in expression was assessed using limma [42,43]. The data were normalised within each array with the printtip loess algorithm to counteract scanning and spatial biases, and further between each array to normalise mean absolute deviations using the 'scale' algorithm [44].

Preliminary analysis using ANOVA methods indicated that many genes had significant differences in expression between treatments, so we proceeded to examine each pairwise contrast in turn. We filtered out less reliable data by selecting genes with p-values adjusted for multiple testing [45] less than 0.05, making use of the moderated t statistics calculated by the eBayes function of limma. Since many genes passing this cutoff showed small changes in expression, we filtered further by absolute log2ratio. The commonly-used cutoff of greater than 2-fold change would have excluded a large number of genes that appeared to change in expression quite consistently, so we used the less stringent criterion of absolute log2ratio >0.5. A lower log2ratio would have included genes with differences in expression too small to be corroborated by other methods. The array design is available from ArrayExpress [46] under the accession A-SGRP-3. The array experiment was deposited in the ArrayExpress database under the accession E-TABM-464.

Quantitative PCR

The same RNA samples subjected to microarray study were used as templates for retrotranscription with High Capacity cDNA Reverse transcription kit (Applied Biosystems) using 250 ng of each RNA in a final volume of 20 μl. For each sample, a triplicated blank was used. This cDNAs served as template in the PCR reaction carried out in 7900 HT Fast Real- Time PCR System using Power Sybrgreen PCR Master Mix 2× with 300 nM oligonucleotides concentration in a final volume of 10 μl. The results were acquired with SDS 2.3 software by Applied Biosystems and handled with EXCEL software by Microsoft. A total of seven genes were studied for each sample and their amount were related to one control gene, DDB0217951, whose expression is not affected by the treatments with the different strains.

Authors' contributions

SC and JC performed the biological experiments and analyzed the data. GB, JS and AI designed and constructed the microarray, and provided informatics and analysis tools; GB contributed to the array experimental design, carried out the array experiments, and contributed to the analysis of results; RK was array project manager. JM contributed to the experimental design of the array and biological experiments. RE designed, coordinated the experiments and drafted the manuscript. All the authors read and approved the final manuscript.

Additional material

Additional file 1

Microsoft excel document containing all the results and genes contained in the microarray.

Click here for file

[http://www.biomedcentral.com/content/supplementary/1471-2180-8-109-S1.xls]

Additional file 2

Microsoft excel document containing the array data for the genes that showed differences in both PAO1 and PA14. The genes were manually annotated and filtered for p < 0.05 and log2 ratio >0.5 or <-0.5. Table 2 was obtained from these data.

Click here for file

[http://www.biomedcentral.com/content/supplementary/1471-2180-8-109-S2.xls]

Additional file 3

Microsoft excel document containing the array data and manual annotation of the genes that showed differential regulation between PAO1 and PA14. The genes were filtered for p < 0.05 and log2 ratio >0.5 or <-0.5. Table 3 was obtained from these data.
Click here for file
[http://www.biomedcentral.com/content/supplementary/1471-2180-8-109-S3.xls]

Acknowledgements

This work was supported by grants BMC2006-00394 from the Spanish Ministerio de Educación y Ciencia (R.E.), CCG07-CSIC/SAL-1959 from Comunidad de Madrid/CSIC (R.E.) and BIO2005-04278, LSHM-CT-2005-518152 and LSHM-CT-2005-018705 to J.M. We would like to thank Theresa Feltwell for technical assistance with the microarray experiment. GB, JS and AI were supported by the Wellcome Trust. JC is recipient of a pre-doctoral fellowship from Spanish Ministerio de Educación y Ciencia.

References

1. Fluit AC, Verhoef J, Schmitz FJ: **Frequency of isolation and antimicrobial resistance of gram-negative and gram-positive bacteria from patients in intensive care units of 25 European university hospitals participating in the European arm of the SENTRY Antimicrobial Surveillance Program 1997–1998.** *Eur J Clin Microbiol Infect Dis* 2001, **20(9):**617-625.
2. Fluit AC, Verhoef J, Schmitz FJ: **Antimicrobial resistance among isolates cultured from patients hospitalized with lower respiratory tract infection in Europe.** *Int J Infect Dis* 2002, **6(2):**144-146.
3. Gibson RL, Burns JL, Ramsey BW: **Pathophysiology and management of pulmonary infections in cystic fibrosis.** *American journal of respiratory and critical care medicine* 2003, **168(8):**918-951.
4. Martinez JL, Baquero F: **Interactions among strategies associated with bacterial infection: pathogenicity, epidemicity, and antibiotic resistance.** *Clin Microbiol Rev* 2002, **15(4):**647-679.
5. Ruiz-Diez B, Sanchez P, Baquero F, Martinez JL, Navas A: **Differential interactions within the Caenorhabditis elegans-Pseudomonas aeruginosa pathogenesis model.** *Journal of theoretical biology* 2003, **225(4):**469-476.
6. Sanchez P, Linares JF, Ruiz-Diez B, Campanario E, Navas A, Baquero F, Martinez JL: **Fitness of in vitro selected Pseudomonas aeruginosa nalB and nfxB multidrug resistant mutants.** *The Journal of antimicrobial chemotherapy* 2002, **50(5):**657-664.
7. Alonso A, Morales G, Escalante R, Campanario E, Sastre L, Martinez JL: **Overexpression of the multidrug efflux pump SmeDEF impairs Stenotrophomonas maltophilia physiology.** *The Journal of antimicrobial chemotherapy* 2004, **53(3):**432-434.
8. Linares JF, Lopez JA, Camafeita E, Albar JP, Rojo F, Martinez JL: **Overexpression of the multidrug efflux pumps MexCD-OprJ and MexEF-OprN is associated with a reduction of type III secretion in Pseudomonas aeruginosa.** *Journal of bacteriology* 2005, **187(4):**1384-1391.
9. Feldman M, Bryan R, Rajan S, Scheffler L, Brunnert S, Tang H, Prince A: **Role of flagella in pathogenesis of Pseudomonas aeruginosa pulmonary infection.** *Infection and immunity* 1998, **66(1):**43-51.
10. Adamo R, Sokol S, Soong G, Gomez MI, Prince A: **Pseudomonas aeruginosa flagella activate airway epithelial cells through asialoGM1 and toll-like receptor 2 as well as toll-like receptor 5.** *American journal of respiratory cell and molecular biology* 2004, **30(5):**627-634.
11. Kipnis E, Sawa T, Wiener-Kronish J: **Targeting mechanisms of Pseudomonas aeruginosa pathogenesis.** *Medecine et maladies infectieuses* 2006, **36(2):**78-91.
12. Van Delden C, Iglewski BH: **Cell-to-cell signaling and Pseudomonas aeruginosa infections.** *Emerging infectious diseases* 1998, **4(4):**551-560.
13. Alonso A, Rojo F, Martinez JL: **Environmental and clinical isolates of Pseudomonas aeruginosa show pathogenic and biodegradative properties irrespective of their origin.** *Environmental microbiology* 1999, **1(5):**421-430.
14. Morales G, Wiehlmann L, Gudowius P, van Delden C, Tummler B, Martinez JL, Rojo F: **Structure of Pseudomonas aeruginosa populations analyzed by single nucleotide polymorphism and pulsed-field gel electrophoresis genotyping.** *Journal of bacteriology* 2004, **186(13):**4228-4237.
15. Lee DG, Urbach JM, Wu G, Liberati NT, Feinbaum RL, Miyata S, Diggins LT, He J, Saucier M, Deziel E, *et al.*: **Genomic analysis reveals that Pseudomonas aeruginosa virulence is combinatorial.** *Genome Biol* 2006, **7(10):**R90.
16. Rahme LG, Stevens EJ, Wolfort SF, Shao J, Tompkins RG, Ausubel FM: **Common virulence factors for bacterial pathogenicity in plants and animals.** *Science* 1995, **268(5219):**1899-1902.
17. Tan MW, Mahajan-Miklos S, Ausubel FM: **Killing of Caenorhabditis elegans by Pseudomonas aeruginosa used to model mammalian bacterial pathogenesis.** *Proc Natl Acad Sci USA* 1999, **96(2):**715-720.
18. Alibaud L, Kohler T, Coudray A, Prigent-Combaret C, Bergeret E, Perrin J, Benghezal M, Reimmann C, Gauthier Y, van Delden C, *et al.*: **Pseudomonas aeruginosa virulence genes identified in a Dictyostelium host model.** *Cellular microbiology* 2008, **10(3):**729-740.
19. Kurz CL, Ewbank JJ: **Infection in a dish: high-throughput analyses of bacterial pathogenesis.** *Current opinion in microbiology* 2007, **10(1):**10-16.
20. Pukatzki S, Kessin RH, Mekalanos JJ: **The human pathogen Pseudomonas aeruginosa utilizes conserved virulence pathways to infect the social amoeba Dictyostelium discoideum.** *Proc Natl Acad Sci USA* 2002, **99:**3159-3164.
21. Cosson P, Zulianello L, Join-Lambert O, Faurisson F, Gebbie L, Benghezal M, van Delden C, Curty LK, Kohler T: **Pseudomonas aeruginosa virulence analyzed in a Dictyostelium discoideum host system.** *J Bact* 2002, **184:**3027-3033.
22. Unal C, Steinert M: **Dictyostelium discoideum as a model to study host-pathogen interactions.** *Methods in molecular biology (Clifton, NJ)* 2006, **346:**507-515.
23. Eichinger L, Pachebat JA, Glockner G, Rajandream MA, Sucgang R, Berriman M, Song J, Olsen R, Szafranski K, Xu Q, *et al.*: **The genome of the social amoeba Dictyostelium discoideum.** *Nature* 2005, **435(7038):**43-57.
24. Navas A, Cobas G, Talavera M, Ayala JA, Lopez JA, Martinez JL: **Experimental validation of Haldane's hypothesis on the role of infection as an evolutionary force for Metazoans.** *Proc Natl Acad Sci USA* 2007, **104(34):**13728-13731.
25. Steinert M, Heuner K: **Dictyostelium as host model for pathogenesis.** *Cellular microbiology* 2005, **7(3):**307-314.
26. Urushihara H, Morio T, Saito T, Kohara Y, Koriki E, Ochiai H, Maeda M, Williams JG, Takeuchi I, Tanaka Y: **Analyses of cDNAs from growth and slug stages of Dictyostelium discoideum.** *Nucl Acids Res* 2004, **32:**1647-1653.
27. Choi JY, Sifri CD, Goumnerov BC, Rahme LG, Ausubel FM, Calderwood SB: **Identification of virulence genes in a pathogenic strain of Pseudomonas aeruginosa by representational difference analysis.** *Journal of bacteriology* 2002, **184(4):**952-961.
28. Farbrother P, Wagner C, Na J, Tunggal B, Morio T, Urushihara H, Tanaka Y, Schleicher M, Steinert M, Eichinger L: **Dictyostelium transcriptional host cell response upon infection with Legionella.** *Cellular microbiology* 2006, **8(3):**438-456.
29. Sarosh BR, Meijer J: **Transcriptional profiling by cDNA-AFLP reveals novel insights during methyl jasmonate, wounding and insect attack in Brassica napus.** *Plant molecular biology* 2007, **64(4):**425-438.
30. Morita T, Amagai A, Maeda Y: **Translocation of the Dictyostelium TRAP1 homologue to mitochondria induces a novel prestarvation response.** *J Cell Sci* 2004, **117(Pt 24):**5759-5770.
31. Muller I, Subert N, Otto H, Herbst R, Ruhling H, Maniak M, Leippe M: **A Dictyostelium mutant with reduced lysozyme levels compensates by increased phagocytic activity.** *J Biol Chem* 2005, **280(11):**10435-10443.
32. Zhang H, Gomez-Garcia MR, Shi X, Rao NN, Kornberg A: **Polyphosphate kinase 1, a conserved bacterial enzyme, in a eukaryote, Dictyostelium discoideum, with a role in cytokinesis.** *Proc Natl Acad Sci USA* 2007, **104(42):**16486-16491.

33. Zhang H, Gomez-Garcia MR, Brown MR, Kornberg A: **Inorganic polyphosphate in Dictyostelium discoideum: influence on development, sporulation, and predation.** *Proc Natl Acad Sci USA* 2005, **102(8):**2731-2735.
34. Kim BJ, Choi CH, Lee CH, Jeong SY, Kim JS, Kim BY, Yim HS, Kang SO: **Glutathione is required for growth and prespore cell differentiation in Dictyostelium.** *Dev Biol* 2005, **284(2):**387-398.
35. Min J, Traynor D, Stegner AL, Zhang L, Hanigan MH, Alexander H, Alexander S: **Sphingosine kinase regulates the sensitivity of Dictyostelium discoideum cells to the anticancer drug cisplatin.** *Eukaryot Cell* 2005, **4(1):**178-189.
36. Ichikawa JK, Norris A, Bangera MG, Geiss GK, van 't Wout AB, Bumgarner RE, Lory S: **Interaction of pseudomonas aeruginosa with epithelial cells: identification of differentially regulated genes by expression microarray analysis of human cDNAs.** *Proc Natl Acad Sci USA* 2000, **97(17):**9659-9664.
37. Huang X, Hazlett LD: **Analysis of Pseudomonas aeruginosa corneal infection using an oligonucleotide microarray.** *Invest Ophthalmol Vis Sci* 2003, **44(8):**3409-3416.
38. Peracino B, Wagner C, Balest A, Balbo A, Pergolizzi B, Noegel AA, Steinert M, Bozzaro S: **Function and mechanism of action of Dictyostelium Nramp1 (Slc11a1) in bacterial infection.** *Traffic* 2006, **7(1):**22-38.
39. Sussman M: **Cultivation and synchronous morphogenesis of Dictyostelium under controlled experimental conditions.** *Meth Cell Biol* 1987, **28:**9-29.
40. Bloomfield G, Tanaka Y, Skelton J, Ivens A, Kay RR: **Widespread duplications in the genomes of laboratory stocks of Dictyostelium discoideum.** *Genome Biol* 2008, **9(4):**R75.
41. Kooperberg C, Fazzio TG, Delrow JJ, Tsukiyama T: **Improved background correction for spotted DNA microarrays.** *J Comput Biol* 2002, **9(1):**55-66.
42. Smyth GK, Michaud J, Scott HS: **Use of within-array replicate spots for assessing differential expression in microarray experiments.** *Bioinformatics* 2005, **21(9):**2067-2075.
43. Smyth GK: **Linear models and empirical bayes methods for assessing differential expression in microarray experiments.** *Stat Appl Genet Mol Biol* 2004, **3:**.
44. Smyth GK, Speed TP: **Normalization of cDNA microarray data.** *Methods* 2003, **31(4):**265-273.
45. Benjamini Y, Hochberg Y: **Controlling the flase discovery rate: a practical and powerful approach to multiple testing.** *J R Statist Soc B* 1995, **57(1):**289-300.
46. **ArrayExpress** [http://www.ebi.ac.uk/arrayexpress]
47. Warnes GR: **Includes R source code and/or documentation contributed by Ben Bolker and Thomas Lumley. gplots: Various R programming tools for plotting data. R package version 2.3.2.** 2007 [http://cran.r-project.org/web/packages/gplots/].

Molecular Biology of the Cell
Vol. 19, 3442–3453, August 2008

Vacuole Membrane Protein 1 Is an Endoplasmic Reticulum Protein Required for Organelle Biogenesis, Protein Secretion, and Development

Javier Calvo-Garrido,* Sergio Carilla-Latorre,* Francisco Lázaro-Diéguez,† Gustavo Egea,† and Ricardo Escalante*

*Instituto de Investigaciones Biomédicas "Alberto Sols," Consejo Superior de Investigaciones Científicas and Universidad Autónoma de Madrid, 28029 Madrid, Spain; †Departament de Biologia Cellular i Anatomia Patològica, Facultat de Medicina, Institut d'Investigacions Biomèdiques August Pi i Sunyer, Institut de Nanociència i Nanotecnologia, Universitat de Barcelona, 08036 Barcelona, Spain

Submitted January 25, 2008; Revised May 22, 2008; Accepted June 4, 2008
Monitoring Editor: Francis A. Barr

Vacuole membrane protein 1 (Vmp1) is membrane protein of unknown molecular function that has been associated with pancreatitis and cancer. The social amoeba *Dictyostelium discoideum* has a *vmp1*-related gene that we identified previously in a functional genomic study. Loss-of-function of this gene leads to a severe phenotype that compromises *Dictyostelium* growth and development. The expression of mammalian Vmp1 in a *vmp1*$^-$ *Dictyostelium* mutant complemented the phenotype, suggesting a functional conservation of the protein among evolutionarily distant species and highlights *Dictyostelium* as a valid experimental system to address the function of this gene. *Dictyostelium* Vmp1 is an endoplasmic reticulum protein necessary for the integrity of this organelle. Cells deficient in Vmp1 display pleiotropic defects in the secretory pathway and organelle biogenesis. The contractile vacuole, which is necessary to survive under hypoosmotic conditions, is not functional in the mutant. The structure of the Golgi apparatus, the function of the endocytic pathway and conventional protein secretion are also affected in these cells. Transmission electron microscopy of *vmp1*$^-$ cells showed the accumulation of autophagic features that suggests a role of Vmp1 in macroautophagy. In addition to these defects observed at the vegetative stage, the onset of multicellular development and early developmental gene expression are also compromised.

INTRODUCTION

One of the hallmarks of eukaryotic cells is the presence of complex intracellular membrane-bound organelles dedicated to specific functions. Part of the structural and functional specificity of these organelles is based on their distinct complement of proteins and membrane lipids. The link between membrane traffic, protein traffic, and organelle biogenesis is now becoming evident in the context of the secretory pathway (Derby and Gleeson, 2007). Failure of any component within the pathway can lead to abnormal targeting of proteins and membrane components that are necessary for organelle function or biosynthesis (Howell *et al*., 2006). Furthermore, some of these defects in organelle biogenesis have been found to be associated with human diseases (Dhaunsi, 2005).

Vacuole membrane protein 1 (Vmp1) is a conserved putative membrane protein with no recognizable functional motifs. The function of Vmp1 is now beginning to be elucidated. Several lines of evidence suggest a possible role of this protein in membrane traffic and organelle organization. It has been described as a stress-induced endoplasmic reticulum (ER) protein in the rat exocrine pancreas that is highly expressed during acute pancreatitis (Dusetti *et al*., 2002; Vaccaro *et al*., 2003). Overexpression of this protein in cell culture leads to vacuole formation and cell death, a process that is observed in pancreatitis (Dusetti *et al*., 2002). A recent report also identified Vmp1 as a novel autophagy-related membrane protein involved in mammalian pancreatitis-induced autophagy (Ropolo *et al*., 2007). In *Drosophila*, Vmp1 (known as TANGO-5) was also identified in a functional genomic screen by using RNA interference. TANGO-5 was found to be required for protein secretion and Golgi organization (Bard *et al*., 2006). In another study, Vmp-1 was localized in the plasma membrane in the kidney cancer cell line Caki-2, and it was found to be essential for cell–cell contact (Sauermann *et al*., 2008). These results suggested a totally different function of Vmp1 in tumor cells. Therefore, the function of this protein remains controversial and seems to depend on the specific cell type studied.

Vmp1 is a conserved protein and the study of its complex function might benefit from the use of simple experimental systems such as *Dictyostelium discoideum*. Using the completed *Dictyostelium* genome sequence, we generated a collection of mutants by targeted disruption of genes with unknown function that are highly conserved between *Dictyostelium* and humans, but also absent from the genomes

This article was published online ahead of print in *MBC in Press* (http://www.molbiolcell.org/cgi/doi/10.1091/mbc.E08–01–0075) on June 11, 2008.

Address correspondence to: Ricardo Escalante (rescalante@iib.uam.es).

Abbreviations used: CV, contractile vacuole; ER, endoplasmic reticulum; GFP, green fluorescence protein; PDI, protein disulfide isomerase; VMP1, vacuole membrane protein 1; TEM, transmission electron microscopy.

of *Saccharomyces cerevisiae* and *Schizosaccharomyces pombe* (Torija *et al*., 2006a,b). Among those genes, we identified Vmp1 (named DupF in that analysis). Its absence in any fungi makes *Dictyostelium* the simplest genetically tractable model system to address its function.

Dictyostelium is a eukaryotic microorganism used as a model to study basic cellular processes, including membrane traffic and the endocytic pathway (Maniak, 2003). These social amoebae live as solitary cells feeding on other microorganisms by phagocytosis. Laboratory strains are also capable of growth in axenic media that is taken up by macropinocitosis. The vacuoles of ingested material fuse with lysosomes and undigested residues are secreted by exocytosis. As in many soil microorganisms, water regulation is essential for survival. A specialized organelle, the contractile vacuole (CV) system, is composed of an independent network of membrane tubules and cisternae that fill up and expel water by transient fusion with the plasma membrane (Gabriel *et al*., 1999). Contractile vacuole biogenesis is dependent on clathrin-coated vesicles and the adaptor-protein complex 1 (AP-1) for transporting protein and membranes required for the CV formation (O'Halloran and Anderson, 1992; Lefkir *et al*., 2003). As a result, defects in AP-1 function lead to impaired osmoregulation.

Besides its interest as a cellular model, *Dictyostelium* has the exceptional ability to form a multicellular organism by aggregation of solitary cells. The differentiation program is triggered by starvation and leads to the formation of a fruiting body composed of spores supported by a stalk (Escalante and Vicente, 2000).

In this report, we describe the first loss-of-function mutation for a Vmp1 homologue in a model system. We have found that Vmp1 is an endoplasmic reticulum protein in *Dictyostelium* necessary for the integrity of this organelle. The lack of this ER protein has pleiotropic defects in several membrane traffic-dependent processes such as organelle biogenesis and structure, endocytosis, and protein trafficking. Our results also suggest that an aberrant pattern of protein secretion during starvation might in part account for the impairment in the transition from growth to development in *Dictyostelium*.

MATERIALS AND METHODS

Dictyostelium *Cell Culture, Transformation, and Development*

Cells were grown axenically in HL5 medium or in association with *Klebsiella aerogenes* in SM plates (Sussman, 1987). Transformations were carried out by electroporation as described previously (Pang *et al*., 1999). For synchronous development, axenically growing cells were washed from culture media by centrifugation, resuspended in PDF buffer (20 mM KCl, 9 mM K_2HPO_4, 13 mM KH_2PO_4, 1 mM $CaCl_2$, and 1 mM $MgSO_4$, pH 6.4) and deposited on nitrocellulose filters (Shaulsky and Loomis, 1993). Because Vmp1 mutant cells do not grow well in axenic HL5 media the strain was initially grown in association with bacteria. For most of the experiments (unless otherwise indicated), ~10,000 cells were mixed with *Klebsiella* (300 μl of an overnight culture) and plated in SM plates. After 3 d, the clear lawn of cells were taken from the plate and used directly or resuspended in HL5. The remaining bacteria were then washed out by centrifugation, and the cells were deposited again in an appropriate volume of HL5 during an overnight, unless otherwise indicated. For filter development mutant cells were taken from SM plates as indicated above, washed, and deposited on the filters. Mutant cells in HL5 or PDF remain viable, and no cell lysis occurs in these conditions.

Generation of Mutant Strains

Disruption of Vmp1 gene in *Dictyostelium* was performed as described previously (Torija *et al*., 2006a). Briefly, DNA fragments ranging from 2 to 2.5 kb containing the genes to be disrupted were cloned by polymerase chain reaction (PCR) from genomic DNA. Insertion of the blasticidin resistance cassette by in vitro transposition by using the vector was performed as described previously (Abe *et al*., 2003). The constructs containing the flanking regions and the transposon were amplified by PCR, and the products were transformed in *Dictyostelium* cells by electroporation. Transformants were plated in association with bacteria for clonal isolation and screened for homologous recombination by PCR by using oligonucleotides surrounding the site of insertion. The DNA of the transformant clones used for PCR was isolated from cells of the growing zone by using the Master amp DNA extraction solution from EPICENTRE.

Gene Expression Analysis, Northern Blots, and Western Blots

RNA was isolated by TRIzol (Invitrogen, Carlsbad, CA), according to manufacturer's instructions. The different RNAs were separated by electrophoresis, transferred to nylon membranes, and hybridized to the indicated radioactive-labeled PCR probes. All DNA/RNA manipulation and Western blot analysis were performed according to methods described previously (Ausubel *et al*., 1992).

Transmission Electron Microscopy

Wild-type (WT) and mutant cells were incubated in Petri dishes with HL5 overnight to allow the attachment of the cells. The media were discarded, and cells were rapidly fixed with 1.25% glutaraldehyde in 0.1 M piperazine-*N*,*N*′-bis(2-ethanesulfonic acid) (PIPES) buffer, pH 6.8, containing 1% sucrose and 2 mM Mg_2SO_4 for 60 min at 37°C. Cells were then gently scraped, pelleted at 200 × *g*, rinsed in PIPES buffer (3 times), postfixed with 1% (wt/vol) OsO_4, 1% (wt/vol) $K_3Fe(CN)_6$ in PIPES buffer for 1 h at room temperature in the dark, and rinsed in PIPES buffer. Cells were treated for 5 min with 0.1% tannic acid in PIPES buffer, dehydrated with graded ethanol solutions, and finally embedded in Epon plastic resin. Ultrathin sections were stained with 2% uranyl acetate for 30 min, and then with lead citrate for 10 min and observed with a JEOL 1010 transmission electron microscope operating at 80 kV with a Gatan BioScan model 792 module for acquisition of digital images with Digital. Micrograph 3.4.3 acquisition software (Gatan, Pleasanton., CA). ImageJ 1.37 software (National Institutes of Health, Bethesda, MD) was used for the morphometric analysis. Data are mean values with SD.

Endocytosis, Exocytosis, and Phagocytosis

Wild-type cells were grown axenically in HL5 and mutant cells were initially grown in SM-plates and then incubated overnight in HL5 before being used for the experiments. Endocytosis, exocytosis, and phagocytosis of fluorescent markers were performed according to Rivero and Maniak, 2006). Results are shown as mean values with SD from duplicates or triplicates of at least three independent experiments. Significance of differences between groups was determined by Student's *t* test.

Conditioned Media, In-Gel Digestion of Proteins, Matrix-Assisted Laser Desorption Ionization-Tandem Mass Spectrometry (MALDI-MS/MS), and Database Searching

Conditioned media were obtained by the incubation of cells in PDF at a concentration of 1 × 10E7 cells/ml during 7 h in shaking culture. The media were washed free of cells by centrifugation at 1000 rpm for 5 min. Conditioned media were subsequently used for the biological experiments and for analysis by SDS-polyacrylamide gel electrophoresis (PAGE). After electrophoresis the gel was silver stained with the silver staining kit from GE Healthcare (Chalfont St. Giles, United Kingdom), according to the instructions that allow the subsequent identification by MALDI-MS/MS. Differential bands between wild type and mutant were excised manually from the gel and then digested automatically using a Proteineer DP protein digestion station (Bruker-Daltonics, Bremen, Germany). The digestion protocol used was that described previously (Shevchenko *et al*., 2006), with minor variations: gel plugs were submitted to reduction with 10 mM dithiothreitol (GE Healthcare) in 50 mM ammonium bicarbonate (99.5% purity; Sigma-Aldrich, St. Louis, MO) and alkylation with 55 mM iodoacetamide (Sigma-Aldrich) in 50 mM ammonium bicarbonate. The gel pieces were then rinsed with 50 mM ammonium bicarbonate and acetonitrile (gradient grade; Merck, Darmstadt, Germany) and dried under a stream of nitrogen. Modified porcine trypsin (sequencing grade; Promega, Madison, WI) at a final concentration of 8 ng/μl in 50 mM ammonium bicarbonate was added to the dry gel pieces and the digestion proceeded at 37°C for 8 h. Finally, 0.5% trifluoroacetic acid (99.5% purity; Sigma-Aldrich) was added for peptide extraction.

An aliquot of the above-mentioned digestion solution was mixed with an aliquot of cyano-4-hydroxycinnamic acid (Bruker Daltonics, Billerica, MA) in 33% aqueous acetonitrile and 0.25% trifluoroacetic acid. This mixture was deposited onto a 600 μm AnchorChip prestructured MALDI probe (Bruker Daltonics) and allowed to dry at room temperature. MALDI-MS(/MS) data were obtained in an automated analysis loop using an Ultraflex time-of-flight (TOF) mass spectrometer (Bruker Daltonics) equipped with a LIFT MS/MS device (Suckau *et al*., 2003). Spectra were acquired in the positive-ion mode at 50-Hz laser frequency, and 100-1000 individual spectra were averaged. For fragment ion analysis in the tandem time-of-flight (TOF/TOF) mode, precur-

sors were accelerated to 8 kV and selected in a timed ion gate. Fragment ions generated by laser-induced decomposition of the precursor were further accelerated by 19 kV in the LIFT cell and their masses were analyzed after passing the ion reflector. Automated analysis of mass data was performed using the flexAnalysis software (Bruker Daltonics). Internal calibration of MALDI-TOF mass spectra was performed using two trypsin autolysis ions with m/z 842.510 and m/z 2211.105; for MALDI-MS/MS, calibrations were performed with fragment ion spectra obtained for the proton adducts of a peptide mixture covering the 800-3200 m/z region. MALDI-MS and MS/MS data were combined through the BioTools program (Bruker Daltonics) to search nonredundant protein databases (National Center for Biotechnology Information, Bethesda, MD; and SwissProt, Swiss Institute for Bioinformatics, Switzerland) by using the Mascot software (Matrix Science, London, United Kingdom) (Perkins *et al*., 1999).

Green Fluorescent Protein (GFP) Expression Constructs, Immunocytochemistry, and Microscopy

The *Dictyostelium vmp1* gene was amplified from genomic DNA by using oligonucleotides containing targets for the restriction enzyme BamH1 and XbaI. The fragment was cloned in pGEMt-easy vector and sequenced to check for possible polymerase errors. The fragment was subsequently cloned into the BamH1 and XbaI sites of the GFP vector pDV-CGFP-CTAP, kindly provided by Pauline Shaap (University of Dundee, Dundee, United Kingdom). The construct, driven by actin15 promoter, contained the complete Vmp1 coding region fused to GFP-TAP. A similar approach was used for cloning the rat Vmp1 vector. In this case, the complete Vmp1 coding region was obtained by reverse transcription (RT)-PCR from RNA isolated from rat tissue.

For immunocytochemistry, WT and mutant cells (incubated previously in HL5 overnight), were allowed to adhere to coverslips and fixed in 4% paraformaldehyde in phosphate-buffered saline (PBS) for 30 min. After two washes with PBS cells were permeabilized with chilled methanol during 2 min and incubated during 20 min in blocking buffer (0.2% bovine serum albumin in PBS). The samples were then incubated with the first antibody in blocking buffer for 1 h. After six washes with blocking buffer the appropriate secondary antibody (labeled with red Alexa 546) was added at a dilution of 1/1000 in blocking buffer for 30 min. After two washes with blocking buffer cells were mounted for microscopic observation. Confocal analysis was performed on a Leica TCS SP5 by using a PL APO 63×/1.4-0.6 objective and a LAS-AF (Leica Application Suite; Lecia, Wetzlar, Germany) software. For excitation of GFP a 488-nm argon laser was used. For fluorescence microscopy, an Olympus DP70 microscope with a Plan Neofluar 100×, 1.30 oil objective was used. The acquisition software was DP controller 2002, Olympus Optical CO.LTD. The antibodies and the dilution used for each were as follows: PDI (221-64-1 ascitis, mouse monoclonal) used at 1:1000; p80 (H161, mouse monoclonal) used at 1:10; Rh50 (rabbit polyclonal), used at 1:500. These antibodies were kindly provided by Pierre Cosson from the University of Geneva (Geneva, Switzerland). VatA (221-35-2 ascitis, mouse monoclonal) used a dilution of 1:3. Kindly provided by Marcus Maniak (Kassel University, Kassel, Germany). AprA (rabbit polyclonal) used at 1:1000. Kindly provided by Richard Gomer (Rice University, Houston, TX).

RESULTS

Disruption of Vmp1 in Dictyostelium Leads to a Severe Defect in Osmoregulation

Dictyostelium vmp1 (DDB0234044) codes for a putative transmembrane protein of 403 amino acids. The level of identity between the human and the *Dictyostelium*-predicted proteins is 41% (Figure 1A). Homologues are also present in other organisms, including *Caenorhabditis elegans*, *Drosophila melanogaster*, and *Arapidopsis thaliana* (Figure 1B). However, no homologues were found in any fungi. Interestingly, it is present in other protists such as pathogenic protozoa, suggesting a specific gene loss during fungi evolution. Furthermore, *Dictyostelium* Vmp1 is more similar to the vertebrate homologues than to other simpler organisms, including other protists. The hydropathicity profile between the *Dictyostelium* and human proteins also showed a high level of similarity, suggesting conservation in the predicted transmembrane domains (Figure 1C). The *Dictyostelium vmp1* gene was disrupted by homologous recombination using an optimized protocol based on in vitro transposition (Torija *et al*., 2006a,b). Figure 1D shows a scheme of the gene and the point of insertion of the blasticidin cassette. Two oligonucleotides surrounding the disruption were used to screen for homologous recombination by PCR as depicted in Figure 1D. Several independent mutants were obtained that showed the same phenotype, and one of them was chosen for further analysis. The lack of expression of *vmp1* mRNA in the disruptant strain suggests that the insertion generated a loss-of-function mutant (Figure 1E). *vmp1* disruption was also generated in other *Dictyostelium* strains (Table 1), and the phenotype was similar regardless of the strain background.

The major consequences of *vmp1* disruption are shown in Figure 2. Growth in association with bacteria was slightly affected as observed by the size of the clearing plaques (Figure 2A). These cells were also deficient in initiating development upon starvation (see also below). Cell growth in axenic media (HL5) was compromised in shaking culture. Cells grew slowly over the first 2 d in culture, and cell growth eventually stopped completely. However, when cells were set in Petri dishes, allowing them to attach to the plastic, their growth was very slow but sustained (data not shown). The possibility of a cytokinesis defect was studied by staining the cells with 4,6-diamidino-2-phenylindole (DAPI). No differences in the number of nuclei per cell were found in any growth condition (data not shown). Intriguingly, when mutant cells were directly taken from SM plates and incubated in water they rapidly rounded up and after few minutes a proportion of them began to burst. This can be recognized by the presence of remaining cell debris (Figure 2B). This aspect of the phenotype is more patently illustrated in Supplemental Movie 1. The same phenotype was observed in cells previously incubated overnight in HL5. *Dictyostelium* cells have a contractile vacuole (CV) system, which allows the cells to efficiently survive hypoosmotic conditions. The presence and the activity of these vacuoles that expel water outside the cell can be visualized under phase contrast microscopy. A high magnification of the cells (Figure 2B) showed that whereas wild type displayed abundance of clear vacuoles that eventually fused with plasma membrane, the mutant cells were round and had a flat appearance with no evident activity of the CV (Figure 2B).

These results suggested a defect in osmoregulation and more specifically in the activity of the CV. To confirm this hypothesis, we incubated wild-type and mutant cells in different concentrations of sorbitol to generate a wide range of osmotic pressure. Figure 2C shows how the morphology of mutant cells became less round as the sorbitol concentration increases. At 100 mM sorbitol the cells looked more normal in appearance but nevertheless they showed no clear vacuole activity as seen in wild type. Mutant cells were able to respond to hyperosmotic stress (400 mM sorbitol) by reducing their volume (also known as cringing) and they showed high refringence, as described for wild type cells (Kuwayama *et al*., 1996). These results suggested a specific defect of the mutant cells in coping with hypoosmotic conditions as a result of impaired CV activity.

Vmp1 Is Required for Contractile Vacuole Biogenesis

To characterize the function of the CV in vivo, we disrupted *vmp1* in a *Dictyostelium* strain expressing the protein Dajumin fused to GFP (see Table 1 for a complete list of strains used in this report). Dajumin is a protein specifically located in the CV (Gabriel *et al*., 1999). Figure 3A shows the expected pattern of fluorescence in wild type. However, GFP fluorescence was hardly detectable in the disruptant strain, confirming the absence of functional vacuoles as observed under phase contrast microscopy. For further confirmation, we used the CV-specific antibody Rh50 (Benghezal *et al*., 2001). Figure 3B shows the immunofluorescence staining in wild type with the expected pattern. However, in this case a weak

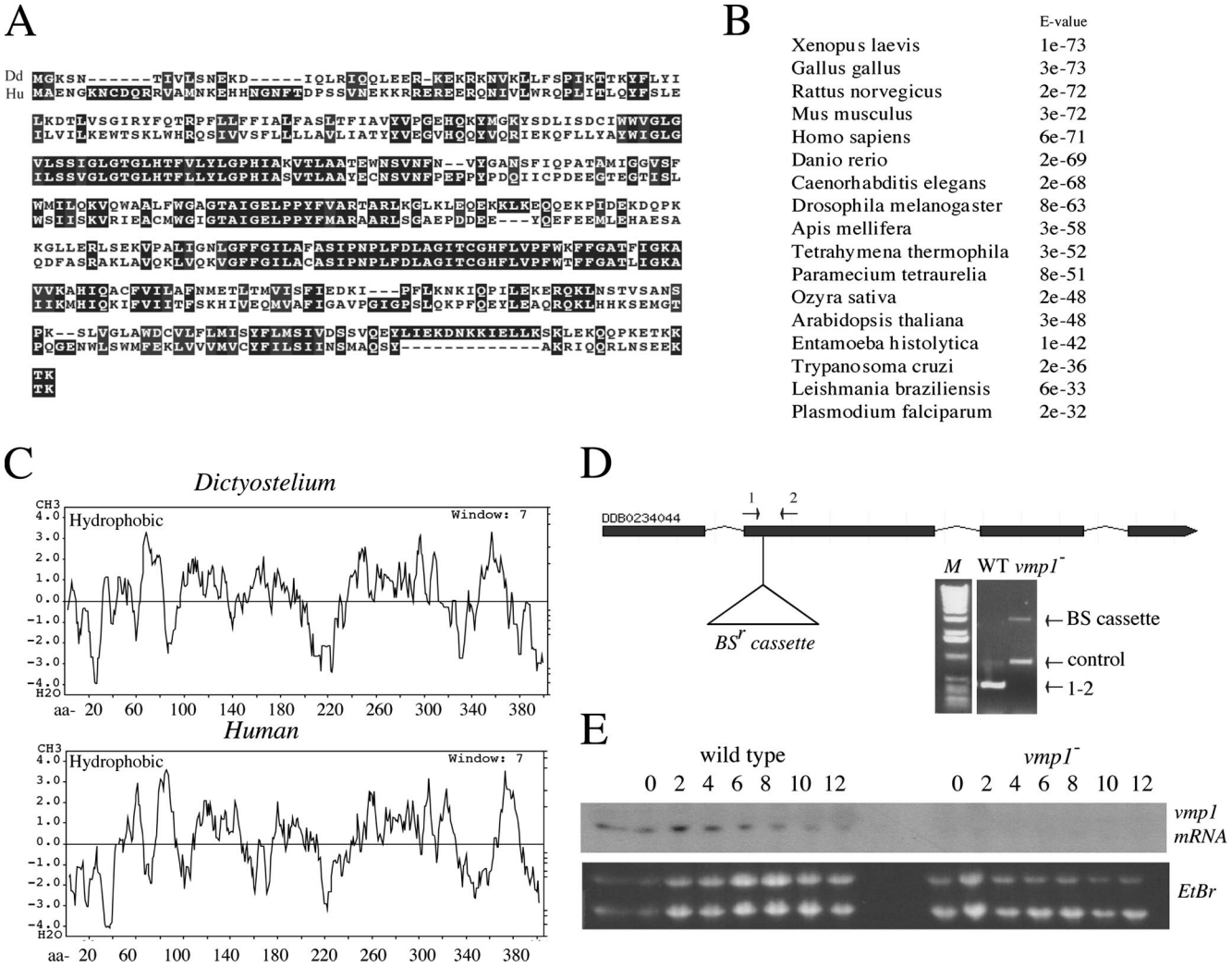

Figure 1. Disruption of the conserved gene *vmp1* in *Dictyostelium*. (A) The sequence of *Dictyostelium* Vmp1 predicted protein (DDB0234044) was aligned with the human homologue (CAG38552) by using the ClustalW program. The letters with black background correspond to identical residues and the gray background to similar residues. (B) The most similar proteins to the *Dictyostelium* Vmp1 are listed in order, from the highest identity to the lowest. (C) The hydropathicity plot of *Dictyostelium* and human Vmp1 predicted proteins are compared. The analysis was performed by the method of Kyte and Doolittle by using the online program at http://workbench.sdsc.edu/. (D) The structure of the *vmp1* gene is shown. Open boxes correspond to coding regions and the thin lines represent the introns. The insertion of the blasticidin cassette took place at the beginning of the second exon (amino acid 89) as indicated below. Disruption of the gene was assessed by PCR using oligonucleotides located at both sides of the insertion as indicated by the arrows. A pair of oligonucleotides from an unrelated locus was used as internal control of the PCR reaction. The panel below shows a typical analysis using DNA isolated from wild type (labeled as WT in the figure) and a disruptant strain (*vmp1*$^-$). The expected band (1–2) shifts to a higher band (BS-cassette) as a consequence of the insertion. M correspond to DNA size markers. (E) RNA isolated at different times of development was hybridized with a radioactive probe derived from the coding sequence of Vmp1. The band detected in wild type is absent in the disruptant strain.

signal was detected in the mutant, although the intensity of the staining and the size and number of vacuoles was greatly reduced (Figure 3B).

Dictyostelium cells contain many large vacuoles, including CVs and also vacuoles of the endocytic pathway, which are mainly devoted to nutrition in *Dictyostelium* (Maniak, 2003). Some of these vacuoles can be distinguished by electron microscopy. As seen in Figure 4, WT cells showed a high number of large electroluscent vesicles. Some of them contained spongy material that is believed to correspond to different degrees of digestion of the axenic media that has been internalized by macropinocytosis (Ryter and de Chastellier, 1977). Some of these vacuoles were completely electron transparent and probably correspond to contractile vacuoles (Ryter and de Chastellier, 1977). Mutant cells showed some striking differences with WT cells. First, there was a remarkable reduction in the number of electroluscent vacuoles, suggesting a defect not only in the biogenesis of the CV system but also in the endocytic pathway (aspect addressed below). Second, mutant cells showed an abnormal accumulation of electrodense vacuoles enclosing large granular and membranous material (Figure 4). The ratio of the number of electroluscent/electrodense vacuolar profiles ($\geq$200 nm) per μm^2 of cytoplasm was determined by morphometric analysis. This ratio in WT was 3.45 $\pm$ 0.98 (number of cells analyzed, n = 14), and it was significantly higher ($p \leq 0.0001$) than that obtained in the mutant, 0.43 $\pm$ 0.11 (number of cells analyzed, n = 14). These electrodense vesicular profiles are very similar to those described in macroautophagy mutants in *Dictyostelium* that are believed to be

Table 1. Strains used in this study

Strain name	Characteristics	Genotype	Parental strain	Reference
AX4	Wild-type strain			
AX2	Wild-type strain			
vmp1$^-$	Gene disrupted at aa-89	BS^r	AX4	This report
vmp1$^-$*/act15*::DdVmp1	Complemented strain by the expression of *Dictyostelium* Vmp1-GFP fusion protein	G418^r; BS^r	Vmp1$^-$	This report
vmp1$^-$*/act15*::rVmp1	Complemented strain by the expression of rat Vmp1-GFP fusion protein	G418^r; BS^r	Vmp1$^-$	This report
Vmp1-GFP	Complemented strain by single homologous recombination	G418^r; BS^r	Vmp1$^-$	This report
act15::ratVmp1	Expression of rat Vmp1 in wild type	G418^r	AX2	This report
Golvesin(C)-GFP	Marker for the Golgi apparatus	G418^r	AX2	Schneider *et al.* (2000)
Golvesin(C)-GFP/Vmp1$^-$	Marker for the Golgi apparatus in *vmp1*$^-$	G418^r; BS^r	Golvesin(C)-GFP	This report
Dajumin-GFP	Marker of the contractile vacuole	G418^r	AX2	Gabriel *et al.* (1999)
Dajumin-GFP/Vmp1$^-$	Marker of the contractile vacuole in *vmp1*$^-$	G418^r; BS^r	Dajumin-GFP	This report

nonmature autophagosomes containing nondigested cytoplasm and organelles (Otto *et al.*, 2003, 2004). This observation suggests a possible implication of Vmp1 in macroautophagy.

Vmp1 Is an Endoplasmic Reticulum Protein in Dictyostelium

We next cloned the entire *Dictyostelium vmp1* gene fused to GFP as a reporter for subcellular localization studies. The expression of the composite gene was driven by the constitutive actin 15 promoter. Mutant cells were transformed with the construct and the resulting strains fully complemented the phenotype in growth, development and osmoregulation (Figure 5, A and B). Complementation of the phenotype strongly suggests that the fused protein is functional. The complemented strain was used for confocal studies to determine the subcellular localization of the protein. The GFP fluorescence pattern as shown in Figure 5C, suggested that the protein was localized in internal membranes. We therefore used several markers of intracellular compartments for colocalization by immunofluorescence. Although a prominent defect in the mutant is related with the CV and the endosomal pathway (see below), Vmp1 did not colocalize with V-ATPase (VatA), a CV/endosomal protein (Clarke *et al.*, 2002), or with the endosomal marker P80 (Supplemental Figure 1). However, as shown in Figure 5D complete colocalization was observed with protein disulfide isomerase (PDI), a typical marker of the ER (Monnat *et al.*, 1997). Moreover, a strong GFP fluorescence labeled the nuclear envelope as can be seen in Figure 5D surrounding several nuclei stained with DAPI.

We next wanted to determine whether the expression of a mammalian Vmp1 in *Dictyostelium* was able to complement the mutant strain. The complete rat Vmp1 was cloned by RT-PCR and placed in frame with GFP in a similar construct as the one described for the *Dictyostelium* protein. This construct was transformed in wild type, and the mutant strains and stable transformants were isolated. As expected by the high conservation of the amino acid sequence, the mammalian protein was also localized in the endoplasmic reticulum in both strains (Supplemental Figure 2). Interestingly, growth in axenic media and development were almost completely recovered as well as the resistance to hypoosmotic conditions as described in Supplemental Figure 2. These results strongly suggest that the mammalian protein is functionally similar to the *Dictyostelium* protein.

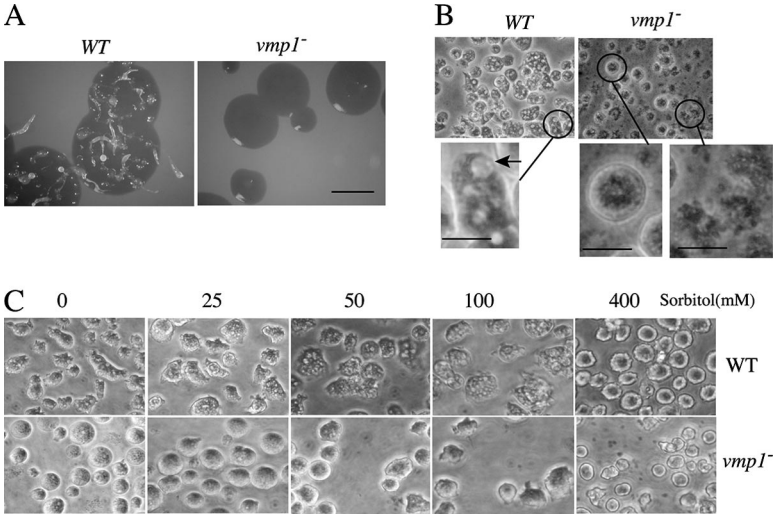

Figure 2. Vmp1 mutant cells are defective in growth, development and osmoregulation. (A) Wild type and *vmp1*$^-$ cells were cultivated in association with *Klebsiella aerogenes* in SM plates. The clearing plaques in the mutant are slightly smaller than those of the WT and do not show any sign of aggregation and development. Bar, 1 cm. (B) Cells were taken from the growing zones of *Klebsiella*-SM plates and incubated in water. After ~30 min, phase contrast photographs were taken with a Nikon Eclipse microscope. Wild type showed extensive vacuolization. A magnified image shows a contractile vacuole before discharging water outside the cell. The mutant cells were round and had a flat appearance with few vacuoles. Some of the mutant cells showed evidence of cell lysis. Magnified images show a mutant cell and cell debris. Bar, 10 μm. (C) Wild-type and mutant cells were incubated at different concentrations of sorbitol to study their response to osmotic pressure. Cell rupture and morphology were gradually recovered in the mutant as the osmotic pressure increased. Bar, 10 μm.

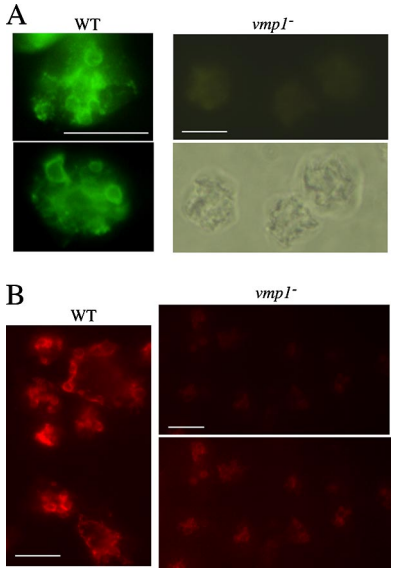

Figure 3. Analysis of the contractile vacuole activity. (A) *vmp1* was disrupted by homologous recombination in a strain expressing Dajumin fused to GFP, a marker of the CV network in *Dictyostelium*. WT and mutant cells were fixed and observed in a Nikon fluorescence microscope. Two representative cells of WT showed the expected pattern. However, fluorescence was barely detected in the mutant (top). Bottom, bright field image of the cells. (B) Immunofluorescence using Rh50, a CV-specific antibody coupled to Alexa 546, was performed in wild-type and mutant cells. A field containing several cells is shown for WT and the mutant. Although some staining was detected in the mutant, the intensity and the size of the vacuoles were reduced. The mutant top panel shows a photograph taken under the same intensity and contrast than the one shown for WT at the left. The bottom panel is the same picture with increased contrast to reveal the weak staining. Bars, 10 μm.

Vmp1 Is Required for ER Integrity and Membrane Traffic-dependent Processes

Although Vmp1 is present in the endoplasmic reticulum, we have shown evidence of defects in the CV. Because the ER is the starting point of the secretory pathway, we hypothesized that a primary defect in the structure of the ER, generated by the loss of Vmp1, could affect the biogenesis and the function of other organelles as a result of defective membrane traffic. To test this hypothesis, we analyzed the structure of the ER and the Golgi apparatus, endocytic trafficking, and the kinetics of protein secretion in the *vmp1*$^{-}$ mutants. We found acute alterations in most of these processes, which are summarized in Figure 6.

The ER in *Dictyostelium*, as observed by immunofluorescence microscopy with the PDI marker, has a typical tubulovesicular structure in WT (Figure 6A). Remarkably, it showed a fragmented appearance in the mutant suggesting a role for Vmp1 in the maintenance of its normal membrane structure. To visualize the Golgi apparatus in the mutant cells, Vmp1 was disrupted in a strain expressing Golvesin fused to GFP, which specifically labels this organelle (Schneider *et al.*, 2000). As displayed in Figure 6B, whereas wild-type cells usually showed fluorescence in a single and restricted area close to the nucleus, most of the mutant cells showed dispersed and fragmented areas of fluorescence.

The endocytic pathway in *Dictyostelium* is primarily dedicated to nutrition, and it depends, as in the rest of eukaryotes, on membrane traffic processes. We have studied the time course of endocytosis and exocytosis as a measure of the functional activity of endocytic organelles. Macropinocytosis as determined by the internalization of fluorescent markers was dramatically affected in the mutant (Figure 6C). Moreover, the staining of F-actin with phalloidin-rhodamine in wild-type and mutant cells showed a clear difference in the presence of crown-like structures (data not shown). Crowns are actin structures located in macropinosomes marking the early stages of macropinocytosis (Hacker *et al.*, 1997). There were almost no such structures in the mutant (data not shown). Exocytosis was difficult to evaluate because the cells accumulated much less fluorescent marker than the wild type shown in Figure 6D. Even so, the slope of the secretion graph at any point was also reduced in the mutant. As anticipated by the ability of the mutant cells to grow in association with bacteria, phagocytosis of fluores-

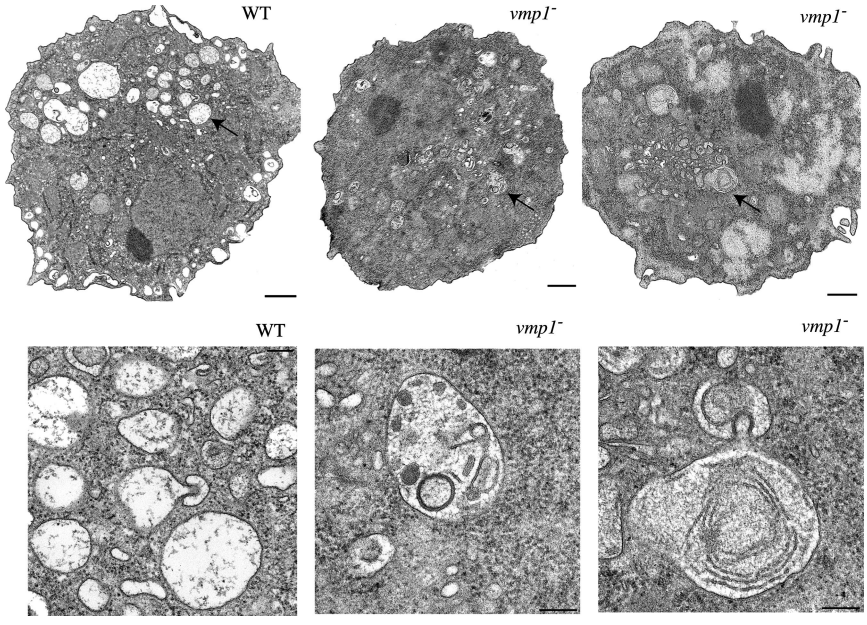

Figure 4. Electronic microscopy of WT and mutant cells. The arrows aim to the magnified area that is shown below. Mutant cells show accumulation of electrodense vacuoles enclosing large granular and membranous material. Bars, 1 μm (top); 200 nm (bottom).

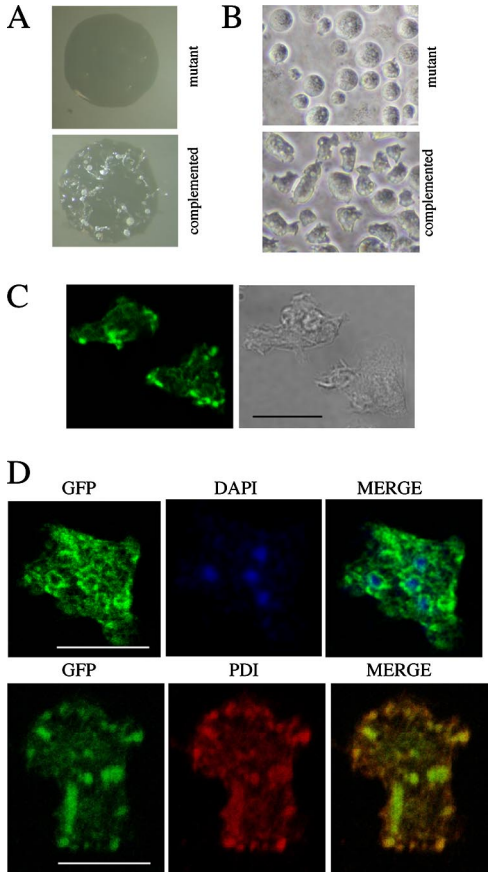

Figure 5. Vmp1 is an endoplasmic reticulum protein in *Dictyostelium*. *Dictyostelium vmp1* gene was fused to GFP and transformed into the *vmp1*$^-$ mutant. The transformant strain showed a WT phenotype with respect to development, osmoregulation and growth. (A) Mutant and complemented strains were grown in SM plates in association with *K. aerogenes*. (B) The strains were incubated in water for 30 min, and the complemented strain showed a normal response to hypoosmotic conditions as can be seen by the irregular shape of the cells and the presence of vacuoles. (C) Complemented cells were fixed and the fused Vmp1-GFP protein was visualized by confocal microscopy. Left, GFP fluorescence Right, bright field of the same cells. Bar, 10 μm. (D) The complemented strain expressing the fusion Vmp1-GFP protein was stained with DAPI (top) or treated for immunodetection of the endoplasmic reticulum marker PDI (bottom). The merged images show the presence of GFP fluorescence in the nuclear envelopes and colocalization with PDI. Bars, 10 μm.

cent beads was observed in the mutant, although at lower rate than in WT (Figure 6E).

Protein secretion is a process dependent on membrane traffic. Therefore, we wanted to determine a possible role of Vmp1 in the kinetics of secretion of AprA, a protein secreted by a conventional mechanism (ER–Golgi transit) that regulates *Dictyostelium* growth (Brock and Gomer, 2005). Wild-type and mutant cells were set in fresh HL5 media, and aliquots were taken at the indicated times. The amount of AprA secreted to the media was analyzed by Western blot (Figure 6F). A rapid accumulation of the protein in the extracellular media was observed in wild type. However, very little protein was detected in the mutant media suggesting a defect in protein secretion. The presence of intracellular AprA was also determined as a control.

Vmp1 Is Necessary for the Transition from Growth to Development

As shown in Figures 2 and 7A, *vmp1*$^-$ mutant cells were unable to aggregate in association with bacteria or on nitrocellulose filters soaked with PDF. We have previously determined that mutant cells, in contrast to their response in water, remained viable in PDF buffer and showed no signs of cell lysis (data not shown). Nevertheless, no aggregation of mutant cells was observed when PDF was supplemented with sorbitol (50 and 100 mM), suggesting that the deficiency in initiating development was not due to their osmosensitivity (data not shown). What aspects of the phenotype could account for such block in development? It is well known that the transition from growth to development in *Dictyostelium* is dependent on the activation of a specific gene expression pattern involving many genes that are regulated by extracellular signals induced by starvation (Kessin, 2001). Among them there are genes coding for the synthesis and relay of cAMP signaling that are essential for aggregation. We studied by Northern blot the expression pattern during early development of some of these markers. As shown in Figure 7B, the level of expression of the cAMP receptor Car1 and the adenylyl cyclase ACA were barely detected in the mutant. The absence of expression of any of these genes would be sufficient to account for the lack of aggregation as seen in the mutant. Discoidin I, in contrast, is a developmentally regulated lectin whose expression depends on cell density. The level of expression during early development was also strongly reduced in the mutant. As a control of constitutive expression, *patA*, a gene coded for a P-type ATPase, was used (Moniakis *et al*., 1995).

In *Dictyostelium*, the expression of these early developmental markers and discoidin are dependent on several secreted proteins during growth and starvation such as prestarvation response factor and conditioned medium factor (Clarke and Gomer, 1995) among others. Therefore, the observed impairment in the starvation response could be due to an abnormal cell response to these extracellular proteins, or to the absence of those signals as a result of abnormal protein secretion, as observed for AprA during growth, or more likely the combination of these two possibilities. Mixing experiments of mutant cells with different proportions of WT were unable to rescue mutant development, suggesting a cell autonomous defect (data not shown). Nevertheless, we undertook a proteomic approach to identify possible differences in the pattern of secreted proteins. Conditioned media was obtained by incubation of cells in starvation during 7 h. The media were then washed free of cells by centrifugation, and the secreted proteins were analyzed by SDS-PAGE electrophoresis. A direct comparison of the protein pattern between wild type and the mutant is shown in Figure 8. Most of the protein bands were present in both media with small differences in abundance. However, some striking differences were observed. Some protein bands were present in wild type but absent in the mutant and more interestingly there were bands present in the mutant that were barely detectable in wild type. This result might indicate a more complex scenario than just the lack of certain protein complement in the mutant suggesting an aberrant regulation of protein secretion.

We next tried to identify the differential protein bands by MALDI-MS/MS. Three different proteins were successfully identified (Figure 8). α-Mannosidase precursor (DDB0201569) and a cysteine proteinase (DDB0219654) were present in WT conditioned media but almost absent in the mutant. These two proteins are secreted by conventional mechanisms (ER/

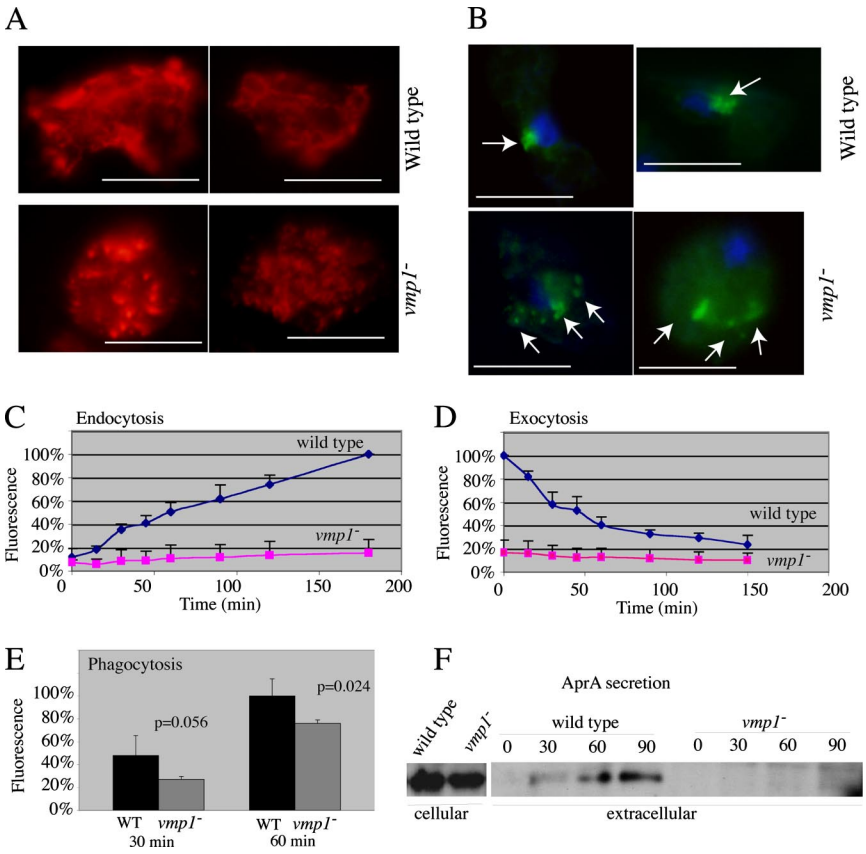

Figure 6. Characterization of defects in other membrane-traffic dependent processes. (A) Antibody label of protein disulfide isomerase (PDI), a marker of the endoplasmic reticulum. Photographs were taken in a fluorescence microscope and two representative cells of each strain are shown. Mutant cells showed fragmented endoplasmic reticulum. Bar, 10 μm. (B) *vmp1* was disrupted in a strain expressing Golvesin-GFP, a marker of the Golgi apparatus. The morphology of the Golgi apparatus was observed by fluorescence microscopy in the mutant and the parental strain. The Golgi apparatus in the mutant seemed disorganized. (C) Endocytosis assay. Wild-type and mutant cells were incubated in the presence of a soluble fluorescent marker. At the times indicated, the internal cellular fluorescence was determined. The mean of three independent experiments and the SD is shown. (D) Exocytosis assay. Cells were first preloaded with the marker and the decrease in internal fluorescence was measured at the times indicated. The mean of three independent experiments, and the SD is shown. (E) Phagocytosis assay. WT and mutant cells were exposed for the indicated times to fluorescent beads. Fluorescence was expressed as arbitrary units. The mean of four independent experiments is shown and the significance of differences is indicated by the p value. Bars show the SD. (F) Protein secretion assay. Wild-type and mutant cells were incubated in HL5 for the indicated times and the secreted AprA was analyzed in the media by Western blot using a specific antibody. The cellular extract was also analyzed as a control.

Golgi), reinforcing the data obtained by AprA (Pannel *et al*., 1982; Wood and Kaplan, 1985). Interestingly, a band overrepresented in the mutant media was identified as 70-kDa hear shock protein (Hsp70) (DDB0219654), a chaperone that has been described to play an additional role as an extracellular protein secreted by nonconventional mechanisms (Mambula *et al*., 2007; Multhoff, 2007). Although a comprehensive proteomic analysis would be necessary to fully characterize the defects in mutant conditioned media, our findings suggest that Vmp1 is also required for normal protein secretion during starvation.

DISCUSSION

Analysis of Vmp1 in Dictyostelium Reveals a Complex Function for This New Protein

Vmp1 is a conserved eukaryotic protein that seems to be lost in the fungi lineage during evolution. Consequently, *Dictyostelium* is one of the simplest genetically tractable model systems to address its function. This is the first loss-of-function mutant described for this gene in an experimental system, and Figure 9 shows a summary of the defects observed in the mutant in the context of the secretory pathway.

Our results show that Vmp1 is an ER protein required to maintain the structure of this organelle. Despite its location, it is involved in a wide range of membrane traffic-dependent processes such as organellar biogenesis and protein secretion. The morphology of the ER itself, the Golgi apparatus and the CV are compromised in the mutant as well as the maturation of autophagosomes and the function of the endocytic pathway. Protein secretion during growth and starvation is also dependent on Vmp1. It is conceivable that a primary defect in the ER, which is the starting point of the secretory pathway, could have an impact on other processes, which are directly dependent on the correct trafficking of protein and membrane components. This is not without precedent. For example, defective ER-resident proteins CLN6 and CLN8 are responsible for lysosomal dysfunctions (Kyttala *et al*., 2006). Secretion of extracellular matrix is impaired when CopII coat component Sec 23a is mutated as a result of defective transport from the ER (Lang *et al*., 2006).

We have found that some of these defects such as the disorganization of ER and Golgi are gradually aggravated over time as the cells remain in HL5 axenic culture. Cells in these conditions are likely to be starved due to the observed defects in nutrient uptake, suggesting that starvation might aggravate those phenotypes. However, other defects such as osmosensitivity and the onset of development do not seem to depend on the growth conditions. Cells taken directly from SM-plates, where they are feeding on bacteria to almost normal rates did not survive hypoosmotic conditions and were unable to initiate multicellular development.

Vmp1 Subcellular Localization and Its Functional Implications

Several lines of evidence suggest that Vmp1 is an ER-resident protein in *Dictyostelium*. We have shown that the fused protein Vmp1-GFP is localized in the endoplasmic reticulum and no colocalization has been observed with CV or endosomal markers. The fused protein showed full complementation of the phenotype when transformed in the mutant strain, suggesting that the protein must be in a functional conformation and also localizes to in the correct cellular compartment. Moreover, a knockin strain was obtained by

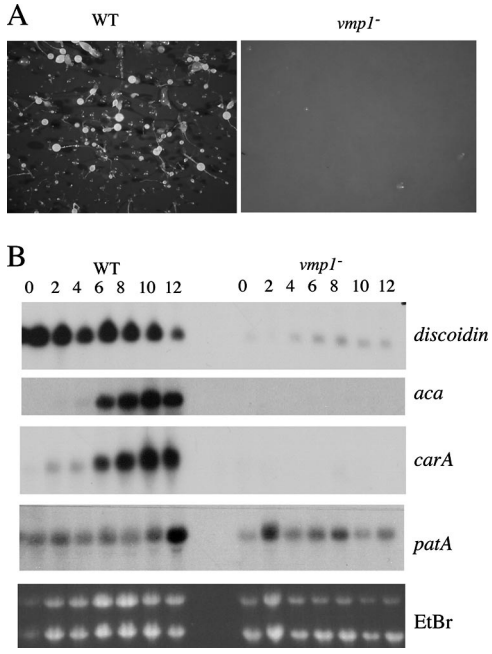

Figure 7. Developmental gene expression in *vmp1*$^{-}$ mutant. (A) WT and mutant cells were deposited in nitrocellulose filters for development and photographs of a representative experiment were taken after 30 h. No aggregation was observed in the mutant. (B) RNA was isolated form cells developed on nitrocellulose filters for the indicated times, transferred to nylon membranes and hybridized to radioactive probes. The same blot was stripped and hybridized several times. The expression of the lectin Discoidin, the adenylyl cyclase ACA, and the cAMP receptor Car 1 was greatly reduced. The expression of P-type ATPase (PatA), which is not developmentally regulated, was used as a control. The staining of ribosomal RNAs by ethidium bromide is shown at the bottom.

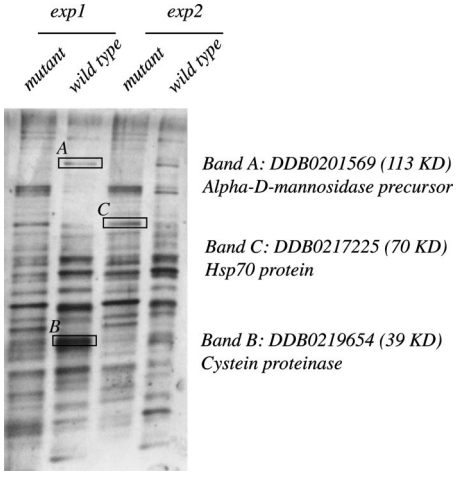

Figure 8. Conditioned medium and protein identification by MALDI-MS/MS. Wild-type and mutant cells were washed free of nutrients and resuspended in PDF for 4 h in shaking culture. Cells were then sedimented by centrifugation and the conditional media analyzed by SDS-PAGE. The gel was silver stained, and the protein pattern was compared. Two independent experiments are shown. Differential bands were cut and analyzed by MALDI-MS/MS. Three bands were successfully identified with a Mascot score of 1.1E-6 (band A), 5.6E-10 (band B), and 7.0E-6 (band C).

single crossover (Charette *et al*., 2006), in which a unique copy of the fused protein was under the control of the endogenous promoter (Supplemental Figure 3). This strain is expected to give rise to a level of expression that is similar to wild-type cells. In fact, the intensity of fluorescence was lower than that obtained in the overexpressor strains (data not shown). Even then, the localization was found in the ER as determined by colocalization with PDI (data not shown).

The amino acid sequence of *Dictyostelium* Vmp1 showed a conserved KKXX-like ER-membrane retention signal at the C terminus as detected by the PSORT program (Nakai and Horton, 1999), resulting in a K-NN prediction 66,7% for ER, which is confirmed by our results. In this connection, an ER localization for Vmp1 has also been described in *Drosophila* (Bard *et al*., 2006) and also in a proteomic study in *Arabidopsis* (Dunkley *et al*., 2006).

Regarding cell localization, the scenario in mammalian cells seems to be more complex. Vmp-1 has been reported to be localized in different subcellular compartments and these results suggest that it may play different roles. The first report by Dusetti *et al*., 2002 localized Vmp1 as a fused protein with GFP in vacuoles, the area of the ER, and the Golgi apparatus. Unfortunately, colocalization analysis with cell markers was not performed in this study to determine the precise localization. The expression of this Vmp1-GFP–fused protein induced vacuolization and death in Cos7 cells (Dusetti *et al*., 2002). Interestingly, our results have shown that a mammalian Vmp1 expressed in *Dictyostelium* also has an ER localization. Remarkably, this construct also complemented the mutant phenotype, suggesting correct subcellular targeting and functional conservation of the protein.

A second report by the same group several years later further defined the vacuolization induced by Vmp1 expression as autophagy in mammalian cells (HeLa293T and NIH3T3) (Ropolo *et al*., 2007). Autophagy is a degradation process of cytoplasmic cellular components that is essential as a survival mechanism during starvation (Klionsky and Emr, 2000). Vmp1 colocalized with LC3, a marker of the autophagosomes and induces autophagosome formation in pancreas acinar cells in transgenic mice (Ropolo *et al*., 2007). The endogenous expression of Vmp1 in HeLa cells was very low and only detectable under conditions inducing autophagome formation such as starvation. In this case, Vmp1 is detected in punctuate structures by immunofluorescence consistent with the autophagosome vesicle formation. It is possible as stated by the authors that a low nondetected basal Vmp1 expression could be related with other physiological processes (Ropolo *et al*., 2007).

Interestingly, a recent report showed that Vmp1 was located in the plasma membrane playing a role in cell–cell contact (Sauermann *et al*., 2008). We have never found *Dictyostelium* Vmp1 in the plasma membrane at the vegetative stage. We also checked the localization pattern during development (finger stage) to determine whether some localization was found in cell–cell contacts. However, the protein remained exclusively at the ER (data not shown).

Together, these results suggest that Vmp1 might be located in the ER in lower organisms, including the social amoebae, insects, and plants, in which it could play a basic role in membrane traffic as we have shown in *Dictyostelium*. In mammalian cells, Vmp-1 may play more diverse roles in different organelles including autophagosome vesicles and the plasma membrane. Whether Vmp1 has a specific role in the ER of mammalian cells as suggested by our results in *Dictyostelium* remains to be investigated.

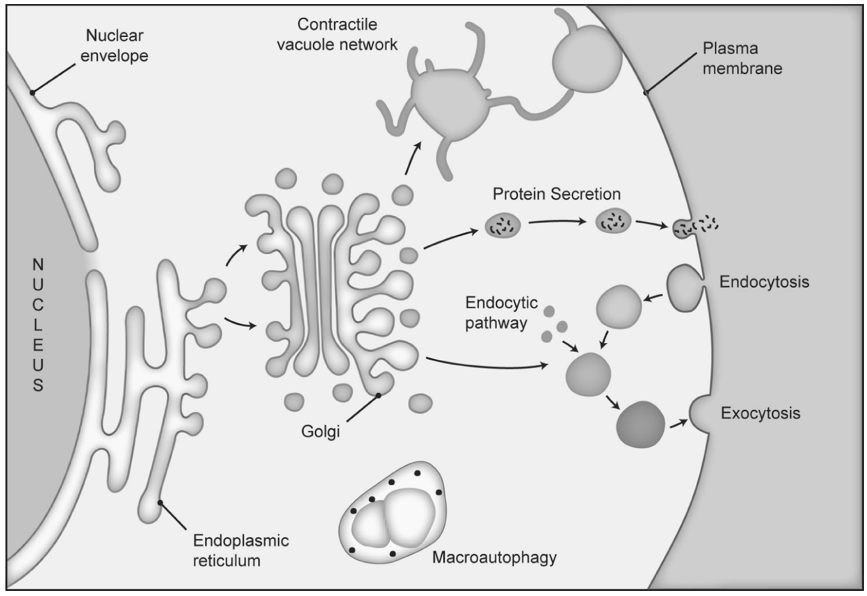

Figure 9. Summary of Vmp1-dependent processes. The amino acid sequence of the encoded protein contains several putative transmembrane domains suggesting that Vmp1 is an integral membrane protein located in the ER. Despite its localization, the loss of this gene in *Dictyostelium* leads to defects in several membrane traffic-dependent processes, including the biogenesis of the CV, the structure of the Golgi apparatus, and the pattern of macroautophagy vacuoles. In contrast, the endocytic pathway, which in *Dictyostelium* is essential for nutrition, is also affected. Endocytosis and exocytosis is severely impaired in the mutant. Protein secretion during growth and probably also during starvation is also defective.

Vmp1 Is Required for Osmoregulation, an Essential Process in Soil Microorganisms

The survival in hypoosmotic conditions is essential for single-celled organisms. These organisms, including *Dictyostelium*, have developed a complex network of vesicles and tubules known as the CV. If CV function is compromised as a result of a general defect in membrane trafficking, the expected phenotype would be dramatic. The cells would not be able to cope with water influx and may burst as a consequence of cell swelling. This is precisely what occurs in the absence of Vmp1 in *Dictyostelium*. A similar phenotype have been reported for a *Dictyostelium* mutant in the AP-1 clathrin-adaptor (Lefkir *et al*., 2003). AP-1 complex participates in vesicle transport from the *trans*-Golgi network to endocytic compartments. This mutant showed a severe growth defect and delayed development and most importantly the biogenesis of the contractile vacuole was compromised. This is another example of a defect in organelle biogenesis as a consequence of defective membrane traffic.

Our results suggest that Vmp1 mutant cells contain very few contractile vacuoles as determine by transmission electron microscopy (TEM) and the use of CV markers. These markers (mainly Rh50) showed a weak staining, labeling few vacuoles in the mutant. This staining did not colocalize with ER or endosomes (data not shown). The reduced levels of these proteins might suggest that the components of the CV system are being degraded or synthesized in lower amounts because they do not seem to be accumulated in other organelles of the secretory pathway.

Mammalian cells lack the contractile vacuole system as they live in an osmotically controlled environment. Therefore, no such behavior is expected to occur by the loss of mammalian Vmp1.

A Possible Role of Vmp1 in Macroautophagy

It has been described that inhibition of Vmp1 expression by small interfering RNA blocks autophagosome formation in mammalian cells (Ropolo *et al*., 2007). Our results in *vmp1*$^-$ mutant in *Dictyostelium* might also support a role in autophagy. TEM images of mutant cells showed the accumulation of autophagic features similar to those described in macroautophagy mutants (Otto *et al*., 2003, 2004). Macroautophagy is induced by starvation and therefore it is probably activated in *vmp1*$^-$ mutant cells in axenic culture as a result of the observed defects in nutrient uptake. Thus, we cannot rule out the possibility that the observed accumulation of vacuoles with unprocessed cellular material might be due to an overactivation of autophagy in the mutant. Other possible explanation is a defect in autophagosome maturation. Such maturation involves dynamic membrane rearrangements and the fusion with lysosomal vesicles that makes the process dependent on the secretory pathway (Mizushima *et al*., 2002). Moreover, the ER itself might, in some cases, be the membrane source for autophagosome formation (Bernales *et al*., 2007; Yorimitsu and Klionsky, 2007). Nevertheless, *Dictyostelium* macroautophagy mutants do not show growth defects or osmotic sensitivity (Otto *et al*., 2003, 2004), suggesting that macroautophagy dysfunction does not account for the overall phenotype of *vmp1*$^-$ mutant. The precise role of Vmp1 in *Dictyostelium* macroautophagy will require further investigation.

Protein Secretion during Growth and Development Depends on Vmp1

We have shown that protein secretion during growth and development is affected by the loss of Vmp1. AprA is an autocrine proliferation repressor in *Dictyostelium*; therefore, a lower level of secretion of this specific factor would induce growth as described previously (Brock and Gomer, 2005). The *vmp1*$^-$ mutant, however, showed a severe growth defect in axenic media. This implies that AprA is not the only factor that is likely to be affected by a general dysfunction in protein secretion. Other unidentified growth-inducing factors may be absent and/or other additional defects may account for the lack of growth in shaking culture.

It is well known that secretion of autocrine factors is necessary for the transition from growth to development in *Dictyostelium* and that this transition is dependent on the onset of a specific gene expression program. We have shown that the expression of representative genes of this program is severely affected and the pattern of protein secretion is also different between wild type and the mutant. If the observed block in development is merely a consequence of the absence of these autocrine factors, we would expect a noncell

autonomous behavior in mixing experiments. However, when mutant cells were mixed with wild-type, mutant cells remained excluded from the aggregates when development was initiated (data not shown). This additional cell-autonomous defect is not surprising if taking into account the severity of the phenotype, which is not only restricted to protein secretion.

The pattern of proteins present in conditioned medium from wild type and the mutant Vmp1 is significantly different. This could be due to differences in protein secretion as well as differences in the expression levels of certain genes because the mutant response to starvation is impaired. Despite our efforts we have been able to identify only few of the differential protein bands. The secreted proteins enriched in the wild-type medium are representative of ER/Golgi-dependent secretory pathway. However, others such as Hsp70 are secreted by nonconventional secretion mechanisms (Nickel, 2005). In this case, Hsp70 was described to be internalized into endolysosmal vesicles by the activity of an ATP-binding cassette transporter, and these vesicles secrete their content by fusing with the plasma membrane (Mambula *et al*., 2007). The high levels of Hsp70 in the mutant supernatant might be related to the activation of stress mechanisms. However, RT-PCR analysis of the hsp70 mRNA levels did not show an induction of the expression of the gene in the mutant (data not shown).

In conclusion, the analysis of Vmp1 null-mutant in *Dictyostelium* has brought us a more comprehensive view of the intricate roles played by this new gene. Our results confirm some data obtained in other experimental systems with regard to the role of Vmp-1 in membrane traffic and protein secretion, but also reveal new functions of Vmp-1, including an essential role in organelle biogenesis and multicellular development.

ACKNOWLEDGMENTS

This work was supported by grants BMC2006-00394 from the Spanish Ministerio de Educación y Ciencia (to R. E.), CCG07-CSIC/SAL-1959 from Comunidad de Madrid/Consejo Superior de Investigaciones Cientificas (to R. E.), and BFU2006-00867/BMC (to G. E.). Sequence data for *Dictyostelium* were obtained from the genome sequencing centers of the University of Cologne (Cologne, Germany); Department of Genome Analysis, Institute of Molecular Biotechnology (Jena, Germany); Baylor Collage of Medicine (Houston, TX); and Sanger Center (Hinxton, Cambridge, United Kingdom). We thank Pauline Shaap for the GFP plasmid and Pierre Cosson, Markus Maniak, and Richard Gomer for providing the antibodies used in this study and for help with the protocols. Thanks to Gunther Gerisch for the strains Dajumin-GFP and Golvesin-C-GFP. Thanks to the Dicty Stock Center (Columbia University in New York City, NY) for providing some of the strains used in the study. We thank R. M. Calvo for help in the cloning of rat Vmp1 and critical reading of the manuscript and Javier Pérez for the artwork. MALDI-MS/MS was performed by the Centro Nacional de Investigaciones Cardiovasculares proteomic service. We also thank the Servicio Interdepartamental de Investigacion-Confocal facility for assistance and Serveis Cientificotècnics-Universitat de Barcelona for help with electron microscopy. We thank Dr. Nancy Wang for revising and correcting the English version of our manuscript. J. C. was recipient of a fellowship from the Spanish Ministerio de Educación y Ciencia.

REFERENCES

Abe, T., Langenick, J., and Williams, J. G. (2003). Rapid generation of gene disruption constructs by in vitro transposition and identification of a Dictyostelium protein kinase that regulates its rate of growth and development. Nucleic Acids Res. *31*, E107.

Ausubel, F. M., Brent, R., Kingston, R. E., Moore, D. D., Seidman, J. G., Smith, J. A., and Struhl, K. (1992). Current Protocols in Molecular Biology. Wiley, New York.

Bard, F. *et al*. (2006). Functional genomics reveals genes involved in protein secretion and Golgi organization. Nature *439*, 604–607.

Benghezal, M., Gotthardt, D., Cornillon, S., and Cosson, P. (2001). Localization of the Rh50-like protein to the contractile vacuole in *Dictyostelium*. Immunogenetics *52*, 284–288.

Bernales, S., Schuck, S., and Walter, P. (2007). ER-phagy: selective autophagy of the endoplasmic reticulum. Autophagy *3*, 285–287.

Brock, D. A., and Gomer, R. H. (2005). A secreted factor represses cell proliferation in *Dictyostelium*. Development *132*, 4553–4562.

Charette, S. J., Cornillon, S., and Cosson, P. (2006). Identification of low frequency knockout mutants in *Dictyostelium discoideum* created by single or double homologous recombination. J. Biotechnol. *122*, 1–4.

Clarke, M., and Gomer, R. H. (1995). PSF and CMF, autocrine factors that regulate gene expression during growth and early development of *Dictyostelium*. Experientia *51*, 1124–1134.

Clarke, M., Kohler, J., Arana, Q., Liu, T. Y., Heuser, J., and Gerisch, G. (2002). Dynamics of the vacuolar H+-ATPase in the contractile vacuole complex and the endosomal pathway of *Dictyostelium* cells. J. Cell Sci. *115*, 2893–2905.

Derby, M. C., and Gleeson, P. A. (2007). New insights into membrane trafficking and protein sorting. Int. Rev. Cytol. *261*, 47–116.

Dhaunsi, G. S. (2005). Molecular mechanisms of organelle biogenesis and related metabolic diseases. Med. Princ. Pract. (14 suppl) *1*, 49–57.

Dunkley, T. P. *et al*. (2006). Mapping the *Arabidopsis* organelle proteome. Proc. Natl. Acad. Sci. USA *103*, 6518–6523.

Dusetti, N. J. *et al*. (2002). Cloning and expression of the rat vacuole membrane protein 1 (VMP1), a new gene activated in pancreas with acute pancreatitis, which promotes vacuole formation. Biochem. Biophys. Res. Commun. *290*, 641–649.

Escalante, R., and Vicente, J. J. (2000). *Dictyostelium discoideum*: a model system for differentiation and patterning. Int. J. Dev. Biol. *44*, 819–835.

Gabriel, D., Hacker, U., Kohler, J., Muller-Taubenberger, A., Schwartz, J. M., Westphal, M., and Gerisch, G. (1999). The contractile vacuole network of *Dictyostelium* as a distinct organelle: its dynamics visualized by a GFP marker protein. J. Cell Sci. *112*, 3995–4005.

Hacker, U., Albrecht, R., and Maniak, M. (1997). Fluid-phase uptake by macropinocytosis in *Dictyostelium*. J. Cell Sci. *110*, 105–112.

Howell, G. J., Holloway, Z. G., Cobbold, C., Monaco, A. P., and Ponnambalam, S. (2006). Cell biology of membrane trafficking in human disease. Int. Rev. Cytol. *252*, 1–69.

Kessin, R. H. (2001). Dictyostelium–Evolution, Cell Biology, and the Development of Multicellularity. Cambridge University Press, Cambridge, United Kingdom.

Klionsky, D. J., and Emr, S. D. (2000). Autophagy as a regulated pathway of cellular degradation. Science *290*, 1717–1721.

Kuwayama, H., Ecke, M., Gerisch, G., and van Haastert, P.J.M. (1996). Protection against osmotic stress by cGMP-mediated myosin phosphorylation. Science *271*, 207–209.

Kyttala, A., Lahtinen, U., Braulke, T., and Hofmann, S. L. (2006). Functional biology of the neuronal ceroid lipofuscinoses (NCL) proteins. Biochim. Biophys. Acta *1762*, 920–933.

Lang, M. R., Lapierre, L. A., Frotscher, M., Goldenring, J. R., and Knapik, E. W. (2006). Secretory COPII coat component Sec23a is essential for craniofacial chondrocyte maturation. Nat. Genet. *38*, 1198–1203.

Lefkir, Y., de Chassey, B., Dubois, A., Bogdanovic, A., Brady, R. J., Destaing, O., Bruckert, F., O'Halloran, T. J., Cosson, P., and Letourneur, F. (2003). The AP-1 clathrin-adaptor is required for lysosomal enzymes sorting and biogenesis of the contractile vacuole complex in *Dictyostelium* cells. Mol. Biol. Cell *14*, 1835–1851.

Mambula, S. S., Stevenson, M. A., Ogawa, K., and Calderwood, S. K. (2007). Mechanisms for Hsp70 secretion: crossing membranes without a leader. Methods *43*, 168–175.

Maniak, M. (2003). Fusion and fission events in the endocytic pathway of *Dictyostelium*. Traffic *4*, 1–5.

Mizushima, N., Ohsumi, Y., and Yoshimori, T. (2002). Autophagosome formation in mammalian cells. Cell Struct. Funct. *27*, 421–429.

Moniakis, J., Coukell, M. B., and Forer, A. (1995). Molecular cloning of an intracellular P-type ATPase from *Dictyostelium* that is up-regulated in calcium-adapted cells. J. Biol. Chem. *270*, 28276–28281.

Monnat, J., Hacker, U., Geissler, H., Rauchenberger, R., Neuhaus, E. M., Maniak, M., and Soldati, T. (1997). *Dictyostelium discoideum* protein disulfide isomerase, an endoplasmic reticulum resident enzyme lacking a KDEL-type retrieval signal. FEBS Lett. *418*, 357–362.

Multhoff, G. (2007). Heat shock protein 70 (Hsp70): membrane location, export and immunological relevance. Methods *43*, 229–237.

Nakai, K., and Horton, P. (1999). PSORT: a program for detecting sorting signals in proteins and predicting their subcellular localization. Trends Biochem. Sci. *24*, 34–36.

Nickel, W. (2005). Unconventional secretory routes: direct protein export across the plasma membrane of mammalian cells. Traffic *6*, 607–614.

O'Halloran, T. J., and Anderson, R. G. (1992). Clathrin heavy chain is required for pinocytosis, the presence of large vacuoles, and development in *Dictyostelium*. J. Cell Biol. *118*, 1371–1377.

Otto, G. P., Wu, M. Y., Kazgan, N., Anderson, O. R., and Kessin, R. H. (2003). Macroautophagy is required for multicellular development of the social amoeba *Dictyostelium discoideum*. J. Biol. Chem. *278*, 17636–17645.

Otto, G. P., Wu, M. Y., Kazgan, N., Anderson, O. R., and Kessin, R. H. (2004). *Dictyostelium* macroautophagy mutants vary in the severity of their developmental defects. J. Biol. Chem. *279*, 15621–15629.

Pang, K. M., Lynes, M. A., and Knecht, D. A. (1999). Variables controlling the expression level of exogenous genes in *Dictyostelium*. Plasmid *41*, 187–197.

Pannel, R., Wood, L., and Kaplan, A. (1982). Processing and secretion of alpha-mannosidase forms by *Dictyostelium discoideum*. J. Biol. Chem. *257*, 9861–9865.

Perkins, D. N., Pappin, D. J., Creasy, D. M., and Cottrell, J. S. (1999). Probability-based protein identification by searching sequence databases using mass spectrometry data. Electrophoresis *20*, 3551–3567.

Rivero, F., and Maniak, M. (2006). Quantitative and microscopic methods for studying the endocytic pathway. In: Methods in Molecular Biology, Vol. 346, The Humana Press, Inc., Clifton, NJ, 423–438.

Ropolo, A. *et al*. (2007). The pancreatitis-induced vacuole membrane protein 1 triggers autophagy in mammalian cells. J. Biol. Chem. *282*, 37124–37133.

Ryter, A., and de Chastellier, C. (1977). Morphometric and cytochemical studies of *Dictyostelium discoideum* in vegetative phase. Digestive system and membrane turnover. J. Cell Biol. *75*, 200–217.

Sauermann, M. *et al*. (2008). Reduced expression of vacuole membrane protein 1 affects the invasion capacity of tumor cells. Oncogene *27*, 1320–1326.

Schneider, N., Schwartz, J. M., Kohler, J., Becker, M., Schwarz, H., and Gerisch, G. (2000). Golvesin-GFP fusions as distinct markers for Golgi and post-Golgi vesicles in *Dictyostelium* cells. Biol. Cell *92*, 495–511.

Shaulsky, G., and Loomis, W. F. (1993). Cell type regulation in response to expression of ricin-A in *Dictyostelium*. Dev. Biol. *160*, 85–98.

Shevchenko, A., Tomas, H., Havlis, J., Olsen, J. V., and Mann, M. (2006). In-gel digestion for mass spectrometric characterization of proteins and proteomes. Nat. Protoc. *1*, 2856–2860.

Suckau, D., Resemann, A., Schuerenberg, M., Hufnagel, P., Franzen, J., and Holle, A. (2003). A novel MALDI LIFT-TOF/TOF mass spectrometer for proteomics. Anal. Bioanal. Chem. *376*, 952–965.

Sussman, M. (1987). Cultivation and synchronous morphogenesis of *Dictyostelium* under controlled experimental conditions. Methods Cell Biol. *28*, 9–29.

Torija, P., Robles, A., and Escalante, R. (2006a). Optimization of a large-scale gene disruption protocol in *Dictyostelium* and analysis of conserved genes of unknown function. BMC Microbiol. *6*, 75.

Torija, P., Vicente, J. J., Rodrigues, T. B., Robles, A., Cerdan, S., Sastre, L., Calvo, R. M., and Escalante, R. (2006b). Functional genomics in *Dictyostelium*: MidA, a new conserved protein, is required for mitochondrial function and development. J. Cell Sci. *119*, 1154–1164.

Vaccaro, M. I., Grasso, D., Ropolo, A., Iovanna, J. L., and Cerquetti, M. C. (2003). VMP1 expression correlates with acinar cell cytoplasmic vacuolization in arginine-induced acute pancreatitis. Pancreatology *3*, 69–74.

Wood, L., and Kaplan, A. (1985). Transit of alpha-mannosidase during its maturation in *Dictyostelium discoideum*. J. Cell Biol. *101*, 2063–2069.

Yorimitsu, T., and Klionsky, D. J. (2007). Eating the endoplasmic reticulum: quality control by autophagy. Trends Cell Biol. *17*, 279–285.

[Autophagy 4:6, 835-837; 16 August 2008]; ©2008 Landes Bioscience

Article Addendum

Vacuole membrane protein 1, autophagy and much more

Javier Calvo-Garrido, Sergio Carilla-Latorre and Ricardo Escalante*

Instituto de Investigaciones Biomédicas Alberto Sols; Consejo Superior de Investigaciones Científicas—Universidad Autónoma de Madrid; Madrid, Spain

Key words: vacuole membrane protein 1, organelle biogenesis, autophagy, protein secretion, osmoregulation, *Dictyostelium*, endoplasmic reticulum

Vacuole membrane protein 1 (Vmp1) is a putative transmembrane protein that has been associated with different functions including autophagy, cell adhesion, and membrane traffic. Highly similar proteins are present in lower eukaryotes and plants although a homologue is absent in the fungi lineage. We have recently described the first loss-of-function mutation for a Vmp1 homologue in a model system, *Dictyostelium discoideum*. Our results give a more comprehensive view of the intricate roles played by this new gene. *Dictyostelium* Vmp1 is an endoplasmic reticulum-resident protein. Cells deficient in Vmp1 display pleiotropic defects in the context of the secretory pathway such as organelle biogenesis, the endocytic pathway, and protein secretion. The biogenesis of the contractile vacuole, an organelle necessary to survive under hypoosmotic conditions, is compromised as well as the structure of the endoplasmic reticulum and the Golgi apparatus. Transmission electron microscopy also shows abnormal accumulation of aberrant double-membrane vesicles, suggesting a defect in autophagosome biogenesis or maturation. The expression of a mammalian Vmp1 in the *Dictyostelium* mutant complements the phenotype suggesting a functional conservation during evolution. We are taking the first steps in understanding the function of this fascinating protein and recent studies have brought us more questions than answers about its basic function and its role in human pathology.

Vmp1, a Membrane Protein of Unknown Function

Vacuole membrane protein 1 (Vmp1) was first described as a gene highly expressed in the pancreas during acute pancreatitis.[1,2] Overexpression of this protein in cell culture induces intracellular vacuolization and cell death.[1,3] These vacuoles were later characterized as autophagosomes, implicating Vmp1 as a novel autophagy protein.[4,5] In a functional genomic RNA-interference screening in Drosophila, Vmp1 (known as TANGO-5) is identified as a protein required for conventional protein secretion and Golgi organization.[6] Another surprise comes from a study in kidney cancer cells where Vmp1 is localized in the plasma membrane and required in adhesion.[7] The study of the function of this new gene is complicated by the fact that no conserved functional motifs are present in its encoded sequence and no homologous genes exist in the fungal models, where most of the autophagy proteins have been studied. The amino acid sequence only indicates the presence of several putative transmembrane regions and an endoplasmic reticulum (ER) retention signal.

Dictyostelium discoideum is a eukaryotic microorganism used as a model system for several cell biology processes including autophagy and non-apoptotic cell death.[8-12] Functional genomics in yeast has proven very valuable to understand the basic function of new genes that later were found to be involved in human diseases. However, there are many genes present in the human genome that are absent in the yeast models. Fortunately, the *Dictyostelium* genome contains many of those genes, being the simplest model system that can be used to address their function.[13,14] Some of these genes do not allow a prediction of their function due to the lack of characterized functional motifs. Vmp1, as explained above, complies with all these characteristics and was selected from a collection of mutants generated in *Dictyostelium* by our group.[13,15] This is the first loss-of-function mutation of Vmp1 analyzed in a model system and our studies reveal unexpected functions for this new protein beyond autophagy.

Subcellular Localization of Vmp1 and its Functional Conservation

The coding sequence of *Dictyostelium* vmp1 (DDB0234044) is highly similar to other homologous genes in other species. Interestingly, it is absent in the fungi lineage but it is present in other protists, plants, and metazoa, suggesting that this gene was lost during fungi evolution (Fig.1). Remarkably, *Dictyostelium* Vmp1 is even more closely related to metazoan genes than to those of other simpler eukaryotes or plants. In order to ascertain the functional conservation of this family, we expressed a mammalian Vmp1 protein in the *Dictyostelium* mutant. The expressed protein is able to complement the phenotype of the mutant and localizes in the same cellular compartment as the *Dictyostelium* protein, suggesting a functional conservation during evolution. Both proteins localize in the endoplasmic reticulum (ER) and no colocalization is observed with endosomal or contractile vacuole markers. There is some evidence of similar localization in plants and Drosophila.[6,16] However, Vmp1

*Correspondence to: Ricardo Escalante; Instituto de Investigaciones Biomédicas Alberto Sols; Consejo Superior de Investigaciones Científicas—Universidad Autónoma de Madrid; Calle Arturo Duperier 4; Madrid 28029 Spain; Tel.: +34.91.585.4494; Fax: +34.91.585.4401; Email: rescalante@iib.uam.es

Submitted: 07/08/08; Revised: 07/09/08; Accepted: 07/09/08

Previously published online as an *Autophagy* E-publication: www.landesbioscience.com/journals/autophagy/article/6574

Addendum to: Calvo-Garrido J, Carilla-Latorre S, Lázaro-Diéguez F, Egea G, Escalante R. Vacuole membrane protein 1 is an endoplasmic reticulum protein required for organelle biogenesis, protein secretion and development. Mol Biol Cell 2008; Epub ahead of print, June 11, 2008.

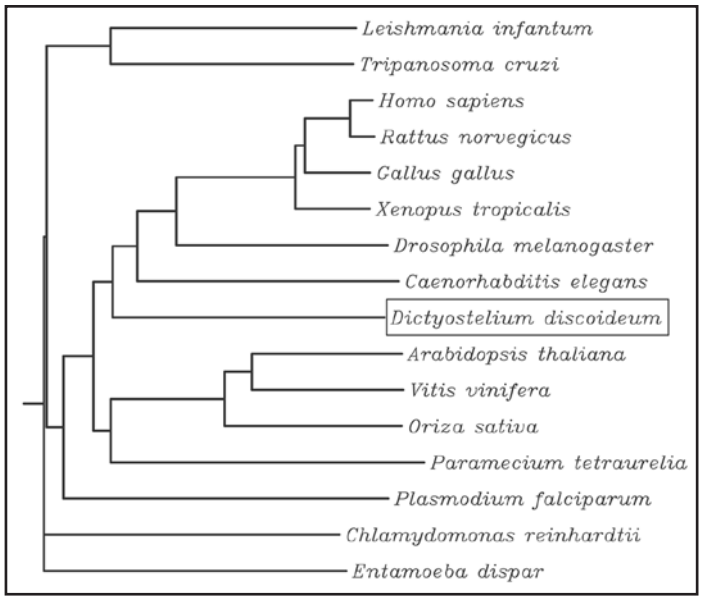

Figure 1. Phylogenetic relationships among Vmp1 proteins from different species. The phylogenetic tree was constructed using Dawgram, a PHILIP rooted phylogenetic tree available at Biology WorkBench (http://workbench.sdsc.edu). The sequences used were: *Dictyostelium discoideum*, XP_638348; *Xenopus tropicalis*, NP_001007877; *Gallus gallus*, XP_415880; *Rattus norvegicus*, NP_620194; *Homo sapiens*, NP_112200; *Caenorhabditis elegans*, NP_499688; *Drosophila melanogaster*, NP_727444; *Vitis vinifera*, CAO71145; *Paramecium tetraurelia*, XP_001432377; *Oryza sativa*, NP_001044428; *Arabidopsis thaliana*, AAM60984; *Entamoeba dispar*, XP_001735614; *Chlamydomonas reinhardtii*, XP_001696213; *Trypanosoma cruzi*, XP_815596; *Plasmodium falciparum*, XP_001348888; *Leishmania infantum*, XP_001470108. The highly divergent *Entamoeba* sequence was used as an outgroup.

Table 1 **Summary of Vmp1-dependent phenotypes in Dictyostelium**

Biological process	Defect and phenotype
Osmoregulation	Contractile Vacuole biogenesis Cell lysis in hypoosmotic conditions
Protein secretion	AprA secretion during growth
Organelle organization	Fragmentation of the ER Fragmentation of the Golgi apparatus
Autophagy	Aberrant autophagosome formation
Endocytic pathway	Impaired macropinocytosis (lack of axenic growth) Impaired exocytosis
Multicellular development	Lack of aggregation Impaired developmental gene expression

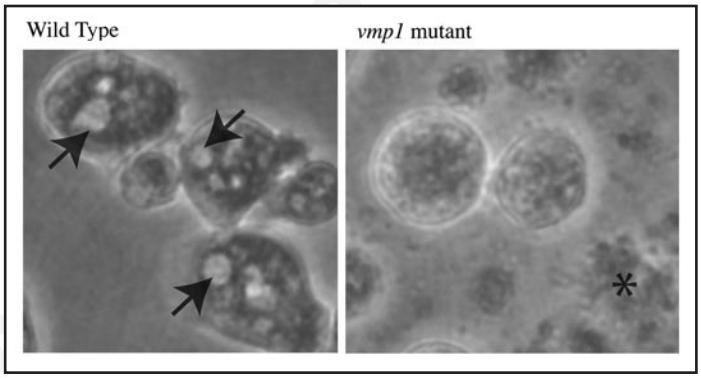

Figure 2. Cell lysis in vmp1 mutant. After a short exposure to water, wild type cells maintain their viability by expelling water through the CV (arrows). Mutant cells, in contrast, were round and showed no sign of CV activity. A large proportion of them lysed rapidly (asterisk) without a large increase in cell volume, suggesting the possibility of additional defects in the stability of the plasma membrane.

localization in mammalian cells is controversial and the protein has been described to be located in autophagosomes[5] and the plasma membrane.[7] We have never observed *Dictyostelium* Vmp1 in the plasma membrane but a possible localization in autophagosomes needs to be determined.

Vmp1 Disruption in *Dictyostelium*, Autophagy and Much More

Disruption of Vmp1 in *Dictyostelium* leads to a severe phenotype that compromises many aspects of this organism's life cycle as described in detail in our recent work.[15] A summary of the defects and phenotypes are displayed in Table 1. The most dramatic consequence is the inability of the mutant cells to cope with hypoosmotic stress. The membrane lysis observed in the mutant cells under hypoosmotic conditions occurs very rapidly. However, cell swelling is not as noticeable as expected (Fig. 2), suggesting an additional defect in membrane stability. *Dictyostelium* is a soil microorganism that has developed a tubulo-vesicular network of membranes known as the contractile vacuole (CV) that fills up and expels water to the exterior of the cell. Our analysis by transmission electron microscopy and specific CV markers shows a defect in the biogenesis of this organelle.

It is well known that organelle biogenesis, including that of the CV system, is dependent on the secretory pathway. Membrane and protein components traffic from the endoplasmic reticulum and Golgi apparatus to their destinations in the different organelles and the plasma membrane.[17-19] Since Vmp1 is an ER-resident protein, it might function at the initial steps of the secretory pathway and consequently might have pleiotropic effects in other organelles. The rest of the phenotypes observed by the lack of Vmp1 might perfectly fit in the context of a secretory pathway defect including the apparent instability of the plasma membrane as described previously in other reports.[20,21]

The autophagy defect in the *Dictyostelium* vmp1 mutant can also be seen in this context. We observe the accumulation of aberrant double-membrane structures in the mutant that is consistent with abnormal autophagic vesicles. The origin and the assembly of the autophagosome is not completely understood and it is conceivable that the ER, as suggested by our results, might be required for the correct assembly or maturation of the phagosome, perhaps by supplying membrane components. Interestingly, a more direct effect in autophagosome formation has been described in mammalian cell culture. In this case Vmp1 is localized in autophagosomes where it interacts with Beclin 1, an essential autophagy protein.[5] Whether or not *Dictyostelium* Vmp1 behaves in the same way remains to be determined.

Concluding Remarks and Future Perspective

The study of the basic function of new proteins with no characterized motifs is difficult and we must take advantage of any available experimental tool. *Dictyostelium* have taught us a few new important things to be considered about Vmp1 and the consequences of its loss-of-function. We have learned that Vmp1 can play an essential role from the ER, having an impact upon many different membrane traffic-dependent processes. However, many questions remain, such as what affects mammalian Vmp1 sub-cellular localization. Is Vmp1 located in the phagosome or plasma membrane depending on the cell type studied and/or the cellular context? Is Vmp1 located in the ER in any cell type or situation in a similar way as seen in lower eukaryotes such as *Dictyostelium*? What is the relationship between Vmp1 localization and function? Our first glimpse into the function of this important conserved protein is intriguing and now the possibility to address its molecular function and its relevance in human disease is within reach.

Acknowledgements

This work was supported by grants BMC2006-00394 from the Spanish Ministerio de Educación y Ciencia and CCG07-CSIC/SAL-1959 from Comunidad de Madrid/CSIC. Thanks to our collaborators Gustavo Egea and Francisco Lázaro-Diéguez. We also want to thank R.M. Calvo for critical reading of the manuscript.

References

1. Dusetti NJ, Jiang Y, Vaccaro MI, Tomasini R, Azizi Samir A, Calvo EL, Ropolo A, Fiedler F, Mallo GV, Dagorn JC, Iovanna JL. Cloning and expression of the rat vacuole membrane protein 1 (VMP1), a new gene activated in pancreas with acute pancreatitis, which promotes vacuole formation. Biochem Biophys Res Commun 2002; 290:641-9.
2. Vaccaro MI, Grasso D, Ropolo A, Iovanna JL, Cerquetti MC. VMP1 expression correlates with acinar cell cytoplasmic vacuolization in arginine-induced acute pancreatitis. Pancreatology 2003; 3:69-74.
3. Jiang PH, Motoo Y, Vaccaro MI, Iovanna JL, Okada G, Sawabu N. Expression of vacuole membrane protein 1 (VMP1) in spontaneous chronic pancreatitis in the WBN/Kob rat. Pancreas 2004; 29:225-30.
4. Vaccaro MI, Ropolo A, Grasso D, Iovanna JL. A novel mammalian trans-membrane protein reveals an alternative initiation pathway for autophagy. Autophagy 2008; 4:388-90.
5. Ropolo A, Grasso D, Pardo R, Sacchetti ML, Archange C, Lo Re A, Seux M, Nowak J, Gonzalez CD, Iovanna JL, Vaccaro MI. The pancreatitis-induced vacuole membrane protein 1 triggers autophagy in mammalian cells. J Biol Chem 2007; 282:37124-33.
6. Bard F, Casano L, Mallabiabarrena A, Wallace E, Saito K, Kitayama H, Guizzunti G, Hu Y, Wendler F, Dasgupta R, Perrimon N, Malhotra V. Functional genomics reveals genes involved in protein secretion and Golgi organization. Nature 2006; 439:604-7.
7. Sauermann M, Sahin O, Sultmann H, Hahne F, Blaszkiewicz S, Majety M, Zatloukal K, Fuzesi L, Poustka A, Wiemann S, Arlt D. Reduced expression of vacuole membrane protein 1 affects the invasion capacity of tumor cells. Oncogene 2008; 27:1320-6.
8. Tekinay T, Wu MY, Otto GP, Anderson OR, Kessin RH. Function of the Dictyostelium discoideum Atg1 kinase during autophagy and development. Eukaryot Cell 2006; 5:1797-806.
9. Otto GP, Wu MY, Kazgan N, Anderson OR, Kessin RH. Dictyostelium macroautophagy mutants vary in the severity of their developmental defects. J Biol Chem 2004; 279:15621-9.
10. Otto GP, Wu MY, Kazgan N, Anderson OR, Kessin RH. Macroautophagy is required for multicellular development of the social amoeba Dictyostelium discoideum. J Biol Chem 2003; 278:17636-45.
11. Golstein P, Kroemer G. Cell death by necrosis: towards a molecular definition. Trends Biochem Sci 2007; 32:37-43.
12. Tresse E, Kosta A, Luciani MF, Golstein P. From autophagic to necrotic cell death in Dictyostelium. Semin Cancer Biol 2007; 17:94-100.
13. Torija P, Vicente JJ, Rodrigues TB, Robles A, Cerdan S, Sastre L, Calvo RM, Escalante R. Functional genomics in Dictyostelium: MidA, a new conserved protein, is required for mitochondrial function and development. J Cell Sci 2006; 119:1154-64.
14. Torija P, Robles A, Escalante R. Optimization of a large-scale gene disruption protocol in Dictyostelium and analysis of conserved genes of unknown function. BMC Microbiol 2006; 6:75.
15. Calvo-Garrido J, Carilla-Latorre S, Lázaro-Diéguez F, Egea G, Escalante R. Vacuole membrane protein 1 is an endoplasmic reticulum protein required for organelle biogenesis, protein secretion and development. Mol Biol Cell 2008; Epub ahead of print, June 11, 2008.
16. Dunkley TP, Hester S, Shadforth IP, Runions J, Weimar T, Hanton SL, Griffin JL, Bessant C, Brandizzi F, Hawes C, Watson RB, Dupree P, Lilley KS. Mapping the Arabidopsis organelle proteome. Proc Natl Acad Sci U S A 2006; 103:6518-23.
17. Dhaunsi GS. Molecular mechanisms of organelle biogenesis and related metabolic diseases. Med Princ Pract 2005; 14 Suppl 1:49-57.
18. Howell GJ, Holloway ZG, Cobbold C, Monaco AP, Ponnambalam S. Cell biology of membrane trafficking in human disease. Int Rev Cytol 2006; 252:1-69.
19. Derby MC, Gleeson PA. New insights into membrane trafficking and protein sorting. Int Rev Cytol 2007; 261:47-116.
20. Lang MR, Lapierre LA, Frotscher M, Goldenring JR, Knapik EW. Secretory COPII coat component Sec23a is essential for craniofacial chondrocyte maturation. Nature Genet 2006; 38:1198-203.
21. Kyttala A, Lahtinen U, Braulke T, Hofmann SL. Functional biology of the neuronal ceroid lipofuscinoses (NCL) proteins. Biochim Biophys Acta 2006; 1762:920-33.

Autophagy 6:6, 686-701; August 16, 2010; © 2010 Landes Bioscience

Autophagy in Dictyostelium
Genes and pathways, cell death and infection

Javier Calvo-Garrido,[1] Sergio Carilla-Latorre,[1] Yuzuru Kubohara,[2] Natalia Santos-Rodrigo,[1] Ana Mesquita,[1] Thierry Soldati,[3] Pierre Golstein[4-6] and Ricardo Escalante[1,*]

[1]Instituto de Investigaciones Biomédicas "Alberto Sols" (CSIC-UAM); Arturo Duperier 4; Madrid, Spain; [2]Institute for Molecular & Cellular Regulation; Gunma University; Maebashi, Japan; [3]Départment de Biochimie; Faculté des Sciences; Université de Genève; Sciences II; Genève-4, Switzerland; [4]Centre d'Immunologie de Marseille-Luminy (CIML); Aix-Marseille Université; [5]INSERM; [6]CNRS; Faculté des Sciences de Luminy; Marseille, France

Key words: Dictyostelium, social amoeba, autophagy, autophagic cell death, autophagy and infection, Vmp1, Atg proteins

The use of simple organisms to understand the molecular and cellular function of complex processes is instrumental for the rapid development of biomedical research. A remarkable example has been the discovery in *S. cerevisiae* of a group of proteins involved in the pathways of autophagy. Orthologues of these proteins have been identified in humans and experimental model organisms. Interestingly, some mammalian autophagy proteins do not seem to have homologues in yeast but are present in Dictyostelium, a social amoeba with two distinctive life phases, a unicellular stage in nutrient-rich conditions that differentiates upon starvation into a multicellular stage that depends on autophagy. This review focuses on the identification and annotation of the putative Dictyostelium autophagy genes and on the role of autophagy in development, cell death and infection by bacterial pathogens.

Introducing Dictyostelium, A Suitable Model to Study Autophagy

Dictyostelium discoideum is a simple eukaryote that lives in the soil and feeds on bacteria by phagocytosis. The individual cells divide by binary fission as long as food is present, however, when bacteria are exhausted, starvation triggers a process of chemotaxis driven by cyclic-AMP (cAMP).[1-3] The resulting cell aggregate is surrounded by a complex extracellular matrix of protein, cellulose and polysaccharides that isolates it from the environment. This cellular association behaves like a true multicellular organism undergoing different stages of development accomplished by the coordination of morphogenesis and cellular differentiation. Eventually, the aggregates give rise to fruiting bodies, each formed by a cellular stalk that supports a mass of spores. The latter will germinate when environmental conditions are adequate.[4-6] The life cycle of the experimental model species *Dictyostelium discoideum* and representative pictures of each stage are illustrated in **Figure 1**.

*Correspondence to: Ricardo Escalante; Email: rescalante@iib.uam.es
Submitted: 04/10/10; Revised: 05/27/10; Accepted: 05/28/10
Previously published online:
www.landesbioscience.com/journals/autophagy/article/12513

Since Dictyostelium cells undergo development in the absence of any source of external nutrients they need to mobilize resources to be able to respond to the high cell activity required for aggregation and morphogenesis. This mobilization is in part achieved by glycogenolysis and autophagy, the degradation and turnover of the cells' own biomolecules. Autophagy is essential for development in many different systems.[7-9] Three types of autophagy have been described, chaperone-mediated autophagy, microautophagy and macroautophagy. In the first one, specific proteins are recognized by chaperones that mediate their translocation across the limiting membrane of the lysosome into the lumen for their degradation.[10] This form of selective autophagy plays an important role in the cell's response to stress and the presence of damaged proteins. In contrast, microautophagy consists of the invagination or protrusion/septation of the lysosome membrane, thus capturing the cargo and delivering it into the lysosomal lumen, again for degradation.[11] We will focus our review on the third type, macroautophagy (referred to as autophagy hereafter), a mechanistically different degradative process characterized by the formation of double-membrane vesicles called autophagosomes that engulf part of the cytosol or even organelles. The outer membrane of the autophagosomes subsequently fuses with lysosomes, forming autolysosomes where the contents and inner membrane of the autophagosome are degraded and the simple molecular constituents recycled. This form of autophagy is essential for temporary cell survival under starvation conditions. Autophagy is also induced in other circumstances such as for the elimination of protein aggregates or defective organelles or in response to intracellular bacteria, and it is therefore of immense importance in diverse pathological processes as well as in aging.[12-14] The origin of the autophagosomal membrane and the mechanism mediating its expansion and maturation are not yet completely understood.

In mammals and Dictyostelium, nascent autophagosomes originate in the cytoplasm from multiple origins, in contrast with *S. cerevisiae,* where these structures are concentrated in a single location of the cytoplasm (named the PAS or phagophore assembly site). These autophagosomes appear in Dictyostelium and higher organisms as a punctate pattern in the cytoplasm when they are analyzed by fluorescence microscopy using specific autophagosome markers like GFP-Atg8/LC3.[15,16] At the molecular level, several proteins involved in autophagosome formation

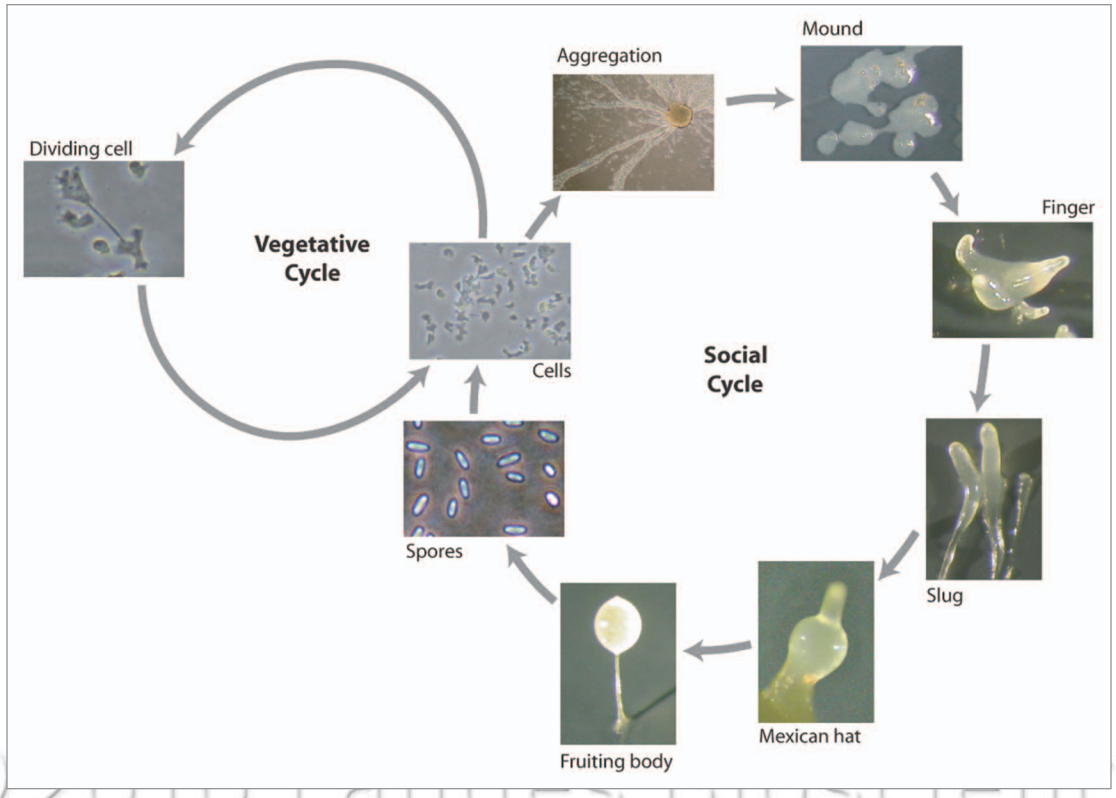

Figure 1. Dictyostelium life cycle. Representative pictures of vegetative and developmental stages are shown. In the wild, Dictyostelium amoeba feed on soil bacteria by phagocytosis but most laboratory strains are also able to grow in liquid axenic media by macropinocytosis. It is important to point out that cells are haploid throughout these vegetative and developmental cycles and this facilitates the generation of knockout strains.

(named Atg for autophagy-related) have historically been identified, primarily in the yeast *S. cerevisiae*. They are grouped in functional complexes required for the origin, elongation, completion and degradation of the autophagosome membrane, although the precise mechanisms of action of many of these proteins and the way in which they are regulated temporally are not yet completely understood (reviewed in ref. 12, 17–19). Two different complexes containing the protein kinase Atg1 and the lipid kinase Vps34 are necessary for induction and nucleation of autophagosomes and to recruit other proteins to the assembly site. Vesicle expansion and completion require two ubiquitin-like conjugation systems involving Atg8 and Atg12. Other proteins like Atg2, Atg9 and Atg18 play a role in membrane traffic and the biogenesis of the autophagosome. Many of these autophagy proteins are conserved in evolution and can be recognized in Dictyostelium by sequence homology analysis as described in detail below.

Despite its simplicity, Dictyostelium shows striking similarities with higher eukaryotes in many biological aspects including chemotaxis,[2,3,20-22] developmental signaling pathways,[4,23,24] the response to bacterial infections,[25-28] the response to therapeutic drugs[29-32] and programmed cell death including autophagic cell death (reviewed in ref. 33). The Dictyostelium genome has been fully sequenced[34] and carefully annotated (http://dictybase.org/) and it is amenable to a wide range of molecular genetic techniques including the generation of mutants by homologous recombination and random genetic screens,[6,33,35-38] that have facilitated the use of comparative genomics to identify relevant genes conserved in the human genome.[37,39]

General Autophagy Mechanisms and Evolutionarily Conserved Autophagy Genes: Induction of Autophagy and the Atg1 Complex

We will now examine the potential of Dictyostelium as a model for autophagy by describing the proteins that are known to be involved in this complex process in other systems and the extent to which they have been conserved in Dictyostelium. **Figure 2** shows a scheme of autophagosome formation and conserved proteins that can be identified in the Dictyostelium genome by comparison with the available information in yeast and mammalian systems.

Autophagy induction and its regulation must be tightly controlled by the energy and nutritional status of the cell. The nutrient sensor TOR (target of rapamycin) belongs to a protein family of conserved serine/threonine kinases known as phosphatidylinositol kinase-related kinases. TOR receives a wide variety of intra- and extracellular signals such as nutrients, energy, growth factors, calcium and amino acids.[40,41] TOR associates with different proteins to form two complexes and only one of them, TORC1, is primarily involved in autophagy. The *S. cerevisiae* TORC1 contains Tor1 or 2, Kog1, Tco89 and Lst8 and is sensitive to rapamycin. As in higher eukaryotes, the Dictyostelium genome codes for proteins highly similar to Tor, Kog1 (also known as Raptor) and

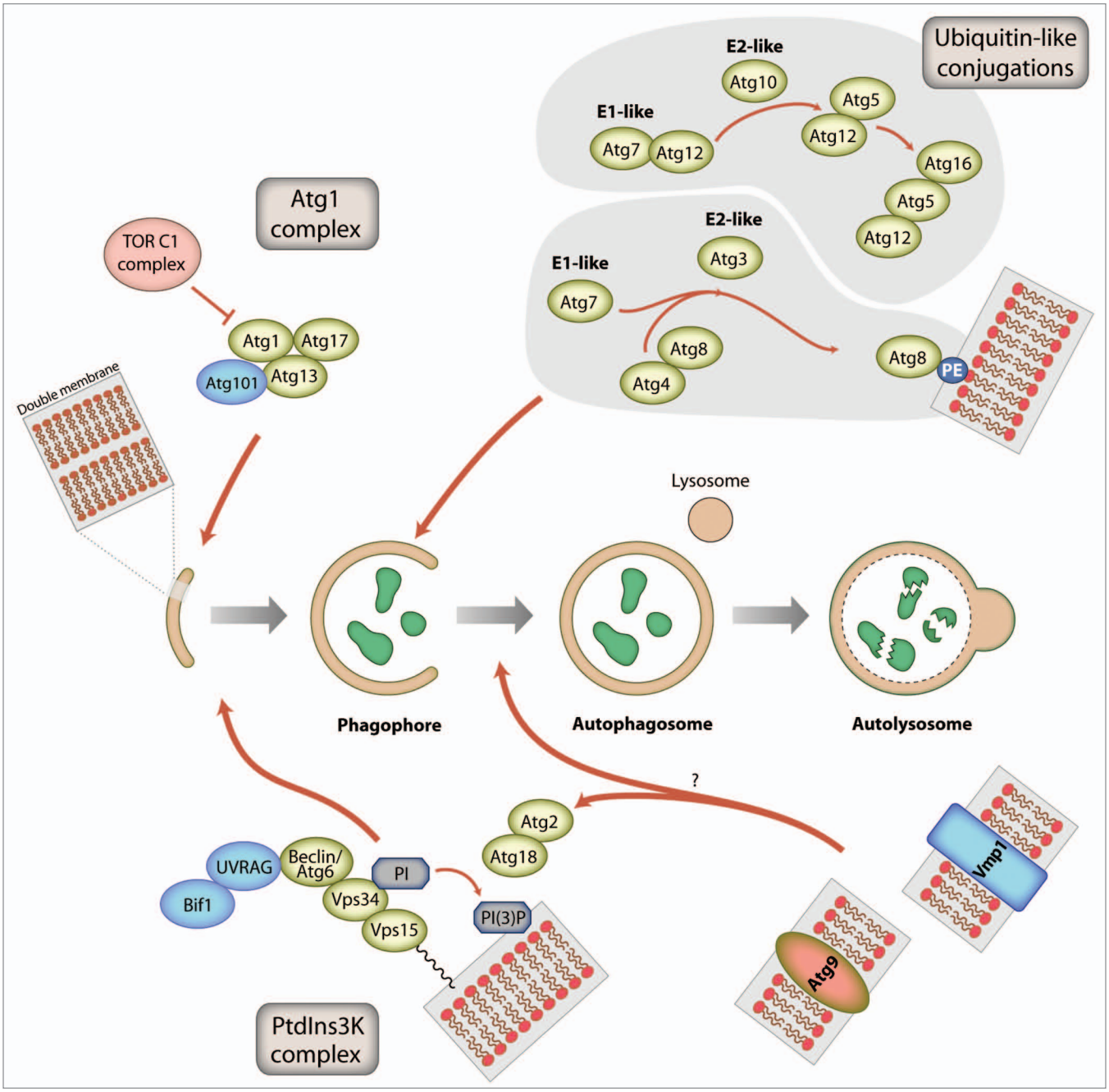

Figure 2. Autophagosome formation and putative signaling pathways in Dictyostelium. The phagophore is a double membrane whose origin is still a matter of debate. This membrane enlarges and finally engulfs parts of the cytoplasm. After fusion with lysosomes the content is degraded and recycled. The predicted Dictyostelium autophagic proteins have been organized in hypothetical functional complexes using the information available from the yeast *S. cerevisiae* and mammalian cells. Some proteins such as Atg101, UVRAG, Bif-1 and Vmp1 seem to be present in Dictyostelium and higher eukaryotes but are absent in *S. cerevisiae*. Vmp1 and Atg9 are transmembrane proteins whose functions are not completely characterized and have been proposed to be involved in membrane trafficking during autophagosome formation.

Lst8. TORC1 regulates many different aspects of cell growth and metabolism and functions upstream of the Atg1 complex, a protein complex containing the kinase Atg1 that plays a central role in the regulation of autophagy by integrating signals from the cellular nutrient status (via its regulation by TOR) and recruiting other autophagy proteins to the site of autophagosome origin (reviewed in ref. 41 and 42). The protein subunit composition of the Atg1 complex and the interplay among these subunits is tightly regulated and depends on TOR activity. Dictyostelium codes for proteins with significant similarity to several Atg1 complex subunits (**Table 1**) and functional analyses have been carried out on Atg1, as described below.

Atg1 is a serine/threonine kinase whose activity is required for autophagy in many different model systems[43-49] including

Table 1. Atg1 protein complex subunits

	Function/features	Dictyostelium	Human	*S. cerevisiae*	E-value Dd-Hu	E-value Dd-Sc
Atg1	Serine/threonine-kinase. (Ma; Cvt)*	Atg1 (DDB_G0292390)	ULK1 (G.ID: 8408) ULK2 (G.ID: 9706)	Atg1 (YGL180W)	1e-38 7e-39	7e-42
Atg13	Atg1 regulator. (Ma; Cvt)	DDB_G0269162	Atg13 related protein (NP_001136145.1)	Atg13 (YPR185W)	n.s.**	n.s.
Atg17	Scaffold protein. (Ma)	Atg17 (DDB0237867)	-	Atg17 (YLR423C)		2e-3
Atg101	Atg1 complex-interacting protein. (Ma)	DDB_G0288287	Atg101 (G.ID: 60673)	-	2e-8	
FIP200	Atg1 complex-interacting protein. (Ma)	DDB_G0268498	FIP200 (G.ID: 9821)	-	1e-3	
Atg29	Atg17-interacting protein. (Ma)	-	-	Atg29 (YPL166W)		
Atg31	Atg17/Atg29-interacting Protein. (Ma)	-	-	Atg31 (YDR022C)		

*Ma, Macroautophagy; Cvt, Cytoplasm-to-vacuole targeting. **The putative Dictyostelium Atg13 shows no significant homology (n.s.) with yeast and human homologues but it contains a conserved pfam Atg13 superfamily domain (as determined by a search of conserved domains at NCBI: http://www.ncbi.nlm.nih.gov/).

Dictyostelium.[16] Dictyostelium Atg1 has an N-terminal kinase domain that shares a high degree of similarity with its counterparts in other organisms, and a poorly conserved C-terminal region. Both domains are separated by an asparagine-rich sequence.[15] The kinase domain is essential for the function of the protein in autophagy, as kinase-dead DdAtg1 has a dominant-negative effect, resulting in a mutant phenotype similar to that observed in the null strain.[16] Interestingly the C terminus contains a short region of significant similarity with human Ulk2 that is also present in other Atg1 proteins such as in Arabidopsis and *C. elegans* but is absent from the *S. cerevisiae* Atg1. The precise function of this domain is unknown, but its presence is required for autophagy.[16]

In *S. cerevisiae,* Atg1 interaction with Atg13 and Atg17 is essential for autophagy induction. This interaction is prevented under nutrient-rich conditions by TOR-dependent phosphorylation of Atg13.[50,51] Starvation conditions inhibit TOR activity and Atg13 becomes rapidly dephosphorylated allowing Atg13 and Atg17 to interact with Atg1 and to activate its kinase activity.[51] Rapamycin, an inhibitor of TOR, is a classic activator of autophagy even under nutrient-rich conditions. A putative Dictyostelium Atg13 homologue has been annotated in the Dictyostelium database (Dicty-base: http://www.dictybase.org/). Although it contains a conserved Atg13 domain that is present in the pfam database (http://pfam.sanger.ac.uk/), Atg13 shows a very low level of similarity between species, suggesting that this protein has largely diverged during evolution.[52]

As seen in **Table 1**, the mammalian Atg1 complex also contains FIP200 (focal adhesion kinase (FAK) family interacting protein of 200 kDa), also known as RB1CC1 (Retinoblastoma 1 inducible coiled coil-1). FIP200 is a multifunctional protein involved in multiple cellular processes besides autophagy such as cell adhesion, migration, cell death and proliferation. It interacts with many different proteins and it is believed to be a functional homologue of Atg17 although they do not share sequence similarity.[53,54] Dictyostelium has putative Atg17 and FIP200, but their level of similarity is too low to decide with some confidence whether or not they are real homologues without any further experimental evidence.

In *S. cerevisiae*, under nutrient-replete growth conditions, Atg1 also regulates the autophagy-dependent cytoplasm-to-vacuole targeting (Cvt) pathway, a mechanism that targets specific hydrolases to the vacuole of *S. cerevisiae*.[55] The hydrolases are packed into autophagosome-like vesicles and delivered to the vacuole in a manner similar to that used during autophagy.[56] This specific and biosynthetic form of autophagy has only been described in *S. cerevisiae* and related yeasts.[57,58] Atg1 and Atg13 are required for both autophagy and the Cvt pathway, but Atg17 is specific to autophagy. A number of other Atg1 complex subunit proteins are known to have specific roles in these pathways. Atg29 and Atg31 are specific for autophagy while Atg11, Atg20 and Atg24 (**Suppl. Table 1**) are only required for the Cvt pathway.[59,60] As in humans, no protein similar to any of these proteins can be recognized by sequence similarity in Dictyostelium (see **Table 1 and Suppl. Table 1**), except for Atg24.

Interestingly, a putative homologue of the mammalian protein Atg101, absent in yeast, can be found in the Dictyostelium genome. Atg101 is a recently described protein essential for autophagy that interacts with Ulk1 in an Atg13-dependent manner. Additionally, it contributes to Atg13 function by protecting Atg13 from proteasomal degradation.[52,61]

Nucleation and the Phosphatidylinositol 3-Kinase (PtdIns3K) Complex

In *S. cerevisiae,* the class III PtdIns3K Vps34 (vacuolar protein sorting 34) is a lipid kinase necessary for autophagy and the Cvt pathway.[62] Its activity generates phosphatidylinositol-3-P (PtdIns3P), believed to be required for binding of other autophagic proteins to the autophagosome nucleation site, such as the

Table 2. PtdIns3K protein complex subunits

	Function/features	Dictyostelium	Human	*S. cerevisiae*	E-value Dd-Hu	E-value Dd-Sc
Atg6/Beclin 1	Subunit of the PtdIns3K complex. (Ma; Cvt)	Atg6B (DDB_G0288021) Atg6A (DDB_G0269244)	BECN1 (G.ID: 8678) BECN1L1 (G.ID: 441925)	Atg6 (YPL120W)	1e-51 2e-27	5e-22 1e-10
Vps34	Class III-phosphatidylinositol 3-kinase. (Ma; Cvt)	PikE (DDB_G0289601) Lower homology to Class I PI3Ks (PikA-H)	PIK3C3 (G.ID: 5289)	Vps34 (YLR240W)	1e-99	1e-121
Vps15	Myristoylated serine/ threonine protein kinase. (Ma; Cvt)	Vps15 (DDB_G0282627) Lower homology at the kinase domain of other proteins	PIK3R4 (G.ID: 30849)	Vps15 (YBR097W)	8e-73	2e-62
UVRAG	Regulates the Beclin1-PtdIns3K complex. (Ma)	DDB_G0288175 DDB_G0283825	UVRAG (G.ID: 7405)	-	1e-28 3e-12	
Bif-1	BAR and SH3-containing protein. (Ma)	DDB_G0284997	SH3GLB1/Bif1 (G.ID: 51100)	-	0.014*	
Atg14	Regulates PtdIns3K. (Ma; Cvt)	DDB_G0278351	KIAA0831	Atg14 (YBR128C)	0.03	n.s.

*The possible Dictyostelium homologue for Bif1 has low homology but contains the expected C-terminal SH3 domain and an N-terminal BAR domain.

phosphoinositide interacting proteins Atg18 and Atg21.[63-65] Besides autophagy, Vps34 is also implicated in other signaling pathways such as the TOR pathway and G-protein signaling to MAPK.[62] Vps34 interacts with Vps15, a myristoylated protein kinase that seems to regulate Vps34.[66,67] This interaction and the kinase domain of Vps15 are necessary for Vps34 activity, although Vps15 does not seem to phosphorylate Vps34 directly.[62,68] A third protein, Atg6 (known as Beclin 1 or Vps30) is also part of the complex.[69] Atg6/Beclin 1 was first identified as a Bcl-2-interacting protein and it is a mammalian tumor suppressor involved in different cancers.[70,71] The complex containing Vps34, Vps15 and Atg6 additionally interacts with two mutually exclusive proteins in *S. cerevisiae*, Vps38 and Atg14. The first one is involved in the Vps pathway and the second one is required for autophagy and the Cvt pathway.

Similar proteins to Vps34, Vps15 and Atg6 can be easily recognized in Dictyostelium and human (**Table 2**). In contrast, Atg14 appears to be present only in close relatives of *S. cerevisiae* and no highly similar proteins can be found in Dictyostelium and higher eukaryotes. However, it should be noted that recently, a distantly related mammalian Atg14 protein has been identified by computational analysis.[72-74] This mammalian Atg14 and UVRAG (UV-radiation resistance-associated gene), another PtdIns3K complex subunit interact with Beclin 1 and Vps34 in a mutually exclusive way. UVRAG has been proposed to be the functional homologue of Vps38 although they do not show significant identity. Therefore, as described in yeast (concerning Atg14 and Vps38), the mammalian cells might also have two different PtdIns3K complexes containing either Atg14 or UVRAG and their mutually exclusive presence might account for the specific functions of this complex in autophagy and other membrane trafficking processes.[73,74] Interestingly, a putative homologue of UVRAG can be detected in the Dictyostelium genome as shown in **Table 2** with a fairly good e-value score. Sequence comparison with Atg14 did not detect any similar protein in Dictyostelium when compared with *S. cerevisiae* Atg14, but identified a protein with a low score when compared with the human Atg14 (**Table 2**).

Besides UVRAG, the mammalian complex might contain additional proteins not identified in yeast such as Ambra1 and Bif-1 whose functions are being characterized.[75,76] Bif-1 interacts with UVRAG and promotes the activation of Vps34. Bif-1 contains two characteristic domains, an amino-terminal N-BAR (Bin-Amphiphysin-Rys) domain, and a carboxy-terminal SH3 (Src-homology 3) and has been proposed to be involved in the biogenesis of the autophagosome membrane due to its membrane binding and bending activities.[77,78] While no similar proteins can be recognized in Dictyostelium for Ambra1, a putative Bif-1 can be identified and, although it shows a low level of similarity, the predicted sequence has the characteristic BAR and SH3 functional domains.

Vesicle Expansion and Ubiquitin-Like Conjugation Systems

Membrane expansion into a fully developed autophagosome requires the function of two ubiquitin-like protein conjugation reactions.[79] In the first conjugation system Atg12 is covalently bound to Atg5, a reaction catalyzed by the E1-type enzyme Atg7 and the E2 enzyme Atg10.[80,81] Atg16 interacts noncovalently with Atg12-Atg5 to form a complex that multimerizes.[82,83] This reaction and the localization of the Atg12-Atg5-Atg16 complex may facilitate the second conjugation reaction, and/or dictate in part where this reaction occurs. In the second reaction the ubiquitin-like protein Atg8 (commonly known as LC3 in mammals) is attached to the expanding autophagosome membrane by conjugation to phosphatidylethanolamine.[84,85] Atg8 is first processed by the protease Atg4 to uncover a conserved glycine at the C terminus that is then used for the covalent binding to the phospholipid with the aid of the E1-type enzyme Atg7, also used in the first conjugation reaction, and the E2-type enzyme Atg3.

The proteins involved in these reactions are very well conserved during evolution and can be easily recognized by sequence similarity in Dictyostelium as shown in **Table 3**. Of note, two Atg8-like proteins are present in Dictyostelium, whereas only one

Table 3. Ubiquitin-like conjugation systems

	Function/features	Dictyostelium	Human	*S. cerevisiae*	E-value Dd-Hu	E-value Dd-Sc
Atg3	E2-like enzyme. (Ma; Cvt)	Atg3 (DDB_G0277319)	Atg3 (G.ID: 64422)	Atg3 (YNR007C)	1e-39	7e-19
Atg4	Cysteine protease. (Ma; Cvt)	Atg4 (DDB_G0273443) DDB_G0283753	Atg4B (G.ID: 23192) Other homologues (Atg4A, C, D)	Atg4 (YNL223W)	3e-19 5e-24	2e-11 1e-12
Atg5	Conjugates with Atg12. (Ma; Cvt)	Atg5 (DDB_G0289881)	Atg5 (G.ID: 9474)	Atg5 (YPL149W)	1e-15	5e-6
Atg7	E1-like enzyme. (Ma; Cvt)	Atg7 (DDB_G0271096)	Atg7 (G.ID: 10533)	Atg7 (YHR171W)	1e-148	1e-116
Atg8	Ubiquitin-like protein that conjugates with phosphatidylethanolamine (PE). (Ma; Cvt)	Atg8 (DDB_G0286191) DDB_G0290491	GABARAP (G.ID: 11337) Other homologues (LC3/ MAP1LC3A; GATE16/ GABARAPL2, etc.,)	Atg8 (YBL078C)	3e-30 2e-21	1e-35 3e-29
Atg10	E2-like enzyme. (Ma; Cvt)	Atg10 (DDB_G0268840)	Atg10 (G.ID: 83734)	Atg10 (YLL042C)	4e-18	0.97
Atg12	Conjugates with Atg5 (Ma; Cvt)	Atg12 (DDB_G0282929)	Atg12 (G.ID: 9140)	Atg12 (YBR217W)	1e-14	8e-7
Atg16	Interaction with Atg12-Atg5 conjugates (Ma; Cvt)	TipD (DDB_G0275323)	Atg16L1 (G.ID: 55054)	Atg16 (YMR159C)	1e-68	1e-4

Table 4. Other autophagic proteins

	Function/features	Dictyostelium	Human	*S. cerevisiae*	E-value Dd-Hu	E-value Dd-Sc
Atg2	Peripheral membrane protein involved in Atg9 cycling (Ma; Cvt)	DDB_G0277419	Atg2A (G.ID: 23130) Atg2B (G.ID: 55102)	Atg2 (YNL242W)	7e-11 4e-24	4e-29
Atg9	Transmembrane protein (Ma; Cvt)	Atg9 (DDB_G0285323)	Atg9A (G.ID: 79065) Atg9B (G.ID: 285973)	Atg9 (YDL149W)	9e-67 1e-26	3e-88
Atg15	Lipase (Ma; Cvt)	-	-	Atg15 (YCR068W)		
Atg18	WD repeat domain phosphoinositide-interacting protein (Ma; Cvt)	Atg18 (DDB_G0285375) Wdr45l (DDB_G0282581)	WIPI-3 (56270) Other homologues (WIPI-1; WIPI-3; WDR45L/WIPI-3)	Atg18 (YFR021W)	1e-37 8e-81	4e-35 8e-29
Atg22	Amino acid export from vacuole (Ma; Cvt)	-	-	Atg22 (YCL038C)		
Atg23	Peripheral membrane protein. (Ma; Cvt)	-	-	Atg23 (YLR431C)		
Atg27	Type I membrane protein. (Ma; Cvt)	-	-	Atg27 (YJL178C)		
Vmp1	Transmembrane protein (Ma)	Vmp1 (DDB_G0285175)	TMEM49 (G.ID: 81671)	-	6e-61	

is present in yeast. Remarkably, the level of similarity between the Dictyostelium and the human proteins is generally higher than that observed between Dictyostelium and *S. cerevisiae* homologues. Another striking similarity is the presence of an extended C terminus in Atg16 containing multiple WD-40 repeats, a feature typically found in the Atg16 homologues of animals but absent in fungi. This domain is probably involved in additional protein-protein interactions that might have been conserved between Dictyostelium and animals. The putative Atg16 homologue (named TipD) was targeted by insertional mutagenesis in a genetic screen for a multi-tipped phenotype but its requirement in autophagy was not addressed.[86] Interestingly the developmental phenotype observed in the *tipD*$^-$ mutant is similar to that described in other Dictyostelium mutants affecting both conjugation reactions, such as *atg7*$^-$, *atg5*$^-$ and *atg8*$^-$.[15,87]

Other Autophagy-Related Proteins

A number of autophagy proteins not included in the above-mentioned functional clusters are involved in other less known processes such as the transport and recycling of components from the autophagosome. As shown in **Table 4**, several of these proteins, such as Atg2, Atg9 and Atg18, can be recognized in the *S. cerevisiae*, Dictyostelium and human genomes. Vmp1 on the other hand is absent in fungi but present in Dictyostelium and higher organisms, another example of the evolutionary proximity of Dictyostelium and animals.

Atg9 is a multispanning membrane protein involved in membrane traffic from not well-defined cellular compartments to the autophagosome and is therefore believed to play a role in the origin and elongation of the autophagic membrane.[88,89] The subcellular localization of Atg9 depends on the organism under study. In *S. cerevisiae,* Atg9 appears to be located on the surface of mitochondria or in vesicles in very close proximity to these organelles.[90,91] In mammalian cells, Atg9 traffics between the Golgi and endosomes suggesting an involvement of the Golgi complex in the autophagic pathway. In Dictyostelium, Atg9 resides in small vesicles that travel from the cell's periphery to the microtubule-organizing center. Its deletion leads to a pleiotropic phenotype including autophagy defects.[92]

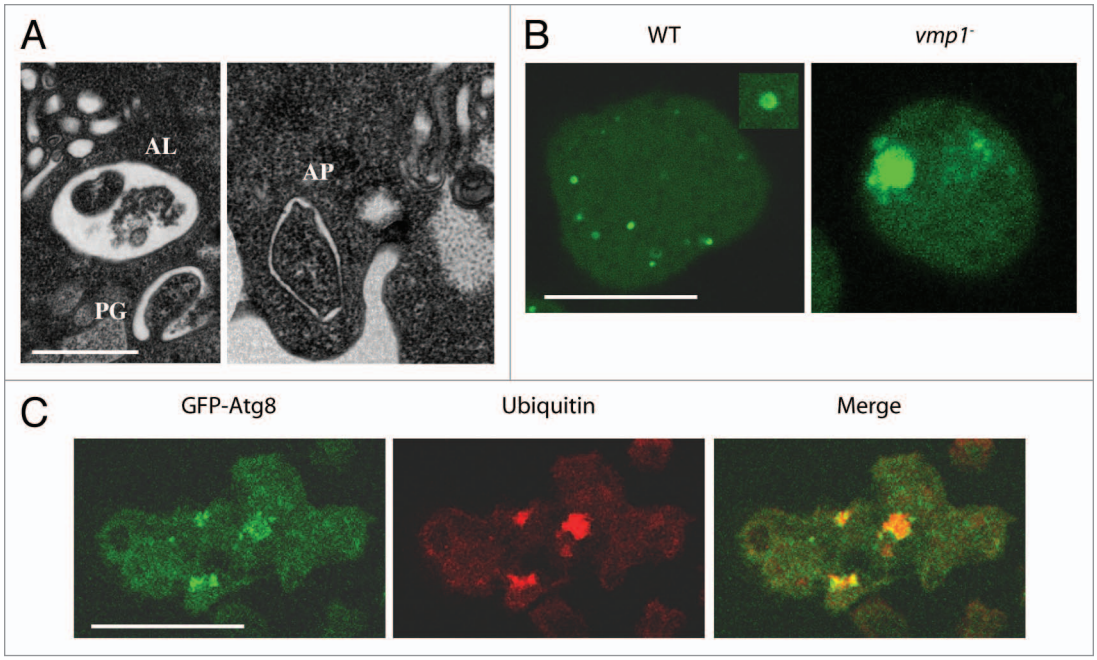

Figure 3. Monitoring autophagy in Dictyostelium. (A) Examples of autophagic structures in Dictyostelium as seen by transmission electron microscopy. PG, AP and AL correspond to putative phagophore, autophagosome and autolysosome respectively. Bar: 0.5 μm. (B) Fluorescence microscopy of wild-type (WT) and *vmp1*- cells expressing the autophagosome marker GFP-Atg8. Close examination of the punctate pattern (see the inset) reveals a vesicle-like appearance of the autophagosomes. In the mutant the marker appears aggregated. Bar: 10 μm. (C) These protein aggregates observed in *vmp1*- organisms (and other autophagic mutants, see the text) colocalize with ubiquitin as determine by immunofluorescence with anti-ubiquitin antibody and contain the scaffold protein p62 as observed in many different protein aggregation diseases.

The fact that Vmp1 and Atg9 are transmembrane proteins known to be required for autophagosome formation in mammalian cells raises interesting questions about their possible role membrane traffic during autophagy.[93-95] In contrast to Atg9, Vmp1 is an endoplasmic reticulum-resident protein in Dictyostelium. It is not yet clear to what extent the autophagosome membrane originates de novo or from pre-existing organelles. The localization of Vmp1 to the ER and its partial colocalization with autophagosomes are in line with other studies that suggest the involvement of the ER in autophagy.[96-99]

Atg18 interacts with Atg2, and this complex is localized to the autophagosome membrane via Atg18 binding to PtdIns(3)P, through the novel conserved motif FRRG.[64,65] This localization is essential for the recruitment of other autophagic proteins and for autophagy, although the precise function of these proteins is unknown.

There are a number of proteins specifically involved in selective autophagy in *S. cerevisiae*. Most of these proteins do not have clear homologues in Dictyostelium and human except for Atg21, a homologue of Atg18 and Atg24, a member of the sorting nexin family with a phosphoinositide binding Phox domain and a BAR domain (**Suppl. Table 1**). This protein is also involved in endosomal protein sorting. The lack of similar proteins is not surprising taking into account that most of these proteins are involved in the Cvt pathway, a process not present in Dictyostelium.

In summary, the Dictyostelium genome codes for most of the basic components that have been described to regulate autophagy. Moreover, the strong similarity with animals and the presence of certain proteins conserved in Dictyostelium and humans that are absent in yeast emphasize the high level of conservation of the basic autophagy machinery between this simple social amoeba and man.

Monitoring Autophagy in Dictyostelium

Transmission electron microscopy (TEM) has been a classical method to monitor autophagy although interpretation of the structures is difficult since autophagosome formation is a very dynamic process with morphologically different stages of maturation. Clear criteria must be applied to determine if a given structure is a bona fide autophagosome, such as the presence of double-membrane vesicles containing organelles or material similar in density to the cytoplasm. This double membrane might have a cup-shape when the formation of the autophagosome has not been completed. When the autophagosome is fused with the lysosomes, the internal membrane and the cytoplasmic material might appear partially degraded. **Figure 3** shows an example of such structures in Dictyostelium. During vegetative growth, TEM images of Dictyostelium cells show very few double membrane autophagosomes, and most of the vacuoles are single membrane and contain spongy material that is believed to correspond to different degrees of digestion of the axenic medium that has been taken up by macropinocytosis.[100,101] Other vesicles are electron-lucent and probably correspond to contractile vacuoles.[100] However, during starvation the number of food vacuoles decreases and double-membrane autophagosomes become

abundant reaching a maximum around 4–5 hours after the initiation of starvation,[100] confirming the activation of autophagy by starvation in Dictyostelium, as described in other organisms. The absence of autophagosomes has been determined by TEM in several Dictyostelium autophagic mutants including *atg1*$^{-}$, *atg6*$^{-}$, *atg8*$^{-}$, *atg7*$^{-}$, *atg5*$^{-}$ *and vmp1*$^{-}$.[15,87,93] Another characteristic feature of TEM images is the progressive disappearance of cytoplasm and organelles during starvation in wild type as a consequence of autophagy. Conversely, the autophagic mutants show dense cytoplasm with little degradation.[15,87]

Molecular markers of autophagy are proteins involved in the autophagy process that can be used to monitor autophagy. The most common marker is Atg8/LC3 that becomes lipidated and attached to the autophagosome membrane, and participates in its elongation. The use of GFP-Atg8/LC3 allows in vivo visualization of autophagy by confocal fluorescence microscopy. In mammalian cells and Dictyostelium, this marker appears as a punctate pattern, as illustrated in **Figure 3**. Since autophagy is a dynamic process involving induction, maturation and degradation, a defect in a particular stage affects the Atg8/LC3 pattern in different ways. For example, a suppression of an early step of autophagosome formation will decrease the number of puncta, but a blockage of late stages might leave the induction unaffected, resulting in an accumulation of puncta.[102,103] In Dictyostelium, the use of the GFP-Atg8 marker reveals some specific features of the system that must be taken into account. Although TEM analysis showed that starvation increases the number of autophagosomes, a number of GFP-Atg8 puncta are present during growth conditions and this number does not seem to be significantly affected during starvation. However, closer examination shows differences in the morphology of puncta. During growth, most of the puncta appear as simple dots. Conversely, during starvation the number of structures showing a cup-like or vesicle-like shape increases (**Fig. 3**). A possible interpretation is that during growth there are many initial autophagosome origins that do not progress in their elongation probably because they require additional signaling events. This signaling would be triggered by starvation to promote the activation of autophagy, and therefore the vesicle-like puncta, reflecting bona fide autophagosomes, become more evident. Alternatively, the dot-like structures observed during growth might represent artifactual aggregation of Atg8/LC3 as described in other systems.[104]

Interestingly, when autophagy is blocked by genetic ablation of Atg1 or Vmp1 in Dictyostelium, the GFP-Atg8 marker colocalizes with large ubiquitinated protein aggregates together with p62 (**Fig. 3**). This phenomenon is less pronounced in other mutants such as Atg7 and Atg5. These aggregates have been described in many other systems where autophagy has been inhibited.[105-107] The accumulation of these aggregates suggests a role for autophagy in their clearance. Other markers that associate with the phagophore have been used in other systems to monitor autophagy, such as Atg5, Atg12, Atg16 and Atg18.[108-110] As described above, Dictyostelium possess proteins highly similar to each of them. They could potentially be used as additional markers to overcome some of the problems observed with GFP-Atg8.

The use of certain substrates to monitor autophagy-dependent protein degradation allows asking whether or not autophagy reaches its last stages, providing information about the autophagic flux. Since Atg8/LC3 and p62 are degraded by autophagy the total amount of these proteins decreases upon autophagy induction despite the expected transcriptional activation. Therefore, the total amount of these markers inversely correlates with autophagic flux.[103,111,112] Dictyostelium cells expressing GFP-Atg8 can be used to monitor the degradation of this marker by western blot using anti-GFP antibodies. As expected we found that the amount of this marker decreases in the first hours of starvation and this decrease is prevented in the autophagic mutant *atg1*$^{-}$ (unpublished observation), suggesting that a similar mechanism operates in Dictyostelium and could be used to monitor autophagy.

The conservation of autophagy genes and the mechanisms involved make us believe that some other techniques used to monitor autophagy in other systems might be applied to Dictyostelium in the future as more research teams join the field and use this model system to study autophagy.

Dictyostelium Autophagy Mutants are Affected in Development

Insertional and knockout mutants have been generated for several Dictyostelium autophagy genes as shown in **Table 5**. They comprise at least one component of each of the described functional complexes: Atg1 from the Atg1 complex,[15] Atg6/Beclin 1 from the PtdIns3K complex,[15] Atg5, Atg7, Atg8 and Atg16[15,86,87] from the ubiquitin-like conjugation systems. Similarly, the two transmembrane proteins identified in mammalian cells to have an essential role in autophagosome formation, Atg9[92] and Vmp1[93,99] have also been ablated in Dictyostelium.

Autophagy is required for multicellular development in Dictyostelium and, interestingly, the severity of the phenotypes depends on the mutated gene. Mutants affected in the ubiquitin-like conjugation systems and Atg6/Beclin 1 have a defect at the mound/finger stage with the formation of multi-tipped structures leading to small or abnormal fruiting bodies.[15,86,87] As described above in **Table 2**, the Dictyostelium genome codes for two homologous Atg6 proteins (Atg6A and Atg6B) and only the first one has been disrupted. As a consequence, the phenotype observed might be affected by partial redundancy.

Stronger phenotypes have been observed in the mutants affecting Atg1 or the transmembrane proteins Atg9 and Vmp1. They show vegetative growth defects, and development is partially or totally arrested at the aggregation or mound stages, depending on the experimental conditions. It should be noted that whereas the proteins involved in ubiquitin-like conjugation reactions seem to play specific roles in autophagy, the Atg1 complex,[42] the PtdIns3K complex,[62] Atg9 and Vmp1[98] might be involved in other membrane trafficking processes. The strong phenotype observed in some of these mutants might therefore be attributed in part to other possible additional defects not directly related to autophagy.

Table 5. Dictyostelium autophagic mutants and related phenotype

Mutant and parental strain	Developmental phenotype	Growth	Survival to starvation	Ubiquitin$^+$ aggregates	References
atg1$^-$ (DH1)	Aggregation/mound arrest	Slow growth	affected	Presence of large aggregates	Otto et al. 2004 (15)
atg5$^-$ (DH1)	Aggregation/Multi-tipped aggregates/ aberrant fruiting bodies	Normal growth	affected	Presence of small aggregates	Otto et al. 2003 (87) Calvo-Garrido and Escalante. 2010 (99)
atg6$^-$ (DH1)	Multi-tipped aggregates/small fruiting bodies	Normal growth	affected	Not detected	Otto et al. 2004 (15)
atg7$^-$ (DH1)	Aggregation/Multi-tipped aggregates/ aberrant fruiting bodies	Normal growth	affected	Presence of small aggregates	Otto et al. 2003 (87)
atg8$^-$ (DH1)	Multi-tipped aggregates/small fruiting bodies	Normal growth	affected	Not detected	Otto et al. 2004 (15)
atg9$^-$ (AX2)	Aggregation/Multi-tipped aggregates/ aberrant fruiting bodies	Slow growth	Not analyzed	Not analyzed	Tung et al. 2010 (92)
TipD/atg16- (AX4)	Multi-tipped aggregates/small fruiting bodies	Not analyzed	Not analyzed	Not analyzed	Stege at al. 1999 (86)
vmp1$^-$ (AX4)	Aggregation/mound arrest	Slow growth	affected	Presence of large aggregates	Calvo-Garrido and Escalante. 2010 (99)

A similar argument, that autophagy may be required during all stages of the Dictyostelium developmental program, arises from the study of temperature-sensitive Atg1 mutants.[16] Development is arrested when the mutant is shifted to the restrictive temperature even after 16 hours of development when the structures are at the slug stage. Development is then resumed when they are set back to the permissive temperature.[16] It seems that a constant turnover of cellular material might be required at all stages of Dictyostelium development. However, as stated before, since Atg1 has been proposed to play additional roles besides autophagy, the Atg1 requirement during development might also involve other functional aspects that have not yet been characterized.

At the cellular level, dysfunction in protein degradation pathways such as in the ubiquitin-proteasome system and autophagy might lead to the persistence of ubiquitin-positive protein aggregates, a hallmark of many degenerative diseases. Interestingly, Dictyostelium *vmp1$^-$* mutants show accumulation of enormous ubiquitin-positive protein aggregates containing the autophagy marker GFP-Atg8 and the putative Dictyostelium p62 homologue as described in many degenerative human diseases.[99] In mammalian cells, p62 functions as a scaffold protein that provides a link between ubiquitinated aggregates and the autophagy machinery via the direct interaction of p62 with ubiquitin and the autophagosome protein Atg8/LC3. The presence of p62 in these ubiquitinated aggregates suggests that a similar mechanism functions in Dictyostelium. The inability of *vmp1$^-$* cells to clear these aggregates by autophagy would explain their accumulation, as described in mutant mice where the autophagy genes *Atg5* and *Atg9* have been knocked out.[113,114]

The analysis of other Dictyostelium autophagic mutants (*atg1$^-$*, *atg5$^-$*, *atg6$^-$*, *atg7$^-$* and *atg8$^-$*) show a correlation between the severity of their corresponding phenotypes and the presence of ubiquitin-positive protein aggregates.[99] An attractive hypothesis is that the phenotypes are aggravated by the presence of aggregates that might function as a sink for interacting proteins altering their normal localization or concentration. This phenomenon has been recently described in Dictyostelium with the formation of actin inclusions in cells by mistargeting VASP, an actin-binding protein, to endosomes. These actin aggregates are reminiscent of Hirano bodies that are often present in neurodegenerative diseases and, in Dictyostelium, are found to sequester other actin-binding proteins and endosomal proteins, promoting their disappearance from the cytoplasm.[115] These Hirano body-like aggregates can also be induced in Dictyostelium by the overexpression of a truncated form of a 34 kDa actin-binding protein.[116] A recent report shows that both autophagy and the proteasome pathway contribute to the degradation of Hirano bodies in Dictyostelium. Moreover, the autophagosome marker protein GFP-Atg8 colocalizes with model Hirano bodies in wild-type Dictyostelium cells, but not in *atg5$^-$* or *atg1$^-$* cells.[117]

Dictyostelium Autophagic Cell Death

Cell death with autophagy has been observed in particular in development and in pathology.[118] Importantly, in recent years a causative role for autophagy in cell death could be demonstrated in certain cases through the decrease of cell death upon inactivation of an autophagy gene, often with no accompanying causative apoptotic or necrotic cell death.[119-132] The question, then, becomes not whether autophagy is causative in some cases of animal cell death (it clearly can be), but how.

The protist Dictyostelium shows, when starved, developmental formation of a fruiting body consisting of viable spores and dead stalk cells.[133] Stalk cell formation can be mimicked in vitro under monolayer culture conditions, where Dictyostelium cells can differentiate from vegetative into "stalk" vacuolated cells[134-136] showing signs of autophagy (see below) and undergoing cell death. This monolayer model shows many advantages for the study of autophagic cell death (ACD)[33] including the absence of

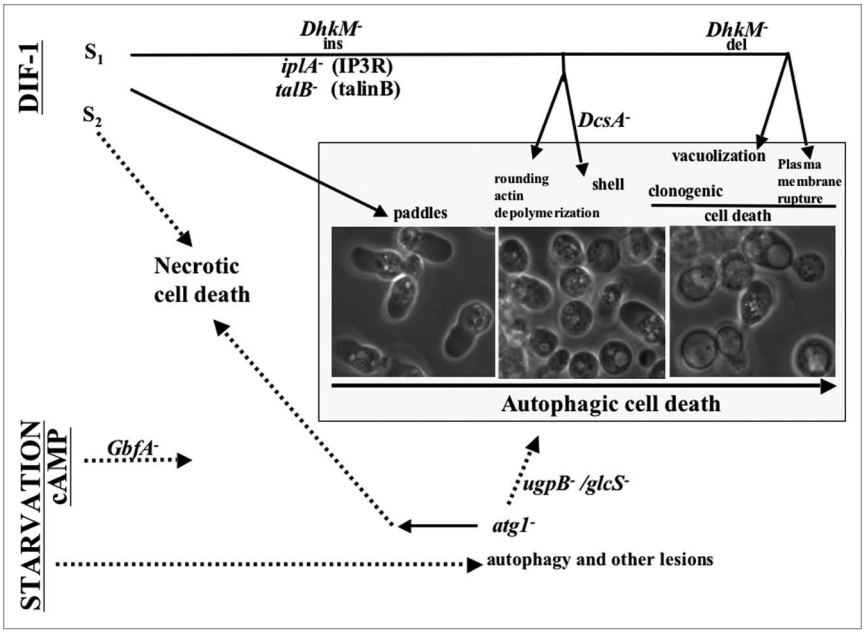

Figure 4. Pathways to cell death in Dictyostelium and mutational analysis thereof. In a first stage (lower half), starvation and cAMP lead to autophagy and sensitize cells to induction by DIF-1 (upper half) of either autophagic (right part) or necrotic (left part) cell death depending on whether the *atg1* gene is wild type or inactivated by mutation. The indicated other mutations allowed the dissection of particular autophagic cell death (see main text).

the main members of the apoptosis machinery that could interfere with it.[137,138]

Importantly, triggering ACD in monolayers requires at least two distinct stimuli. The first stimulus is starvation together with cAMP.[135,139,140] These induce, on the one hand, autophagy, as manifested by the appearance of autophagosomes,[136,141,142] and on the other hand, major mitochondrial lesions.[143] Starvation, cAMP and the resulting alterations including autophagy do not by themselves lead to ACD. To induce cell death, a second stimulus is required, namely the main stalk differentiation-inducing factor DIF-1, a small dichlorinated molecule.[144-147] DIF-1 is naturally synthesized during starvation-induced development. In monolayer experiments, ACD can be induced by addition of cAMP and DIF-1 to starved cells undergoing autophagy.[134-136] ACD includes first the emergence of polarized "paddle" cells, then their rounding and acquisition of a cellulose shell. Small vacuoles then fuse to form large vacuoles ultimately occupying most of the cell volume (**Fig.** 4). Plasma membrane rupture occurs later (50% at around 40 hours of treatment) as judged by propidium iodide staining.[134,136] The whole sequence of ACD subcellular events is shown in **Figure** 4.

ACD has been further investigated in this model, mostly using random insertional mutagenesis,[33] and here its requirements and genetic control are briefly reviewed (summarized in **Fig.** 4). Starvation-induced events are blocked by mutations of *gbfA* (G-box binding factor; a transcription factor)[33] and of *ugpB* (UDP-glucose pyrophosphorylase)/*glcS* (glycogen synthase).[141] The DIF-1-triggered pathway leading to ACD was also studied by insertional mutagenesis. The correct functioning of this pathway from its triggering by DIF-1 to the induction of ACD requires the following genes: *iplA* (IP3 receptor),[148] *talB* (talin B),[33] and *DhkM* (receptor histidine kinase M).[149] Mutation of these genes dissociates the autophagic cell death phenotype into several subcellular traits under various molecular controls.[33,149]

In this system, is autophagy itself mechanistically required for or only accompanying ACD? If autophagy were required for ACD in the Dictyostelium model, mutation of one of the *atg* genes essential for the autophagic pathway should prevent not only autophagy, but also most or all of the signs of ACD. Indeed, an *atg1*$^{-}$ mutation decreases autophagy[15,150] and suppresses ACD.[150] Cell death, however, still occurs upon addition of DIF-1 to starved *atg1*$^{-}$ cells, but as necrotic cell death (NCD), quite distinct from ACD. NCD involves immediate and massive mitochondrial uncoupling, perinuclear clustering of mitochondria, lysosomal permeabilization and rapid plasma membrane rupture.[150-152] Several mutations that inhibit the pathway leading to ACD do not affect or affect much less, the pathway leading to NCD,[33,141,148] and NCD and ACD differ as to the specificity of their DIF-1 signaling.[153] These data are compatible with the interpretation that a mutation of the autophagy gene *atg1* could at the same time affect two distinct types of cell death, leading to NCD and preventing ACD. However, in this model NCD occurs much sooner and quicker than ACD and may thus preempt the occurrence of ACD, leading to the alternative interpretation that the *atg1*$^{-}$ mutation would just favor the more rapid NCD, without any significance as to an Atg1 requirement for ACD. Current investigations aiming at rigorously checking an Atg1 requirement for ACD are based on drastic suppression of NCD. A first approach includes the differential reversibility of ACD and NCD upon early removal of the inducer. Specifically, removal of DIF-1 15 min after its addition led, in *atg1*$^{-}$ cells to full reversal of early signs of NCD and ultimately to no or little death, but in wild-type cells to almost no reversal of ACD, which proceeded to vacuolization and death (reviewed in ref. 136, 151). A second approach is to use as a death-inducer not DIF-1, but a given DIF-1 derivative called 107 or desmethyl-DIF-1, which induces ACD, but almost no NCD.[153] Preliminary experiments using early removal of 107, or yet other approaches, or combinations of these, to prevent induction and/or completion of NCD strongly suggest that ACD is indeed dependent on Atg1 in this model.

Altogether, in this Dictyostelium monolayer model, autophagic cell death triggering requires a first signal, starvation/cAMP, leading to autophagy and a second signal, DIF-1, leading from autophagy to ACD. Autophagy is not directly causative of death (since autophagy is not sufficient) but primes for a mechanism that is (the DIF-1 pathway to ACD can occur only if *atg1* is intact). We think that such a second signal or something homologous to it, may well exist to trigger ACD in less simple eukaryotes,

where it is still buried in complexity. While we do not know yet to what extent this mechanism is conserved for instance in mammalian cells, in some cases the latter can show vacuolizing ACD morphologically very similar to that seen in Dictyostelium.[154] On the pathway triggered by DIF-1, some mutations specifically affect ACD, not autophagy. These mutations dissociate ACD into distinct, separately controlled subcellular lesions. To pursue this genetic analysis of ACD in this very favorable model, a search for further ACD mutants is ongoing.

Autophagy and Infection in Dictyostelium

The first line of defense against invading bacteria is comprised of phagocytic cells of the innate immune system. These cells are specialized in the recognition of invading pathogens and respond by activating antimicrobial immune responses (reviewed in ref. 155). These cells recognize and contain microbes early during infection via complement activation, phagocytosis, autophagy and immune activation by families of pattern recognition receptors (PRRs). The response relies on recognition of evolutionarily conserved structures of commensals and pathogens, termed pathogen-associated molecular patterns (PAMPs). The family of TLRs is the major and most extensively studied class of PRRs. The main bactericidal strategy relies on phagocytosis, the process by which cells engulf particles, which is conserved during evolution. In organisms such as amoebae, "phagotrophy" is used for feeding and appears as a distinguishing feature in the last common ancestor of eukaryotes.[156] In immune phagocytes, the bactericidal and degradation machineries have been harnessed to meet the needs for presentation of antigenic peptides.

Studies of autophagy identified important functions in the regulation of innate immunity and inflammation (reviewed in ref. 157). Xenophagy refers to the use of the autophagy pathway to digest foreign rather than self-constituents. The PRR-triggered pathways and the autophagy process intersect at many different levels: TLRs can regulate autophagy induction, the autophagy machinery can be used to deliver pathogen genetic material for binding to endosomal TLRs, and TLRs may act in the recruitment of autophagy proteins to phagosomal membranes. Indeed, Atg proteins have been identified in the major proteomic investigations of phagosomal components.[158] The pathways leading from bacterial sensing to xenophagy are very complex and have not been completely deciphered yet. Nevertheless, a picture is emerging with a central axis of signaling making use of the general nutrient-sensing cascade involving the energy sensor AMP-activated protein kinase (AMPK) that, in response to high AMP/ATP ratios, inhibits TORC1 and leads to induction of autophagy (reviewed in ref. 159). In addition, during evolution, before the NFkappaB pathway emerged as the central coordinator of the immune response, the p38 mitogen-activated protein kinase (MAPK) cascade served as the ancestral antimicrobial defense-coordinating pathway.[160]

Facing the evolution of ever more efficient bacterial sensing and killing mechanisms, microorganisms subject to predation were under strong selective pressure to develop the traits needed to survive phagocytic cells, including passive (resistant capsule) or active (toxin secretion) defense mechanisms, but also the ability to replicate directly within the predator cell. This results in a paradox: many microorganisms, although they only accidentally infect mammals, have evolved sophisticated mechanisms to do so.[161] One of the clearest examples is Legionella that did not infect humans before the invention of air conditioning. Indeed, the virulence traits of Legionella and pathogens such as Chlamydia and waterborne Mycobacteria[162] were probably selected to fight amoebae long before the appearance of metazoans. Despite evolutionary perfection, phagocytic cells can be hijacked by intracellular pathogens that overcome their killing mechanisms and establish themselves a vacuolar or cytosolic niche to survive and/or proliferate. Upon cell invasion, bacteria must confront xenophagy, an efficient intracellular defense machinery. Beside bacteria that are completely controlled by autophagy as part of the innate surveillance mechanism, several bacterial pathogens have evolved virulence strategies to either inhibit autophagy to establish a persistent infection or even to take advantage of autophagy to generate a replication niche and to succeed in colonization and spreading (reviewed in ref. 163).

The amoeba Dictyostelium is an attractive model system to study host-pathogen interactions.[25,164] Recent reports suggest that self-nonself discrimination[165] and innate immunity[166] already evolved in amoebae. Dictyostelium cells feed on soil bacteria and, throughout their life, ingest, kill and digest microorganisms at a rate of at least one per minute. Thus, Dictyostelium is likely to have evolved mechanisms that enable it to discriminate and respond appropriately to various bacteria to optimize feeding and to avoid subversion by pathogens. Indeed, genome-wide mutagenesis screening reveals pathways of uptake and killing mechanisms specific to $Gram^+$ or $Gram^-$ bacteria.[167] Several transcriptomic analyses of Dictyostelium's reaction to different bacterial species have been carried out and reveal strong modulation of thousands of transcripts.[168-170] Many of these genes belong to a set of "innate immunity-related" genes that bear homologies to plant and insect innate immune defenses, as well as to the mammalian pathways,[27,168] confirming that Dictyostelium can recognize bacteria and modulate its response.[26] In the multicellular slug, a special cell-type, the sentinel cell, patrols in search of xenobiotics and bacteria.[166]

Because of its ease of manipulation and the conservation of cell-autonomous defense pathways, Dictyostelium has been successfully used and instrumental in the study of virulence mechanisms of Pseudomonas, Legionella and *Vibrio cholera*.[171-174] Most interesting in the view of autophagy, Dictyostelium is an experimental host to pathogens that interact and interfere with xenophagy such as Salmonella, mycobacteria and especially Legionella.[175]

Salmonella enterica serovar Typhimurium is a food-borne pathogen that is usually restricted to the gastrointestinal tract, but can cause severe extra-intestinal diseases in the elderly. In epithelial and other cell types, Salmonella escapes the phagosome pathway and establishes a replication compartment that retains some characteristics of the endosomal pathway. Contrary to the fate of many intracellular pathogens for which the course of infection in Dictyostelium is similar to the one in macrophages, Salmonella is killed and degraded hours after ingestion by the

amoeba.[176] Interestingly, Salmonella appears to evade the common fate of nonpathogenic bacteria such as *E. coli* and escapes phagosome maturation. But, even though Salmonella does not succumb to the bactericidal activities of the phagosomal pathway, it is nevertheless surrounded by GFP-Atg8-positive membranes about 2 hours post-infection and finally is degraded in autolysosomes.[177] Confirming the restrictive role of autophagy, infection of *atg1*-, *atg6*- and *atg7*-null mutants results in the formation of a standard Salmonella-containing vacuole (SCV) and bacteria proliferation. This is finally detrimental to these autophagy-defective Dictyostelium mutants, which die within 1–3 days of infection.[177]

Like many other bacterial pathogens, *M. tuberculosis* can reside in various compartments of its host. As a facultative intracellular pathogen, it can reside outside cells, in the interstitial space or inside necrotic granulomatous lesions. After uptake by immune phagocytes and inducing an arrest of their phagocytic maturation pathway, it resides intracellularly, first inside a replication vacuole[178] and then in the cytosol.[179] In Dictyostelium, the establishment and course of an infection by *M. marinum* are similar to those observed for pathogenic mycobacteria in other host systems. Importantly, as is the case in animal macrophages, during infection of Dictyostelium, *M. marinum* escapes its vacuole and continues to proliferate in the cytosol.[180] It is worth noting that, in activated macrophages, autophagy appears to be able to overcome the phagosome maturation block imposed by mycobacteria and thus controls *M. bovis* BCG infection by directing the replication vacuole to fuse with lysosomes and kill the bacteria.[181] Whether this might also be relevant for infections by *M. marinum* and *M. tuberculosis* still awaits further studies. However, recent studies point to a causality link between vacuole rupture, *M. marinum* exposure to the cytosol, ubiquitination and the spatial recruitment of Atg8-positive membranes, indicating the intervention of adapter proteins such as p62/sequestosome 1. Interestingly, for some cytosolic pathogens, the cell wall is a target for ubiquitination,[182] whereas for others, the damaged vacuole is the target.[183] Furthermore, it is suggested that bactericidal peptides derived from ubiquitin and ribosomal proteins are brought in contact with the mycobacteria via p62-mediated autophagy.[184] Because most of these proteins and processes are conserved in Dictyostelium, including p62,[99] it will be exciting to investigate whether these mechanisms are also active during infection of Dictyostelium by *M. marinum*.

Legionella pneumophila is the prototype of an accidental pathogen for human, because its natural hosts are unicellular protozoa, such as Acanthamoeba. This explains why the use of the amoeba Dictyostelium to study the mechanisms of Legionella virulence and host resistance has been increasingly popular, and represents the "flagship" of host-pathogen studies in this model system. The many successes in this field of research have been very recently and comprehensively reviewed (see ref. 175), and here we will concentrate on the interactions of Legionella with autophagy. Studies in macrophages, mainly using pharmacological tools, had pointed to a potential positive involvement of autophagy in the biogenesis of the replication compartment.[185] For example, starvation-induced autophagy had a modest stimulatory effect on proliferation.[186] But this claim remained disputed, until a seminal study using the genetic power of Dictyostelium demonstrated that the absence of either Atg1, Atg5, Atg6, Atg7 or Atg8 had little or no impact on the establishment of the replication compartment, and even slightly enhanced the proliferation of Legionella.[187] These findings were compatible with a role of autophagy in the control of Legionella infection, but this was not further examined until a few recent studies. The starting point was the finding that the global transcriptomic response to Legionella infection includes the prominent regulation of three autophagy genes encoding Atg8, Atg9 and Atg16.[172] Among these, the multi-transmembrane protein Atg9 was chosen to study the impact of gene ablation in Legionella infection.[92] First, surprisingly, the absence of Atg9 results in a significant decrease in phagocytic uptake, possibly reflecting a direct or indirect coupling between phagocytosis and autophagy. Then, a careful quantitative analysis of the early phase of infection reveals that, in wild-type Dictyostelium, Legionella is rapidly and strongly cleared from the amoeba in the first hours post uptake, and that this is strongly defective in *atg9* null cells.[92] These findings confirm and extend the previous conclusions that autophagy plays a protective role to limit infection by Legionella.

But three recent studies indicate that the case is probably not definitively closed and that the interaction of Legionella with the autophagic pathway might be more complex than initially thought. First, it was recently discovered that an effector secreted by Legionella, AnkB, represents a case of molecular mimicry by which Legionella subverts the polyubiquitination machinery of its host, be it a macrophage or a Dictyostelium cell.[188] This protein contains a noncanonical F-box domain, the integrity of which is essential for rapid acquisition of polyubiquitinated proteins by the Legionella-containing vacuole and for bacteria proliferation. AnkB is proposed to act via a pathway including the SCF1 (RBX1-CUL1-SKP1) ubiquitin ligase complex that is highly conserved throughout eukaryotes.[188] Second, while studying the causes of increased susceptibility of patients with mitochondrial diseases to Legionella infection, Paul Fisher's group highlighted the profound impact of an upregulation of the energy-sensing protein kinase AMPK.[189] Upregulation of AMPK is a primary response to the impaired energy production in such diseases, but the resulting dysfunction on the containment of Legionella infection was a relative surprise. Overexpression of AMPK in wild-type Dictyostelium phenocopied the situation in mutant cells, identifying AMPK as a dominant regulator of intracellular immunity to Legionella,[189] possibly via the TOR-autophagy or p38ERK-MAPK cascade pathways. More work is required to answer these exciting developments, but another study might point in that direction. High-throughput screening to identify host proteins that modulate Legionella growth in Dictyostelium reveal a pivotal role for DupA in the genesis of the replication niche.[169] DupA is a putative tyrosine/dual specificity phosphatase that appears to regulate ERK1 phosphorylation and activation of the MAPK cascade. Also of interest is the finding that many genes are regulated both in *dupA* null cells and upon infection with bacteria, including the *tirA* and *slrA* genes that encode proteins suggested to play an immune-like function in sentinel cells during development.[166]

Concluding Remarks

Autophagy is a fast emerging field and although a big leap has been taken recently by identifying a group of proteins involved in the mechanism and regulation of autophagy, the molecular function of many of these Atg proteins is still poorly defined. It is very likely that a number of proteins involved in autophagy are still unknown and the use of simple experimental models should help us define these new components. Autophagy in the social amoeba Dictyostelium plays essential roles in its natural life that makes it a suitable model where autophagy can be studied in the context of a whole organism. The differences between Dictyostelium and the yeast model *S. cerevisiae* will enrich the possibilities of study while still maintaining the simplicity of the microorganisms. Its powerful molecular genetics, the availability of the genome sequence and the similarities with higher organisms will help shed light on many of the still unanswered questions and help discover new genes involved in this exciting field.

Acknowledgements

This work was supported by grants BFU2006-00394 and BFU2009-09050 to R.E. from the Spanish Ministerio de Ciencia e Innovación. We thank Javier Pérez for the art work. Sequence data for Dictyostelium were obtained from the Genome Sequencing Centers of the University of Cologne. Germany; the Institute of Molecular Biotechnology, Department of Genome Analysis, Jena; the Baylor Collage of Medicine in Houston, Texas USA; and the Sanger Center in Hinxton, Cambridge, United Kingdom. The access to the sequence data was performed using Dicty-base (the central resource for Dictyostelid genomics).

Note

Supplementry materials can be found at:
www.landesbioscience.com/supplement/CalvoGarridoAUTO6-6-Sup.pdf

References

1. Willard SS, Devreotes PN. Signaling pathways mediating chemotaxis in the social amoeba, *Dictyostelium discoideum*. Eur J Cell Biol 2006; 85:897-904.
2. Janetopoulos C, Firtel RA. Directional sensing during chemotaxis. FEBS Lett 2008; 582:2075-85.
3. King JS, Insall RH. Chemotaxis: finding the way forward with Dictyostelium. Trends Cell Biol 2009; 19:523-30.
4. Strmecki L, Greene DM, Pears CJ. Developmental decisions in *Dictyostelium discoideum*. Dev Biol 2005; 284:25-36.
5. Annesley SJ, Fisher PR. *Dictyostelium discoideum*-a model for many reasons. Mol Cell Biochem 2009; 329:73-91.
6. Escalante R, Vicente JJ. *Dictyostelium discoideum*: a model system for differentiation and patterning. Int J Dev Biol 2000; 44:819-35.
7. Meléndez A, Levine B. Autophagy in *C. elegans*. WormBook 2009; 1-26.
8. McPhee CK, Baehrecke EH. Autophagy in *Drosophila melanogaster*. Biochim Biophys Acta 2009; 1793:1452-60.
9. Cecconi F, Levine B. The role of autophagy in mammalian development: cell makeover rather than cell death. Dev Cell 2008; 15:344-57.
10. Kon M, Cuervo AM. Chaperone-mediated autophagy in health and disease. FEBS Lett 2009; 284:1399-404.
11. Uttenweiler A, Mayer A. Microautophagy in the yeast *Saccharomyces cerevisiae*. Methods in molecular biology. Clifton NJ 2008; 445:245-59.
12. Levine B, Kroemer G. Autophagy in the pathogenesis of disease. Cell 2008; 132:27-42.
13. Marino G, Lopez-Otin C. Autophagy and aging: new lessons from progeroid mice. Autophagy 2008; 4:807-9.
14. Mellen MA, de la Rosa EJ, Boya P. The autophagic machinery is necessary for removal of cell corpses from the developing retinal neuroepithelium. Cell Death Differ 2008; 15:1279-90.
15. Otto GP, Wu MY, Kazgan N, Anderson OR, Kessin RH. Dictyostelium macroautophagy mutants vary in the severity of their developmental defects. J Biol Chem 2004; 279:15621-9.
16. Tekinay T, Wu MY, Otto GP, Anderson OR, Kessin RH. Function of the *Dictyostelium discoideum* Atg1 kinase during autophagy and development. Eukaryot Cell 2006; 5:1797-806.
17. Xie Z, Klionsky DJ. Autophagosome formation: core machinery and adaptations. Nat Cell Biol 2007; 9:1102-9.
18. Uchiyama Y, Shibata M, Koike M, Yoshimura K, Sasaki M. Autophagy-physiology and pathophysiology. Histochem Cell Biol 2008; 129:407-20.
19. Reggiori F. Membrane origin for autophagy. Curr Topics Dev Biol 2006; 74:1-30.
20. Van Haastert PJ, Veltman DM. Chemotaxis: navigating by multiple signaling pathways. Sci STKE 2007; 2007:40.
21. Stephens L, Milne L, Hawkins P. Moving towards a better understanding of chemotaxis. Curr Biol 2008; 18:485-94.
22. Kay RR, Langridge P, Traynor D, Hoeller O. Changing directions in the study of chemotaxis. Nat Rev 2008; 9:455-63.
23. Harwood AJ. Dictyostelium development: a prototypic Wnt pathway? Meth Mol Biol 2008; 469:21-32.
24. Fountain SJ. Neurotransmitter receptor homologues of *Dictyostelium discoideum*. J Mol Neurosci 2010; 41:263-9.
25. Steinert M, Heuner K. Dictyostelium as host model for pathogenesis. Cellular Microbiology 2005; 7:307-14.
26. Bozzaro S, Bucci C, Steinert M. Phagocytosis and host-pathogen interactions in Dictyostelium with a look at macrophages. Int Rev Cell Mol Biol 2008; 271:253-300.
27. Cosson P, Soldati T. Eat, kill or die: when amoeba meets bacteria. Curr Opin Micro 2008; 11:271-6.
28. Jin T, Xu X, Fang J, Isik N, Yan J, Brzostowski JA, Hereld D. How human leukocytes track down and destroy pathogens: lessons learned from the model organism *Dictyostelium discoideum*. Immunol Res 2009; 43:118-27.
29. Shaulsky G, Escalante R, Loomis WF. Developmental signal transduction pathways uncovered by genetic suppressors. Proc Natl Acad Sci USA 1996; 93:15260-5.
30. Escalante R, Loomis WF. Whole-mount in situ hybridization of cell-type-specific mRNAs in Dictyostelium. Dev Biol 1995; 171:262-6.
31. Alexander S, Min J, Alexander H. *Dictyostelium discoideum* to human cells: pharmacogenetic studies demonstrate a role for sphingolipids in chemoresistance. Biochim Biophys Acta 2006; 1760:301-9.
32. Williams RS. Pharmacogenetics in model systems: defining a common mechanism of action for mood stabilisers. Prog Neuropsychopharmacol Biol Psychiatry 2005; 29:1029-37.
33. Giusti C, Tresse E, Luciani M-F, Golstein P. Autophagic cell death: analysis in Dictyostelium. Biochim Biophys Acta 2009; 1793:1422-31.
34. Eichinger L, Pachebat JA, Glockner G, Rajandream MA, Sucgang R, Berriman M, et al. The genome of the social amoeba *Dictyostelium discoideum*. Nature 2005; 435:43-57.
35. Kuspa A, Loomis WF. Tagging developmental genes in Dictyostelium by restriction enzyme-mediated integration of plasmid DNA. Proc Natl Acad Sci USA 1992; 89:8803-7.
36. Kuspa A, Loomis WF. Transformation of Dictyostelium—Gene disruptions, insertional mutagenesis and promoter traps. Meth Mol Genet 1994; 3:3-21.
37. Torija P, Robles A, Escalante R. Optimization of a large-scale gene disruption protocol in Dictyostelium and analysis of conserved genes of unknown function. BMC Microbiol 2006; 6:75.
38. Urushihara H. The cellular slime mold: eukaryotic model microorganism. Exp Anim 2009; 58:97-104.
39. Torija P, Vicente JJ, Rodrigues TB, Robles A, Cerdan S, Sastre L, et al. Functional genomics in Dictyostelium: MidA, a new conserved protein, is required for mitochondrial function and development. J Cell Sci 2006; 119:1154-64.
40. Schmelzle T, Hall MN. TOR, a central controller of cell growth. Cell 2000; 103:253-62.
41. Mizushima N. The role of the Atg1/ULK1 complex in autophagy regulation. Curr Opin Cell Biol 2010; 22:132-9.
42. Chan EY, Tooze SA. Evolution of Atg1 function and regulation. Autophagy 2009; 5:758-65.
43. Matsuura A, Tsukada M, Wada Y, Ohsumi Y. Apg1p, a novel protein kinase required for the autophagic process in *Saccharomyces cerevisiae*. Gene 1997; 192:245-50.
44. Melendez A, Tallóczy Z, Seaman M, Eskelinen EL, Hall DH, Levine B. Autophagy genes are essential for dauer development and life-span extension in *C. elegans*. Science 2003; 301:1387-91.
45. Scott RC, Schuldiner O, Neufeld TP. Role and regulation of starvation-induced autophagy in the Drosophila fat body. Dev Cell 2004; 7:167-78.
46. Chan EY, Kir S, Tooze SA. siRNA screening of the kinome identifies ULK1 as a multidomain modulator of autophagy. J Biol Chem 2007; 282:25464-74.
47. Chang YY, Neufeld TP. An Atg1/Atg13 complex with multiple roles in TOR-mediated autophagy regulation. Mol Biol Cell 2009; 20:2004-14.
48. Ganley IG, Lam du H, Wang J, Ding X, Chen S, Jiang X. ULK1·ATG13·FIP200 complex mediates mTOR signaling and is essential for autophagy. J Biol Chem 2009; 284:12297-305.

49. Hosokawa N, Hara T, Kaizuka T, Kishi C, Takamura A, Miura Y, et al. Nutrient-dependent mTORC1 association with the ULK1-Atg13-FIP200 complex required for autophagy. Mol Biol Cell 2009; 20:1981-91.
50. Kamada Y, Funakoshi T, Shintani T, Nagano K, Ohsumi M, Ohsumi Y. Tor-mediated induction of autophagy via an Apg1 protein kinase complex. J Cell Biol 2000; 150:1507-13.
51. Kabeya Y, Kamada Y, Baba M, Takikawa H, Sasaki M, Ohsumi Y. Atg17 functions in cooperation with Atg1 and Atg13 in yeast autophagy. Mol Biol Cell 2005; 16:2544-53.
52. Mercer CA, Kaliappan A, Dennis PB. A novel, human Atg13 binding protein, Atg101, interacts with ULK1 and is essential for macroautophagy. Autophagy 2009; 5.
53. Hara T, Mizushima N. Role of ULK-FIP200 complex in mammalian autophagy: FIP200, a counterpart of yeast Atg17? Autophagy 2009; 5:85-7.
54. Hara T, Takamura A, Kishi C, Iemura S, Natsume T, Guan JL, Mizushima N. FIP200, a ULK-interacting protein, is required for autophagosome formation in mammalian cells. J Cell Biol 2008; 181:497-510.
55. Huang WP, Klionsky DJ. Autophagy in yeast: a review of the molecular machinery. Cell Struct Funct 2002; 27:409-20.
56. Khalfan WA, Klionsky DJ. Molecular machinery required for autophagy and the cytoplasm to vacuole targeting (Cvt) pathway in *S. cerevisiae*. Curr Opin Cell Biol 2002; 14:468-75.
57. Wang CW, Klionsky DJ. The molecular mechanism of autophagy. Mol Med 2003; 9:65-76.
58. Farre JC, Vidal J, Subramani S. A cytoplasm to vacuole targeting pathway in *P. pastoris*. Autophagy 2007; 3:230-4.
59. Kabeya Y, Noda NN, Fujioka Y, Suzuki K, Inagaki F, Ohsumi Y. Characterization of the Atg17-Atg29-Atg31 complex specifically required for starvation-induced autophagy in *Saccharomyces cerevisiae*. Biochem Biophys Res Commun 2009; 389:612-5.
60. Kawamata T, Kamada Y, Suzuki K, Kuboshima N, Akimatsu H, Ota S, et al. Characterization of a novel autophagy-specific gene, *ATG29*. Biochem Biophys Res Commun 2005; 338:1884-9.
61. Hosokawa N, Sasaki T, Iemura S, Natsume T, Hara T, Mizushima N. Atg101, a novel mammalian autophagy protein interacting with Atg13. Autophagy 2009; 5:973-9.
62. Backer JM. The regulation and function of Class III PI3Ks: novel roles for Vps34. Biochem J 2008; 410:1-17.
63. Krick R, Tolstrup J, Appelles A, Henke S, Thumm M. The relevance of the phosphatidylinositolphosphat-binding motif FRRGT of Atg18 and Atg21 for the Cvt pathway and autophagy. FEBS Lett 2006; 580:4632-8.
64. Obara K, Sekito T, Niimi K, Ohsumi Y. The Atg18-Atg2 complex is recruited to autophagic membranes via phosphatidylinositol 3-phosphate and exerts an essential function. J Biol Chem 2008; 283:23972-80.
65. Nair U, Cao Y, Xie Z, Klionsky DJ. The roles of the lipid-binding motifs of Atg18 and Atg21 in the cytoplasm to vacuole targeting pathway and autophagy. J Biol Chem 2010; 285:11476-88.
66. Herman PK, Stack JH, DeModena JA, Emr SD. A novel protein kinase homolog essential for protein sorting to the yeast lysosome-like vacuole. Cell 1991; 64:425-37.
67. Stack JH, Herman PK, Schu PV, Emr SD. A membrane-associated complex containing the Vps15 protein kinase and the Vps34 PI 3-kinase is essential for protein sorting to the yeast lysosome-like vacuole. EMBO J 1993; 12:2195-204.
68. Stack JH, Emr SD. Vps34p required for yeast vacuolar protein sorting is a multiple specificity kinase that exhibits both protein kinase and phosphatidylinositol-specific PI 3-kinase activities. J Biol Chem 1994; 269:31552-62.
69. Cao Y, Klionsky DJ. Physiological functions of Atg6/Beclin 1: a unique autophagy-related protein. Cell Res 2007; 17:839-49.
70. Aita VM, Liang XH, Murty VV, Pincus DL, Yu W, Cayanis E, Kalachikov S, Gilliam TC, Levine B. Cloning and genomic organization of *beclin 1*, a candidate tumor suppressor gene on chromosome 17q21. Genomics 1999; 59:59-65.
71. Miracco C, Cosci E, Oliveri G, Luzi P, Pacenti L, Monciatti I, Mannucci S, et al. Protein and mRNA expression of autophagy gene Beclin 1 in human brain tumours. Int J Oncol 2007; 30:429-36.
72. Sun Q, Fan W, Chen K, Ding X, Chen S, Zhong Q. Identification of Barkor as a mammalian autophagy-specific factor for Beclin 1 and class III phosphatidylinositol 3-kinase. Proc Natl Acad Sci USA 2008; 105:19211-6.
73. Itakura E, Kishi C, Inoue K, Mizushima N. Beclin 1 forms two distinct phosphatidylinositol 3-kinase complexes with mammalian Atg14 and UVRAG. Mol Biol Cell 2008; 19:5360-72.
74. Itakura E, Mizushima N. Atg14 and UVRAG: mutually exclusive subunits of mammalian Beclin 1-PI3K complexes. Autophagy 2009; 5:534-6.
75. Fimia GM, Stoykova A, Romagnoli A, Giunta L, Di Bartolomeo S, Nardacci R, et al. Ambra1 regulates autophagy and development of the nervous system. Nature 2007; 447:1121-5.
76. Takahashi Y, Coppola D, Matsushita N, Cualing HD, Sun M, Sato Y, et al. Bif-1 interacts with Beclin 1 through UVRAG and regulates autophagy and tumorigenesis. Nature Cell Biol 2007; 9:1142-51.
77. Takahashi Y, Meyerkord CL, Wang HG. Bif-1/Endophilin B1: a candidate for crescent driving force in autophagy. Cell Death Differ 2009; 16:947-55.
78. Takahashi Y, Meyerkord CL, Wang HG. BARgaining membranes for autophagosome formation: Regulation of autophagy and tumorigenesis by Bif-1/Endophilin B1. Autophagy 2008; 4:121-4.
79. Geng J, Klionsky DJ. The Atg8 and Atg12 ubiquitin-like conjugation systems in macroautophagy. EMBO Rep 2008; 9:859-64.
80. Tanida I, Mizushima N, Kiyooka M, Ohsumi M, Ueno T, Ohsumi Y, Kominami E. Apg7p/Cvt2p: A novel protein-activating enzyme essential for autophagy. Mol Biol Cell 1999; 10:1367-79.
81. Shintani T, Mizushima N, Ogawa Y, Matsuura A, Noda T, Ohsumi Y. Apg10p, a novel protein-conjugating enzyme essential for autophagy in yeast. EMBO J 1999; 18:5234-41.
82. Mizushima N, Sugita H, Yoshimori T, Ohsumi Y. A new protein conjugation system in human. The counterpart of the yeast Apg12p conjugation system essential for autophagy. J Biol Chem 1998; 273:33889-92.
83. Mizushima N, Noda T, Ohsumi Y. Apg16p is required for the function of the Apg12p-Apg5p conjugate in the yeast autophagy pathway. EMBO J 1999; 18:3888-96.
84. Kirisako T, Baba M, Ishihara N, Miyazawa K, Ohsumi M, Yoshimori T, et al. Formation process of autophagosome is traced with Apg8/Aut7p in yeast. J Cell Biol 1999; 147:435-46.
85. Ichimura Y, Kirisako T, Takao T, Satomi Y, Shimonishi Y, Ishihara N, et al. A ubiquitin-like system mediates protein lipidation. Nature 2000; 408:488-92.
86. Stege JT, Laub MT, Loomis WF. Tip genes act in parallel pathways of early Dictyostelium development. Dev Genet 1999; 25:64-77.
87. Otto GP, Wu MY, Kazgan N, Anderson OR, Kessin RH. Macroautophagy is required for multicellular development of the social amoeba *Dictyostelium discoideum*. J Biol Chem 2003; 278:17636-45.
88. Webber JL, Young ARJ, Tooze SA. Atg9 trafficking in mammalian cells. Autophagy 2007; 3:54-6.
89. Mari M, Reggiori F. Atg9 trafficking in the yeast *Saccharomyces cerevisiae*. Autophagy 2007; 3:145-8.
90. He C, Klionsky DJ. Atg9 trafficking in autophagy-related pathways. Autophagy 2007; 3:271-4.
91. Reggiori F, Shintani T, Nair U, Klionsky DJ. Atg9 cycles between mitochondria and the pre-autophagosomal structure in yeasts. Autophagy 2005; 1:101-9.
92. Tung SM, Unal C, Ley A, Pena C, Tunggal B, Noegel AA, et al. Loss of Dictyostelium ATG9 results in a pleiotropic phenotype affecting growth, development, phagocytosis and clearance and replication of *Legionella pneumophila*. Cell Microbiol 2010; 12:765-80.
93. Calvo-Garrido J, Carilla-Latorre S, Lazaro-Dieguez F, Egea G, Escalante R. Vacuole membrane protein 1 is an endoplasmic reticulum protein required for organelle biogenesis, protein secretion and development. Mol Biol Cell 2008; 19:3442-53.
94. Vaccaro MI, Ropolo A, Grasso D, Iovanna JL. A novel mammalian trans-membrane protein reveals an alternative initiation pathway for autophagy. Autophagy 2008; 4:388-90.
95. Ropolo A, Grasso D, Pardo R, Sacchetti ML, Archange C, Lo Re A, et al. The pancreatitis-induced vacuole membrane protein 1 triggers autophagy in mammalian cells. J Biol Chem 2007; 282:37124-33.
96. Simonsen A, Stenmark H. Self-eating from an ER-associated cup. J Cell Biol 2008; 182:621-2.
97. Axe EL, Walker SA, Manifava M, Chandra P, Roderick HL, Habermann A, et al. Autophagosome formation from membrane compartments enriched in phosphatidylinositol 3-phosphate and dynamically connected to the endoplasmic reticulum. J Cell Biol 2008; 182:685-701.
98. Calvo-Garrido J, Carilla-Latorre S, Escalante R. Vacuole membrane protein 1, autophagy and much more. Autophagy 2008; 4:835-7.
99. Calvo-Garrido J, Escalante R. Autophagy dysfunction and ubiquitin-positive protein aggregates in Dictyostelium cells lacking Vmp1. Autophagy 2010; 6:100-9.
100. de Chastellier C, Ryter A. Changes of the cell surface and of the digestive apparatus of *Dictyostelium discoïdeum* during the starvation period triggering aggregation. J Cell Biol 1977; 75:218-36.
101. Neuhaus EM, Almers W, Soldati T. Morphology and dynamics of the endocytic pathway in *Dictyostelium discoideum*. Mol Biol Cell 2002; 13:1390-407.
102. Klionsky DJ, Abeliovich H, Agostinis P, Agrawal DK, Aliev G, Askew DS, et al. Guidelines for the use and interpretation of assays for monitoring autophagy in higher eukaryotes. Autophagy 2008; 4:151-75.
103. Mizushima N, Yoshimori T, Levine B. Methods in mammalian autophagy research. Cell 2010; 140:313-26.
104. Kuma A, Matsui M, Mizushima N. LC3, an autophagosome marker, can be incorporated into protein aggregates independent of autophagy: caution in the interpretation of LC3 localization. Autophagy 2007; 3:323-8.
105. Pankiv S, Clausen TH, Lamark T, Brech A, Bruun JA, Outzen H, et al. p62/SQSTM1 binds directly to Atg8/LC3 to facilitate degradation of ubiquitinated protein aggregates by autophagy. J Biol Chem 2007; 282:24131-45.
106. Kaniuk NA, Kiraly M, Bates H, Vranic M, Volchuk A, Brumell JH. Ubiquitinated-protein aggregates form in pancreatic β-cells during diabetes-induced oxidative stress and are regulated by autophagy. Diabetes 2007; 56:930-9.
107. Szeto J, Kaniuk NA, Canadien V, Nisman R, Mizushima N, Yoshimori T, et al. ALIS are stress-induced protein storage compartments for substrates of the proteasome and autophagy. Autophagy 2006; 2:189-99.
108. Mizushima N, Yamamoto A, Hatano M, Kobayashi Y, Kabeya Y, Suzuki K, et al. Dissection of autophagosome formation using Apg5-deficient mouse embryonic stem cells. J Cell Biol 2001; 152:657-68.

109. Mizushima N, Kuma A, Kobayashi Y, Yamamoto A, Matsubae M, Takao T, et al. Mouse Apg16L, a novel WD-repeat protein, targets to the autophagic isolation membrane with the Apg12-Apg5 conjugate. J Cell Sci 2003; 116:1679-88.
110. Proikas-Cezanne T, Pfisterer SG. Assessing mammalian autophagy by WIPI-1/Atg18 puncta formation. Methods Enzymol 2009; 452:247-60.
111. Bjørkøy G, Lamark T, Pankiv S, Øvervatn A, Brech A, Johansen T. Monitoring autophagic degradation of p62/SQSTM1. Methods Enzymol 2009; 452:181-97.
112. Mizushima N, Yoshimori T. How to interpret LC3 immunoblotting. Autophagy 2007; 3:542-5.
113. Rubinsztein DC. The roles of intracellular protein-degradation pathways in neurodegeneration. Nature 2006; 443:780-6.
114. Hara T, Nakamura K, Matsui M, Yamamoto A, Nakahara Y, Suzuki-Migishima R, et al. Suppression of basal autophagy in neural cells causes neurodegenerative disease in mice. Nature 2006; 441:885-9.
115. Schmauch C, Claussner S, Zoltzer H, Maniak M. Targeting the actin-binding protein VASP to late endosomes induces the formation of giant actin aggregates. Eur J Cell Biol 2009; 88:385-96.
116. Maselli AG, Davis R, Furukawa R, Fechheimer M. Formation of Hirano bodies in Dictyostelium and mammalian cells induced by expression of a modified form of an actin-crosslinking protein. J Cell Sci 2002; 115:1939-49.
117. Kim DH, Davis RC, Furukawa R, Fechheimer M. Autophagy contributes to degradation of Hirano bodies. Autophagy 2009; 5:44-51.
118. Bursch W. The autophagosomal-lysosomal compartment in programmed cell death. Cell Death Differ 2001; 8:569-81.
119. Yu SW, Baek SH, Brennan RT, Bradley CJ, Park SK, Lee YS, et al. Autophagic death of adult hippocampal neural stem cells following insulin withdrawal. Stem Cells 2008; 26:2602-10.
120. Yu L, Wan F, Dutta S, Welsh S, Liu Z, Freundt E, et al. Autophagic programmed cell death by selective catalase degradation. Proc Natl Acad Sci USA 2006; 103:4952-7.
121. Yu L, Alva A, Su H, Dutt P, Freundt E, Welsh S, et al. Regulation of an *ATG7-beclin 1* program of autophagic cell death by caspase-8. Science 2004; 304:1500-2.
122. Shimizu S, Kanaseki T, Mizushima N, Mizuta T, Arakawa-Kobayashi S, Thompson CB, Tsujimoto Y. Role of Bcl-2 family proteins in a non-apoptotic programmed cell death dependent on autophagy genes. Nat Cell Biol 2004; 6:1221-8.
123. Puyal J, Vaslin A, Mottier V, Clarke PG. Postischemic treatment of neonatal cerebral ischemia should target autophagy. Ann Neurol 2009; 66:378-89.
124. Pattingre S, Tassa A, Qu X, Garuti R, Liang XH, Mizushima N, et al. Bcl-2 antiapoptotic proteins inhibit Beclin 1-dependent autophagy. Cell 2005; 122:927-39.
125. Koike M, Shibata M, Tadakoshi M, Gotoh K, Komatsu M, Waguri S, et al. Inhibition of autophagy prevents hippocampal pyramidal neuron death after hypoxic-ischemic injury. Am J Pathol 2008; 172:454-69.
126. Hoyer-Hansen M, Bastholm L, Mathiasen IS, Elling F, Jaattela M. Vitamin D analog EB1089 triggers dramatic lysosomal changes and Beclin 1-mediated autophagic cell death. Cell Death Differ 2005; 12:1297-309.
127. Hofius D, Schultz-Larsen T, Joensen J, Tsitsigiannis DI, Petersen NH, Mattsson O, et al. Autophagic components contribute to hypersensitive cell death in Arabidopsis. Cell 2009; 137:773-83.
128. Espert L, Denizot M, Grimaldi M, Robert-Hebmann V, Gay B, Varbanov M, et al. Autophagy is involved in T cell death after binding of HIV-1 envelope proteins to CXCR4. J Clin Invest 2006; 116:2161-72.
129. Denton D, Shravage B, Simin R, Mills K, Berry DL, Baehrecke EH, Kumar S. Autophagy, not apoptosis, is essential for midgut cell death in Drosophila. Curr Biol 2009; 19:1741-6.
130. Chen Y, McMillan-Ward E, Kong J, Israels SJ, Gibson SB. Oxidative stress induces autophagic cell death independent of apoptosis in transformed and cancer cells. Cell Death Differ 2008; 15:171-82.
131. Berry DL, Baehrecke EH. Autophagy functions in programmed cell death. Autophagy 2008; 4:359-60.
132. Baek SH, Kim EK, Goudreau JL, Lookingland KJ, Kim SW, Yu SW. Insulin withdrawal-induced cell death in adult hippocampal neural stem cells as a model of autophagic cell death. Autophagy 2009; 5:277-9.
133. Whittingham WF, Raper KB. Non-viability of stalk cells in Dictyostelium. Proc Natl Acad Sci USA 1960; 46:642-9.
134. Levraud JP, Adam M, Luciani MF, de Chastellier C, Blanton RL, Golstein P. Dictyostelium cell death: early emergence and demise of highly polarized paddle cells. J Cell Biol 2003; 160:1105-14.
135. Kay RR. Cell differentiation in monolayers and the investigation of slime mold morphogens. Meth Cell Biol 1987; 28:433-48.
136. Cornillon S, Foa C, Davoust J, Buonavista N, Gross JD, Golstein P. Programmed cell death in Dictyostelium. J Cell Sci 1994; 107:2691-704.
137. Roisin-Bouffay C, Luciani MF, Klein G, Levraud JP, Adam M, Golstein P. Developmental cell death in Dictyostelium does not require paracaspase. J Biol Chem 2004; 279:11489-94.
138. Lam D, Levraud JP, Luciani MF, Golstein P. Autophagic or necrotic cell death in the absence of caspase and bcl-2 family members. Biochem Biophys Res Commun 2007; 363:536-41.
139. Yamada Y, Okamoto K. Cell-type-specific responsiveness to cAMP in cell differentiation of *Dictyostelium discoideum*. Dev Biol 1992; 149:235-7.
140. Berks M, Kay RR. Cyclic AMP is an inhibitor of stalk cell differentiation in *Dictyostelium discoideum*. Dev Biol 1988; 126:108-14.
141. Tresse E, Kosta A, Giusti C, Luciani MF, Golstein P. A UDP-glucose derivative is required for vacuolar autophagic cell death. Autophagy 2008; 4:680-91.
142. de Chastellier C, Ryter A. Changes on the cell surface and of the digestive apparatus of *Dictyostelium discoideum* during the starvation period triggering aggregation. J Cell Biol 1977; 75:218-36.
143. Kosta A, Luciani MF, Geerts WJ, Golstein P. Marked mitochondrial alterations upon starvation without cell death, caspases or Bcl-2 family members. Biochim Biophys Acta 2008; 1783:2013-9.
144. Town CD, Gross JD, Kay RR. Cell differentiation without morphogenesis in *Dictyostelium discoïdeum*. Nature 1976; 262:717-9.
145. Town C, Stanford E. An oligosaccharide-containing factor that induces cell differentiation in *Dictyostelium discoideum*. Proc Natl Acad Sci USA 1979; 76:308-12.
146. Sobolewski A, Neave N, Weeks G. The induction of stalk cell differentiation in submerged monolayers of *Dictyostelium discoideum*. Characterization of the temporal sequence for the molecular requirement. Differentiation 1983; 25:93-100.
147. Morris HR, Taylor GW, Masento MS, Jermyn KA, Kay RR. Chemical structure of the morphogen differentiation inducing factor from *Dictyostelium discoideum*. Nature 1987; 328:811-4.
148. Lam D, Kosta A, Luciani MF, Golstein P. The IP3 receptor is required to signal autophagic cell death. Mol Biol Cell 2008; 19:691-700.
149. Giusti C, Luciani MF, Ravens S, Gillet A, Golstein P. Autophagic cell death in Dictyostelium requires the receptor histidine kinase DhkM. Mol Biol Cell 2010; 21:1825-35.
150. Kosta A, Roisin-Bouffay C, Luciani MF, Otto GP, Kessin RH, Golstein P. Autophagy gene disruption reveals a non-vacuolar cell death pathway in Dictyostelium. J Biol Chem 2004; 279:48404-9.
151. Giusti C, Luciani MF, Klein G, Aubry L, Tresse E, Kosta A, Golstein P. Necrotic cell death: From reversible mitochondrial uncoupling to irreversible lysosomal permeabilization. Exp Cell Res 2009; 315:26-38.
152. Laporte C, Kosta A, Klein G, Aubry L, Lam D, Tresse E, et al. A necrotic cell death model in a protist. Cell Death Differ 2007; 14:266-74.
153. Luciani MF, Kubohara Y, Kikuchi H, Oshima Y, Golstein P. Autophagic or necrotic cell death triggered by distinct motifs of the differentiation factor DIF-1. Cell Death Differ 2009; 16:564-70.
154. Turcotte S, Chan DA, Sutphin PD, Hay MP, Denny WA, Giaccia AJ. A molecule targeting VHL-deficient renal cell carcinoma that induces autophagy. Cancer Cell 2008; 14:90-102.
155. Mogensen TH. Pathogen recognition and inflammatory signaling in innate immune defenses. Clin Microbiol Rev 2009; 22:240-73.
156. Cavalier-Smith T. Predation and eukaryote cell origins: a coevolutionary perspective. Int J Biochem Cell Biol 2009; 41:307-22.
157. Virgin HW, Levine B. Autophagy genes in immunity. Nat Immunol 2009; 10:461-70.
158. Dieckmann R, Gopaldass N, Escalera C, Soldati T. Monitoring time-dependent maturation changes in purified phagosomes from *Dictyostelium discoideum*. Methods Mol Biol 2008; 445:327-37.
159. Arsham AM, Neufeld TP. Thinking globally and acting locally with TOR. Curr Opin Cell Biol 2006; 18:589-97.
160. Irazoqui JE, Urbach JM, Ausubel FM. Evolution of host innate defence: insights from *Caenorhabditis elegans* and primitive invertebrates. Nat Rev Immunol 2010; 10:47-58.
161. Casadevall A, Pirofski LA. Accidental virulence, cryptic pathogenesis, martians, lost hosts and the pathogenicity of environmental microbes. Eukaryot Cell 2007; 6:2169-74.
162. Lamoth F, Greub G. Amoebal pathogens as emerging causal agents of pneumonia. FEMS Microbiol Rev 2009; In press.
163. Campoy E, Colombo MI. Autophagy in intracellular bacterial infection. Biochim Biophys Acta 2009; 1793:1465-77.
164. Dorer MS, Isberg RR. Non-vertebrate hosts in the analysis of host-pathogen interactions. Microbes Infec 2006; 8:1637-46.
165. Benabentos R, Hirose S, Sucgang R, Curk T, Katoh M, Ostrowski EA, et al. Polymorphic members of the lag gene family mediate kin discrimination in Dictyostelium. Curr Biol 2009; 19:567-72.
166. Chen G, Zhuchenko O, Kuspa A. Immune-like phagocyte activity in the social amoeba. Science 2007; 317:678-81.
167. Benghezal M, Fauvarque MO, Tournebize R, Froquet R, Marchetti A, Bergeret E, et al. Specific host genes required for the killing of Klebsiella bacteria by phagocytes. Cell Microbiol 2006; 8:139-48.
168. Sillo A, Bloomfield G, Balest A, Balbo A, Pergolizzi B, Peracino B, et al. Genome-wide transcriptional changes induced by phagocytosis or growth on bacteria in Dictyostelium. BMC Genom 2008; 9:291.
169. Li Z, Dugan AS, Bloomfield G, Skelton J, Ivens A, Losick V, Isberg RR. The amoebal MAP kinase response to *Legionella pneumophila* is regulated by DupA. Cell Host Microbe 2009; 6:253-67.
170. Carilla-Latorre S, Calvo-Garrido J, Bloomfield G, Skelton J, Kay RR, Ivens A, et al. Dictyostelium transcriptional responses to *Pseudomonas aeruginosa*: common and specific effects from PAO1 and PA14 strains. BMC Microbiol 2008; 8:109.
171. Pukatzki S, Ma AT, Sturtevant D, Krastins B, Sarracino D, Nelson WC, et al. Identification of a conserved bacterial protein secretion system in *Vibrio cholerae* using the Dictyostelium host model system. Proc Natl Acad Sci USA 2006; 103:1528-33.
172. Farbrother P, Wagner C, Na J, Tunggal B, Morio T, Urushihara H, et al. Dictyostelium transcriptional host cell response upon infection with Legionella. Cell Microbiol 2006; 8:438-56.

173. Cosson P, Zulianello L, Join-Lambert O, Faurisson F, Gebbie L, Benghezal M, et al. *Pseudomonas aeruginosa* virulence analyzed in a *Dictyostelium discoideum* host system. J Bact 2002; 184:3027-33.
174. Solomon JM, Isberg RR. Growth of *Legionella pneumophila* in *Dictyostelium discoideum*: a novel system for genetic analysis of host-pathogen interactions. Trends Microbiol 2000; 8:478-80.
175. Clarke M. Recent insights into host-pathogen interactions from Dictyostelium. Cell Microbiol 2010; 12:283-91.
176. Skriwan C, Fajardo M, Hagele S, Horn M, Wagner M, et al. Various bacterial pathogens and symbionts infect the amoeba *Dictyostelium discoideum*. Int J Med Microbiol 2002; 291:615-24.
177. Jia K, Thomas C, Akbar M, Sun Q, Adams-Huet B, Gilpin C, Levine B. Autophagy genes protect against *Salmonella typhimurium* infection and mediate insulin signaling-regulated pathogen resistance. Proc Natl Acad Sci USA 2009; 106:14564-9.
178. Russell DG. Who puts the tubercle in tuberculosis? Nat Rev 2007; 5:39-47.
179. van der Wel N, Hava D, Houben D, Fluitsma D, van Zon M, et al. *M. tuberculosis* and *M. leprae* translocate from the phagolysosome to the cytosol in myeloid cells. Cell 2007; 129:1287-98.
180. Hagedorn M, Soldati T. Flotillin and RacH modulate the intracellular immunity of Dictyostelium to *Mycobacterium marinum* infection. Cell Microbiol 2007; 9:2716-33.
181. Gutierrez MG, Master SS, Singh SB, Taylor GA, Colombo MI, Deretic V. Autophagy is a defense mechanism inhibiting BCG and *Mycobacterium tuberculosis* survival in infected macrophages. Cell 2004; 119:753-66.
182. Collins CA, De Maziere A, van Dijk S, Carlsson F, Klumperman J, Brown EJ. Atg5-independent sequestration of ubiquitinated mycobacteria. PLoS Path 2009; 5:1000430.
183. Dupont N, Lacas-Gervais S, Bertout J, Paz I, Freche B, Van Nhieu GT, et al. Shigella phagocytic vacuolar membrane remnants participate in the cellular response to pathogen invasion and are regulated by autophagy. Cell Host Microbe 2009; 6:137-49.
184. Ponpuak M, Davis AS, Roberts EA, Delgado MA, Dinkins C, Zhao Z, et al. Delivery of cytosolic components by autophagic adaptor protein p62 endows autophagosomes with unique antimicrobial properties. Immunity 2010; 32:329-41.
185. Dorn BR, Dunn WA Jr, Progulske-Fox A. Bacterial interactions with the autophagic pathway. Cell Microbiol 2002; 4:1-10.
186. Swanson MS, Isberg RR. Association of *Legionella pneumophila* with the macrophage endoplasmic reticulum. Infect Immun 1995; 63:3609-20.
187. Otto GP, Wu MY, Clarke M, Lu H, Anderson OR, Hilbi H, et al. Macroautophagy is dispensable for intracellular replication of *Legionella pneumophila* in *Dictyostelium discoideum*. Mol Microbiol 2004; 51:63-72.
188. Price CT, Al-Khodor S, Al-Quadan T, Santic M, Habyarimana F, Kalia A, Kwaik YA. Molecular mimicry by an F-box effector of *Legionella pneumophila* hijacks a conserved polyubiquitination machinery within macrophages and protozoa. PLoS Path 2009; 5:1000704.
189. Francione L, Smith PK, Accari SL, Taylor PE, Bokko PB, Bozzaro S, et al. *Legionella pneumophila* multiplication is enhanced by chronic AMPK signalling in mitochondrially diseased Dictyostelium cells. Dis Model Mech 2009; 2:479-89.

Protocol manuscript

A proteolytic cleavage assay to monitor autophagy in *Dictyostelium discoideum*

Javier Calvo-Garrido, Sergio Carilla-Latorre, Ana Mesquita and Ricardo Escalante

Instituto de Investigaciones Biomédicas Alberto Sols. C.S.I.C./U.A.M. Calle Arturo Duperier 4, 28029 Madrid. Spain.

Author for correspondence: Ricardo Escalante, Tel: +34-91-585-4467. Fax: +34-91-585-4401. e-mail: rescalante@iib.uam.es

Key words: macroautophagy, autophagic flux, proteolytic assay, *Dictyostelium discoideum.*

Abstract

Dictyostelium discoideum **is a good model of autophagy. However, the lack of autophagic flux techniques hinders the assessment of new mutants or drugs. One of these techniques, which has been used successfully in yeast and mammalian cells, but has not yet been described in *Dictyostelium,* is based on the presence of proteolytic fragments derived from autophagic degradation of expressed fusion proteins. Lysosomotropic agents such as NH_4Cl penetrate acidic compartments and raise their pH, thus allowing the accumulation and measurement of these cleaved fragments, which otherwise would be rapidly degraded. We have used this property to detect the presence of free GFP fragments derived from the fusion protein GFP-Tkt-1, a cytosolic marker. We demonstrate that this proteolytic event is dependent on autophagy and can be used to detect differences in the level of**

autophagic flux among different mutant strains. Moreover, treatment with NH_4Cl also facilitates the assessment of autophagic flux by confocal microscopy using the marker RFP-GFP-Atg8.

1. Introduction

Macroautophagy (hereafter referred to as autophagy) is a very dynamic process comprising different stages from the induction, expansion and completion of a double membrane autophagosome, to the fusion of this vesicle with lysosomes and subsequent degradation and recycling of its cargo. The experimental observation of this complex process is difficult and most techniques only give snapshots of specific steps. For example in mammalian cells, the number of puncta revealed by the classical marker GFP-Atg8 strictly reflects the steady-state levels of early autophagosomes. An increase in the number of puncta can be either the consequence of an induction of autophagy or it can be due to inhibition of later steps of maturation. Therefore, this assay is insufficient to determine the stage at which autophagy is actually affected. It is important to determine autophagic flux for a given cargo until its degradation in order to have a more accurate picture of the entire process.[1]

Although most of our current knowledge about autophagy derives from the popular simple model *Saccharomyces cerevisiae*, development of autophagy techniques in other alternative experimental models such as zebrafish[2] or *Magnaporthe*[3] will make it possible to address new aspects of this important process. *Dictyostelium discoideum* has some advantages in the study of autophagy including the presence of several conserved autophagy genes, which are absent in *S. cerevisiae.*[4] Despite this potentiality, techniques to monitor autophagy in *Dictyostelium* are rather limited and a simple assay to measure autophagic flux has not been available.

The accumulation of free GFP fragments derived from autophagic degradation of GFP fusion proteins has become a useful technique to monitor autophagic flux in several systems, including yeast and mammalian cells.[5,6] These free GFP fragments can be detected because of their relative resistance to proteolytic degradation in the lysosome.[7] A recent report highlights the importance of lysosomal pH as a critical factor in the formation of these fragments from GFP-LC3 degradation in mammalian cells.[6] In certain cell types, the level of free GFP fragments is only detectable in the presence of non-saturating levels of lysosomal inhibitors or under conditions attenuating lysosomal acidity. Since the yeast vacuolar pH is higher than that of mammalian lysosomes (6.2 and 4.7, respectively), even low levels of free GFP fragments are detectable in yeast without the necessity of using lysosomotropic compounds.[5]

Remarkably, the lysosomal pH in *Dictyostelium* is extremely acidic (pH<3.5).[8] Thus, the lack of detectable free GFP fragments in this system could be the result of this highly acidic environment that rapidly degrades cargo proteins. The use of the lysosomotropic compound NH_4Cl has been previously described to increase lysosomal pH in *Dictyostelium.*[8,9] Using this compound, we have optimized the conditions to monitor the proteolytic cleavage of the GFP protein fused to cytosolic markers (Fig. 1). In order to test the approach, we have used different strains deficient in autophagy: *atg5*[-],[10] *atg6*[-],[11] *atg7*[-],[10] *atg8*[-],[11] and *vmp1*[-],[12] in which, as expected, the level of cleaved GFP is reduced or absent. Conversely, *midA*[-],[13] a strain in which the mitochondrial AMPK is overactive,[14] showed increased basal autophagy (Fig. 1).

The autophagy marker RFP-GFP-Atg8 (or RFP-GFP-LC3) has also been used as a tool to monitor autophagic flux in other systems. It is well known that RFP fluorescence is more resistant to the acidic and protease-rich conditions of the lysosome, whereas GFP fluorescence is rapidly quenched.[15] Therefore, the red-green puncta label

early autophagosomes, and the presence of red puncta that lack the green fluorescence (red/not-green) is indicative of the fusion event of autophagosomes with lysosomes. *Dictyostelium* cells expressing this marker showed a clear increase in the number of cells with red/not-green puncta upon NH_4Cl treatment, further confirming the usefulness of this approach (Fig. 2). The lack of autophagy in the *atg1*$^-$ mutant results in the absence of red/not-green puncta even during NH_4Cl treatment, and the formation of huge red-green aggregates, confirming our previous results.[12] Interestingly, we have found a high level of cleaved GFP during growth in axenic media (HL5), suggesting a high level of basal autophagy in *Dictyostelium*. These results are consistent with other observations such as the presence of GFP-Atg8[12] and RFP-GFP-Atg8 puncta (in this study) in HL5 and the slow growth phenotype observed in *atg1*$^-$ and *vmp1*$^-$ mutants.[10-12]

In conclusion, we have observed that slowing down the autophagy process is necessary to reveal autophagic flux in *Dictyostelium*. We show here the specific experimental conditions to measure nonselective bulk autophagy in *Dictyostelium* using the cleavage of a cytosolic marker fused to GFP, but certainly a variety of other experimental set-ups based on this property could be further optimized for specific purposes. With these autophagic flux techniques now within reach, *Dictyostelium* as a model in autophagy studies will be further strengthened.

2. Materials

2.1. Strains and culture media

The strains used in this study were derived from the DH1 (WT, *atg5*$^-$, *atg6*$^-$, *atg7*$^-$ and *atg8*$^-$) and obtained from the DictyStock Center (kindly deposited by Grant Otto[10,11]) and AX4 (WT and *vmp1*$^-$) strains. Transfections were carried out as previously described.[16]

The media used for growth was HL5 (Formedium; HLB0102) and PDF was used for starvation (20 mM KCl, 9 mM K_2HPO_4, 13 mM KH_2PO_4, 1 mM $CaCl_2$, 1 mM $MgSO_4$, pH 6.4). 6-well plates were from Becton Dickinson (353046) and P35 plates were from Ibidi (80136).

2.2. Chemicals and antibodies

DAPI was from Sigma (D95421). A stock solution (1000X) was prepared in dimethylformamide at 1 mg/ml.

G418 was from Gibco (11811-023). A stock solution was prepared in water at 50 mg/ml.

Blasticidin (BS) was from Calbiochem (203350). A stock solution was prepared in water at 10 mg/ml.

GFP antibody was from Sigma (G1544) and secondary antibody was from Santa Cruz (SC2030).

RIPA buffer: 50 mM Tris-HCl, pH 8, 1% NP-40, 0.1% SDS, 0.5% sodium deoxycholate, 150 mM NaCl, 2 mM EDTA. Protease inhibitor was added to RIPA buffer before use at 1:1,000 (Sigma, P8340).

TBST: 20 mM Tris-HCl, pH 7.52, 150 mM NaCl, 0.05% Tween 20.

2.3. Plasmid constructs

The genes coding for Tkt-1 (DDB_G0272618) and PgkA (DDB_G0287595) were amplified by RT-PCR using RNA isolated from growing cells. The fragments were then cloned into the *Xho*I-*Xba*I sites of the vector pTX-GFP (kindly deposited in the Dicty Stock Center by Tom Egelhoff[17]).

The construct RFP-GFP-Atg8 was generated using a GFP-Atg8 fragment amplified by PCR from the vector pA15/GFP-Apg8 (kindly deposited in Dicty Stock Center by Grant Otto). This fragment was then cloned in frame using a *Xho*I site at the C terminus of the RFP protein from the vector pTX-RFPmars (kindly deposited in the Dicty Stock Center by Clement Nizak).

2.4. Western blot and microscopy

The ECL detection kit was from GE HealthCare (RPN2209), and the western blot membrane was from Pall corporation (Biotrace PVDF; 66543).

Confocal microscopy was performed in a LeicaTCS SP5 using a PL APO 63X/1.4-0.6 objetive and LAS-AF (Leica Application Suite) software.

3. Methods

3.1. Cleavage assay

(1) Grow the different *Dictyostelium* strains transformed with the construct GFP-Tkt-1 in HL5 with G418 (10 μg/ml) and blasticidin (5 μg/ml) when appropriate (see technical notes 1 and 2).

(2) Grow cells to a density of approximately 1-2x10^6 in HL5. For each condition, harvest 10^6 cells by centrifugation at 250g for 5 min at room temperature and wash once with 1 ml of PDF. After centrifugation at 250g for 5 min, resuspend cells at 10^6 cells/ml in PDF (or HL5) and deposit 1 ml of cell suspension in each well of a 6-well plate.

(3) Add NH_4Cl (from a 2 M stock solution in water) to reach different concentrations ranging from 0-250 mM (usually 0, 50 mM, 100 mM, 150 mM, 250 mM). Incubate for 2 h at 22º C (see technical note 3).

(4) After 2 h add the same amount of NH_4Cl and further incubate during 2 additional h. This additional treatment increases the effect of the drug.

(5) After the incubation, resuspend the cells by pipetting, and transfer to 1.7 ml microcentrifuge tubes. Pellet by centrifugation at 250g for 5 min at room temperature and resuspend in 50 µl of RIPA buffer supplemented with protease inhibitors. Keep the cells on ice for a 15-30 min incubation to allow complete cell lysis (see technical note 4).

(6) Determine the amount of protein in the extracts by the Bradford method using BSA to generate the standard curve. Use 3-10 µg of protein for western blot analysis. Complement with loading buffer, boil, and separate using a standard 12% acrylamide SDS-PAGE gel.

(7) Transfer the gel to a PVDF membrane for Western-blot analysis. Block the filter overnight at 4ºC with TBST containing 1% skim-milk. Incubate for 3 h at room temperature with anti-GFP antibody diluted 1:4,000 in TBST containing 0.5% skim-milk with gentle shaking. Wash the filter twice for 10 min each with TBST containing 0.5% skim-milk and two more times with TBST. Incubate for 45 min with the secondary antibody diluted at 1:5,000 in TBST and wash three times for ten min each with TBST.

(8) Reveal with ECL using the appropriate exposure time to avoid saturation of the signal.

(9) Quantify using the software ImageJ (http://rsbweb.nih.gov/ij/) to measure the relative amount of signal of the cleaved GFP and the complete GFP-Tkt-1 protein (see technical note 5).

3.2. RFP-GFP-Atg8 assay

(1) Cells expressing RFP-GFP-Atg8 are grown exponentially in HL5 with the appropriate antibiotics (G418 and/or blasticidin).

(2) For each condition, harvest 10^6 cells by centrifugation at 250g for 5 min at room temperature and wash once with 1 ml of HL5. After centrifugation at 250g for 5 min, resuspend cells at 10^6 cells/ml in HL5 and deposit 500 µl on P35 plates (IBIDI). Add NH_4Cl at the same concentration as described for the cleavage assay. Incubate for 2 h at 22ºC.

(3) After 2 h add the same amount of NH_4Cl and incubate an additional 2 h.

(4) Visualize the cells in vivo in the same plates using a LeicaTCS SP5 confocal microscope.

4. Technical notes

1. We have found differences in the expression levels of the marker between different strains (for example AX4 and DH1 in this study) and, thus, the same background should be used when wild-type and mutant strains are compared.

2. Similar results were obtained with another cytosolic marker, the glycolytic enzyme phosphoglycerate kinase (PgkA) fused with GFP as previously described in yeast.[5]

3. The range of NH_4Cl must include unsaturating and saturating concentrations giving rise to partial and complete suppression of autophagy, respectively. We have found that unsaturated concentrations between 100-150 mM NH_4Cl give the maximum response, and 250 mM largely inhibits the accumulation of free GFP probably due to a complete suppression of lysosomal function, but the precise range must be optimized for each strain and condition. We recommend a preliminary assay with different concentrations in the range between 0-250 mM as shown in Figure 1.

4. Once in RIPA buffer, cells must be kept on ice, and cell lysis can be checked by light microscopy. At this point, cell extracts can be stored frozen (-70ºC). To continue with the analysis allow cells to thaw on ice.

5. Quantification is required to discern slight differences in autophagic flux. In this case, the experiment should be repeated at least three times to allow statistical analysis. Possible differences in the level of expression among strains can be calculated by densitometry of the GFP-Tkt-1 band in a preliminary western blot analysis. These data can be used to adjust the amount of protein loaded in subsequent experiments.

Acknowledgements

This work was supported by grant BFU2009-09050 from the Spanish Ministerio de Ciencia e Innovación. We thank the SIDI-Confocal facility for their assistance with confocal microscopy and the Dicty-Stock center for providing some of the strains used in this study. We wish to thank Pascale Gaudet for revising the English of the manuscript.

References

1. Klionsky DJ, Abeliovich H, Agostinis P, Agrawal DK, Aliev G, Askew DS, et al. Guidelines for the use and interpretation of assays for monitoring autophagy in higher eukaryotes. Autophagy 2008; 4:151-75.
2. He C, Klionsky DJ. Analyzing autophagy in zebrafish. Autophagy 2010; 6.
3. Xu F, Liu XH, Zhuang FL, Zhu J, Lin FC. Analyzing autophagy in *Magnaporthe oryzae*. Autophagy 2011; 7.

4. Calvo-Garrido J, Carilla-Latorre S, Kubohara Y, Santos-Rodrigo N, Mesquita A, Soldati T, et al. Autophagy in Dictyostelium: genes and pathways, cell death and infection. Autophagy 2010; 6:686-701.
5. Welter E, Thumm M, Krick R. Quantification of nonselective bulk autophagy in S. cerevisiae using Pgk1-GFP. Autophagy 2010; 6:794-7.
6. Ni HM, Bockus A, Wozniak AL, Jones K, Weinman S, Yin XM, et al. Dissecting the dynamic turnover of GFP-LC3 in the autolysosome. Autophagy 2011; 7:188-204.
7. Mizushima N, Yoshimori T, Levine B. Methods in mammalian autophagy research. Cell 2010; 140:313-26.
8. Marchetti A, Lelong E, Cosson P. A measure of endosomal pH by flow cytometry in Dictyostelium. BMC Res Notes 2009; 2:7.
9. Cardelli JA, Richardson J, Miears D. Role of acidic intracellular compartments in the biosynthesis of Dictyostelium lysosomal enzymes. The weak bases ammonium chloride and chloroquine differentially affect proteolytic processing and sorting. J Biol Chem 1989; 264:3454-63.
10. Otto GP, Wu MY, Kazgan N, Anderson OR, Kessin RH. Macroautophagy is required for multicellular development of the social amoeba *Dictyostelium discoideum*. J Biol Chem 2003; 278:17636-45.
11. Otto GP, Wu MY, Kazgan N, Anderson OR, Kessin RH. Dictyostelium macroautophagy mutants vary in the severity of their developmental defects. J Biol Chem 2004; 279:15621-9.
12. Calvo-Garrido J, Escalante R. Autophagy dysfunction and ubiquitin-positive protein aggregates in Dictyostelium cells lacking Vmp1. Autophagy 2010; 6:100-9.
13. Torija P, Vicente JJ, Rodrigues TB, Robles A, Cerdan S, Sastre L, et al. Functional genomics in *Dictyostelium*: MidA, a new conserved protein, is required for mitochondrial function and development. J Cell Sci 2006; 119:1154-64.
14. Carilla-Latorre S, Gallardo ME, Annesley SJ, Calvo-Garrido J, Grana O, Accari SL, et al. MidA is a putative methyltransferase that is required for mitochondrial complex I function. J Cell Sci 2010; 123:1674-83.
15. Kimura S, Noda T, Yoshimori T. Dissection of the autophagosome maturation process by a novel reporter protein, tandem fluorescent-tagged LC3. Autophagy 2007; 3:452-60.
16. Pang KM, Lynes MA, Knecht DA. Variables controlling the expression level of exogenous genes in Dictyostelium. Plasmid 1999; 41:187-97.
17. Levi S, Polyakov M, Egelhoff TT. Green fluorescent protein and epitope tag fusion vectors for *Dictyostelium discoideum*. Plasmid 2000; 44:231-8.

Figure legends

Figure 1

Western blot analysis of the cytosolic marker GFP-Tkt-1. (A) *Dictyostelium* cells were transformed with a construct expressing the fusion protein GFP-Tkt-1. Cells were

stained with DAPI and visualized by confocal microscopy. GFP fluorescence is homogeneously distributed in the cytosol, a prerequisite for a good marker of nonselective bulk autophagy. DAPI (blue staining) labels the nuclei. Bar: 10 μm. (B) Western blot analysis of *Dictyostelium* cells expressing GFP-Tkt-1 using a GFP antibody reveals a cleaved GFP fragment in AX4 and DH1 cells. Cells were treated with different concentrations of NH_4Cl during a 4-h incubation in PDF. The arrow indicates the presence of the cleaved GFP fragment corresponding approximately to the size of free GFP (not shown). Asterisks indicate background signal. In the left panel, AX4 cells were used and the concentration of NH_4Cl was 0, 15, 25, 40, 80 and 100 mM. In the right panel, higher concentrations were tested in DH1 cells (0, 50, 100, 250, 500 mM). The concentration range 0, 50, 100, 150, 250 mM is considered appropriate to cover unsaturated and saturated concentrations, 100 mM being the optimal. (C, D, E) The presence of the free-cleaved GFP fragment is dependent on autophagy. Different autophagy mutants (*atg5*$^-$, *atg6*$^-$, *atg7*$^-$ and *atg8*$^-$, whose background parental strain is DH1) were used in comparison with DH1 using concentrations of NH_4Cl ranging from 0-250 mM in PDF (0, 100, 250 mM in panel C; 0, 50, 100, 250 mM in panel D; 0, 100, 150, 250 mM in panel E). The cleaved GFP fragment is largely reduced or absent in all saturated or non-saturated concentrations. (F) AX4 and DH1 wild-type strains show a high basal autophagic flux during growth (HL5) and starvation (PDF). In these experiments, the concentration of NH_4Cl was 0, 50 100 and 250 mM (left panel) and 0,100, 250, 400 mM (right panel). (G) Autophagy dependency of the cleaved GFP fragment in the AX4 background. A different autophagy mutant (*vmp1*$^-$) whose parental strain is AX4 was also tested after incubation with different concentrations of NH_4Cl in HL5 for 4 h (0, 100, 250 mM in the wild type, and 100, 250 mM in the mutant). It should be noted that in this case the expression level of the construct was lower in the

mutant and thus, the amount of protein loaded in the gel was 5 times higher than that of the wild type, and the western blot was exposed longer. The difference in the expression level was calculated by densitometry in a previous western blot. In any case, no specific signal was detected in the *vmp1*$^{-}$ mutant. (H) In order to test if this technique can be used to detect higher levels of autophagy, a mutant strain defective in a mitochondrial protein, MidA, was used. AX4 wild-type and mutant strains were treated in HL5 with 0, 50, 100, 250 mM NH_4Cl. Western blot analysis revealed an increase in the level of the cleaved-GFP at 100 mM. An example of quantification by densitometry is shown on the right, where the ratio between the complete GFP-Tkt-1 and the cleaved GFP was calculated using the software ImageJ. All the experiments shown here are representative of at least three independent experiments.

Figure 2

Use of NH_4Cl in confocal analysis using the RFP-GFP-Atg8 marker. Wild-type (WT) and *atg1*$^{-}$ mutant cells expressing the construct RFP-GFP-Atg8 (shown schematically at the top) were treated with 100 mM NH_4Cl or left untreated (0) and analyzed by confocal microscopy *in vivo*. *atg1*$^{-}$ cells were used due to the presence of protein aggregates as previously described.[12] (Upper panel) WT cells showed the typical green/red punctate pattern. Only a few cells showed red/not-green puncta (arrow) indicating the presence of basal autophagy. Under these conditions the treatment with NH_4Cl revealed the presence of a large number of cells with red/not-green puncta (arrows) confirming the presence of a rapid autophagic flux, which is only clearly detectable when autophagy is slowed down by non-saturating concentrations of NH_4Cl. (Lower panel) The *atg1*$^{-}$ mutant under the same conditions. In this case, huge aggregates were detected as

described previously, showing red-green fluorescence, while no red/not-green puncta could be observed under all conditions, indicating a block in autophagic flux.

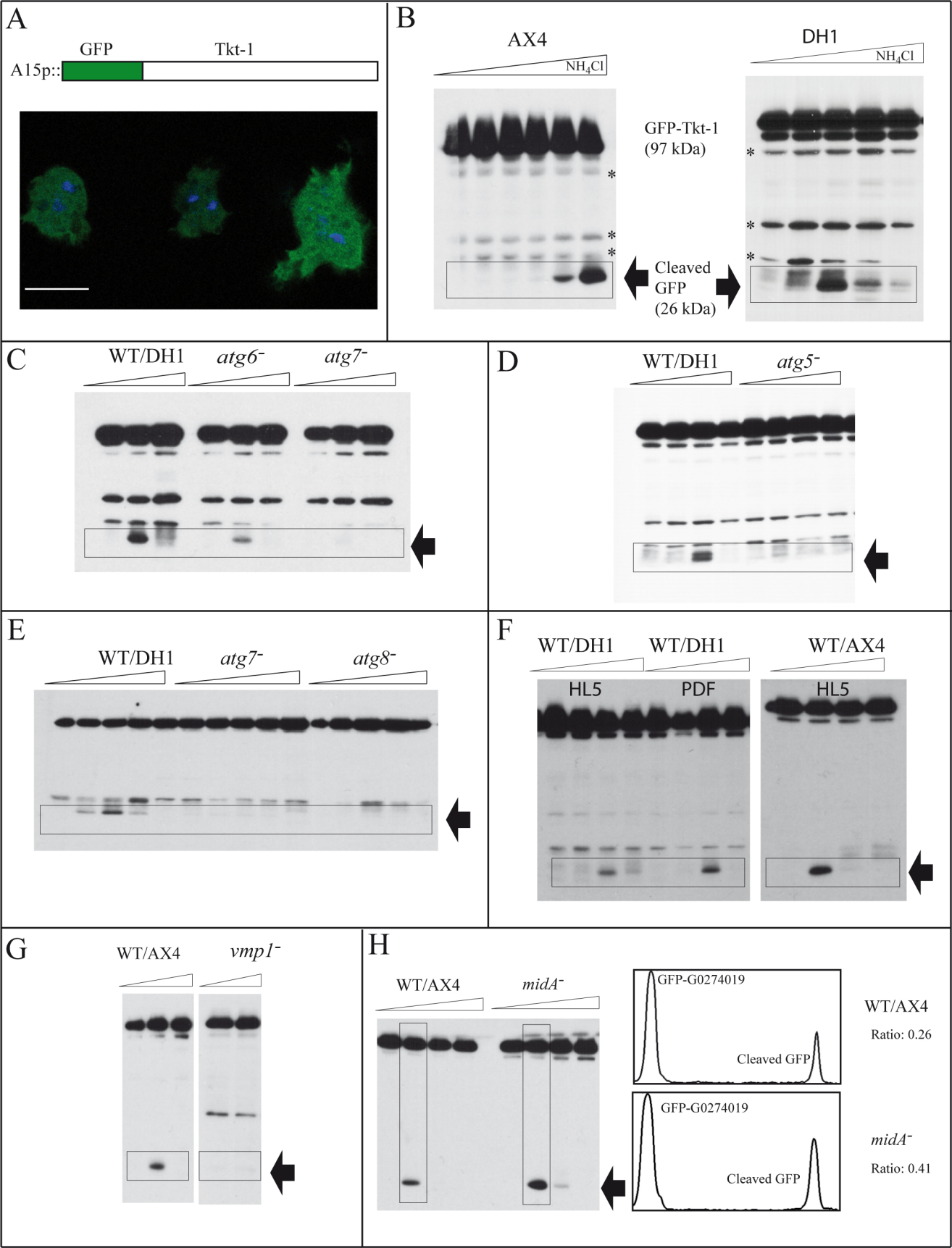
A
GFP
Tkt-1
A15p::
B
AX4
NH4Cl
DH1
NH4Cl
GFP-Tkt-1
(97 kDa)
Cleaved
GFP
(26 kDa)
C
WT/DH1
atg6-
atg7-
D
WT/DH1
atg5-
E
WT/DH1
atg7-
atg8-
F
WT/DH1
WT/DH1
WT/AX4
HL5
PDF
HL5
G
WT/AX4
vmp1-
H
WT/AX4
midA-
GFP-G0274019
Cleaved GFP
WT/AX4
Ratio: 0.26
GFP-G0274019
Cleaved GFP
midA-
Ratio: 0.41

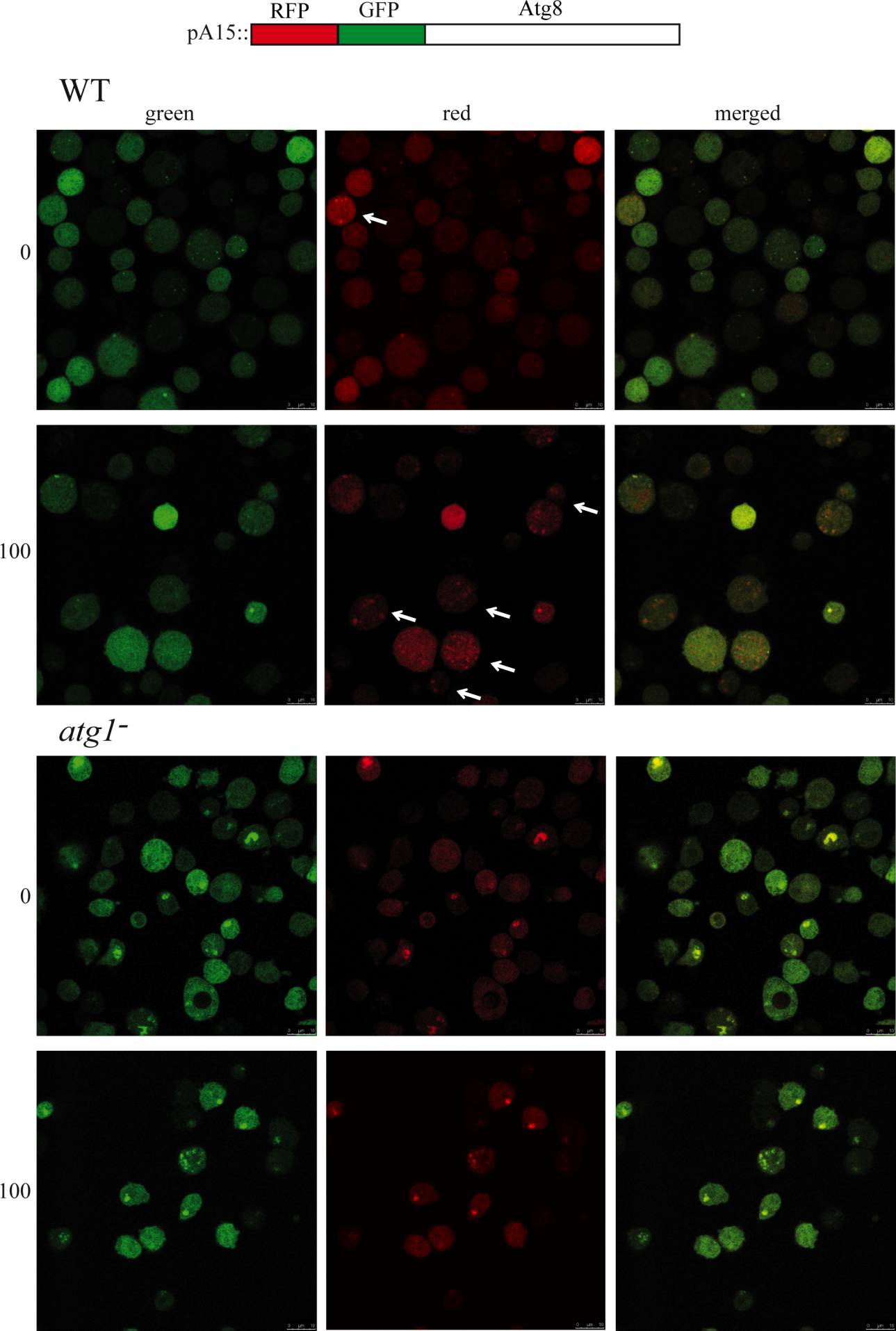
RFP
GFP
Atg8
pA15::
WT
green
red
merged
0
100
atg1-
0
100